UNIVERSITY
OF TASMANIA

Organolanthanide Complexes of the Calix[2]phenylene[2]pyrrolide Macrocyclic Ligand

By

Adele Jane Wilson, B. Sc. (Hons), Grad. Dip. (Sci. Comm.)

A thesis submitted in fulfilment of the requirements

for the degree of Doctor of Philosophy

University of Tasmania, May 2015

This thesis contains no material which has been accepted for the award of any other degree or diploma in any tertiary institution, and to the best of my knowledge and belief, contains no material previously published or written by another person, except where due reference is made in the text of the thesis.

This thesis may be made available for loan and limited copying and communication in accordance with the Copyright Act 1968.

Adele Wilson

May, 2015

Acknowledgements

My sincere thanks go to my supervisor Associate Professor Michael Gardiner, whose valuable guidance and support has been instrumental in bringing this work together.

Thanks also to my predecessors in this research, Dr Jun Wang, Dr Alistair Frey, and in particular Dr Adam James, providing advice and great company alongside our co-workers in the laboratory Dr James Suttil, Dr Bryce Lockhart-Gillett, Dr Sam Karpiniec, Dr Peter Molesworth, Dr Roderick Jones, Dr Curtis Ho, Ms Catriona Vanston and Ms Helen Thomas. Dr Nathan Kilah and Professor Brian Yates have offered advice and support as co-supervisors, for which I am grateful.

Thanks to Dr Thomas Rodemann and Assoc. Prof Noel Davies who provided advice in elemental analysis and GC-MS analysis, respectively, and to the scientists at the small molecule crystallography beamlines at the Australian Synchrotron in Melbourne.

I have been lucky to receive encouragement and support from great friends; in particular Andrew Burgess, Anthia Lyons, Jarrod Coad, Brendon Schollum, Reyne Pullen, Jeremy Just, Murray Frith, Dr Peter Traill and Jeannie-Marie LeRoi, thank you all from the bottom of my heart.

Finally, I am very grateful to my family for providing encouragement and happy distractions. Thank you Paul, Peter, David, Celina, Samuel and Thomas Wilson, Tony Prins and my parents Shirley O'Brien and Richard Wilson; I couldn't have done this without you.

Abstract

This thesis describes the synthesis and characterisation of lanthanide complexes of the macrocyclic ligand calix[2]phenylene[2]pyrrolide. The reactivity of these complexes is investigated and discussed. The reductive abilities of these complexes are tested through reaction with a series of pyridines and diazines. The flexibility and reactivity of the macrocyclic ligand is contrasted with a related, more rigid ligand.

Chapter 1 establishes a background of the lanthanide metals and organolanthanide chemistry. Organolanthanide complexes of the ubiquitous cyclopentadienyl and pentamethylcyclopentadienyl ligands are introduced. Non-cyclopentadienyl ligands are briefly discussed, with a focus on the use of calix[4]pyrrolide as a macrocyclic ligand. Modifications of the calix[4]pyrrolide ligand are introduced, with a focus on *trans*-*N*,*N'*-dimethyl-*meso*-octaethylcalix[4]pyrrolide and *meso*-octamethyl-calix[2]phenylene[2]pyrrolide.

Chapter 2 discusses the preparation and characterisation of precursors, key reagents and benchmark lanthanide(II) and (III) reference complexes. Conformational characteristics of these complexes are compared, with a focus on detail of the solid state structures obtained by single crystal X-ray diffraction. The contrasting structures of dilithiated calix[2]phenylene[2]pyrrole and an analogous potassium complex are described. Metathesis of the dilithiated macrocycle with samarium diiodide is shown to form complexes with samarium bound within the macrocyclic cavity. The effect of ancillary

coordinated solvent molecules on the conformation of these complexes is investigated. The oxidation state of lanthanides in macrocyclic complexes is discussed. Unambiguous europium(II) and samarium(III) complexes are synthesised and characterised in order to identify whether conformational changes to the macrocycle indicate the oxidation state of the lanthanide metal centre. An interesting polymeric samarium complex free of ancillary ligands is described.

Chapter 3 focuses on the preparation of a series of samarium calix[2]phenylene[2]pyrrolide complexes with pyridine and pyridine-based ligands. Where possible, analogous europium complexes are also described in order to compare their structural characteristics in the solid state. This investigation produced some unexpected results, such as an easily-reducible molecule observed acting as neutrally charged ancillary ligand. This Chapter covers the reactivity of selected pyridines, diazines, and sterically bulky linked- or fused-ring heterocyclic molecules with a samarium macrocyclic complex. Where relevant, comparisons are drawn with analogous samarium cyclopentadienyl-based complexes and complexes of the related macrocyclic ligand *trans*-*N*,*N'*-dimethyl-*meso*-octaethylcalix[4]pyrrolide.

Concluding remarks and avenues of work warranting future investigation are presented in Chapter 4. The experimental syntheses and characterisation data of complexes prepared in this thesis are provided in Chapter 5. Single crystal X-ray diffraction data has been included electronically in the form of crystallographic information files (.CIF) in Appendix A.

Table of Contents

Abbreviations

Å	Ångströms, 10^{-10} m
br	broad
bipy	2,2'-bipyridine
*n*BuLi	*n*-butyl lithium
COT^{2-}	cyclooctatetraendiyl dianion
Et	ethyl
$(Et_8N_4Me_2)^{2-}$	*trans*-*N*,*N'*-dimethyl-*meso*-octaethylcalix[4]pyrrolide
L	ligand
Ln	lanthanide
M	metal
m	multiplet
Me	methyl
$Me_8N_2Ph_2H_2$	*meso*-octamethylcalix[2]phenylene[2]pyrrole
$(Me_8N_2Ph_2)^{2-}$	*meso*-octamethylcalix[2]phenylene[2]pyrrolide
NMR	nuclear magnetic resonance
Ph	phenyl (or phenylene)
phen	1,10-phenanthroline
ppm	parts per million
py	pyrrolide
pyr	pyridine
R	alkyl, aryl
s	singlet
SIR	sterically induced reduction
*t*Bu	*tertiary*-butyl
terpy	2,2';6',2"-terpyridine
t	tertiary
THF	tetrahydrofuran
δ	chemical shift

Chapter 1

Introduction

1.1 The Lanthanides

The *f*-block of the periodic table consists of two rows customarily shown below the main body of the table. These two rows are split into the lanthanides (elements 57–71) and the actinides (elements 89–103). The lanthanide elements lanthanum (57) and lutetium (71) are sometimes defined as Group 3 elements, but are formally included with the *f*-block.[1] Group 3 elements scandium and yttrium are also chemically similar to the lanthanides and are sometimes included in the series. These elements together are also known as the rare earths or *lanthanoids*. The term 'rare earth' is somewhat of a misnomer as these elements are actually quite abundant. The lanthanide neodymium, for example, is more commonly found in the Earth's crust than gold.[2, 3] Even the least abundant lanthanide, thulium, is four times more abundant than silver.[4] The exception to this is radioactive promethium, with its half-life of 18 years, which is produced by irradiation of neodymium or praseodymium.[5, 6] The name perhaps better describes the scarcity of the rare earth mineral ore deposits which led to the relatively late identification of these elements.[5-11]

Mixtures of lanthanides are found in naturally occurring ore. The reliable separation and isolation of lanthanide metals is a relatively recent development as the chemical and physical properties of lanthanides are very similar to one another. Only minor

differences in solubility and complex formation allow for their separation. The lanthanoids are now commonly utilised in a number of industrial processes.

In recent years *f* block chemistry has been an area of growing interest as these metals show some strong and novel reductive behaviour.[12, 13] Organolanthanide complexes are already utilised in industrial and specific catalysis reactions, such as trivalent organolanthanide complexes which have applications as polymerisation catalysts.[14-23]

Common uses of *f* metals are in catalysis[24, 25] and polymerisation reactions.[14, 26] Catalytic converters in internal combustion engines often use a cerium catalyst to reduce atmospheric pollution.[27] Some lanthanide oxides are used in detection of gases such as hydrogen, oxygen or nitrous oxide.[28-31] Lanthanide reagents also have applications in numerous organic reactions,[32] in photonics (optical fibres, lasers, laser-protective filters and night vision goggles),[33, 34] organic light emitting diodes (OLEDs),[35, 36] solar energy conversion,[37, 38] photocatalytic decomposition of pollutants,[39, 40] phosphors for lighting and plasma displays,[41, 42] and luminescent probes for biological sciences.[43-46] Specific *f* metals and their alloys have become ubiquitous in the production of strong magnets.[47] Strong samarium-cobalt and neodymium magnets are used in computer hard drives, superconductors and in batteries. Single-molecule nanoscale magnets are of great interest in the development of high speed computers and hard drives.[48-50] The strong magnetic properties of rare earths have been utilised in the development of permanent-magnet motors free of bearings.[51, 52] Rare earth alloys also play a role in cryogenics and magnetic refrigeration.[53-59] The radioactive isotopes ^{138}La, ^{147}Sm, $^{143/144}$Nd and ^{176}Lu

have long half-lives and can be used to date rock and mineral samples.[60-63] Lanthanum can be used as an alternative to Ca^{II} in some biological reactions as they are similar in size, bonding and coordination.[27] Addition of lanthanides improves the physical and mechanical properties of steel,[27] whilst lanthanide salts can inhibit corrosion[27] and are also used as pigments for glass, enamels, ceramics and paints.[64] Gadolinium(III), with its seven unpaired electrons, is used as a strong contrast agent for Magnetic Resonance Imaging (MRI).[65]

Elements of the *f*-block represent the filling of the seven 4*f* and 5*f* orbitals. The marked similarity of properties across the group suggests that *f* electrons are not heavily involved in bonding. The most notable physical difference between the *f* elements is the small decrease in metal ionic radius across the row, listed in Table 1.

This *f*-block contraction is similar to the *d*-block contraction seen in transition metals, and is caused in part by relativistic effects. The *f* orbitals lie close to the nucleus where they are shielded by the larger *p* and *d* orbitals, meaning they have less importance in lanthanide complexes than the *d* orbitals in transition metal complexes. It is accepted the *f* electrons play little or no role in organolanthanide bonding, which makes ligand effects more important than metal orbital effects in organolanthanide chemistry.[66-68]

Table 1: Atomic and ionic radii of the formal lanthanides (C.N. = coordination number).[6,9,27,69,70]

Element		Number	Atomic radius (Å)	Ln^{III} radius (C.N.=8) (Å)	Ln^{III} radius (C.N.=6) (Å)	Ln^{III} radius (Å)
La	Lanthanum	57	1.877	1.16	1.032	1.06
Ce	Cerium	58	1.825	1.14	1.010	1.03
Pr	Praseodymium	59	1.828	1.13	0.990	1.01
Nd	Neodymium	60	1.821	1.11	0.983	0.99
Pm	Promethium	61	1.810	1.09	0.970	0.98
Sm	Samarium	62	1.802	1.08	0.958	0.96
Eu	Europium	63	2.042	1.07	0.947	0.95
Gd	Gadolinium	64	1.802	1.05	0.938	0.94
Tb	Terbium	65	1.782	1.04	0.923	0.92
Dy	Dysprosium	66	1.773	1.03	0.912	0.91
Ho	Holmium	67	1.766	1.02	0.901	0.89
Er	Erbium	68	1.757	1.00	0.889	0.88
Tm	Thulium	69	1.746	0.99	0.880	0.87
Yb	Ytterbium	70	1.940	0.99	0.868	0.86
Lu	Lutetium	71	1.734	0.98	0.861	0.85

The chemical similarities between these elements in combination with the lanthanide contraction leads to a unique opportunity for fine tuning reactivity; the lanthanides are a set of chemically similar metals with a range of sizes. Ligands can be chosen and manipulated for steric control, and the complex can then be fine-tuned by changing the size of the metal to optimise activity. The hydrogenolysis reaction in Scheme 1 is an example of a reaction heavily influenced by the metal centre, where decreasing the metal centre radius by 0.02 Å reduces the yield of product drastically, from 55% to only trace amounts.[71, 72] Although it is tempting to expect trends in structures across the lanthanide series due to the changing metal radius, this is not always the case, even with simple halide ligands.[70]

Scheme 1: Hydrogenolysis reactivity influenced by lanthanide centre in analogous complexes.

For Ln = Er (radius 1.004 Å) yield = 55%; Ln = Yb (radius 0.985 Å) yield = trace.

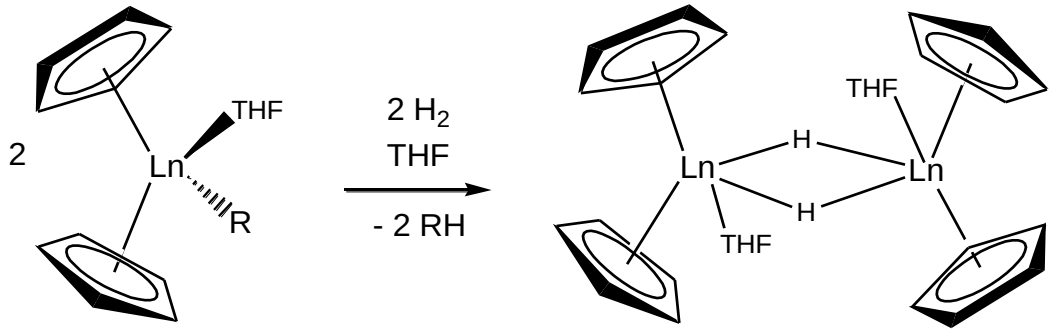

The most common oxidation state found for lanthanide metals is 3+. Cerium can be found in a 4+ oxidation state, as the loss of 4 electrons achieves the noble gas configuration, but it is the only lanthanide to attain this state without the use of the extremely electronegative fluoride ligand. The 2+ oxidation state is well established for samarium, europium and ytterbium and until recently these were believed to be the only lanthanide metals able to form stable Ln^{II} compounds. This will be further discussed in Section 1.7.

Europium(II) and ytterbium(II) have half-filled and fully-filled *f* shells respectively, giving them stability in the 2+ state, whilst samarium(II) has a $4f^{6}$ electronic configuration which approaches a half-filled shell. The redox potentials of samarium, europium and ytterbium are related to their electronic configurations, shown in Table 2.

These standard potentials in acidic solution are the smallest of the lanthanides: Eu^{2+}/Eu^{3+} is −0.35 V, while the Yb^{2+}/Yb^{3+} couple is −1.05 V. The larger standard

potential of Sm^{2+}/Sm^{3+} of −1.55 V indicates the strongly favoured oxidation of Sm^{II} to Sm^{III}. This reactivity, in combination with the relative accessibility of samarium(II), makes this a desirable target for further investigation. More recent work has also isolated neodymium, dysprosium, thulium and lanthanum in 2+ oxidation states.[73-75]

Table 2: Electronic configuration of the lanthanides in atomic and 3+ oxidation state, and the standard reduction potentials of each Ln^{3+}/Ln^{2+}couple.[10, 76, 77]

Symbol	**Name**	**Atomic configuration**	**Ln^{3+} configuration**	**Ln^{3+}/Ln^{2+} E^o (V)**
La	Lanthanum	$[Xe]5d^1\ 6s^2$	$4f^0$	−2.94
Ce	Cerium	$[Xe]4f^1\ 5d^1\ 6s^2$	$4f^1$	−2.92
Pr	Praseodymium	$[Xe]4f^3\ 6s^2$	$4f^2$	−2.84
Nd	Neodymium	$[Xe]4f^4\ 6s^2$	$4f^3$	−2.62
Pm	Promethium	$[Xe]4f^5\ 6s^2$	$4f^4$	−2.44
Sm	Samarium	$[Xe]4f^6\ 6s^2$	$4f^5$	−1.55
Eu	Europium	$[Xe]4f^7\ 6s^2$	$4f^6$	−0.34
Gd	Gadolinium	$[Xe]4f^7\ 5d^1\ 6s^2$	$4f^7$	−2.85
Tb	Terbium	$[Xe]4f^8\ 5d^1\ 6s^2$	$4f^8$	−2.83
Dy	Dysprosium	$[Xe]4f^{10}\ 6s^2$	$4f^9$	−2.56
Ho	Holmium	$[Xe]4f^{11}\ 6s^2$	$4f^{10}$	−2.79
Er	Erbium	$[Xe]4f^{12}\ 6s^2$	$4f^{11}$	−2.87
Tm	Thulium	$[Xe]4f^{13}\ 6s^2$	$4f^{12}$	−2.22
Yb	Ytterbium	$[Xe]4f^{14}\ 6s^2$	$4f^{13}$	−1.05
Lu	Lutetium	$[Xe]4f^{14}\ 5d^1\ 6s^2$	$4f^{14}$	−2.25

Research in this thesis will focus primarily on the lanthanide metal samarium, which was first spectroscopically described in 1853 by Jean Charles Galissard De Margnac and first isolated in 1879 by Paul Émile Lecoq do Boisbaudran. Samarium can be extracted from minerals such as monazite and samarskite, where it is found mixed with other lanthanides including cerium and gadolinium. Some rare earth alloys have permanent magnetisation, as seen in neodymium and samarium-cobalt magnets.[47, 50] Isotopes of samarium are used in the treatment of some types of cancer and disease,[78, 79] and in nuclear reactor control rods as a neutron absorber.[80] The properties of samarium also give it a range of other applications in catalysis,[81, 82] lasers,[83] and determining the age of geological samples using the $^{147}Sm/^{143}Nd$ ratio.[84-87]

In 1977 Kagan noted that the thermodynamically favourable oxidation of readily available Sm^{II} to Sm^{III} would make it a useful one-electron reducing agent.[88] A simple synthetic method was presented reacting samarium metal with 1,2-diiodoethane in THF to form samarium diiodide.[89] In following years SmI_2 was found to be useful in a range of organic reactions, including selective coupling reactions,[90, 91] functional group conversions and reductions.[4, 32, 81, 90-93] Requiring only mild reaction conditions, samarium diiodide has become a staple in organic and organometallic synthesis. Additives such as HMPA or transition metal salts are commonly used alongside SmI_2 to increase its reactivity in organic transformations.[94-96] Dysprosium diiodide is also a powerful reducing agent.[97]

In transition metal chemistry, covalent bonds are predominantly formed between a ligand and metal centre. Ligand influence on the reactivity of transition metal complexes is attributed to these covalent bonds. While it is generally accepted that in lanthanide complexes the ligand-metal bond is ionic, ligand influence on reactivity is still present.[98, 99]

There are a number of factors that can influence the appearance of an NMR spectrum, not the least of which is the presence of a paramagnetic metal.[66] Unlike paramagnetic transition metals, the electron spin relaxation time in paramagnetic lanthanides is usually short enough that resonances can still be observed, however broadening generally results in the loss of structural information such as the nature of coupling between resonances.[66] A paramagnetic metal complex will show shifted resonances for protons in proximity to the metal centre.[100-102] Most lanthanide ions are paramagnetic and will cause shifting of resonances in an NMR spectrum, making the observation and assignment of resonances challenging.[66, 100] This property of paramagnetic lanthanides does make them useful as NMR shift reagents which can help to resolve resonances.[103-106] Because of this, NMR spectroscopy is not always useful in the characterisation of organolanthanide complexes. The paramagnetism of a particular organolanthanide depends on the metal ion and the ligands involved, and the understanding of even a simple organolanthanide NMR spectrum requires a quite different approach to the interpretation of ^{1}H and ^{13}C NMR spectra of diamagnetic compounds.[100, 107] The magnetic moment of selected lanthanides, averaged from observed data, are shown in Figure 1 below.

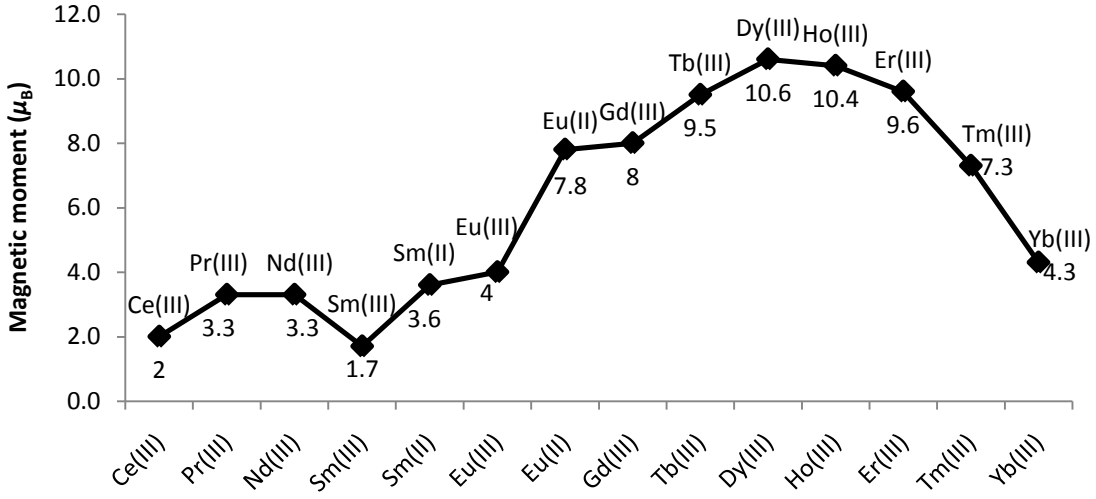

Figure 1: Magnetic moments (μ_B) of selected lanthanide ions (average observed values).[108, 109]

Proton chemical shifts in paramagnetic molecules are determined by factors proportional to magnetic susceptibility.[110] While the high magnetic moment of gadolinium(III) makes it useful as an MRI contrasting agent, this property also rules out NMR spectroscopy as a useful characterisation method. Europium(II), with an average magnetic moment of 7.8 μ_B is too paramagnetic to allow for useful NMR spectral characterisation. Samarium(II) also has a high magnetic moment of 3.6 μ_B, which can hinder characterisation by NMR spectroscopy. Samarium(III) has a lower magnetic moment of 1.7 μ_B, and can generally be characterised using NMR spectroscopy.

1.2 Organolanthanide Complexes

One of the most notable milestones in organometallic chemistry was the synthesis and characterisation of ferrocene, $[(\eta^5\text{-}C_5H_5)_2Fe]$, shown in Figure 2, in 1951 by Pauson and Kealy.[111] The sandwich structure of ferrocene was postulated by Woodward and

Wilkinson shortly afterwards,[112] and the structure was confirmed crystallographically by Eiland and Pepinsky in 1952.[113] The iron centre in ferrocene sits π-bound between two anionic cyclopentadienide ligands, in what is commonly referred to as a metallocene, or sandwich complex.

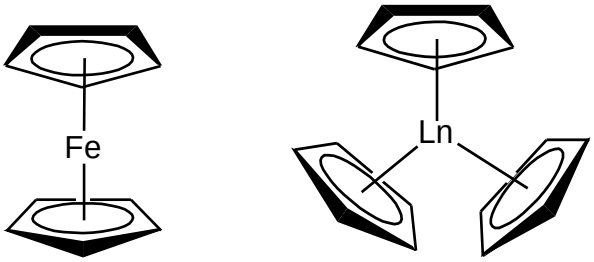

Figure 2: Ferrocene; $[(\eta^5\text{-}C_5H_5)_2Fe]$ and the lanthanide tris(cyclopentadienyl)complex $[(\eta^5\text{-}C_5H_5)_3Ln]$.

Cyclopentadienyl, $(\eta^5\text{-}C_5H_5)^-$, hereafter expressed as $(C_5H_5)^-$, is a mono anionic ligand which is normally non-participative in reactions.[114] It provides steric and electronic stability, occupying a relatively large amount of the coordination sphere with respect to its monoanionic status. Metallocene complexes are known for many metals, as the cyclopentadienyl orbitals interact favourably with metal *d* orbitals.

The first organolanthanide complexes were reported two years after ferrocene. Wilkinson and Birmingham isolated tris(cyclopentadienyl)lanthanide(III) complexes of Sc, Y, La, Ce, Pr, Nd, Sm and Gd in 1954,[115] and complexes of Dy, Er and Yb in 1956.[116, 117] These larger *f* metal centres require three cyclopentadienyl ligands to satisfy charge balancing issues and their coordination sphere permits this binding. The cyclopentadienyl ligands are π-bound and the M–cyclopentadineyl interactions are

formally ionic with the lanthanide metal centre in a 3+ state, as confirmed by magnetic moment calculations in 1963.[115,118,119] The air-sensitive crystalline $[(C_5H_5)_3Ln]$ complexes share similar solubility, reactivity and are uniformly ionic in nature. The tris(cyclopentadienyl) europium complex $[(C_5H_5)_3Eu(THF)]$ was reported in 1964 by Dubeck and Manastyrskyj,[120] and the first bis(cyclopentadienyl) complex of europium was reported by Fischer in the same year.[121]

Dubeck prepared halogenated bis(cyclopentadienyl) complexes of the general formula $[(C_5H_5)_2LnCl]$ (where Ln = Sm, Gd, Dy, Ho, Er, Yb and Lu) and $[(C_5H_5)LnCl_2(THF)_3]$ (where Ln = Sm, Eu, Gd, Dy, Ho, Er, Yb, Lu) in 1963 (Figure 3).[118, 119] Two synthetic pathways were reported, through the reaction of lanthanide trichlorides with sodium cyclopentadienide or by reaction of lanthanide tris(cyclopentadienyl) complexes with their corresponding lanthanide trichloride. These complexes provided a stepping stone to the investigation of numerous novel complexes of the form $[(C_5H_5)_2LnR]$, which the authors demonstrated by preparing alkyl, amide, methoxide, phenoxide and acylate derivatives.[119]

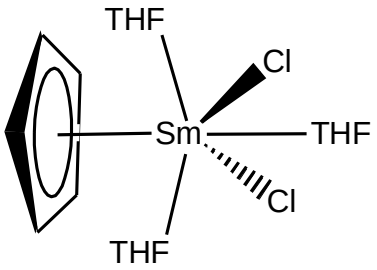

Figure 3: Cyclopentadienyl samarium chloride complex $[(\eta^5\text{-}C_5H_5)SmCl_2(THF)_3]$.

The pyrophoric bis(cyclopentadienyl) samarium(II) complex [Sm(C_5H_5)$_2$(THF)], shown in Figure 4, was prepared in 1969 by Watt and Gillow using a modified method developed for the synthesis of their related pyrophoric zirconium complex, [Zr(C_5H_5)$_2$].[122] This was achieved by stirring tris(cyclopentadienyl) samarium(III) with potassium in THF, yielding an insoluble purple samarium(II) product. It was observed that exposure to trace amounts of air caused an immediate colour change from purple to yellow, accompanied by a significant reduction in paramagnetism indicating that a Sm^{II} product was being oxidised to Sm^{III}. Bis(cyclopentadienyl)samarium, [(C_5H_5)$_2$Sm], is another easily prepared reducing agent[123] and has numerous roles in organic reactions. A recent report, for example, shows that [(C_5H_5)$_2$Sm] is an effective initiator of lactone ring-opening polymerisation.[124]

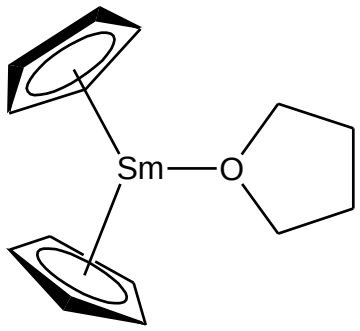

Figure 4: Pyrophoric [(C_5H_5)$_2$Sm(THF)].

f-Element analogues of ferrocene were at first predicted to be unstable, as two cyclopentadienyl ligands would not satisfy the lanthanide centre requirements for coordinative saturation. The first reported 'true' *f*-block sandwich complex was uranocene [(η^8-C_8H_8)$_2$U],[125] Figure 5, which was followed by the synthesis of related lanthanide complexes of the form K[(C_8H_8)$_2$Ln] and [{(C_8H_8)LnCl(THF)$_2$}$_2$].[99, 126, 127] A

larger carbon ring is required for *f* elements to utilise π-bonding to satisfy the high coordination number (and 8–10 electron pairs) required to make a stable sandwich complex.

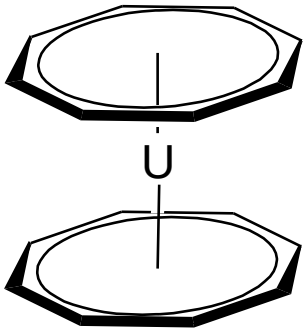

Figure 5: Uranocene [$(\eta^8\text{-}C_8H_8)_2U$].

Permethylation of cyclopentadienyl gives the bulkier pentamethylcyclopentadienyl ligand $(\eta^5\text{-}C_5Me_5)^-$. Increasing steric bulk of the ligand encourages crystallinity and stability of resulting complexes, making characterisation in the solid state more accessible. The larger pentamethylcyclopentadienyl ligand occupies more of the coordination sphere, occupying three adjacent coordination sites whilst retaining the monoanionic nature of the smaller cyclopentadienyl ligand. In lanthanide chemistry the most common binding mode is $(\eta^5\text{-}C_5Me_5)^-$, hereafter referred to as $(C_5Me_5)^-$, and is not generally open to decomposition or fragmentation. As pentamethylcyclopentadienyl is more electron-rich than cyclopentadienyl, it is a stronger donor and harder to remove from the metal centre.

The pentamethylcyclopentadienyl complex $[(C_5Me_5)_2Sm(THF)_2]$, prepared by Evans in 1981, was the first reported soluble organosamarium(II) complex (Figure 6).[128] Crystallographic characterisation of this samarium(II) metallocene revealed a pseudo-tetrahedral shape including two ancillary THF molecules, presumably to satisfy the coordination sphere of the metal ion. Isolating this soluble complex allowed for a wider exploration of the reduction chemistry of samarium(II). The complex was found to be an active catalyst, polymerising ethene and acting as a catalyst precursor for the hydrogenation of 3-hexyne to *cis*-3-hexene.[128] Evans also formed samarium methyl complexes by reacting $[(C_5Me_5)_2Sm(THF)_2]$ with trimethylaluminium.[129]

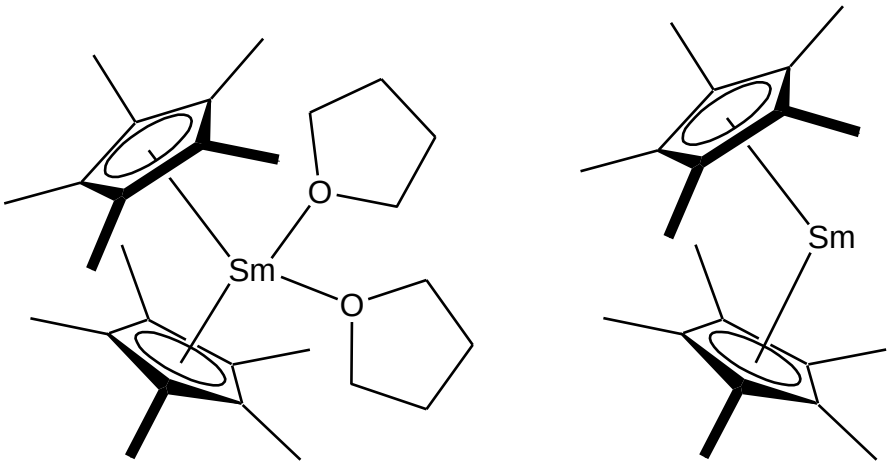

Figure 6: The Sm^{III} complexes$[(C_5Me_5)_2Sm(THF)_2]$, and desolvated bent decamethylsamarocene $[(C_5Me_5)_2Sm]$.

Sublimation of $[(C_5Me_5)_2Sm(THF)_2]$ under vacuum resulted in the removal of the coordinated THF to give decamethylsamarocene, $[(C_5Me_5)_2Sm]$ (Figure 6).[130] The bent metallocene structure is retained, with a slightly larger (C_5Me_5)–Sm–(C_5Me_5) (centroid) angle compared to the solvated complex (140.1 ° vs 136.7 °). The increased reactivity of

[$(C_5Me_5)_2Sm$] is due to both the strong reduction potential of samarium and the open, unsaturated coordination sphere of the complex.

The bent metallocene structure was unanticipated, as sterically a parallel metallocene geometry would be expected. In order to explain this structure, Evans drew a comparison between decamethylsamarocene and the isomorphous europium analogue [$(C_5Me_5)_2Eu$], concluding that neither simple electrostatic considerations, molecular orbital calculations, steric effects nor electronic configuration predicted the bent structure observed in both complexes.[130-132] The pentamethylcyclopentadienyl rings are planar, and displacement of the methyl groups from the plane of the cyclopentadienyl ring is the same as that observed in the disolvated complex. This unusual bent structure may be attributed to intermolecular interactions and crystal packing, although as Evans notes, these interactions would still be possible with a parallel metallocene structure instead of the bent structure. Evans concludes that the parallel between bent and linear alkaline earth metal dihalide complexes may provide the best explanation for this unusual bent metallocene - polarisation of the metal cation by one anionic ligand may decrease the electrostatic interaction between the metal and a second ligand lying opposite.[66]

Both [$(C_5Me_5)_2Sm(THF)_2$] and [$(C_5Me_5)_2Sm$] show interesting reactivities in the reduction of unsaturated organic substrates,[133-136] the isomerisation of *cis*-stilbene to *trans*-stilbene,[137] and in the activation of small molecules such as N_2 and CO.[133, 138] Evans noted the tendency of these divalent organosamarium complexes to form 2:1

complexes when reacted with unsaturated substrates, in which the substrate is reduced by two electrons.[137, 139-141] This reactivity is demonstrated in the preparation of the first lanthanide dinitrogen complex, $[\{(C_5Me_5)_2Sm\}_2(\mu\text{-}N_2)]$.[142] This was the first reported side-on dinitrogen complex of any metal system, with the dinitrogen bridging between two $\{(C_5Me_5)_2Sm\}^+$ units as shown in Figure 7. The yttrium complex $[\{(C_5Me_5)_2YH\}_2]$ also reduces dinitrogen to make an analogue of the above samarium complex.[143] Interestingly, the reaction of $[(C_5Me_5)_2Sm(THF)_2]$ with acetylene formed a acetylide complex which showed end-on binding in the single crystal structure determined by X-ray diffraction.[139]

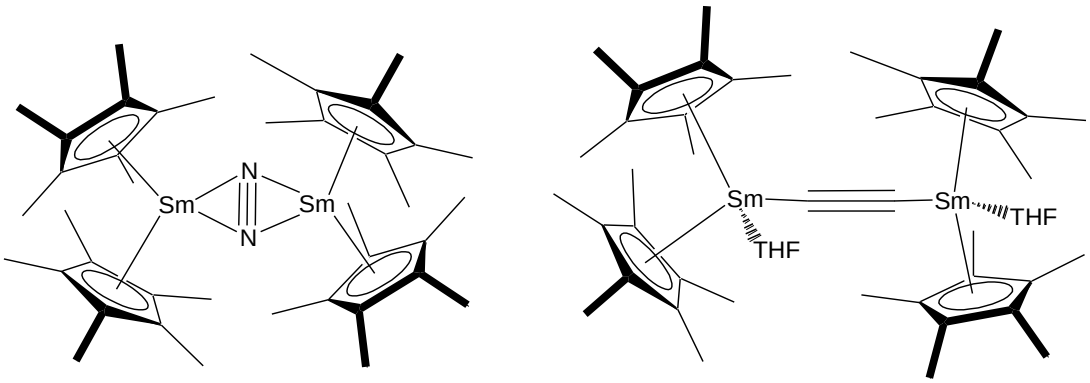

Figure 7: The dinitrogen complex $[\{(C_5Me_5)_2Sm\}_2(\mu\text{-}N_2)]$ and carbine complex $[\{(C_5Me_5)_2Sm(THF)\}_2(\mu\text{-}\eta^1\text{:}\eta^1\text{-}C_2]$.

The bis(pentamethylcyclopentadienyl)lanthanide(II) complexes have led to a number of discoveries; the unusual bent structure of lanthanocenes,[130-132] the isolation of complexes with (or transformations of) alkenes,[134, 137, 145] alkynes,[146-148] hydrocarbons,[149] azobenzene[150, 151] and zintl ions.[152, 153] They have also played a part in

the development of active and unusual CO insertion reactions[154] and catalytic olefin hydrogenations.[141, 155-157]

Whilst exploring the reaction chemistry of decamethylsamarocene with unsaturated hydrocarbons, Evans attempted to prepare a sterically strained bimetallic complex incorporating cyclooctatetraendiyl, $(C_8H_8)^{2-}$, in order to determine whether the ligand would be planar or distorted. Instead the reaction yielded an unexpected mono-cyclopentadienyl samarium cyclooctatetraendiyl product and, surprisingly, the first isolated tris(pentamethylcyclopentadienyl) metal complex (Scheme 2).[158]

Scheme 2: Reaction of $[(C_5Me_5)_2Sm]$ with C_8H_8 to form $[(C_5Me_5)_3Sm]$ and $[(C_5Me_5)Sm(\eta^8\text{-}C_8H_8)]$.

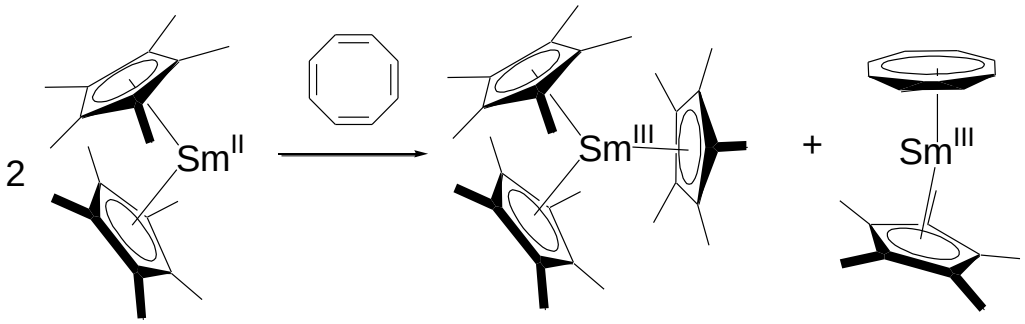

This begged the question of how had a tris(pentamethylcyclopentadienyl) complex formed? It had been widely accepted for a decade that the bulk of the pentamethylcyclopentadienyl groups would only allow only two of the ligands to attach to a metal centre.[159] In both decamethylsamarocene and $[(C_5Me_5)_2Sm(THF)_2]$, the cone angle of a pentamethylcyclopentadienyl ligand to the metal centre is 142 °, depicted in Figure 8. Three ligands with 142° cone angles simply cannot fit around one metal centre. In order to allow the three bulky ligands to fit around the metal centre,

observations showed that the metal-ligand bonds were lengthened and ligand methyl groups displaced, splaying outwards to decrease the cone angle of the ligand to 120°.[158]

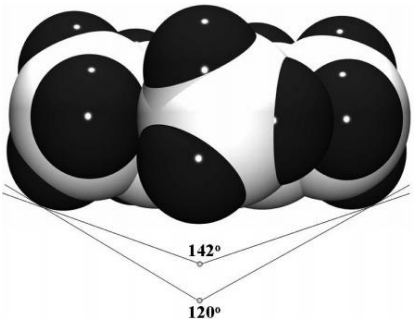

Figure 8: The cone angle of the pentamethylcyclopentadienyl ligand is usually 142°, but is just 120° for $[(C_5Me_5)_3Sm]$, reproduced from literature.[160]

Each of the three pentamethylcyclopentadienyl groups show some level of methyl group displacement, one quite drastically and one with only minor difference to a normal pentamethylcyclopentadienyl ligand (Figure 9). The average Sm–(C_5Me_5) bond length in this complex is 2.82(5) Å, with the longest at 2.910(3) Å is the longest Sm–C bond of any trivalent (C_5Me_5)/Sm system.[161] Strain from the steric saturation combined with the elongated metal-ligand bond could make this group particularly prone to removal.

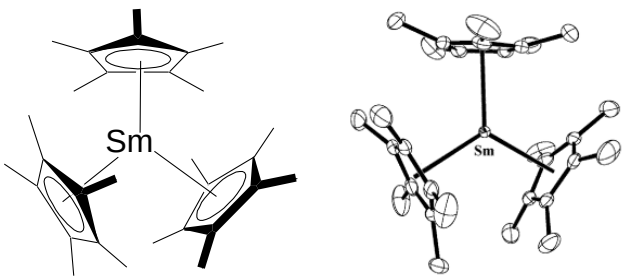

Figure 9: Tris(pentamethylcyclopentadienyl)samarium, showing the splayed methyl groups.[158]

Although sterically saturated, $[(C_5Me_5)_3Sm]$ was found to initiate the polymerisation of ethylene.[162] There is no room for an olefin to approach the sterically saturated metal centre of $[(C_5Me_5)_3Sm]$, which indicated the possible presence of an (η^1-C_5Me_5) intermediate, which would lower the steric strain of the $[(C_5Me_5)_3Sm]$ complex.

This sterically crowded complex was found to be similar to decamethylsamarocene in reductive ability, an unexpected result as a Sm^{3+}/Sm^{4+} redox couple is not known.[7] Evans performed a number of reductions of simple substrates,[163] showing that the products formed were the same whether $[(C_5Me_5)_3Sm]$, $[(C_5Me_5)_2Sm]$ or $[(C_5Me_5)_2Sm(THF)_2]$ were used. A $(C_5Me_5)_2$ dimer by-product was observed whilst Sm^{IV} products were not, leading to the conclusion that this is a ligand-based reduction utilising a $(C_5Me_5)/(C_5Me_5)^-$ redox couple.[163] This opens up the possibility of extending reduction chemistry for other trivalent lanthanides.[164] There have been promising results with a number of different lanthanides showing an unexpected ligand-based reductive ability,[160, 165-167] whilst similar work with uranium opens up the possibility of multi-electron reductions.[162, 168-171] This reactivity is now defined as SIR (Sterically-Induced Reduction), referring to how steric crowding trigger such ligand-based reduction chemistry. This emphasises the importance of tailoring both the metal centre and ligands of a complex to optimise reactivity.

This was not the first case of ligand-based reductions, but was the first instance where the ligand reduction is seen only in very sterically crowded complexes, perhaps linked to the elongated metal-ligand bond and its decreased electrostatic stabilisation.

Heavily substituted cyclopentadienyl-based ligands are still the most common ligands seen in organolanthanide chemistry. The π-binding ligand occupies significant portions of the coordination sphere while providing electrons necessary to stabilise low-valent metal centres. The success of heavily substituted π-bound ligands gives a strong structural principle for the development of non-cyclopentadienyl ligands.

1.3 Non-Cyclopentadienyl Ligands

The monoanionic cyclopentadienyl ligand occupies a relatively large proportion of the coordination sphere. It is an excellent spectator ligand that can be modified through the addition of substituents to tune steric and electronic properties. For a long time organolanthanide chemistry was largely focussed on cyclopentadienyl and aromatic ligands. Alternatives to the ubiquitous cyclopentadienyl ligands, based on alkyl, aryl, alkenyl, alkynyl derivatives and heterocycles were uncommon in organolanthanide chemistry until relatively recently. There are a number of reviews that provide a good background on non-cyclopentadienyl organolanthanide chemistry.[3, 68, 172-176]

The synthesis of simple alkyl or aryl ligated lanthanide complexes is encumbered by the large lanthanide metal ion, which requires a high coordination number to form stable complexes. Alkyl or aryl organolanthanides normally involve ancillary solvent coordination in order to satisfy the coordination number of the lanthanide. In order to form ancillary solvent-free alkyl organolanthanides, a sterically bulky ligand such as tris(trimethylsilyl)methyl is require as demonstrated in the ytterbium(II) complex

$[Yb\{C(SiMe_3)_3\}_2]$, (Figure 10).[177] Anionic methyl lanthanide complexes have been prepared with the chelating ligand tetramethylethylenediamine (tmed).[178, 179]

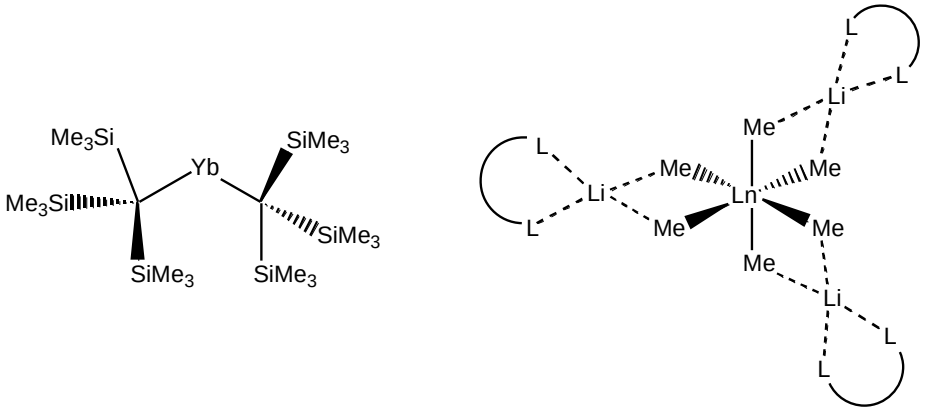

Figure 10: Alkyl organolanthanide complexes, $[Yb\{C(SiMe_3)_3\}_2]$,[177] and $[\{Li(tmed)\}_3Ln(CH_3)_6]$.[178]

Pentadienyl is a common ligand in organometallic chemistry, generally bound η^5 although it can also bind η^3 or η^1. Pentadienyl organolanthanide complexes with η^5 and/or η^3 exist for Yb,[180-182] Sm, [182, 183] Nd, [182, 184, 185] and Lu,[186] shown in Figure 11. Neodymium, lanthanum and yttrium dimethylpentadienyl complexes have been shown to be precatalysts for the polymerisation of butadiene.[36]

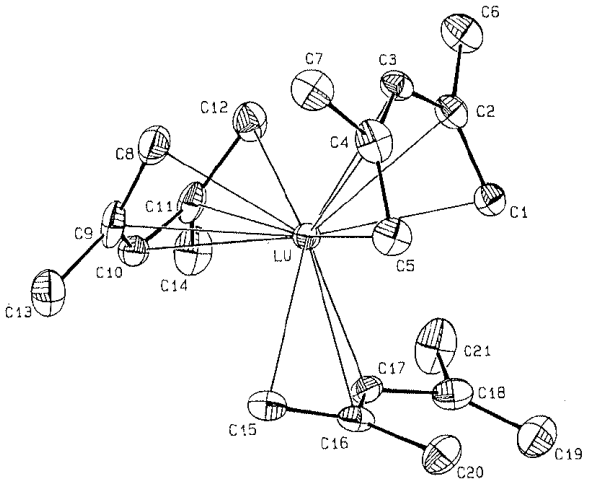

Figure 11: Ortep representation of [Lu(η^3-C_7H_{11})(η^5-C_7H_{11})$_2$] reproduced from literature.[186]

In reacting an aryl-substituted alkene, Evans formed a bimetallic complex containing an η^2-arene lanthanide bond.[137] The first phenyl lanthanides, of the form [$Ph_3Ln(THF)_3$] (Ln = Er, Tb), were formed five years later and were found to have a distorted octahedral shape.[187] A chelating ligand with an additional donor atom can help complete the coordination sphere in lieu of coordinated solvent, as seen in [Lu{*o*-$C_6H_4CH_2N(CH_3)_2$}$_3$].[188] These complexes are shown in Figure 12. Carbenes such as 1,2,4,5-tetramethyl-2-methyleneimidazoline and 1,3-dimethylimidazol-2-ylidene form thermally stable complexes with lanthanides (Figure 13).[21, 176, 189-191]

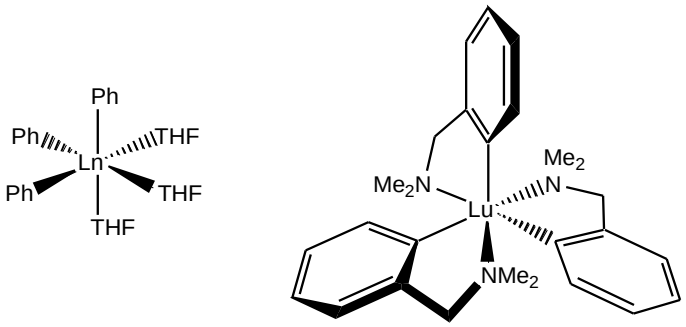

Figure 12: Aryl organolanthanide complexes; $[Ph_3Ln(THF)_3]$, (Ln = Er, Tb) and $[Lu\{o\text{-}C_6H_4CH_2N(CH_3)_2\}_3]$.

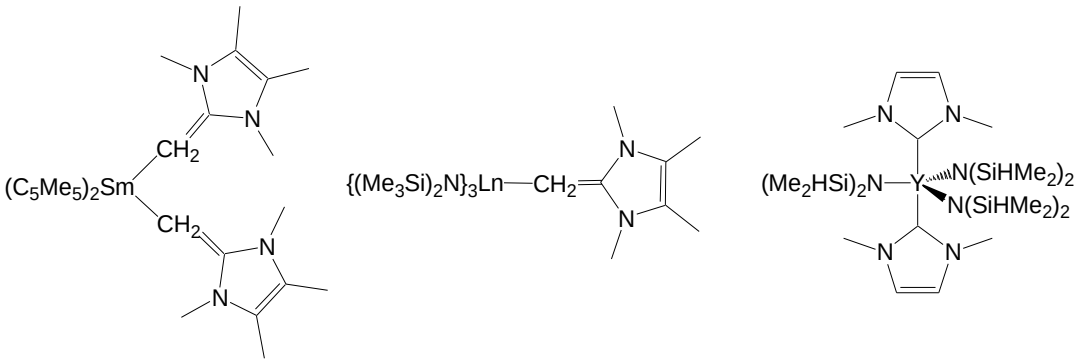

Figure 13: *N*-heterocyclic carbene organolanthanide complexes $[(C_5Me_5)_2Sm$(1,2,4,5-tetramethyl-2-methyleneimidazoline)$]$[176], $[Ln\{N(SiMe_3)_2\}_3$(1,2,4,5-tetramethyl-2-methyleneimidazoline)$]$.[176] and $[Y\{N(SiHMe_2)_2\}_3$(1,3-dimethyllimidazol-2-ylidene$)_2]$.[189]

N-Heterocyclic carbenes have allowed the isolation of unusual complexes such as the neodymium-iron complex seen in Figure 14.[192] This was the first reported complex with an unsupported 4*f*–3*d* metal-metal bond that was stable enough to be isolated. The use of metal-based ligands to form heterometallic metal–metal bonds in *f* element chemistry is a relatively new area, despite the long history of *d*- and *p*-block metal-metal bonded complexes.[68, 193]

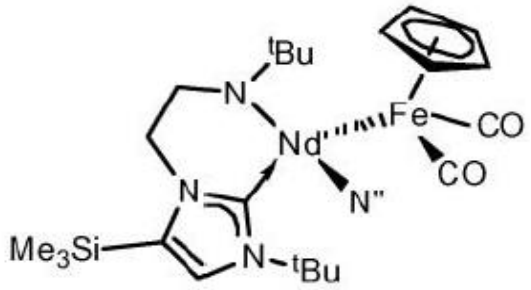

Figure 14: An organoneodymium complex with chelating *N*-heterocyclic carbene and a Nd-Fe bond (from literature).[192]

Phosphorus ligands are well established in organometallic chemistry, and are not uncommon in complexes of *f* elements.[194, 195] Phosphorus-containing heterocycles have similar properties to the ubiquitous cyclopentadienyl ligands, although due to the lower electronegativity of phosphorus relative to nitrogen, they are less likely to σ-bind a metal centre, instead preferring π-binding. Some phosphorus organolanthanide complexes are shown in Figure 15. The reactivity of phospholyl organolanthanide complexes will be discussed in Chapter 3. Phosphorus analogues of indenyl and fluorenyl can σ- or π- bond to form complexes with samarium.[196]

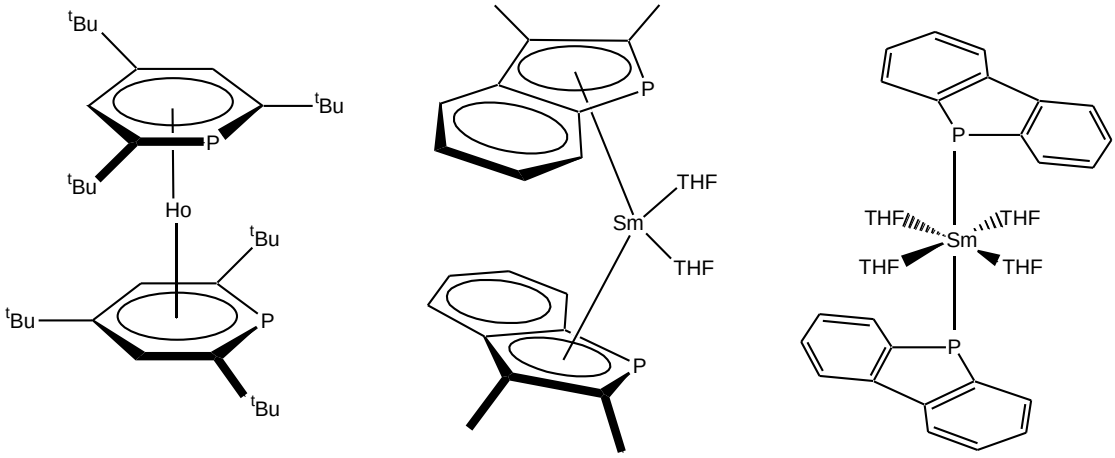

(a) (b) (c)

Figure 15: Phosphorus containing ligands in organolanthanide complexes; (a) [Ho(η-$PC_5H_2tBu_3$-2,4,5)$_2$][197] (b) [bis(η^5-2,3-dimethylphosphindolyl)Sm(THF)$_2$],[196] (c) [bis(η^1-dibenzophospholyl)Sm(THF)$_4$].[196]

f-Block metals are electropositive Lewis acids and thus tend to preferentially bind with hard Lewis bases, making for strong coordination with nitrogen or oxygen.[5] Oxygen donor ligands are common in organolanthanide chemistry,[198-202] as are those containing nitrogen. Diazabutadiene,[203-209] benzylamines[188, 210] and heterocyclic ligands such as pyridyl, pyrrolyl[211] and diphenyldipyrrolide[212] are known (Figure 16). Pyrrolides are discussed further in Chapter 1.4, and pyridyls in Chapter 3.

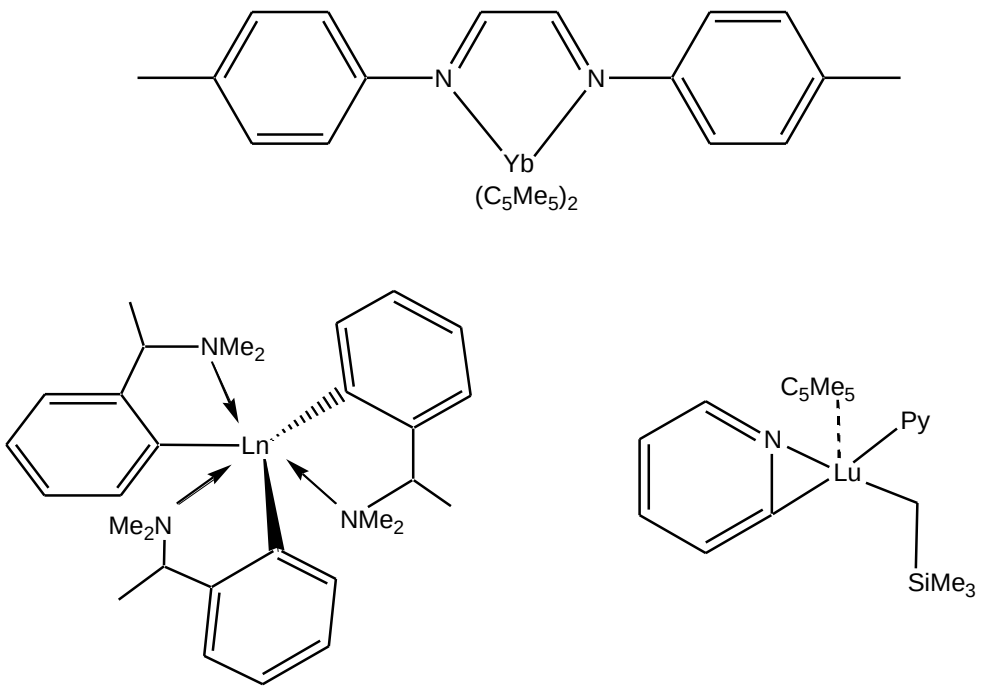

Figure 16: Nitrogen-containing ligands in organolanthanide complexes.[203,210,213]

Like cyclopentadienyl ligands, pyrrolide ligands also have an anionic aromatic 5-membered ring, which can bind η^5 to a metal through its six aromatic π-electrons. In contrast, pyrrolide substituents tend to form σ metal-nitrogen bonds due to the electronegativity of the nitrogen atom with its lone pair of electrons. This preference for σ- over π-binding is dependent on substituents present on the pyrrolide ring.

1.4 Macrocyclic ligands - Calix[4]pyrrolides

Organolanthanide complexes have great potential as highly reactive reagents in synthesis. Samarium diiodide is widely used as a reducing reagent but has limited scope for modification, whereas organometallic samarium(II) analogues allow for numerous

modifications to tailor their reactive properties. Identifying the most appropriate ligands to optimise stability and reactivity is a vital step toward realising new organolanthanides in novel chemistry. Ligands come in many forms, with a range of steric and electronic properties. These include the ubiquitous cyclopentadienyl and pentamethylcyclopentadienyl ligand systems, and less common non-cyclopentadienyl ligands including harder Lewis basic donor centres such as nitrogen, phosphorus or oxygen. Macrocyclic lanthanide complexes have long had roles in biochemistry and extraction but their application in synthetic and redox chemistry is relatively new.[27]

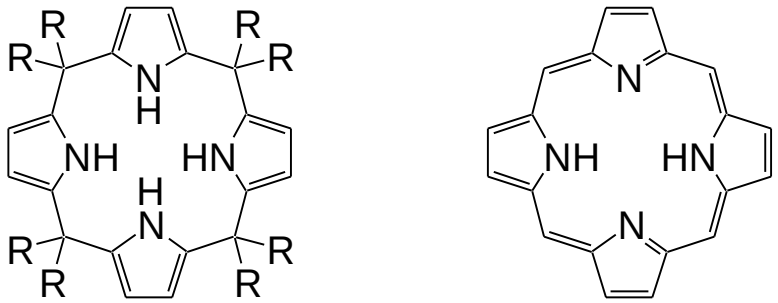

Figure 17: *meso*-Octaalkylporphyrinogen and porphyrin.

Porphyrinogens, as shown in Figure 17, are macrocycles consisting of four pyrroles linked through the 2 and 5 carbons by sp^3 carbons. The *meso*-carbons are sp^3 hybridised, effectively making four linked pyrrole units. This differs from porphyrin which is highly conjugated with resonance throughout the macrocycle and adopts a planar conformation. A porphyrinogen with hydrogens on the *meso*-carbons is easily oxidised to form a porphyrin. Octa-alkyl or -aryl substitution at the *meso*- positions as seen in Figure 17 prevents this conversion. The pyrrole units of porphyrinogens act somewhat independently, increasing the variety of possible macrocyclic conformations.

In the solid state they typically adopt an alternating 1,3-conformation, with pyrrole units orientated in opposite directions.[214]

The tetrapyrrolic macrocycle *meso*-octamethylporphyrinogen was first reported in 1886 by Baeyer. It is prepared by an acid-catalysed condensation of pyrrole and acetone, Scheme 3. Baeyer speculated on its structure, sparking interest from Dennstedt and Zimmerman who also published on the macrocycle in 1887,[215] 1888,[216] and 1890.[217] Decades later Chelintzev and Tronov[218] proposed a structure for the product, calling it 'acetonepyrrole'. Fischer later renamed the product *α,β,γ,δ*-octamethylporphyrinogen in a 1934 book.[219] In 1955 the structure was partially confirmed by Rothemund.[220]

Scheme 3: Condensation reaction to form *meso*-octamethylporphyrinogen (calix[4]pyrrole).

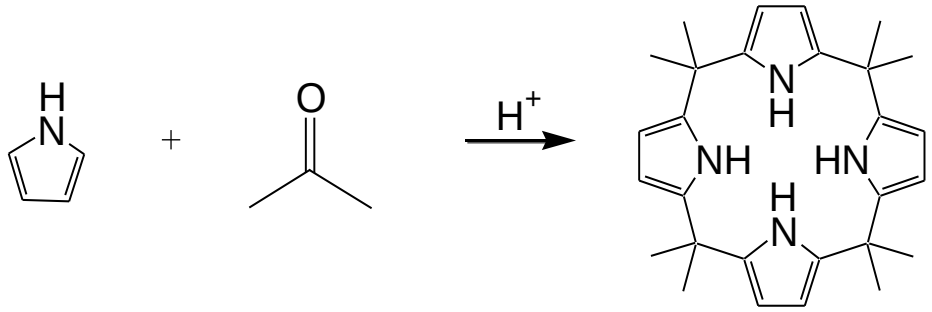

The alternating pyrrole ring structure of *meso*-octamethylporphyinogen was confirmed by Floriani in 1991.[221] Sessler later published on the structure of the octaethyl system[222] and proposed the name calix[4]pyrrole for this class of macrocycle in reference to the structurally-related calixarene systems (Figure 18).[223]

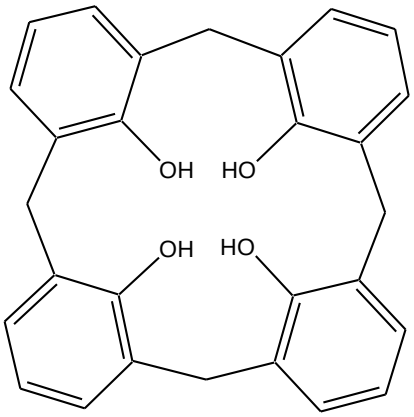

Figure 18: Calix[4]arene.

This class of tetrapyrrolic macrocycle is still commonly referred to as a porphyrinogen. However even this term is somewhat misleading as it is not a precursor to porphyrin. Throughout the rest of this work, for consistency this framework will be referred to as *meso*-octaalkylcalix[4]pyrrole.

Tetrapyrrolic macrocycles have widespread applications across chemistry, biology, medicine and material science.[224] Calix[4]pyrroles can bind anions,[222, 225] neutral substrates,[226] and can be deprotonated and utilised as ligands to form organometallic complexes. Sessler recently referred to the capacity of calixpyrroles as molecular switches, which could act as logic gates for electron transfer reactions, or as precursors or self-assembled materials.[227] A short review by Gale describes the different applications of calix[4]pyrroles.[228] In recent years there has been increasing interest in utilising deprotonated calix[4]pyrroles as flexible non-conjugated macrocyclic ligands for organometallic chemistry.[221]

Each of the pyrrolide units in calix[4]pyrrolide can rotate, giving a large range of possible conformations. Neutral calix[4]pyrrole adopts a 1,3-alternating conformation in the solid state (Figure 19). This conformation is generally retained when binding neutral substrates, whereas a cone conformation is observed in binding anions.[222] In coordination complexes the pyrrolide units of the macrocycle will adapt their conformations to different steric and electronic environments.

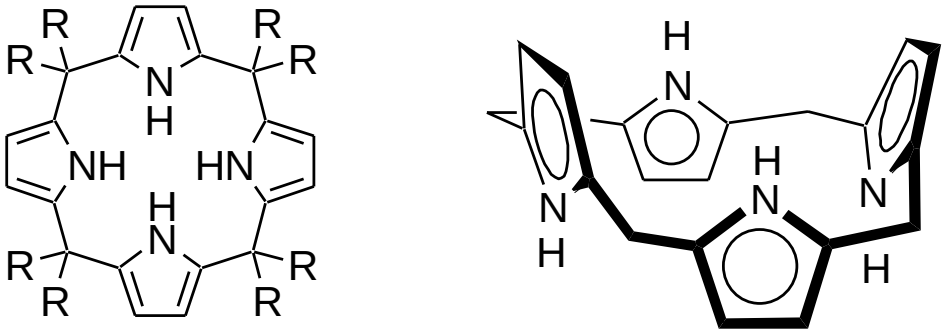

Figure 19: Calix[4]pyrrole, and side-on projection showing the most common 1,3-alternating conformation.

Deprotonation of calix[4]pyrrole gives tetraanionic calix[4]pyrrolide, in which each pyrrolide unit is able to bind η^1, η^3 or η^5 to a metal centre. This is a ligand rich in electrons, able to provide from 8 to 16 electrons to a metal centre depending upon its bonding mode. Metal complexes with *meso*-octamethylcalix[4]pyrrolide were first reported by Floriani in 1991.[221, 229] In some systems the metal is σ-bound between the nitrogens, but other metals adopt a combination of σ and π binding modes.

Transition metal complexes of iron(III), molybdenum(V), zirconium(IV) and nickel(II) with calix[4]pyrrolide (Figure 20) can be prepared by deprotonation using *n*-butyl lithium and a subsequent metathesis reaction.[229-231] Numerous transition metal complexes with the calix[4]pyrrolide ligand are now known.[221, 223, 229, 232-242] Noting that a pyrrolide group bound σ- to the metal centre can also π-bind η^3 or η^5 to a second metal ion, Floriani termed this an acid/base bifunctionality.[230, 231] He demonstrated this by forming complexes of electron-rich nickel(II), in which the metal centre is bound square planar within a flattened octaethylcalix[4]pyrrolide macrocycle. This conformation contrasts with that of a relatively electron-poor zirconium(IV) complex. With no *d* electrons on the zirconium(IV) metal, two pyrrolide groups of the ligand adopt a η^5 binding mode in order to satisfy the coordination sphere of the metal centre.

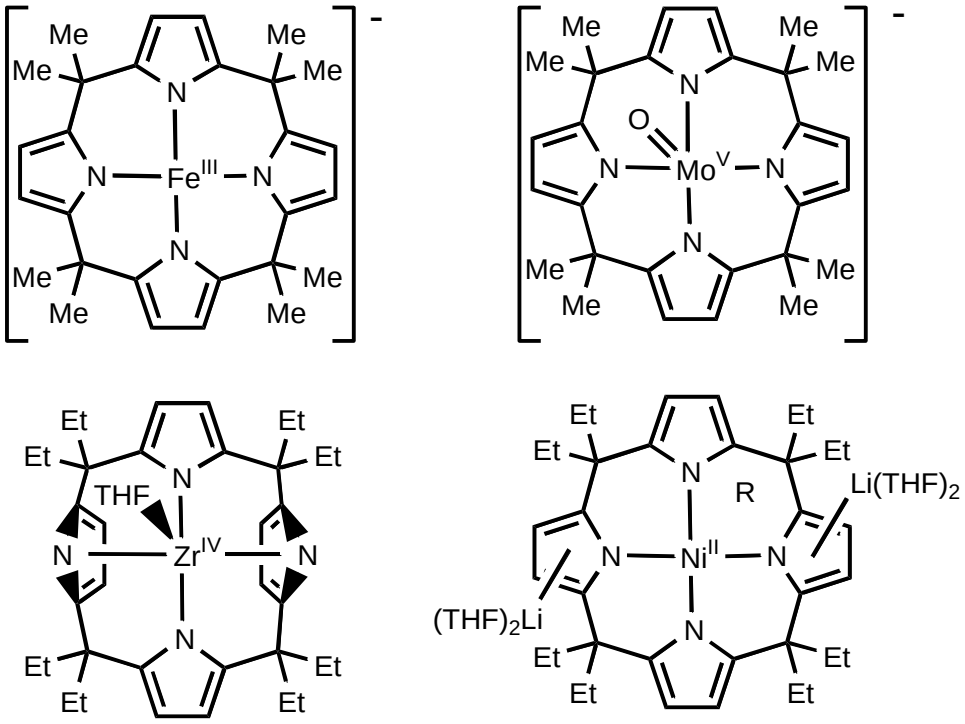

Figure 20: Fe^{III}, Mo^{V}, Zr^{IV} and Ni^{II} *meso*-octaalkylcalix[4]pyrrolide complexes.[229, 230]

The iron(III) is square planar, with the metal centre σ-bound between the four nitrogen centres. The molybdenum(V) complex has an oxo-functionality on the metal centre, giving a slightly puckered macrocycle conformation with the metal sitting above the plane of the four nitrogen centres. In both complexes there is interaction between the Fe centre or the oxo-functionality of the Mo with hydrogens on the *meso*-methyl groups of the macrocycle. In the case of the zirconium complex the macrocycle binds alternately σ- and π- to the metal centre, η^1:η^5:η^1:η^5, with the two π-binding pyrrolyl units tilted to sandwich the metal centre between them.[221] Other complexes formed with calix[4]pyrrole exist for Cu^{II}, Ni^{III} and Pd^{II} as reported by Blangy.[223] Jacoby reported a series of lithium-transition metal complexes which also showed mixed binding modes.[241]

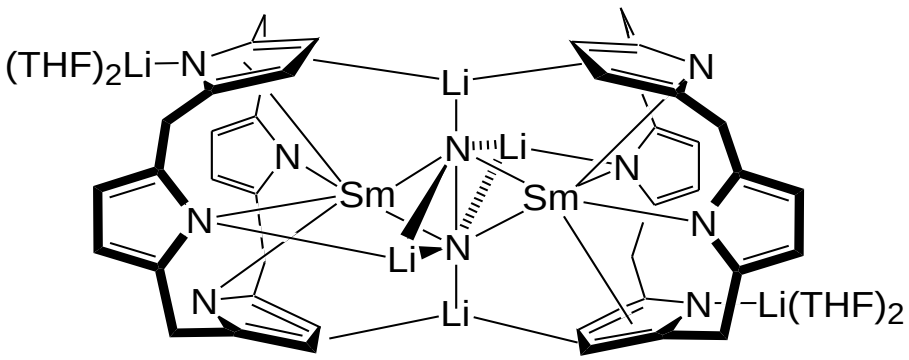

Figure 21: Gambarotta's samarium hydrazide tetralithium salt;
[{$(THF)_2$Li(octaethylcalix[4]pyrrole)Sm}$_2$(N_2Li_4)] (*meso*-octaethyl substituents not shown).[243]

The first lanthanide calix[4]pyrrolide complex was reported by Gambarotta who used *meso*-octaethylcalix[4]pyrrolide to prepare a samarium(II) complex.[243] This complex was found to react with dinitrogen to form a dimeric tetralithium hydrazide salt (Figure

21). Here the macrocycles adopt distorted 1,3-alternating conformations, each binding η^5:η^1:η^1:η^1 to a samarium(III) metal centre. Lithium atoms bridge between the samarium, dinitrogen and macrocycles. The N–N bond length indicates that this is a single bond, consistent with a four electron reduction of dinitrogen. Two of these electrons have been obtained from the coordinated samarium centre, meaning that the remaining two electrons have come from another source.

The first yttrium calix[4]pyrrolide complex was reported shortly thereafter, which contains an ethoxide indicative of THF cleavage *in situ*.[239] Cleavage of THF had been previously observed in the presence of a vanadium calix[4]pyrrolide complex.[233, 244] Further investigation of this process led Gambarotta to suggest that the source of these extra two electrons was in fact the macrocyclic ligand itself. Gambarotta published the first low valent dinuclear samarium complex containing a short Sm–Sm distance shortly thereafter, describing the radical-like character of the samarium(II) and it's reductive ability with regard to dinitrogen.[245]

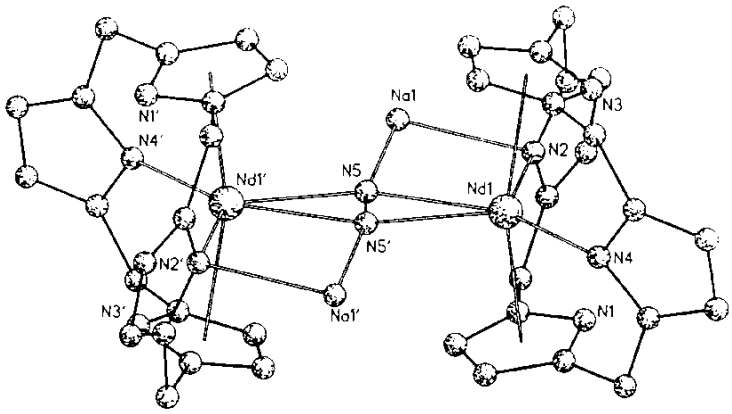

Figure 22: Dinitrogen complex of Nd calix[4]pyrrolide, reproduced from literature.[246]

Other lanthanide complexes using the calix[4]pyrrole scaffold include Floriani's neodymium and praseodymium complexes which were also found to reduce dinitrogen to N_2^{2-}, as shown in Figure 22.[246] Reversible fixation of ethylene on a samarium calix[4]pyrrolide complex was reported one year later by Gambarotta,[247] Floriani further reported the complexation of a range of lanthanide(III) ions by *meso*-octaethylcalix[4]pyrrolide,[248, 249] including acetylene and ethylene bridging complexes.[250] Praseodymium, neodymium, samarium, europium, gadolinium and ytterbium complexes were obtained by reacting the appropriate lanthanide trichloride with a sodium derivative of the macrocycle. Floriani has written about the similarities in behaviour between cyclopentadienyl ligands and the conformationally flexible pyrrolyl moieties in calix[4]pyrrolide macrocyclic ligands.[249]

Deprotonated calix[4]pyrrole has a charge of 4−. In lanthanide(II) or (III) complexes this high negative charge on the ligand is often balanced by the inclusion of more than one metal centre, or the presence of counter-cations. The presence of alkali metals

and/or counter cations can be problematic for further reaction, but can be avoided by making changes to the macrocyclic structure.

There are a number of steric and electronic modifications that can be made to the calix[4]pyrrole macrocycle. The addition of substituents and/or modifying the structure of the macrocycle can affect the binding mode, conformation and charge of the ligand, and can be used to prevent the inclusion of undesired alkali metals. These modifications can be made by changing the *meso*-carbon substituents or by adding substituents to the pyrrolide units, either on the nitrogen (*N*-rim) or the back of the pyrrolide (*C*-rim), as shown in Figure 23. Changing the *meso*-substituents on the sp^3 carbons or adding substituents to the *C*-rim or *N*-rim open a large variety of modifications to the basic calix[4]pyrrolic macrocycle.

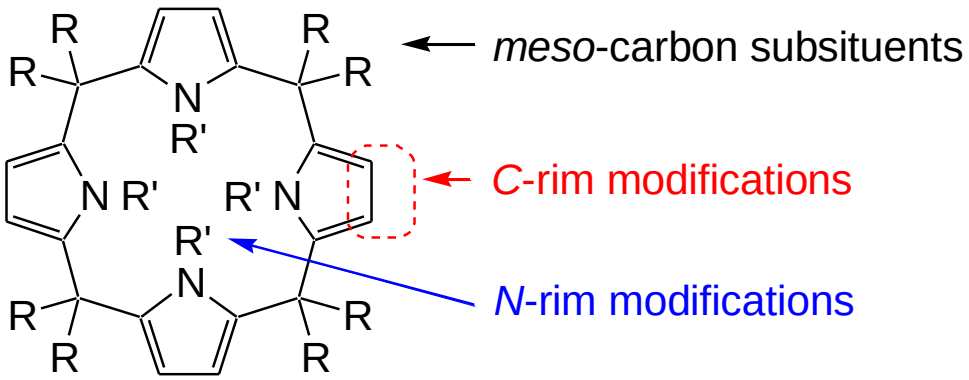

Figure 23: Calix[4]pyrrole showing *N*-rim, *C*-rim and *meso*-carbon sites open to modification.

More drastic changes to the macrocycle can be made by changing the number of pyrrole units in the macrocycle,[251] or by modifying the type of units that make up the macrocycle. For example one or more pyrrole groups can be substituted for a pyridine,

phenol, arene or other cyclic group. There have been a number of reports into these modifications and functionalisations of calix[4]pyrroles, and the resulting changes to the properties of the macrocycle.[252]

Meso-substituents point away from the macrocycle and are unlikely to impede on metal binding in the cavity. *Meso*-substitution prevents the porphyrinogen from converting to a porphyrin. The substituents of the sp^3 *meso*-carbons of a calix[4]pyrrole are determined by the ketone used in the synthesis of the macrocycle. The simplest of these are acetone or 3-pentanone, which yield methyl or ethyl *meso*-substituents. One of the earliest of these modifications reported is the *meso*-cyclohexylcalix[4]pyrrole (tetraspirocyclohexylcalix[4]pyrrole) (Figure 24).[253] There are some examples where the substituents are not distributed evenly, or where not every *meso* carbon has two substituents (Figure 25). Using 'pre-strapped' diketones in the macrocycle synthesis produces strapped calix[4]pyrroles.[254] Including the strap imposes restrictions on the shape of the macrocycle, forming cryptand-like structures.[255, 256]

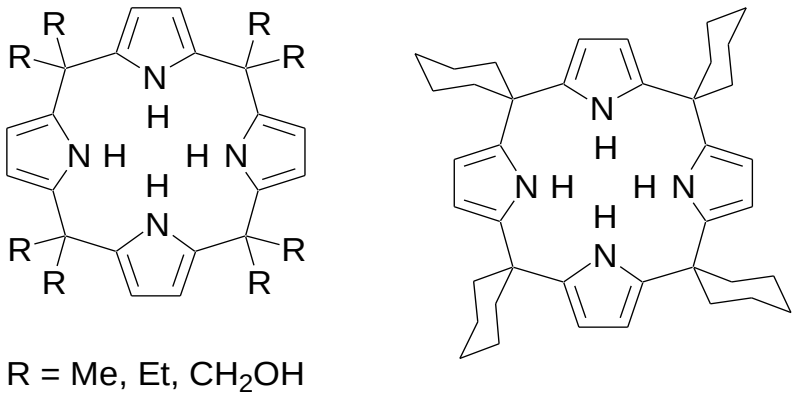

Figure 24: *meso*-Octaalkylcalix[4]pyrrole and tetraspirocyclohexylcalix[4]pyrrole.

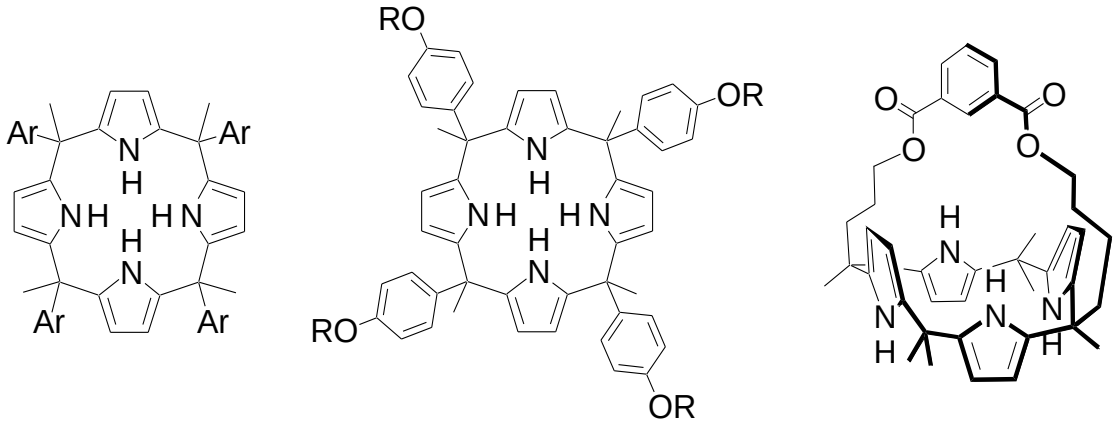

Figure 25: Unevenly distributed *meso*-substituted macrocycles.

Substituents on the carbons of the pyrrolide ring (the *C*-rim) have a greater effect on metal binding than the *meso*-substituents. Substituents on the pyrrolide ring can have steric effects on the macrocyclic cavity, the location and angle of the pyrrolide units in complexes as well as changing the electronic properties of the macrocycle.

Gale and Sessler reported the syntheses of *C*-rim substituted calix[4]pyrroles with the aim of investigating their comparative anion-binding strength.[257] Utilising 3,4-disubstituted pyrroles and ketones to directly prepare a substituted product was successful in producing a *β*-octamethoxy-*meso*-tetraspirocyclohexylcalix[4]pyrrole. Direct modification of *meso*-octamethylcalix[4]pyrrole by electrophilic attack was also achieved, yielding mono- and di-substituted ester products. A *β*-octabromo-*meso*-octamethylcalix[4]pyrrole was prepared by reacting with *N*-bromosuccinimide. Later Sessler utilised the metal-mediated Sonogashira coupling reaction to introduce aryl/alkynyl functionality, (Figure 26).[258]

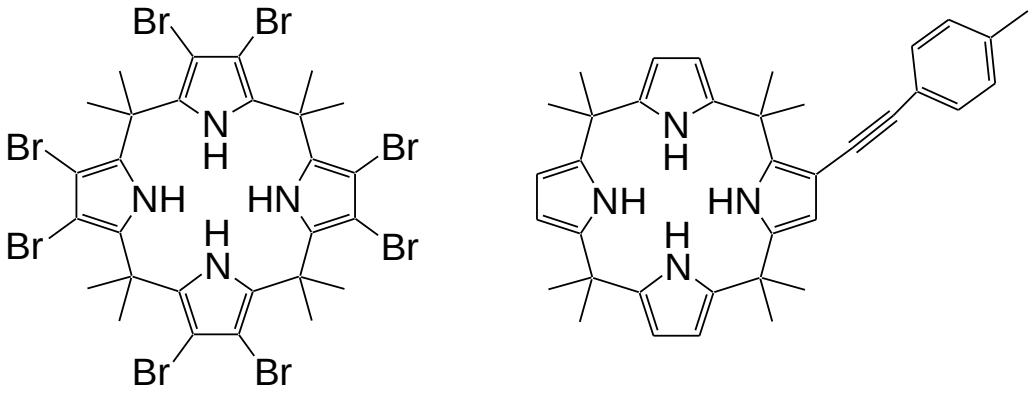

Figure 26: *β*-Octabromo-*meso*-octamethylcalix[4]pyrrole and arylalkynyl-*meso*-octamethylcalix[4]pyrrole.

N-substituents have great steric influence on the macrocyclic cavity. An *N*-substituent occupies a nitrogen site, lowering the charge of the overall complex, making the ligand more suitable for the stabilisation of low-valent metals as counter cations are no longer required to balance the charge. Figure 27 shows two *N*-substituted macrocycles; a strapped calix[4]pyrrole,[259] and an *N*-tetramethylated calix[4]pyrrole.[260]

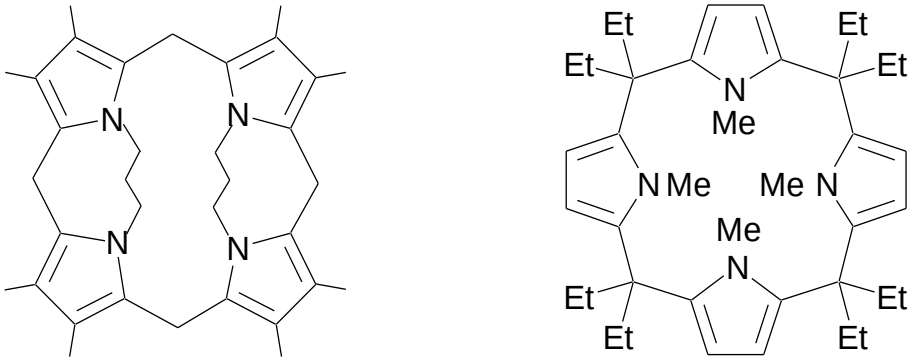

Figure 27: A strapped porphyrinogen, and *N*,*N*',*N*'',*N*'''-tetramethyl-octaethylcalix[4]pyrrole.

1.5 *trans*-*N*,*N*'-Dimethyl-*meso*-octaethylcalix[4]pyrrolide $(Et_8N_4Me_2)^{2-}$

Takata reported in 1998 that reacting *meso*-octaethylcalix[4]pyrrole with NaH and MeI in the presence of 18-crown-6 produced *N*-methylated products (see Scheme 4).[261] The main products of this reaction are *N*-methyl, *cis*- and *trans*-*N*,*N*'-dimethyl, *N*,*N*',*N*''-trimethylated and the tetramethylated calix[4]pyrroles.

Scheme 4: Synthesis of *trans*-*N*,*N*'-dimethyl-*meso*-octaethylcalix[4]pyrrolide.

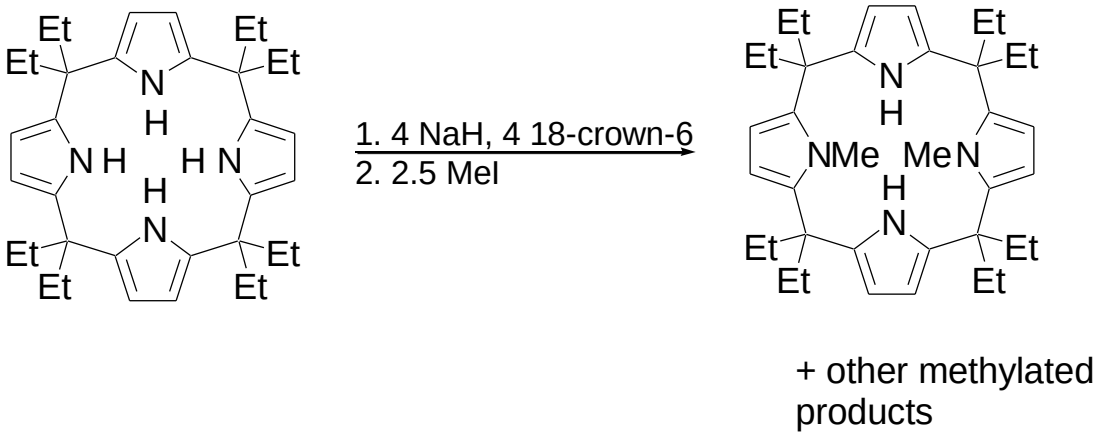

The *N*-methylation occurs at one or more nitrogens, with the ratio of products unevenly distributed. Both *cis*- and *trans*- dimethylation products were observed with the *trans*-product favoured. The products can be separated by flash chromatography.

The ligand *trans*-*N*,*N*'-dimethyl-*meso*-octaethylcalix[4]pyrrolide, $(Et_8N_4Me_2)^{2-}$, has similar (adaptable) binding modes to *meso*-octaalkylcalix[4]pyrrolide. The *N*-

methylation of two opposite pyrrolide groups restricts the flexibility of the macrocycle and reduces the charge of the deprotonated ligand. The deprotonated *trans-N,N'*-dimethyl macrocycle is an interesting ligand, with a rigid conformation and overall anionic charge well suited to form neutral complexes with samarium(II).

In *trans-N,N'*-dimethyl-*meso*-octaethylcalix[4]pyrrolide the methylation of two opposite nitrogen centres blocks one face of the macrocyclic cavity of the dianionic ligand, leaving a binding cavity with one open face. Figure 28 shows a spacefilling structure depicting both the blocked and open faces of the cavity.

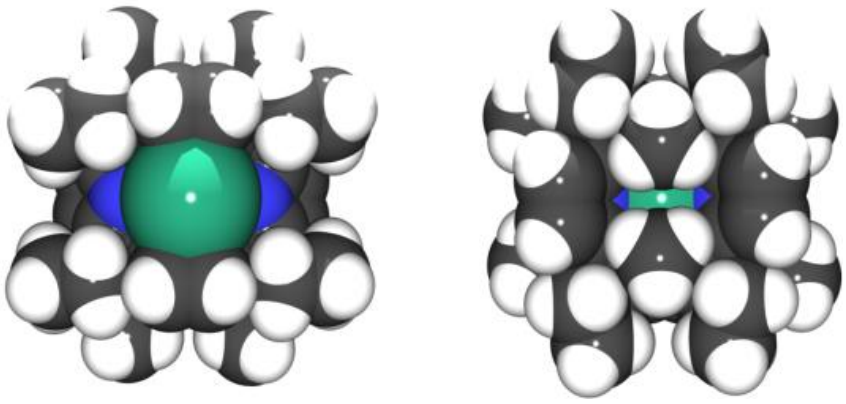

Figure 28: Space filling view of *N,N'*-dimethyl-*meso*-octaethylcalix[4]pyrrolide samarium(II) complex with two THF maolecules removed, view of the macrocyclic cavity from above (left) and below (right).

The rigidity of this ligand creates a controlled coordination environment supporting a $\eta^1:\eta^5:\eta^1:\eta^5$ binding mode to a large metal centre, with the *N*-methylated pyrrolides coordinating η^5 to the metal, whilst the remaining two pyrrolides are free to bind σ to the metal centre as shown in Figure 29.

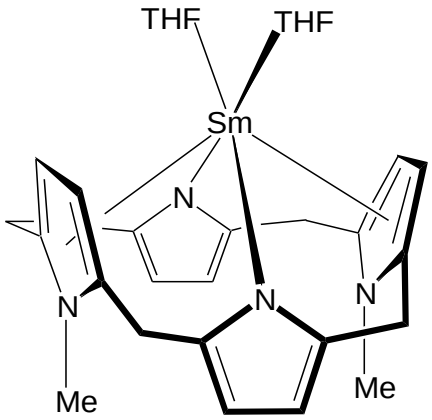

Figure 29: Structure of $[(Et_8N_4Me_2)Sm(THF)_2]$, showing the $\eta^1{:}\eta^5{:}\eta^1{:}\eta^5$ binding mode.

This macrocycle is dianionic when deprotonated, unlike the tetranionic calix[4]pyrrolide. The lower charge on the ligand better suits a low valent metal centre, reducing cation inclusion in metal complex products. This modified ligand can stabilise a metal centre with its high coordination number and low anionicity, whilst the conformation still allows the metal centre to bind a limited number of ancillary ligands.

Using the rigid macrocyclic ligand $(Et_8N_4Me_2)^{2-}$ led to good structural control of *s*- and *f*-block metals in complexes[262, 263] which has led both to novel reactivity[264] as well as increased stabilisation[265] of reactive metal centres. This *N*-methylated ligand has already yielded a number of interesting and novel results in organosamarium complexes, including unusual steric strain,[266] CO_3^{2-} complexes,[267] an end-on dinitrogen complex[268] and a reversible Sm^{II}/Sm^{III} redox reaction.[264] Where relevant, complexes of this rigid macrocyclic ligand $(Et_8N_4Me_2)^{2-}$ will be referred to for comparison throughout this work.

1.6 *meso*-Octamethylcalix[2]phenylene[2]pyrrolide $(Me_8N_2Ph_2)^{2-}$

The macrocycles mentioned above are all based on a calix[4]pyrrole system. Changing the units of the macrocycle, for example substituting furan in place of pyrrole, or adding additional units, reveals further information about the resulting metal complexes and their binding.

Replacing two opposing pyrrolide groups with furanyl rings (Figure 30) yields a macrocyclic ligand with two nitrogen and two oxygen atoms which can bind to a metal centre.[263] Samarium(II) complexes of this ligand were shown to be generally bimetallic, with the Lewis base donor oxygens binding samarium on one face of the macrocycle whilst the anionic nitrogen centres bind alkali metals on the opposite face.

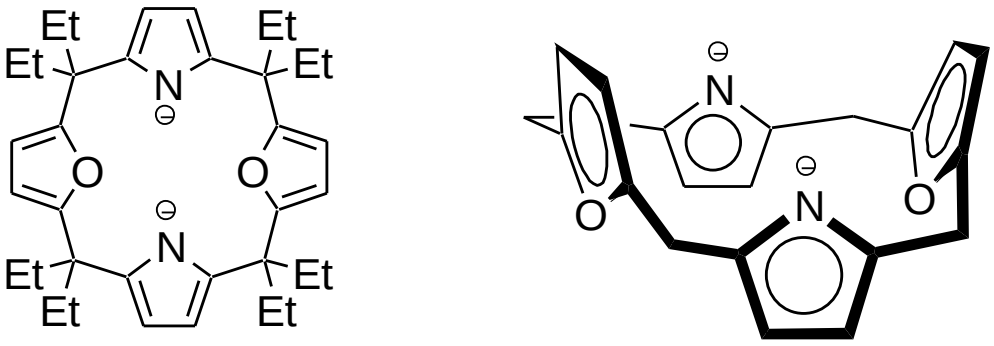

Figure 30: *trans*-Dioxa-*meso*-octaethylcalix[4]pyrrole.[263]

A hybrid macrocycle containing phosphole and thiophene reported by Matano is pictured in Figure 31.[269] This was the first reported calixpyrrole containing a phosphole, following on from calix[4]arene derivatives containing phosphorus functionalities.

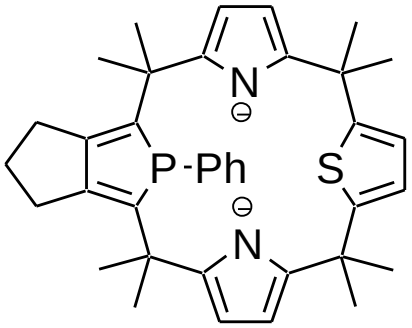

Figure 31: Calix[1]phosphole[1]thiophene[2]pyrrolide.

Calix[4]arene organometallic chemistry is well established, utilising π-bonding to stabilise metal centres.[270-276] When deprotonated, the pyrrolide groups in calix[4]pyrroles can bind either π or σ (via the nitrogen) to a metal.[229, 277, 278] A number of researchers have reported substituting different unit types such as pyridine or arenes in place of one or more pyrrole groups of calix[4]pyrrole.[214, 254, 272, 279-281] A ligand containing both arene and pyrrolide groups may have interesting properties utilising one or both types of bonding.

The flexibility of this ligand type opens up a range of possible uses. A ligand that can both stabilise low valent *f* elements and allow a metal centre enough room to be utilised in reactivity is certainly a desirable target. A calix[2]phenylene[2]pyrrolide ligand is the subject of investigation throughout this thesis, and will be introduced in Chapter 2.

1.7 Novel Lanthanide(II) and Reduction Chemistry

Organolanthanide chemistry generally involves lanthanides in their most common 3+ oxidation state.[32, 282, 283] For many years it was assumed that only samarium, europium and ytterbium were accessible in the 2+ oxidation state.[88, 284] Europium and ytterbium metals are soluble in liquid ammonia,[285, 286] leading to their use in the first divalent organolanthanide complexes. These divalent lanthanides had multiple applications, most commonly in aqueous redox chemistry.[287]

Divalent organosamarium complexes were developed later using metal vapour synthesis.[128] It had been thought that the larger and more reactive samarium metal would be more difficult to stabilise with steric saturation, hence the much later synthesis of divalent samarium complexes.[288] The development of $SmI_2(THF)_x$ in 1980[88, 89] was the starting point for the development of more easily synthesised samarium(II) complexes.[289] It was not until the turn of the century that, other divalent lanthanides including lanthanum,[290, 291] thulium,[8, 73, 74, 292-294] dysprosium[8, 74, 295] and neodymium[74, 296, 297] were isolated and found to be stable in solution for limited periods of time.

These Lewis acidic divalent complexes are very reactive and powerful reducing agents, able to reduce dinitrogen at room temperature and atmospheric pressure.[298, 299] The strong reducing nature of the more reactive divalent lanthanides means they have great potential as useful reagents in synthesis,[97, 284, 300, 301] however it also limits the practicality of utilising lanthanide(II) complexes in industrial-scale reactions.

Bochkarev noted unusual behaviour of NdI_2 and DyI_2 in THF solution when in the presence of aromatic hydrocarbons. The THF solutions appear stable for up to 24 hours, but if even a small amount of aromatic hydrocarbon such as benzene or toluene are present the diiodide will cleave the THF solvent.[302]

The more recently isolated lanthanide(II) metals are highly reducing ($E°$ of Tm = −2.3 V; Dy = −2.6 V; Nd −2.6 V) therefore the preparation of stable divalent organometallic complexes will rely on appropriate ligands. Lanthanide(II) compounds prepared by alkali metal reduction of $(C_5H_5)_3La^{III}$ indicate that even these highly reducing lanthanides can still be accessible ($E°$ of La = −3.1 V).[291]

The isolation of strongly reducing divalent lanthanides as stable reactive complexes is important as they have many potential applications.[24, 291, 303-305] The challenge lies in stabilising these reactive lanthanide(II) metals with appropriate ligands, and also having the reaction conditions and solvents tailored to limit undesired reactions or competition between ligands and solvent molecules.

1.8 General Research Aims

This work will use modified calix[4]pyrrolides as ligands to synthesise novel lanthanide complexes. The reactivity of resulting novel samarium complexes will be explored with a series of heterocycles.

Europium complexes will be synthesised and their structural characteristics compared with analogous samarium complexes. This comparison with a europium(II) complex may be useful for gleaning information where the oxidation state of a samarium metal centre is unclear given the very similar ionic radii of Eu^{II} and Sm^{II}. An unambiguously samarium(III) complex will be prepared to extend this comparison between lanthanide(II) and lanthanide(III) complexes of the modified macrocyclic ligand.

.

Chapter 2

Calix[2]phenylene[2]pyrrolide Metal Complexes

2.1 Introduction

Meso-octamethylcalix[2]phenylene[2]pyrrole ($Me_8N_2Ph_2H_2$), **1**, is a macrocycle incorporating alternating phenylene and pyrrole groups (Figure 32). It was first synthesised by Sessler[272] as one of a series of hybrid heterocalix[4]arene analogues including pyrrole, benzene, methoxy-substituted benzene and pyridine subunits. Condensation of pyrrole and bis-carbinol forms the macrocycle which adopts a 1,3 alternating conformation similar to the *N*,*N'*-dimethylated calix[4]pyrrole mentioned in Chapter 1.

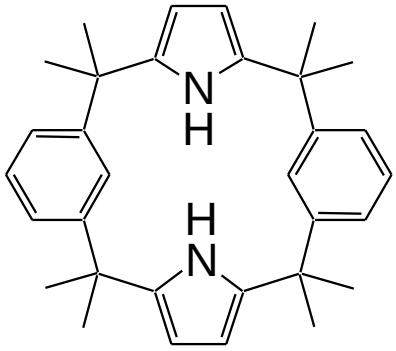

1

Figure 32: *meso*-Octamethyl-*trans*-calix[2]phenylene[2]pyrrole, **1**.

The solid state structure of **1** obtained by single crystal X-ray diffraction can be seen in Figure 33, alongside the structure of the macrocycle with a CH_2Cl_2 molecule included in the macrocyclic cavity. The structure of **1** is slightly twisted, with the pyrrole groups

oriented at different angles. Protons in the C2 position of the phenylene point in opposite directions to the pyrrolide NH protons, analogous to calix[4]pyrrole.

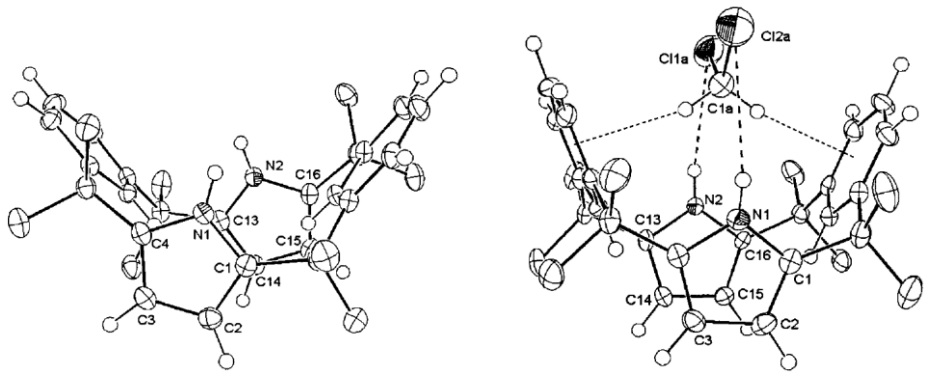

Figure 33: Molecular structure of calix[2]phenylene[2]pyrrole and a second structure with CH_2Cl_2 bound within the macrocyclic cavity, reproduced from literature.[272]

When coordinating to CH_2Cl_2, the macrocycle draws inwards with the phenylenes lying 'steeper' (closer to being parallel) and the macrocycle adopting a more symmetrical shape. The CH_2Cl_2 σ-binds the pyrrolide nitrogens and π-binds to the phenylene groups to sit within the macrocyclic cavity. This η^6:η^1:η^6:η^1 binding and the related conformation of the macrocycle will be seen again later in this Chapter.

Temperature-dependant ^{1}H NMR and NOESY spectroscopy indicated that a slightly flattened 1,3-alternating conformation of *trans*-calix[2]phenylene[2]pyrrole exists in solution at low temperature (188 K).[272] At room temperature it is believed that the macrocycle shows 'breathing' motions between the flattened and regular 1,3-alternating conformations as shown in (Figure 34), although the authors could not rule out rapid conversion between 1,3-alternating and a flattened partial cone conformation.

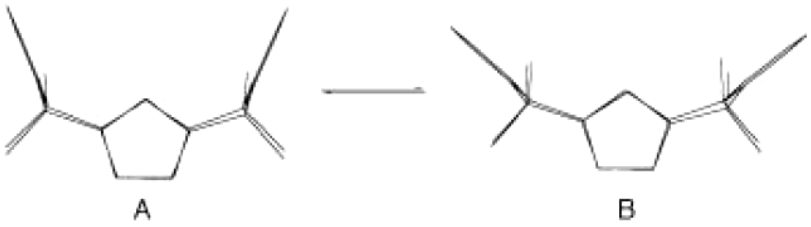

Figure 34: The 'breathing' motion of **1** believed to occur in solution.[272]

The two pyrrolide nitrogens can be deprotonated to yield the dianionic macrocycle *meso*-octamethyl-*trans*-calix[2]phenylene[2]pyrrolide, $(Me_8N_2Ph_2)^{2-}$, (Figure 35). Like calix[4]pyrrolide complexes reviewed in Chapter 1, the pyrrolide groups of this $(Me_8N_2Ph_2)^{2-}$ ligand may adopt σ- or π- binding to a metal centre. In the case of $(Me_2N_2Ph_2)^{2-}$ π-bonding may also be seen between the phenylene groups and the metal centre. This added flexibility in binding makes the ligand adaptable to metals with different sizes and electronic characteristics. This is also a dianionic ligand, which compared with the tetranionic calix[4]pyrrolide is better suited to form cation-free complexes with low valent lanthanide(II) metal centres. Some samarium complexes of this ligand have been reported by Gambarotta[306] and Frey,[307] and will be discussed further in Section 2.2 and Chapter 3.

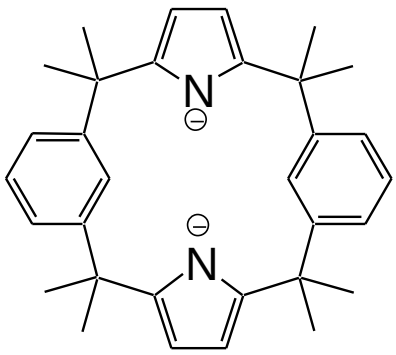

Figure 35: Deprotonated *meso*-octamethyl-*trans*-calix[2]phenylene[2]pyrrolide, $(Me_8N_2Ph_2)^{2-}$.

Numerous samarium macrocyclic complexes appear in this thesis, many featuring ancillary ligands that are non-innocent regarding redox activity. The oxidation state of samarium in these complexes is sometimes unclear. Colour can be a useful indicator of oxidation state, as for most lanthanides there is a distinct colour change between the Ln^{II} and Ln^{III} states.[140] It is not, however, a definitive measure of oxidation state, which is also affected by other factors. In cases where a ligand has been reduced this can be seen through characteristic bond distances. A mono-adduct complex may be neutral Ln^{2+}–L^{0} or the radical anion Ln^{3+}–$L^{\bullet-}$. Theoretical work by James utilised computational methods to investigate the oxidation state of Sm in complexes of the *trans-N,N´*-dimethyloctaethylcalix[4]pyrrolide ligand.[268] He found that the samarium metal centre can exist in an oxidation state between samarium(II) and samarium(III), which will be discussed further throughout this thesis.

Structural characteristics and binding modes are likely to differ between lanthanide(II) and lanthanide(III) macrocyclic complexes due to changes in metal ion size. Bond lengths between the metal and ligand can be compared with those in known lanthanide(II) or lanthanide(III) complexes where the coordination number is the same. With this in mind, europium(II) analogues of selected complexes were prepared, featuring various mono- and bis- ancillary ligands, along with an unambiguous samarium(III) chloride complex. This allowed for structural comparisons to be made between complexes of unknown oxidation state and these known lanthanide(II) and lanthanide(III) complexes.

Research Aim

The synthesis and characterisation of complexes of the macrocyclic ligand $(Me_8N_2Ph_2)^{2-}$ are the subject of this Chapter. Group 1 metal complexes are investigated with the aim of identifying an improved synthetic method for the preparation of samarium complexes, with the desired target of a synthetic method that reduces or removes the formation of *N*-confused macrocyclic products.

Lanthanide complexes prepared from a lithium precursor complex will be reacted with different coordinating solvents with the aim of determining which solvent molecules will coordinate to the metal and whether the bonding model conformation of the macrocyclic ligand is affected. Comparisons will be drawn between related lanthanide complexes, with a focus on the binding geometry of the macrocyclic ligand in different coordinating environments.

The binding mode of europium complexes is to be evaluated with comparison to analogous samarium complexes. The lanthanide metal europium is well established to be very stable in the 2+ oxidation state, and has a similar metallic radius to samarium(II). Any differences in macrocyclic binding between analogous samarium and europium complexes will be noted. A complex that is unambiguously samarium(III) is a desired target in this Chapter. The preparation and characterisation of a Sm^{III} complex will provide a good benchmark of the macrocyclic binding conformation for comparison of a Ln^{III} with known Ln^{II} examples, if these differ.

2.2 Results and Discussion

2.2.1 Group 1 Metal Salts with the *trans*-Calix[2]phenylene[2]pyrrolide Macrocyclic Ligand

The condensation reaction between pyrrole and bis-carbinol to form *trans*-calix[2]phenylene[2]pyrrole (**1**) was first reported by Sessler.[272] In this synthesis a stoichiometric amount of $BF_3 \cdot OEt_2$ is stirred with the reactants for one hour, quenched with aqueous NaOH, extracted with ethyl acetate and separated chromatographically before the crude product is recrystallised from ethanol to yield the desired macrocycle.

A modification by Frey replaces equimolar $BF_3.OEt_2$ with 0.5 mol % scandium triflate catalyst (Scheme 5).[307] Scandium trifluromethanesulfonate is an active Lewis acid catalyst.[14, 308-314] The reaction takes place over 7 days without stirring, with product forming as colourless crystals. Whilst this is a longer reaction time and results in a slightly lower yield (9% vs 16%), the convenience of a one-step reaction makes this a favourable preparation method. This modified synthesis was used in this work to prepare *trans*-calix[2]phenylene[2]pyrrole, $Me_8N_2Ph_2H_2$ (**1**).

Scheme 5: Synthesis of $Me_8N_2Ph_2H_2$ (**1**) in a $Sc(OTf)_3$ catalysed condensation reaction.

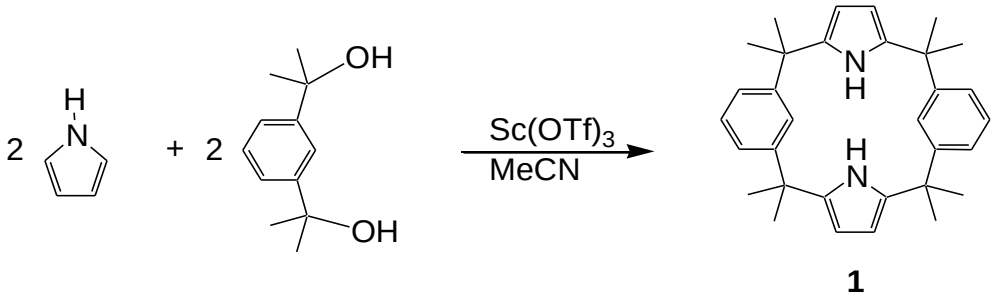

1

Analysis by ^{1}H and ^{13}C NMR spectroscopy confirmed the product was the desired *meso*-octamethyl-*trans*-calix[2]phenylene[2]pyrrole (**1**) (9 % crude yield). Vacuum sublimation of the product (1.5 hrs at 220 °C / 1 x 10^{-3} mmHg) separated colourless crystals of (**1**) from a trace amount of uncharacterised dark brown liquid.

Deprotonation of the $Me_8N_2Ph_2H_2$ macrocycle (**1**) was achieved by Frey using potassium metal to form the potassium complex $[(Me_8N_2Ph_2)K_2(THF)]$.[307] Potassium was added to a THF/PhMe solution of **1** and stirred at 70 °C for 24 – 72 hours under argon, as seen in Scheme 6. The potassium complex is insoluble in toluene, hexanes and benzene, and only slightly soluble in THF. Determination of the number of THF molecules in this structure by ^{1}H NMR spectroscopy proved inconclusive, with results varying from ⅔– 2 molecules per macrocycle. A single crystal suitable for X-ray diffraction was obtained by heating a solution of $[(Me_8N_2Ph_2)K_2(THF)]$ in toluene to form the THF-free complex $[\{(Me_8N_2Ph_2)K_2.⅔(PhMe)\}_n]$. The structure of contains the potassium metal centres bound within each face of the macrocyclic cavity, which makes a polymeric structure with low solubility in organic solvents. The insolubility of both of

the THF-inclusive and THF-free potassium complexes may indicate that this polymeric structure exists in both cases.

Scheme 6: Preparation of $[Me_8N_2Ph_2K_2(THF)]$ and $[(Me_8N_2Ph_2)K_2]_n.⅔(PhMe)$. *Meso*-methyl groups omitted for clarity.

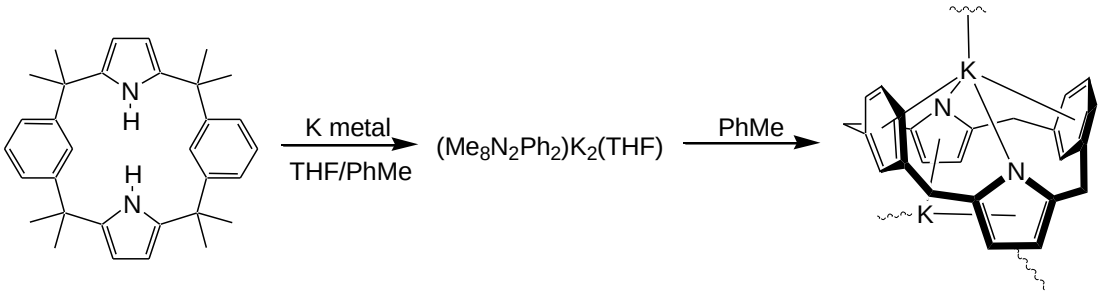

1

Addition of 2 equivalents of *n*-butyl lithium to calix[2]phenylene[2]pyrrole, (**1**), in hexane solution immediately yielded a white powder. This product was isolated, dried *in vacuo* and dissolved in THF to form a clear solution. Reducing the volume of solvent under reduced pressure gave colourless crystals of $[(Me_8N_2Ph_2)Li_2(THF)_4]$, **2**, as shown in Scheme 7.

Scheme 7: Deprotonation of 1 using *n*BuLi to form $[(Me_8N_2Ph_2)Li_2(THF)_4]$, **2**.

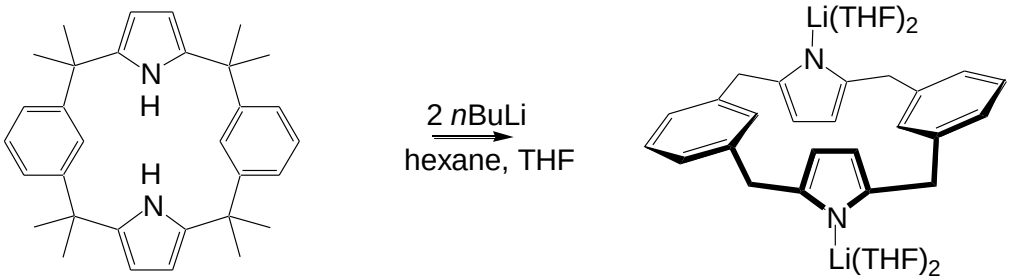

1 **2**

The dilithiated complex (**2**) is insoluble in hexane, slightly soluble in benzene and soluble in THF. Characterisation by ^{1}H NMR spectroscopy of **2** was carried out in C_6D_6. Variable temperature studies were not undertaken as this product is not a main focus of this study.

A single methyl resonance at 1.57 ppm is assigned to the *meso*-methyl protons, indicating that the eight *meso*-methyl groups are fluxional and equivalent in solution. This most likely involves either a ring-flip or cleavage and re-coordination of the lithium cations. Three overlapping resonances in the 6 — 8 ppm region are attributed to the protons on the pyrrolide and phenylene rings. A solid state structure obtained by X-ray crystallography (below) shows inequivalent protons on the methyl and pyrrolide groups, but the presence of single resonances for the methyl and pyrrolide hydrogens in the NMR spectrum support a fluxional structure with ring conformational changes in solution.

Colourless block crystals of $[(Me_8N_2Ph_2)Li_2(THF)_4]$ (**2**) suitable for single crystal X-ray diffraction were obtained from the diffusion of hexane into a THF solution of **2** over 48 hrs. The crystals belong to the monoclinic space group *P*2/*n* (No. 11) with a = 10.668(2), b = 15.302(2), c = 12.976(2) Å, β = 90.335(6) °. The asymmetric unit consists of half of one macrocyclic unit of crystallographic centrosymmetry, with two molecules in the unit cell. The solid state structure of **2** is shown in Figure 36.

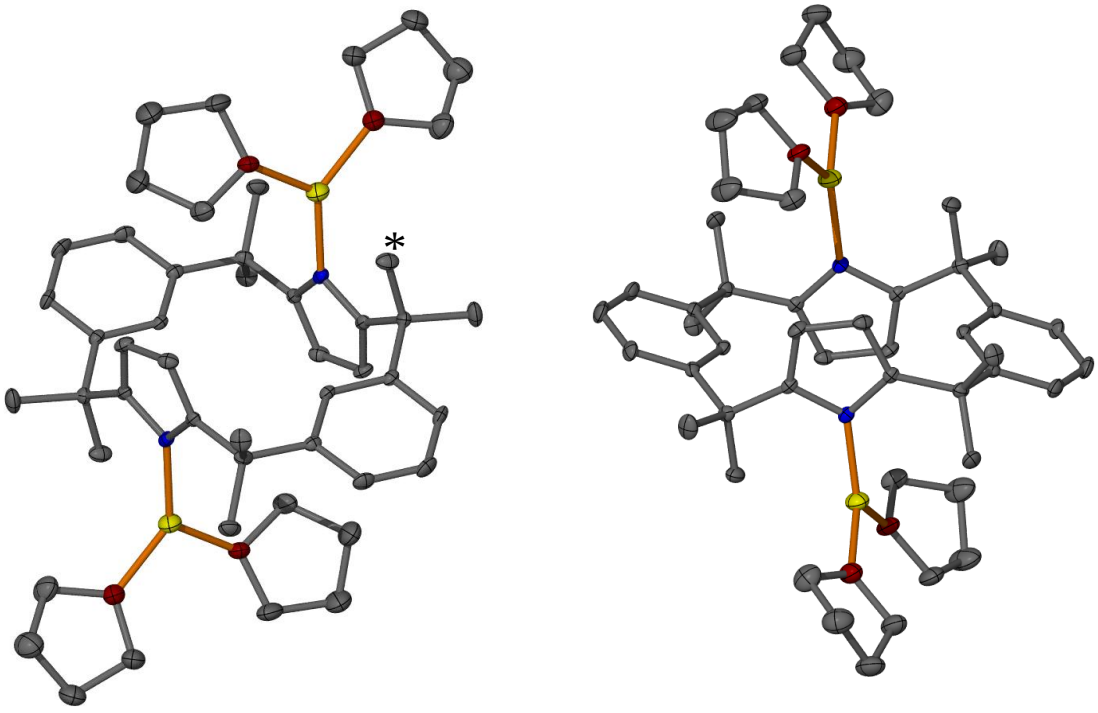

Figure 36: Molecular structure of $[(Me_8N_2Ph_2)Li_2(THF)_4]$, (**2**), with thermal ellipsoids at 50% probability (protons omitted for clarity). Views (a) and (b) show the complex from two different angles. The carbon to which a weak agostic Li...H–C interaction exists is marked with *****.

The solid state structure of **2** has a doubly flattened partial cone conformation. The pyrrolide groups lie antiparallel to each other, with the nitrogens of each group oriented in opposite directions. The phenylene groups splay outwards, laying parallel with no interaction with lithium or THF molecules. The two lithium centres each σ-bind to the nitrogen of a pyrrolide group, and to the oxygen atoms of two THF molecules in a distorted trigonal planar geometry. *meso*-Methyl groups on the macrocyclic framework sit close enough to allow weak agostic interactions between lithium and the closest C–H, as close as 2.06 Å.

The potassium complexes [{($Me_8N_2Ph_2$)K_2(⅔PhMe)}$_n$] and [($Me_8N_2Ph_2$)K_2(THF)] obtained by Frey have an 1,3-alternating double cone conformation similar to calix[2]phenylene[2]pyrrolide, (**1**), as shown in Figure 37.[315] The location and binding of one of the potassium atoms in the macrocyclic cavity between the phenylene moeties has strong similarity to the calix[2]phenylene[2]pyrrolide bound to DCM seen earlier in Figure 33. The potassium centre bound in the phenylene-face of the ligand is bound η^6:η^1:η^6:η^1 to the macrocycle, whilst the potassium at the opposite face is η^5-bound between the pyrrolide moeities, bridging to bind to the pyrrolide backbone of an adjacent complex.

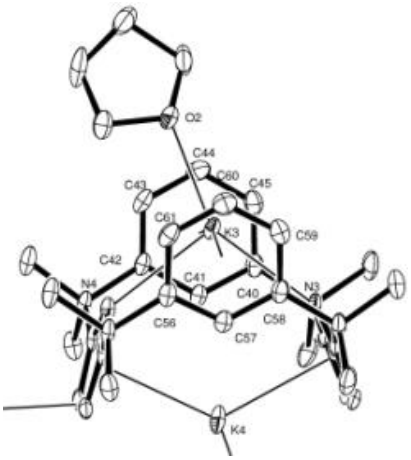

Figure 37: Single crystal solid state structure of [{($Me_8N_2Ph_2$)K_2(THF)}$_n$].[315]

The potassium metal centre within the macrocyclic cavity is large enough for the macrocycle to retain the 1,3-alternate conformation seen earlier in $Me_8N_2Ph_2H_2$ (**1**) and $Me_8N_2Ph_2H_2$**.**CH_2Cl_2. This contrasts with the lithiated complex **2**, where two of the smaller lithium metal centres are required to form a stable complex, with the macrocycle adopting a significantly different conformation, with the pyrrolide moieties

binding σ- to lithium and no π-binding is observed. The polymeric structure of the potassium complex results in a greatly lowered solubility which prevented characterisation by NMR spectroscopy.

As noted in Chapter 1, metal centres binding to pyrrolides are normally observed σ-bound to the electronegative nitrogen atom. A pyrrolide with bulky substituents at the 2 and 5 positions, such as 2,5-di(*t*-butyl)pyrrolide, can force the pyrrolide to adopt η^5 π-binding to a metal centre as seen in Figure 38.[316-318] Due to its small size, lithium can still bind η^1 despite the steric influence of the large *t*-butyl groups Figure 38.[319] Short bond lengths for Li–O and Li–N are present in [{2,5-di(*t*-butyl)pyrrolide}Li(THF)$_2$].[319]

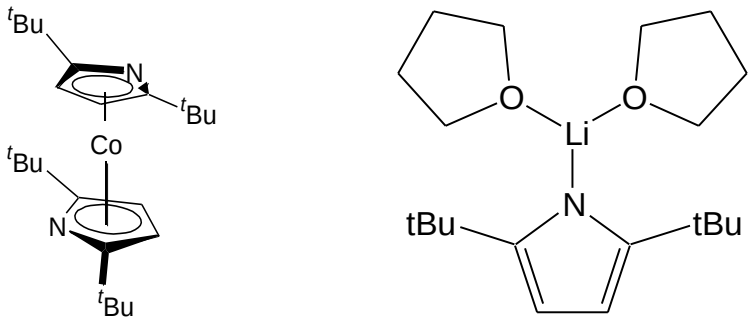

Figure 38: [{2,5-di(*t*-butyl)pyrrolide}$_2$Co],[316] and [{2,5-di(*t*-butyl)pyrrolide}Li(THF)$_2$].[319]

The mixed lithium/aluminium complex [Li(C_4Me_4N)$AlMe_2$)$_2$(μ-Cl)] (Figure 39) features π-binding due to the aluminium centres outcompeting lithium to σ-bind the pyrrolide nitrogen atom.[320] In this case a lithium metal centre is sandwiched between two linked pyrrolide units.

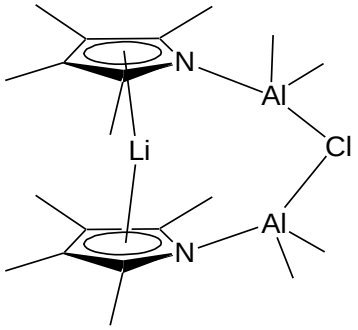

Figure 39: The lithium/aluminium complex [Li{(C_4Me_4N)$AlMe_2$}$_2$(μ-Cl)].[320]

Gambarrota's [{(octaethylcalix[4]pyrrole)Li_4}(t-BuLi)$_2$], Figure 40, contains both η^1 and η^5 Li–pyrrolide interactions.[321] Four lithium atoms η^5-bind to the four pyrrolyl rings of the distorted macrocycle. The μ^3 carbanionic centre establishes a triangular array of three lithium centres that sit directly over each face of the macrocycle.

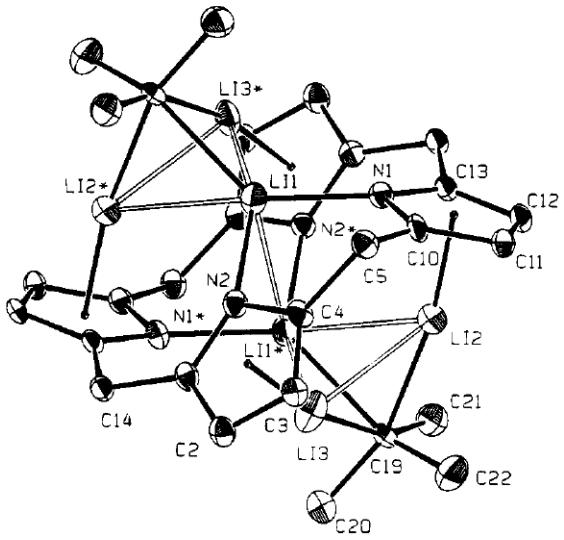

Figure 40: [{(octaethylcalix[4]pyrrole)Li_4}(tBuLi)$_2$], reproduced from literature.[321]

A further example of a lithiated macrocycle containing different Li–pyrrolide interactions is the tetralithiated octaethylcalix[4]pyrrolide, Figure 41.[322] Originally this complex was isolated with four coordinated THF molecules, drying *in vacuo* or by

recrystallising from toluene causes the loss of one THF. A central lithium is σ-bound to the four pyrrolic nitrogen atoms. The remaining three lithium atoms each bind η^2 to a pyrrole ring, σ- to the nitrogen of an adjacent pyrrole, and to one THF molecule.

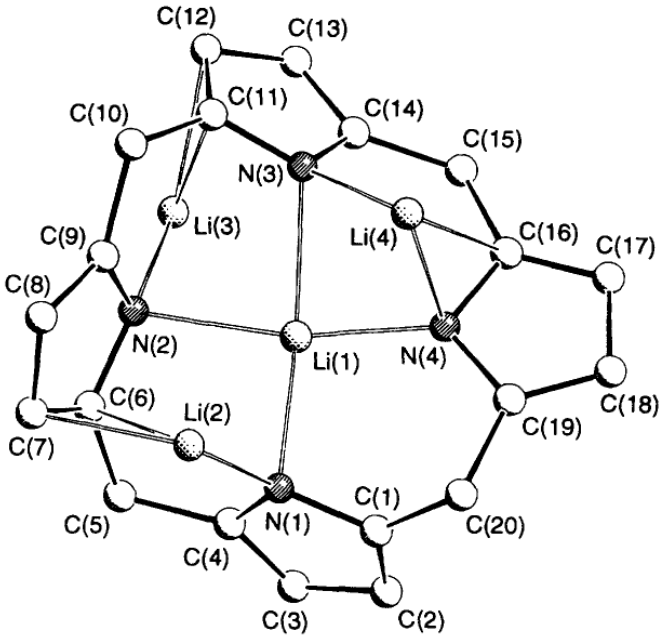

Figure 41: Tetralithiated tris(THF)octaethylcalix[4]pyrrolide (hydrogens, *meso*-ethyl groups and THF molecules omitted for clarity) reproduced from literature.[322]

In dilithium transition metal complexes of the octaethylcalix[4]pyrrolide ligand each lithium is bound to two THF molecules and one pyrrolide group, as seen in Figure 42.[241] In these cases the lithium is π-bound η^3 to the pyrrolide groups, differing from the σ-binding seen in the trigonal planar lithium in the 2,5-di(*t*-butyl)pyrrolide earlier (Figure 39).

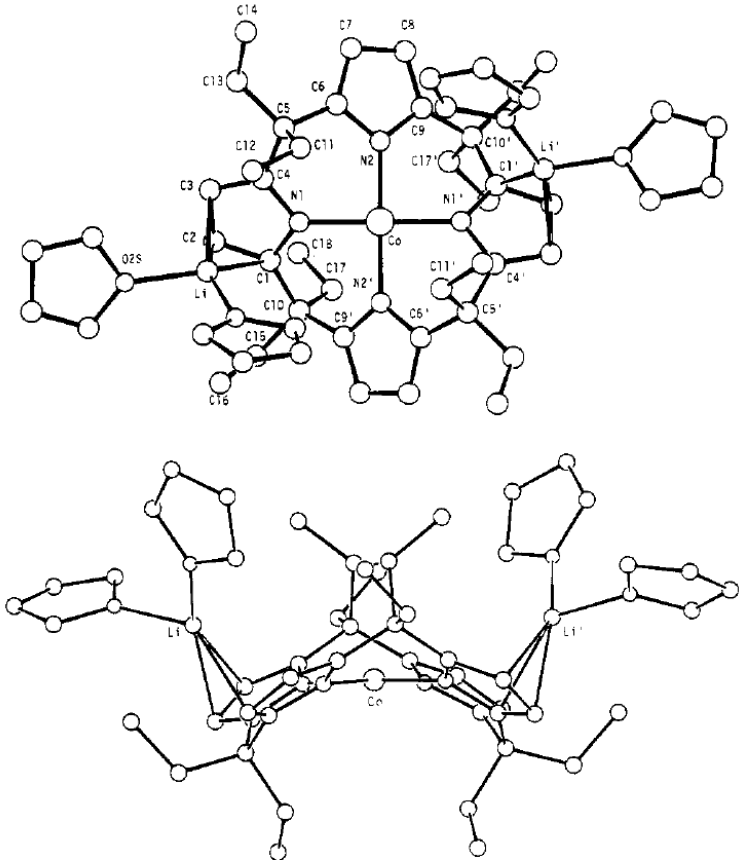

Figure 42: Molecular structure of $[Li_2Co(Et_8N_4)THF_4]$, reproduced from literature.[241]

2.2.2 Lanthanide Calix[2]phenylene[2]pyrrolide Complexes

The salt metathesis reaction of $[(Me_8N_2Ph_2)Li_2(THF)_4]$ (**2**) with samarium diiodide in THF yields $[(Me_8N_2Ph_2)Sm(THF)_2]$, (**3**) as dark purple crystals. Complex **3** is slightly soluble in THF and only sparingly soluble in benzene. Recrystallisation of **3** from benzene or toluene yields the mono(THF) complex $[(Me_8N_2Ph_2)Sm(THF)]$, (**4**), as seen

in Scheme 8. Complex **4** is a purple crystalline product, visually indistinguishable from the bis(THF) complex.

Scheme 8: Metathesis of the precursor **2** to Sm^{II} complexes **3** and **4** (methyl groups omitted).

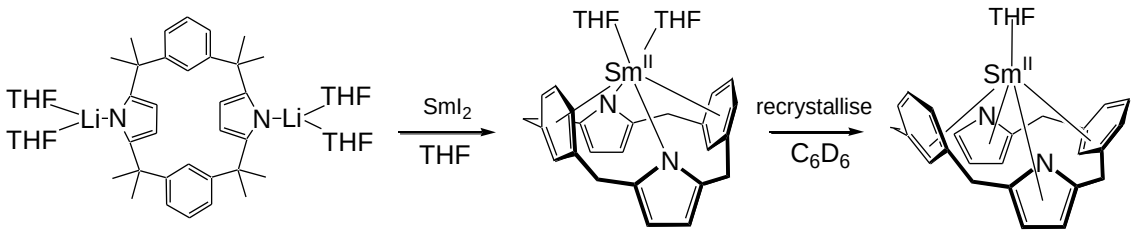

2 3 4

Frey noted that an *N*-confused product (Figure 43) was also formed in the room temperature metathesis reaction of $[(Me_8N_2Ph_2)K_2(THF)_n]$ with SmI_2 in THF, despite the reactants ($Me_8N_2Ph_2H_2$) and potassium products being free of *N*-confused complexes.[307] Gambarotta has also reported *N*-confused products from a lithiated calix[4]pyrrolide precursor.[323]

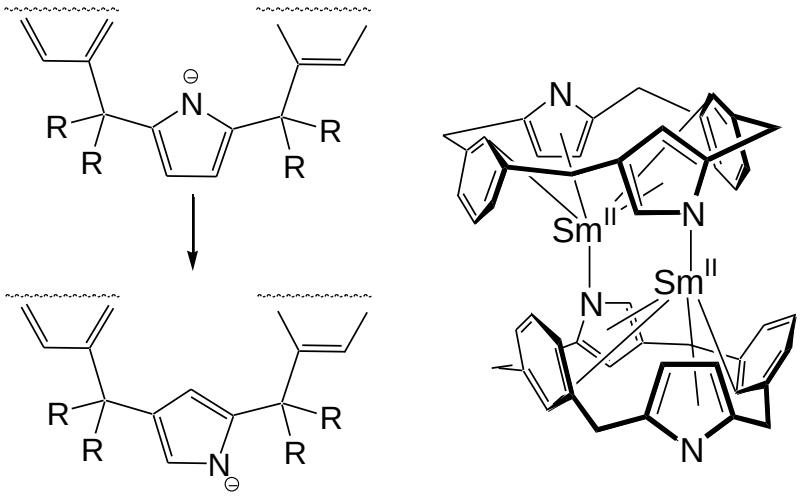

Figure 43: *N*-confused complexes.

Samarium complexes **3** and **4** formed from the lithiated precursor **2** in this work do not appear to include noticeable amounts of *N*-confused macrocyclic product. Only one *N*-confused complex was observed in this work: a non-reproducible low-yielding europium(II) example which was identified by X-ray crystallography.

This drastically lowered incidence of *N*-confused products in lanthanide complexes formed from the lithium precursor **2** opened the way for wider reactivity studies with the $(Me_8N_2Ph_2)^{2-}$ ligand which were not possible in previous work using the potassium precursor.

The bis- and mono-THF complexes **3** and **4** were characterised by ^{1}H NMR spectroscopy. Low solubility in deuterated solvents prevented useful characterisation by ^{13}C or 2D NMR spectra, despite numerous attempts and long data collection times. As introduced in Chapter 1, the presence of paramagnetic samarium causes shifting and broadening of resonances, which can limit the usefulness of NMR spectroscopy in the characterisation of lanthanide complexes.[324] As noted in Section 1.1 (Figure 1) samarium(II) is more paramagnetic than samarium(III), with magnetic moments of 3.6 and 1.7 μ_B, respectively. Therefore NMR spectroscopic characterisation is likely to be more challenging when a samarium(II) metal centre is present. This work contains both samarium(II) and samarium(III) chemistry, and NMR spectroscopy has been attempted and assignments made where possible.

There are clear and distinct resonances in the chemical shift range between −13 and 11 ppm in the ^{1}H NMR spectra of **3** and **4**, along with a dramatically shifted broad resonance at approximately 120 ppm. The ^{1}H NMR spectrum of the mono-THF complex **4**, seen in Figure 44.

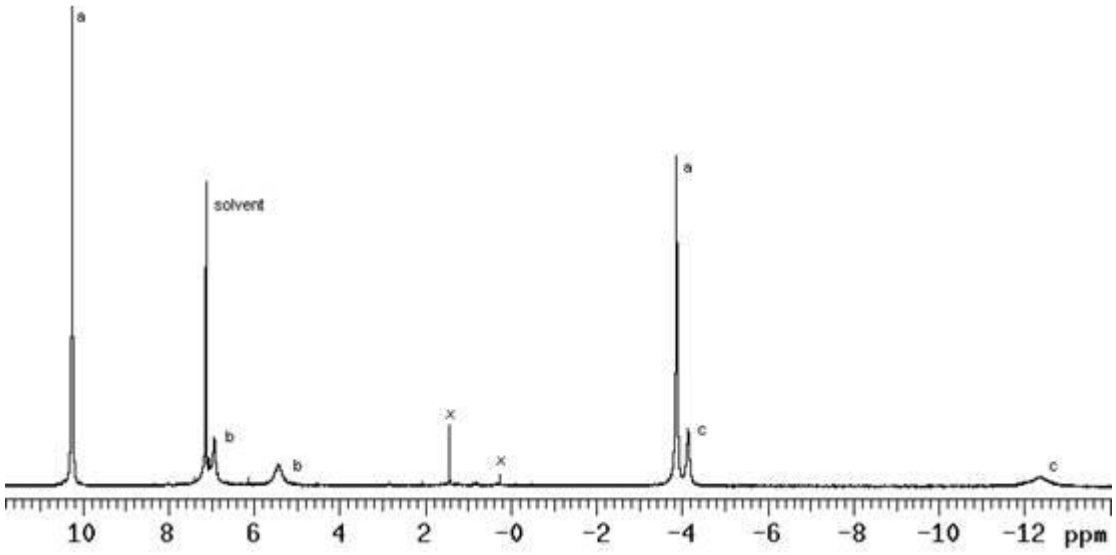

Figure 44: ^{1}H NMR spectrum of $[(N_2Ph_2)Sm(THF)]$, (**4**), (C_6D_6, 299.91 MHz, 298 K, ppm) (a. *meso*-CH_3 protons, b. aromatic protons, c. THF protons, x = impurity, broad resonance at 120 ppm not shown).

Single resonances at 10.29 and −3.83 ppm were attributed to the *meso*-methyl groups, which face either toward or away from the samarium metal centre in this conformation, giving two distinctly shifted singlets. Two resonances at −4.10 and −12.33 ppm are due to the THF hydrogens. A singlet at 5.47 ppm is due to the four pyrrolide protons (CH). Singlet resonances observed at 7.16 and 6.97 ppm were attributed to six phenylene CH protons. The remaining phenylene proton, C(1)H, is in close proximity to the samarium

metal centre and, as a result, has been shifted far downfield; it was observed as a broad resonance at 120 ppm. This could not be confirmed with 2D NMR spectroscopy, presumably due to the proximity of the paramagnetic metal. Previous work on this complex by Frey did not observe this resonance, likely because of its location far downfield from the rest of the resonances.

The ^{1}H NMR spectrum of the bis(THF) complex **3** is similar to that of **4**, indicating that it exists as the mono-THF complex in solution, with rapid THF exchange. The preparation of mono(THF) complex is indeed achieved by recrystallising bis(THF) from benzene, lending support to the complex being mono-solvated when in solution.

The major difference between the two NMR spectra are the THF resonances, which are observed at −4.48 and −1.42 ppm in the bis-solvated complex and at −3.87 and −11.68 ppm for the mono(THF). The strong similarity of the bis- and mono-THF NMR spectra indicate that the bis(THF) complex exists as mono-THF when in benzene solution, indicting rapid THF exchange. With the exception of the newly-identified broad resonance downfield at 120 ppm, these ^{1}H NMR spectra are consistent with those reported by Frey.[307]

The solid state structures of complexes **3** and **4**, obtained from the lithiated precursor **2**, were confirmed by X-ray single crystallography to be identical to products formed from Frey's potassium complex. Superficially, these complexes differ only in the number of ancillary THF molecules coordinated to the metal centre, however this has a marked

effect on the conformation and coordination of the complexes, pictured in Figure 45. The structures of **3** and **4** will be discussed in detail in Section 2.2.4.

In order to discuss the coordination environment across different complexes in this work, some general parameters describing the features of the different macrocyclic conformations and binding modes are described below. These bond lengths and angles will be used throughout this work to describe and compare the conformation and binding of lanthanide complexes of the *trans*-calix[2]phenylene[2]pyrrolide ligand. The binding modes and conformations of complexes **3** and **4** will be used to define these general parameters.

In the bis(THF) complex **3** shown in Figure 45, the samarium centre is located centrally relative to the two phenylene groups, which will be described as 'high' in the macrocyclic cavity. The macrocycle adopts a 1,3-alternate conformation. The phenylene moieties are approximately parallel, each π-binding η^6 to sandwich the metal centre in a metallocene-like structure. The pyrrolides σ-bind η^1 to the metal through the nitrogen. Overall the macrocycle binds η^6:η^1:η^6:η^1 (phenylene:pyrrolide:phenylene:pyrrolide) to the samarium metal centre.

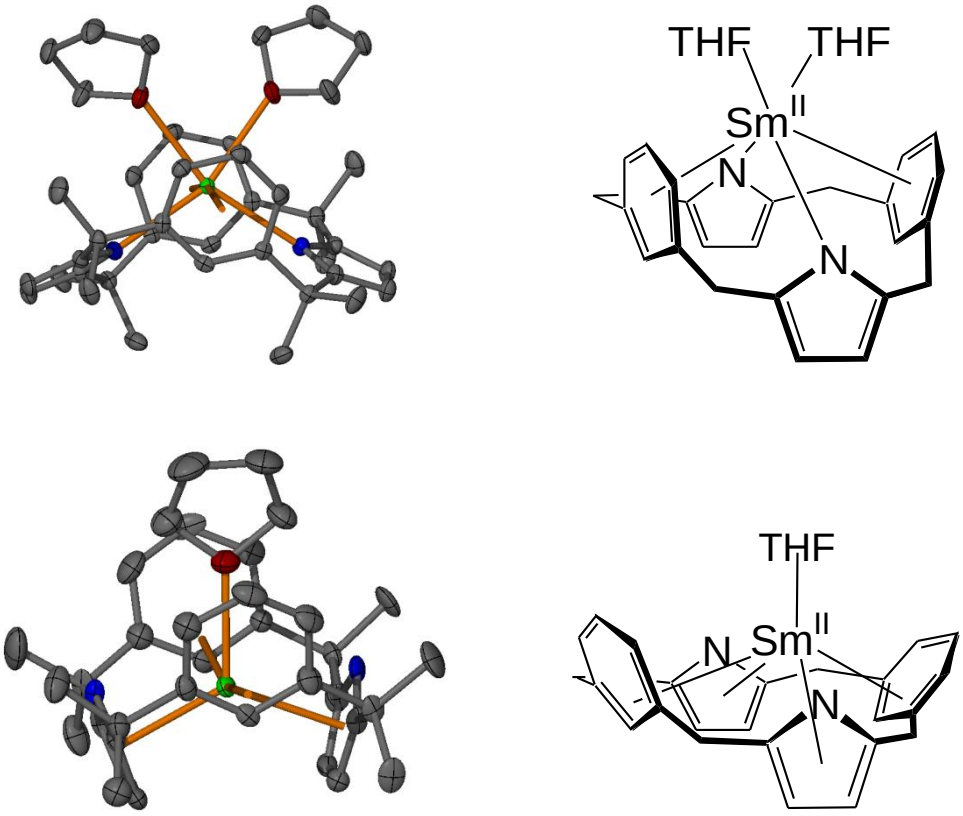

Figure 45: [$(Me_8N_2Ph_2)Sm(THF)_2$], **3** (above), and [$(Me_8N_2Ph_2)Sm(THF)$], **4** (below), demonstrating 'high' (η^6:η^1:η^6:η^1) and 'low' (η^3:η^5:η^3:η^5) metal centre location within the macrocyclic cavity.

The mono-THF complex **4** has the metal centre located at a point approximately between the phenylene C2 carbons, which will be described as 'low' within the macrocyclic cavity. The macrocycle has a cone-shaped conformation, with the phenylene groups splayed outward to bind η^3 to the samarium metal centre. The pyrrolide units each bind η^5 to the metal centre, giving an overall binding mode of η^3:η^5:η^3:η^5 between the macrocyclic ligand and the samarium metal. There is a 'twist' to the macrocycle in the bis(THF) complex, highlighted by the staggering of the phenylene groups relative to each other. This differs from the mono(THF) complex, where the phenylene groups are eclipsed.

In order to better describe the relationship between the phenylene groups and the metal centre, an angle (Φ) is measured between the two planes of the phenylene rings. This describes whether the phenylenes are parallel or splayed outwards. A second angle is measured between phenylene ring centroids and the metal centre (θ_{ph}), akin to a metallocene bend angle. These phenylene-related measurements are shown in Figure 46.

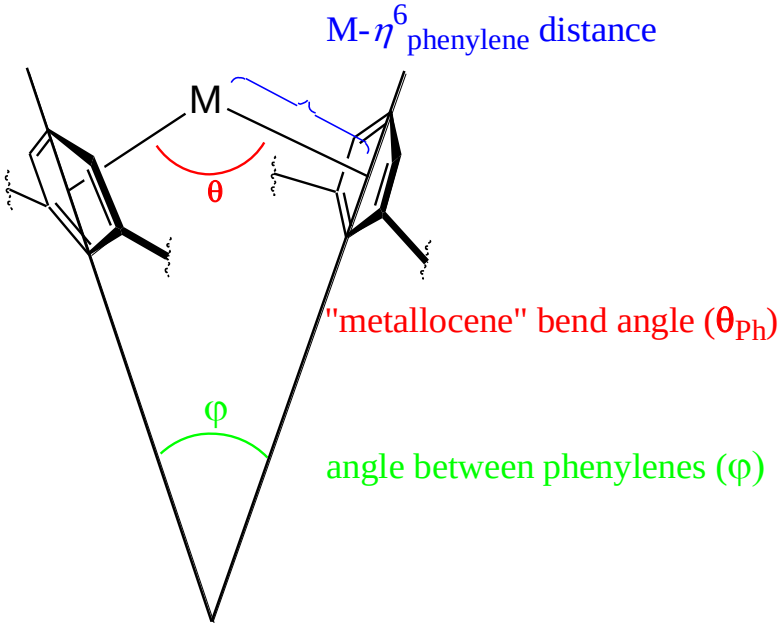

Figure 46: Phenylene moiety angles and distance measurements.

In previous work on complexes of the related $(Et_8N_4Me_2)^{2-}$ macrocycle, a plane described by the four sp^3 hybridised carbons (the '*meso*-plane') made a useful parameter for comparing structural characteristics of the lanthanide complexes.[268] Due to 'twisting' of the $(Me_8N_2Ph_2)^{2-}$ macrocycle seen in the majority of complexes in this work, the four *meso* carbons are rarely planar and distance/angle metrics relative to the *meso*-plane is

not a useful measurement. The macrocyclic 'twist' in complexes of the $(Me_8N_2Ph_2)^{2-}$ ligand is visible in the staggering of the phenylene groups.

The most significant change in conformation between the two complexes **3** and **4** is the ring flipping of the pyrrolide group, which changes from η^1 binding through the nitrogen atom in **3** to η^5 π-binding in **4**. This changes the macrocycle between 1,3-alternating and a doubly-flattened conformation. Where the pyrrolides bind η^5 to the metal centre, the 'metallocene' angle between centroids of the pyrrolides and the metal centre, θ_{py}, is measured (Figure 47). Bond distance between the metal centre and pyrrolide ring centroids is measured where π-bonding exists (M–η^5_{py}), otherwise the bond distance is measured between the metal centre and the nitrogen atom of the pyrrolide (M–η^1_{py}).

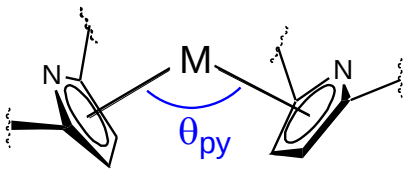

Figure 47: Angle measured where pyrrolide-metal binding is η^5.

2.2.3 Complexes of $(Me_8N_2Ph_2)^{2-}$ with Europium

Europium(II) is similar to samarium(II) in size, with ionic radii of 1.09 and 1.11 Å respectively.[325] Europium(II) has an electronic configuration of $4f^7$, and forms stable compounds in this oxidation state. In complexes with the dianionic $(Me_8N_2Ph_2)^{2-}$ ligand

a samarium metal centre may be present as Sm^{II} or oxidised to Sm^{III} if an easily reduced ligand is present. In some samarium complexes with a macrocyclic ligand it can be difficult to identify with certainty whether the metal centre is present as Sm^{II} or Sm^{III}. The more stable Eu^{II} metal centre, supported by a divalent macrocyclic ligand, is less likely to be oxidised.

If analogous samarium and europium complexes in this work are observed to have nearly identical structural details, it is likely that both metals are present in the 2+ oxidation state. If the analogous complexes have significantly different conformations this may indicate that the metals have different oxidation states, for example an Eu^{II} and Sm^{III}, as the Sm^{III} ionic radii is much smaller at 1.09 compared to 1.31 Å.

In his 2011 thesis James used computational methods supported by structural and spectroscopic results to confirm that analogous europium complexes provide a reliable benchmark for the behaviour of a lanthanide(II) metal in $(Et_8N_4Me_2)^{2-}$ organolanthanide complexes.[268] Europium analogues of samarium complexes **3** and **4** were prepared by salt metathesis of **2** with $EuI_2.THF_x$ as shown in Scheme 9.

Scheme 9: Metathesis of lithated precursor complex **2** to form europium(II) complexes **5** and **6**.

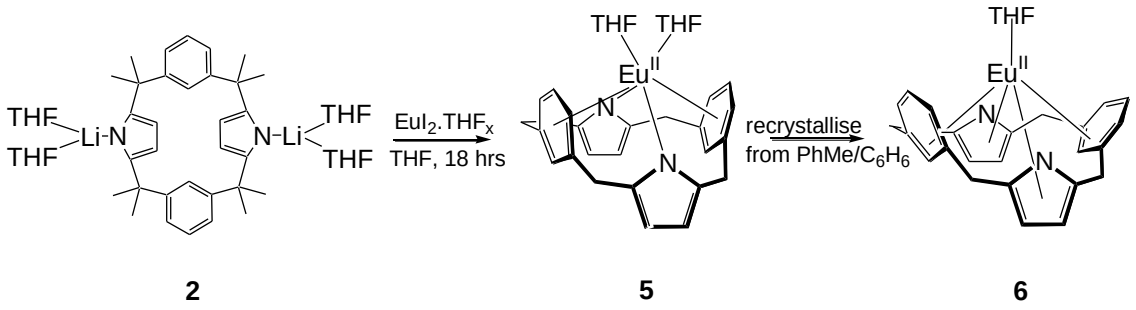

2 **5** **6**

A metathesis reaction between $[(Me_8N_2Ph_2)Li_2(THF)_4]$ (**2**) and $EuI_2.THF_x$ afforded orange crystals of $[(Me_8N_2Ph_2)Eu(THF)_2]$, (**5**). Recrystallisation from benzene caused the loss of one ancillary solvent ligand, yielding the orange mono-solvated complex $[(Me_8N_2Ph_2)Eu(THF)]$, (**6**). Single crystal X-ray diffraction structures of **5** and **6** were obtained from crystals grown in THF and benzene, respectively. The high paramagnetism of europium prevented effective characterisation of these complexes by NMR spectroscopy. Characterisation of **5** and **6** relies on microanalysis and X-ray structures to confirm bulk and structural assignments, respectively.

Large bright orange crystals of complex **5** were obtained and recrystallised from THF. The crystal belongs to the orthorhombic space group $P2_12_12$ (No. 18) with a = 13.200(5), b = 13.400(8), c = 9.382(1) Å. The asymmetric unit consists of half a molecule with C_2 symmetry generating the rest of the molecule. There is a pronounced twist to the macrocycle as seen in Figure 48. There are four molecules in the unit cell. The bis(THF) Eu complex **5** is isomorphous to the samarium complex **3**.

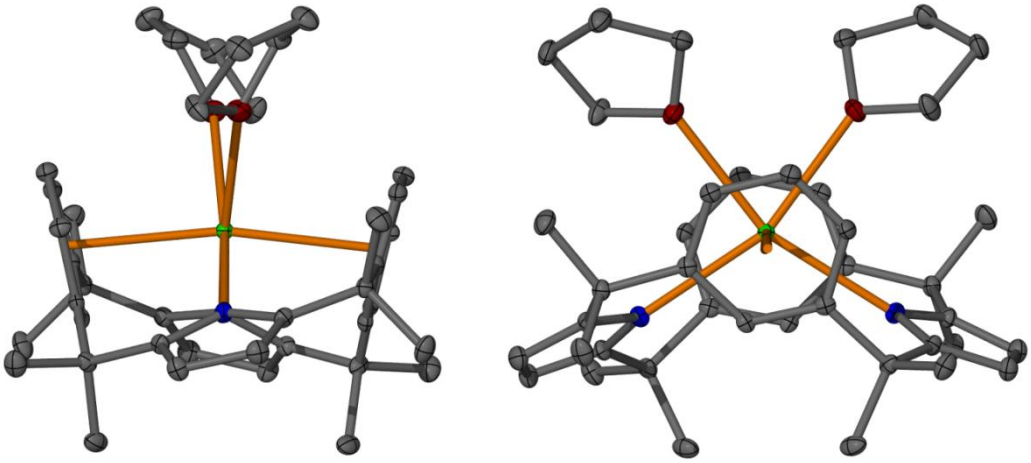

Figure 48: Molecular structure of $[Me_8N_2Ph_2Eu(THF)_2]$, (**5**), isomorphous with $[Me_8N_2Ph_2Sm(THF)_2]$, (**3**), with thermal ellipsoids drawn at 50% probability (protons omitted for clarity).

In the isomorphous samarium and europium bis(THF) complexes **3** and **5** the metal centre sits high in the macrocyclic cavity, sandwiched between the two phenylene units. The metal centres are bound η^6:η^1:η^6:η^1 to the macrocyclic ligand. Measurements below are for the europium analogue.

The phenylene groups have an Φ angle of 27.1 ° between them (as defined in Section 2.2.2). The M–η^6_{Ph} distance is 2.75 Å. The θ_{ph} 'metallocene angle' formed between the phenylene centroids and the metal centre is 167.9 °. The two pyrrolide groups bind η^1 through the nitrogen with a M–η^1_{Py} distance of 2.618(3) Å. Two THF molecules occupy the top cavity of the macrocycle and are bound to the metal centre with a M–O distance of 2.635(3) Å.

Orange rod crystals of the mono(THF) europium complex (**6**) suitable for single crystal X-ray diffraction were formed from recrystallisation of the bis(THF) complex (**5**) from benzene at room temperature under an atmosphere of nitrogen. The crystal belongs to the orthorhombic space group $P2_12_12_1$ (No. 19) with a = 15.413(2), b = 18.754(2), c = 10.371(3) Å. The asymmetric unit contains one molecule, with four molecules in the unit cell. The solid state structure obtained by single crystal X-ray diffraction can be seen in Figure 49. The europium mono(THF) complex **6** is isomorphous to the samarium complex **4**. The europium analogue is described below.

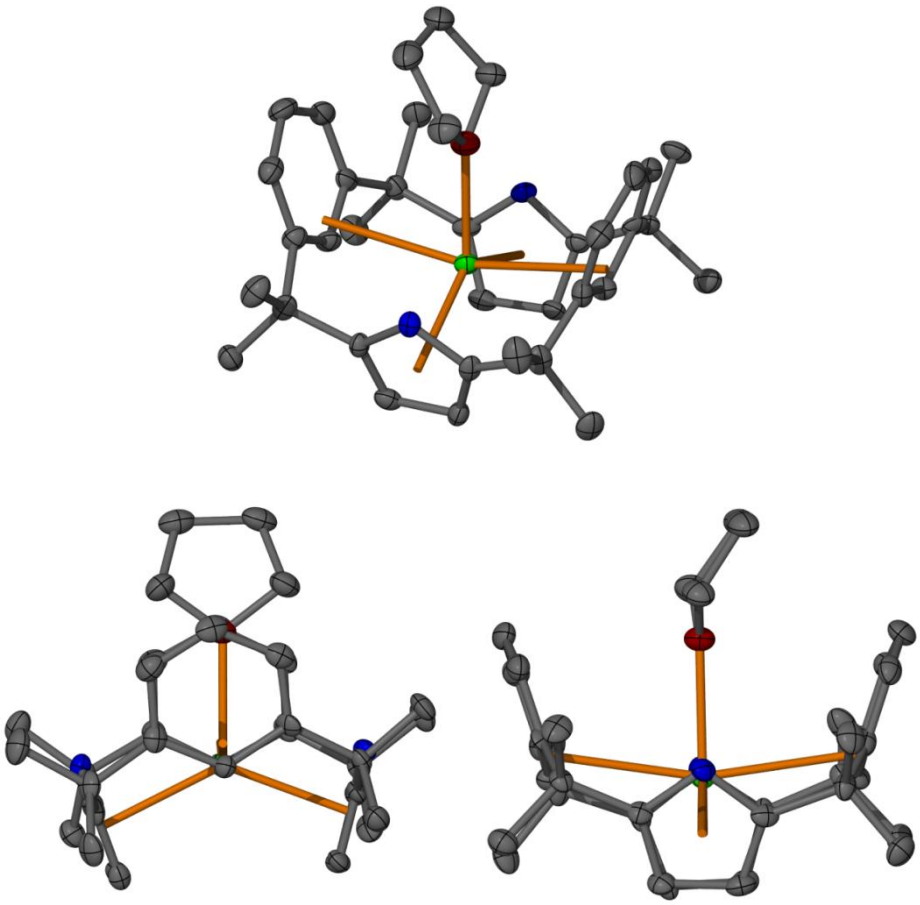

Figure 49: Molecular structure of [($Me_8N_2Ph_2$)Eu(THF)], (**6**), with thermal ellipsoids drawn at 50% probability (protons omitted for clarity).

The metal centre is seated deep within the macrocyclic cavity of the mono(THF) complex, located approximately in line between the C2 carbons of the phenylene groups (C–Eu–C forms an angle of 170 °). The THF molecule is pulled further into the macrocyclic cavity by the deeper seated samarium centre and is flanked by the phenylene rings, causing the alignment of the THF in this narrow binding cleft. The macrocycle is in a cone conformation (though 1,3 alternate, unlike calix[4]arene analogies), binding η^3:η^5:η^3:η^5 to the metal centre. Selected measurements of the europium mono(THF) crystal structure obtained by X-ray diffraction are listed in Section 2.2.4. Unlike the bis(THF) complexes, the macrocyclic ligand is not twisted in the mono(THF) complexes **4** and **6**.

2.2.4 Structural Comparisons of [(Me$_8$N$_2$Ph$_2$)Ln(THF)$_x$] Complexes (Ln = Sm, Eu; x = 1,2)

The crystal structures of the europium complexes [(Me$_8$N$_2$Ph$_2$)Eu(THF)$_2$], (**5**) and [(Me$_8$N$_2$Ph$_2$)Eu(THF)], (**6**) are isomorphous to samarium complexes **3** and **4**. The Eu^{II} metal centre has a similar ionic radius to Sm^{II} (1.09 and 1.11 Å, respectively).[27] Selected bond lengths and angles are listed in Table 3 below.

Table 3: Selected bond lengths (Å) and angles (°) of $[(Me_8N_2Ph_2)Ln(THF)_n]$ for Ln = Sm, Eu and n = 1,2 ($L = (Me_2N_2Ph_2)^{2-}$)

	[LSm(THF)$_2$] (3)	**[LEu(THF)$_2$] (5)**	**[LSm(THF)] (4)**	**[LEu(THF)] (6)**
M in cavity	High	High	Low	Low
M–O (Å)	2.638(3)	2.635(3)	2.523(4)	2.510(5)
M–$\eta^x_{(Ph)}$	2.77 (η^6)	2.75 (η^6)	2.90, 2.91 (η^3)	2.86, 2.87 (η^3)
$\theta_{(Ph)}$ (°)	167.6 (η^6)	167.9 (η^6)	NA	NA
Φ (°)	27.6	27.1	33.5	34.4
M–$\eta^x_{(Py)}$	2.614(3) (η^1)	2.618(3) (η^1)	2.53, 2.53 (η^5)	2.53, 2.54 (η^5)
$\theta_{(Py)}$ (°)	NA	NA	131.6	132.1

The angle from phenylene centroid-metal-phenylene centroid angle is 167.9 ° in the europium bis(THF) complex. The phenylene groups are nearly parallel, which allows them to sandwich the metal centre with η^5-binding on either side. In both the samarium and europium mono(THF) complexes the phenylenes are splayed outwards, with M–C distances indicating η^3-binding to the metal centre. Distances between the metal centre and the phenylene carbons in the samarium and europium mono(THF) complexes are shown in Figure 50.

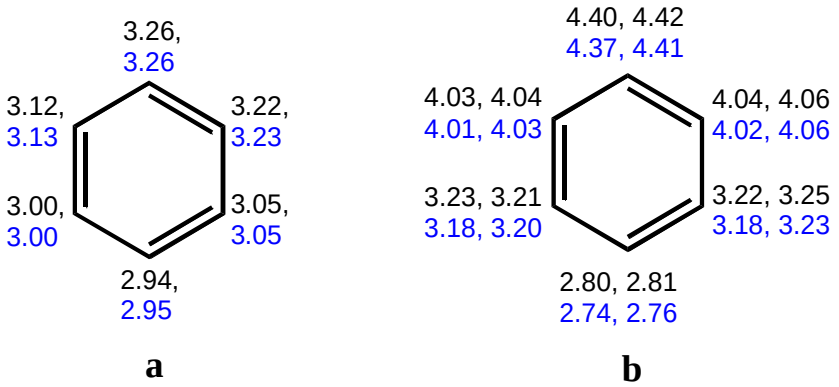

Figure 50: Metal centre (Sm, Eu) to phenylene carbon distances (Å) in (a) the bis(THF) complexes **3** & **5** (η^6-binding) and (b) the mono(THF) complexes **4** & **6** (η^3-binding).

The number of coordinated solvent ligands appears to be related to the macrocycles conformation and bonding. When two THF molecules are coordinated, the metal centre sits high in the macrocyclic cavity between two near-parallel phenylene groups. The coordination sphere of the metal is satisfied by two ancillary solvent molecules, π-binding from the phenylenes, and σ-bonds through the nitrogen atoms of the pyrrolide moeities.

In the mono(THF) complex the metal centre is seated deeper within the cone-shaped macrocyclic cavity, although with slightly shorter M–O bond distance than in the bis(THF) complex. The loss of a coordinated THF molecule reduces the coordination number and in turn reduces the effective ionic radii of the metal centre. When the metal is drawn into the macrocyclic cavity the pyrrolide groups flip to π-bind η^5 to the metal centre, which requires the phenylene groups to splay outward, binding η^3- to the metal. This change in conformation achieves a high coordination number for the metal centre, compensating for the loss of one THF solvent molecule.

2.2.5 A Samarium(III) Chloride Complex, [(Me$_8$N$_2$Ph$_2$)SmCl], 7

A samarium(III) halide complex allows access to samarium(III) derivatives through metathetical exchange of the halide. In addition, it also acts as a good structural benchmark of a lanthanide(III) complex for comparison with the lanthanide(II) complexes **3**–**6** and others described in Chapter 3.

Scheme 10: Synthesis of [($Me_8N_2Ph_2$)$Sm^{III}Cl$], **7**

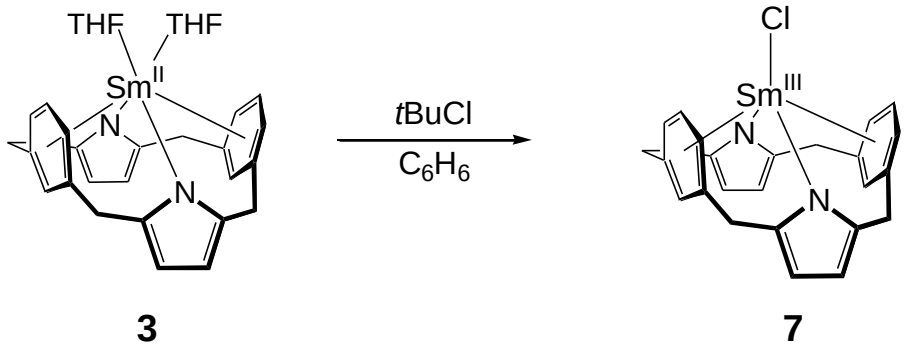

3 **7**

The chloride complex [($Me_8N_2Ph_2$)$Sm^{III}Cl$] **7** was prepared by the addition of *t*BuCl to a solution of (**3**) in benzene (Scheme 10). The chloride complex forms as orange crystals which are stable when stored under an inert atmosphere. This rapid colour change from dark purple to orange is consistent with rapid oxidation of samarium(II) to samarium(III).[140] The crystals were characterised by ^{1}H NMR spectroscopy, elemental analysis and single crystal X-ray structure determination. As this is a Sm^{III} complex, there is less influence of the paramagnetic metal centre on the NMR spectrum relative to the previous Sm^{II} complexes. However, the ^{1}H NMR spectrum of **7** still contained some broadening and shifted resonances, which prevented full assignment. While low solubility prevented further investigation, the partial characterisation of the complex met the structural benchmark for a samarium(III) monoligated η^6:η^1:η^6:η^1 structure type.

Two resonances attributed to the methyl groups are located at 1.45 and 1.92 ppm, indicating that methyl protons are equally distributed between facing either towards or away from the metal centre, consistent with the THF complexes. This is also supported by the solid state crystal structure described below.

An alternative preparation of [($Me_8N_2Ph_2$)$Sm^{III}Cl$] was reported in the literature through the course of this study.[306] This complex was prepared by deprotonation of ($Me_8N_2Ph_2H_2$) with KH followed by salt metathesis of with $SmCl_3(THF)_3$. Comparison of single crystal X-ray diffraction data from Gambarotta suggests that this is the same complex as **7**, however the reported ^1H NMR spectrum is inconsistent with our findings.[306]

Gambarotta attributed all methyl protons to only one resonance at 1.46 ppm, which differs significantly from NMR spectra collected throughout this work: all lanthanide complexes have given inequivalent methyl proton resonances on either face of the macrocycle. Gambarotta's NMR assignment also differs from this in identification of the pyrrolide protons; where he reported the four pyrrolide protons as "*four separate sets of resonances as two sharp doublets at 6.25 and 6.16 ppm non-coupled to each other and each coupled instead to poorly* [re]*solved broad resonances at 6.92 and 6.74 respectively*", instead only one resonance in the spectrum of **7** was attributed to the four pyrrolide protons. A further inconsistency is identified in the assignment of the phenylene protons, reported by Gambarotta as "*four multiplets at 7.37, 6.85 and 6.53 all coupled together with an additional weak coupling to a broad multiplet at 7.02, probably generated by the hydrogen located between the two ring attachments*." In this work, there were three resonances attributed to the phenylene protons, consistent with the NMR spectra of similar samarium complexes throughout this work.

Bright orange crystals of complex **7** suitable for single crystal X-ray diffraction were isolated and washed with benzene. The crystal belongs to the monoclinic space group *C*2/*c* (No. 15) with *a* = 18.988(4), *b* = 14.995(3), *c* = 10.13(4) Å, β = 110.06(1) °. The asymmetric unit contains half a molecule of C_2 symmetry, with four molecules in the unit cell. The solid state structure can be seen in Figure 51.

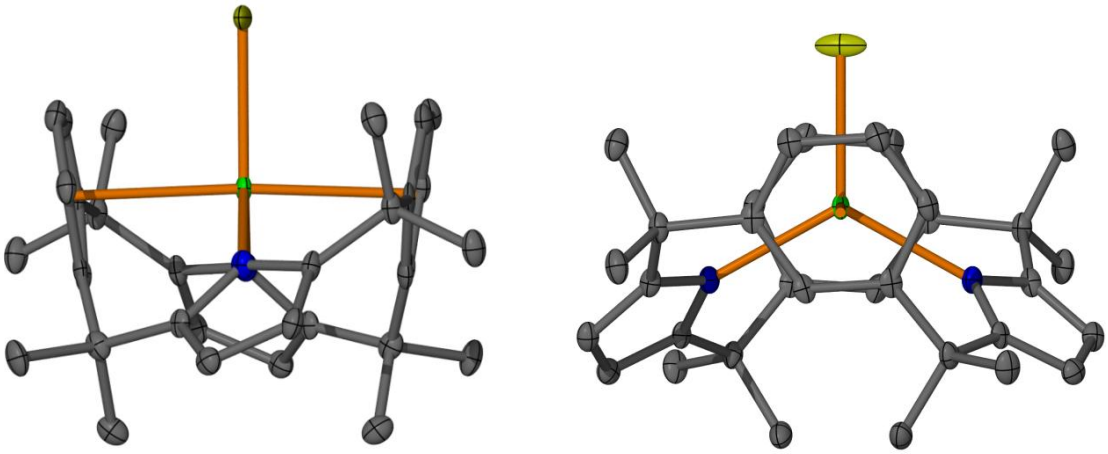

Figure 51: Molecular structure of [($Me_8N_2Ph_2$)SmCl], (**7**) with thermal ellipsoids drawn at 50% probability (protons omitted for clarity).

In this mononuclear samarium(III) complex the macrocycle binds the samarium η^6:η^1:η^6:η^1, similar to the bis(THF) complex **3**. This differs from the mono(THF) complex **4**, suggesting that perhaps the larger Cl^- ligand prevents the deeper η^3:η^5:η^3:η^5 binding mode of the macrocycle. The macrocycle has twisted to such an extent that the phenylenes are eclipsed by the 60 ° twist. Bond lengths and angles measured from the single crystal X-ray diffraction structure of this samarium(III) complex are compared

with the mono- and bis(THF) samarium(II) complexes in Table 4. The smaller radius of Sm^{III} in 7 is apparent.

Table 4: Selected metrics of [LSmCl] (**7**), [LSm(THF)$_2$] (**3**) and [LSm(THF)],(**4**), (L = $(Me_8N_2Ph_2)^{2-}$).

	[LSmCl] (7)	**[LSm(THF)$_2$] (3)**	**[LSm(THF)] (4)**
M in cavity	High	High	Low
M–Cl or M–O	2.6396(13)	2.638(3)	2.523(4)
M–$\eta^x_{(Ph)}$ (Å)	2.61 (η^6)	2.77 (η^6)	2.90, 2.91 (η^3)
$\theta_{(Ph)}$ (°)	175.8 (η^6)	167.6 (η^6)	NA
Φ (°)	16.0	27.6	33.5
M–$\eta^x_{(Py)}$ (Å)	2.415(3) (η^1)	2.614(3) (η^1)	2.53, 2.53 (η^5)
$\theta_{(Py)}$ (°)	NA	NA	131.6

Gambarotta reported that the samarium(III) chloride complex was reacted with MeLi to form a C–H activated complex [{$Me_8N_2Ph_2$(-H)}Sm^{III}(THF)] in which one of the phenylene rings has metallated and the two pyrrolide units have adopted a π-binding mode, (Figure 52).[326]

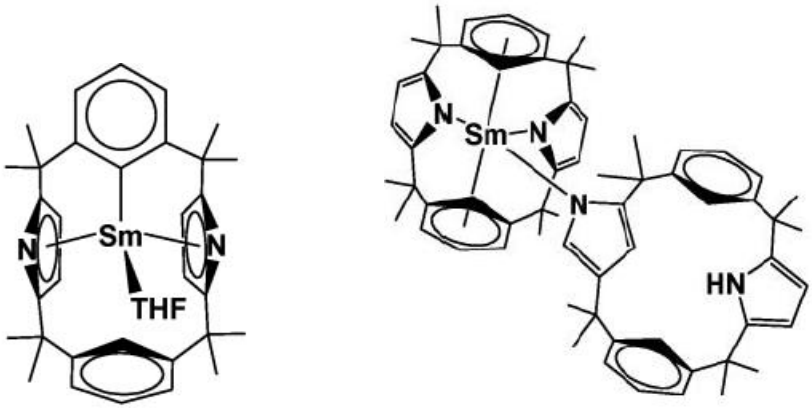

Figure 52: Gambarotta's metallated [{$Me_8N_2Ph_2$(-H)}Sm^{III}(THF)] complex and an *N*-confused product formed in the same reaction, reproduced from literature.[306]

An *N*-confused minor product was also formed, which contains one Sm^{III} metal centre between one macrocyclic ligand and one *N*-confused macrocyclic ligand. In this minor product, the normal macrocyclic ligand adopts a conformation similar to the [$(Me_8N_2Ph_2)Sm^{III}Cl$], whilst the *N*-confused ligand acts as a σ-bound monodentate ligand, binding through one nitrogen of an *N*-confused pyrrolide ring, whilst the other pyrrolide nitrogen has been protonated. Gambarotta reports that the formation of this *N*-confused complex is 'unavoidable' and could not be separated from the metallated THF complex. Pure samples of the *N*-confused complex in their work were prepared by reacting the $Sm^{III}Cl$ complex with NaH.

These findings of Gambarotta may indicate some support to the earlier suggestion that larger Group 1 metals are implicated in the formation of *N*-confused products. Whilst he did report the *N*-confused product as a systematic contaminant of the reaction between [$(Me_8N_2Ph_2)SmCl$] and MeLi, by using NaH in the reaction the *N*-confused complex becomes the major product. He compared the calix[2]phenylene[2]pyrrolide ligand to dipyrrolebenzene and calix[4]pyrrole, concluding that the replacement of two pyrrolide groups with purely π-donating aromatic rings increased the reactivity of the samarium metal centre.

Gambarotta noted the lack of samarium(II) products, and concluded that the samarium(II) complexes produced were not stable enough to be isolated. This is in contrast to the results of work in this thesis, where numerous samarium(II) complexes were isolated and shown to be stable as solid and in solution for weeks or months.

2.2.6 Synthesis of $[(Me_8N_2Ph_2)Ln(NCMe)_2]$, Ln = Sm (8), Eu (9)

Nitriles and isonitriles have carbon-nitrogen triple bonds and a lone pair available for coordination to metals (on the nitrogen or carbon atoms respectively). There are a number of examples of nitrile and isonitriles forming adducts with lanthanide(II) and (III) metal centres,[327] such as $[(C_5H_5)_3Ln(NCR)_2]$,[328] $[(C_5H_5)_3Ln(NCMe)]$ (Ln = Nd, Sm, Yb) and $[(C_5H_5)_2Yb(NCMe)]$.[329] Tris(pentamethylcyclopentadienyl) lanthanide complexes also form adducts with neutral nitriles and isonitriles.[163, 330]

Organolanthanide complexes can also cleave acetonitrile and/or undergo rearrangement into other products. Nitriles and isonitriles can be reduced to form samarium(III) cyanides through single electron reduction and cleavage at the C–N or C–C bond.[331-333] Reductive cleavage of isocyanide occurs in the presence of $[(C_5Me_5)_2Sm(THF)_2]$, forming a cyclic trimer with cyanide ligands bridging the metal centres and an additional unreacted isonitrile on each metal, (Figure 53).[332] Similarly, the addition of excess *t*-butyl isonitrile to $[(Et_8N_4Me_2)Sm(THF)_2]$ also forms a Sm(III) cyclic trimer cyanide complex through reductive C–N cleavage, $[\{(Et_8N_4Me_2)Sm(\mu\text{-}C{\equiv}N)\}_3]$.[268,333]

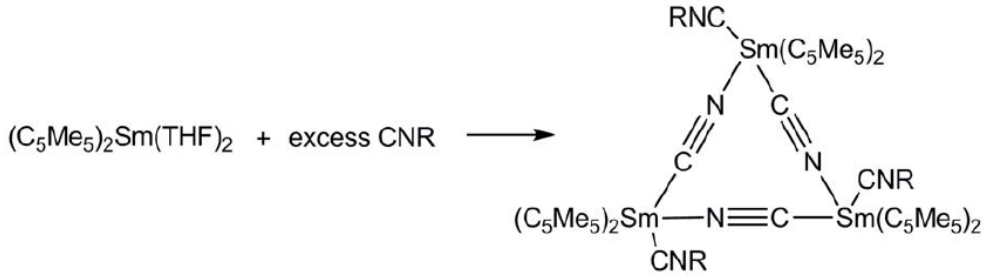

Figure 53: Reductive cleavage of isocyanide to form cyanide ligands in a trimeric complex.

Addition of excess acetonitrile to $[(Et_8N_4Me_2)Sm(THF)_2]$ in aromatic solvent yields crystalline $[(Et_8N_4Me_2)Sm(NCMe)_2]$ in a reversible solvent-driven reaction.[268] Washing the insoluble crystalline $[(Et_8N_4Me_2)Sm(NCMe)_2]$ with benzene gave a purple solution which bleaches to colourless within minutes. Attempts to isolate product from the purple solution, presumed to be a partially desolvated mono-acetonitrile complex, were not successful.[268] Orange crystals formed from the colourless solution over 24 hrs, which single crystal X-ray diffraction identified as $[\{(Et_8N_4Me_2)Sm(C\equiv N)\}_3]$ (Figure 54). This product of reductive cleavage of the acetonitrile indicates that a Sm^{III} methyl product is also likely to be present.

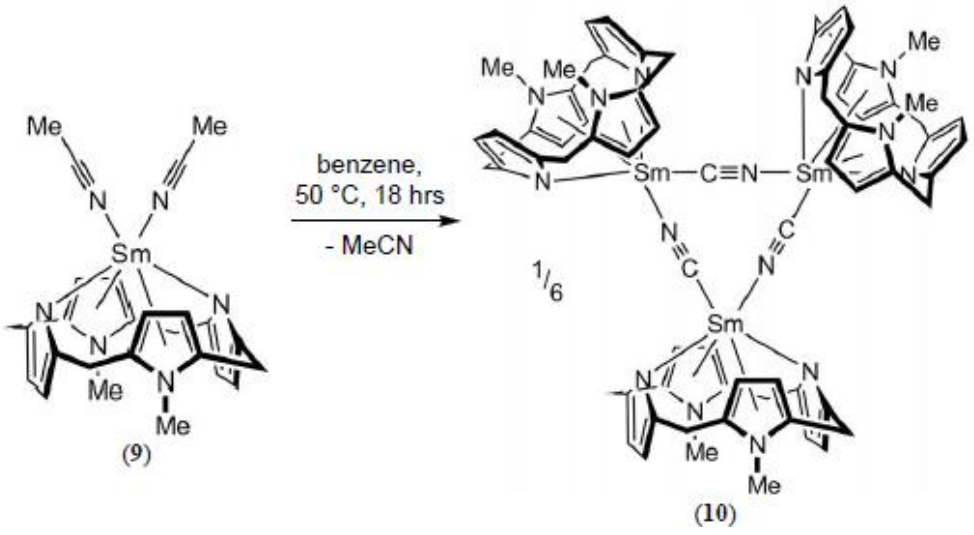

Figure 54: Formation of a cyanide trimer from $[(Et_8N_4Me_2)Sm(NCMe)_2]$, reproduced from literature.[268]

The bis(acetonitrile) complexes $[(Me_8N_2Ph_2)Sm(NCMe)_2]$, **8**, and $[(N_2Ph_2)Eu(NCMe)_2]$, **9**, were prepared by addition of acetonitrile to a benzene solution of **3** and **5** respectively (Scheme 11). The samarium complex **8** forms over 24–48 hrs as large dark red crystals. The europium complex **9** forms as bright orange crystals which are visually indistinguishable from the bis(THF) reactant.

Scheme 11: Preparation of Sm^{II} and Eu^{II} acetonitrile complexes.

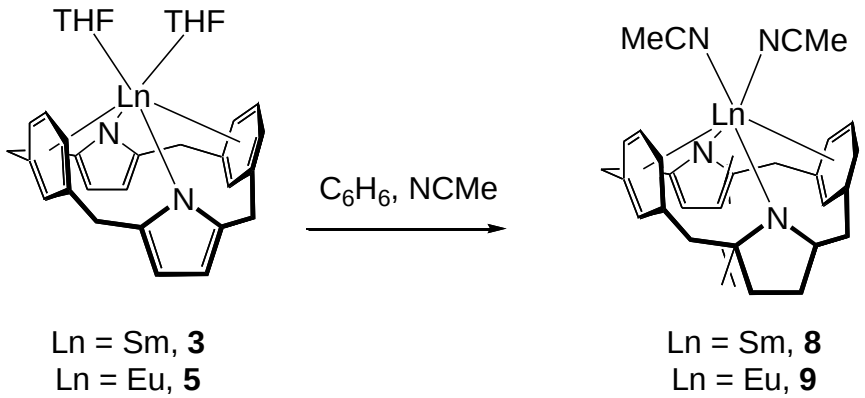

Dark red crystals of complex **8** and orange needle crystals of complex **9** suitable for single crystal X-ray diffraction were isolated and washed with benzene. The two solid state crystal structures were found to be isomorphous. The crystal of **8** belongs to the orthorhombic space group *P*nma (No. 62) with a = 11.70(1), b = 19.21(1), c =15.20(1) Å. Orange needle crystals of complex **9** (a = 11.719(2), b = 19.240(2), c = 15.193(4) Å) has an asymmetric unit containing half of a macrocyclic unit lying on a mirror plane that contains the metal centre, both arene rings and an acetonitrile lattice solvent molecule. The solid state structure of the samarium complex can be seen in Figure 55.

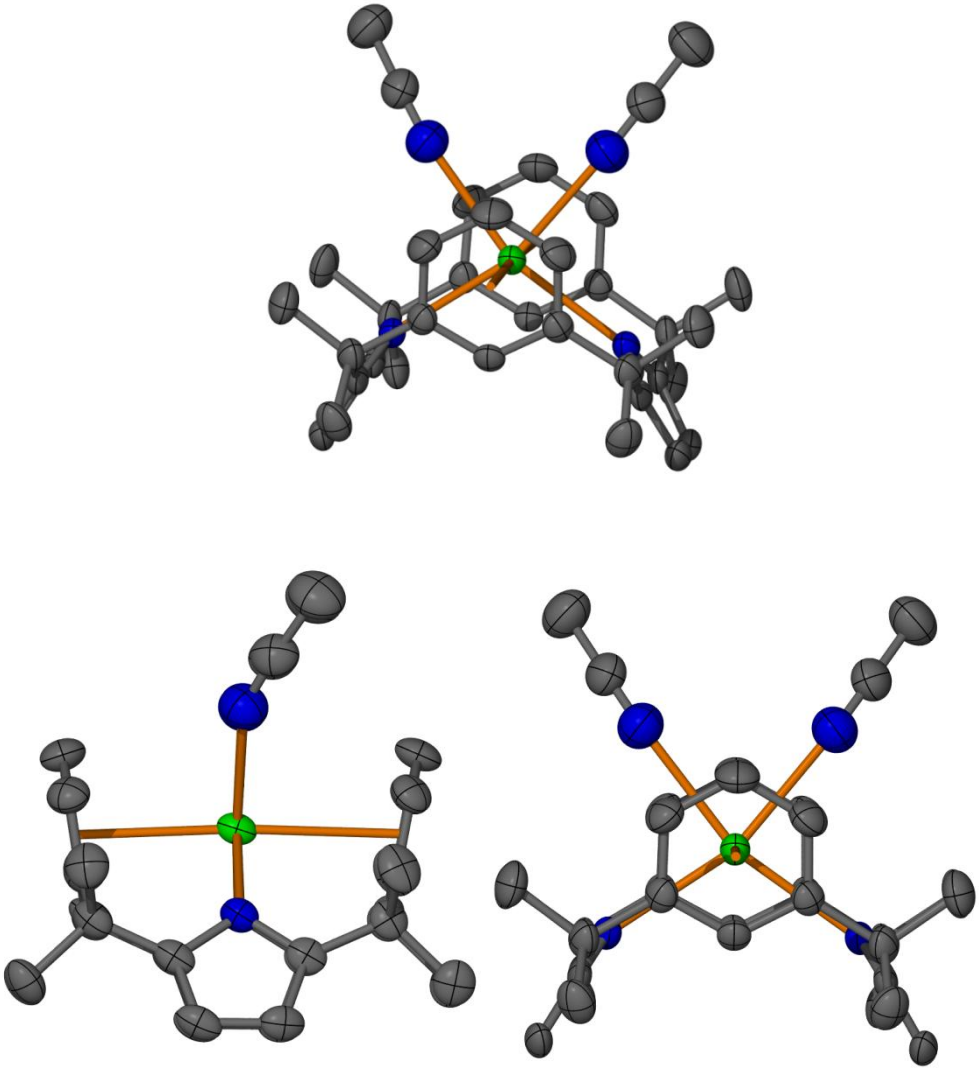

Figure 55: Molecular structure of[$Me_8N_2Ph_2Sm(NCMe)_2$], **8**, (isomorphous to [$Me_8N_2Ph_2Eu(NCMe)_2$], **9**, with thermal ellipsoids drawn at 50% probability (protons omitted for clarity).

In the lanthanide bis-acetonitrile complexes **8** and **9** the metal centre sits high in the macrocyclic cavity, approximately between the centroids of the phenylene units. The metal centre binds η^6:η^1:η^6:η^1 to the macrocyclic ligand. The structural data is summarised in Table 5.

Table 5: Structural data for [LLn(NCMe)$_2$] and [LLn(THF)$_2$] (Ln = Sm, Eu; L = $(Me_8N_2Ph_2)^{2-}$).

	[LSm(NCMe)$_2$] (8)	**[LEu(NCMe)$_2$] (9)**	**[LSm(THF)$_2$] (3)**	**[LEu(THF)$_2$] (5)**
M in cavity	High	High	High	High
M-NCMe/THF	2.648(9)	2.698(5)	2.638(3)	2.635(3)
M–$\eta^x_{(Ph)}$ (Å)	2.72, 2.79 (η^6)	2.74, 2.79 (η^6)	2.77 (η^6)	2.75 (η^6)
$\theta_{(Ph)}$ (°)	176.2 (η^6)	174.4 (η^6)	167.6 (η^6)	167.9 (η^6)
Φ (°)	18.7	19.5	27.6	27.1
M–$\eta^x_{(Py)}$ (Å)	2.589(6) (η^1)	2.632(3) (η^1)	2.614(3) (η^1)	2.618(3) (η^1)

Whilst similar in ionic radii, a samarium(II) metal centre is larger than europium(II) metal centre by around 0.02 Å. Surprisingly, the solid state structural data in Table 5 indicate that in analogous complexes of both NCMe and THF, for some metrics it is the the samarium complexes that have shorter metal–ligand bond lengths, whilst most are statistically equal. This may indicate that there is some partial electron transfer from the metal to the ligand, shortening the M–L bond without formally changing the metal oxidation state or cleaving the acetonitrile ligand. This partial electron transfer has also been observed in some samarium pyridine complexes, and will be discussed further in Chapter 3.

The [$(Me_8N_2Ph_2)Sm(NCMe)_2$] complex was heated in benzene with the aim of investigating whether cleavage of the nitrile would occur, as has been observed for [$(C_5Me_5)_2Sm(THF)_2$] and [$(Et_8N_4Me_2)Sm(THF)_2$].[163, 268, 332] Deuterated benzene was used in order to monitor the extent of solvation by ^{1}H NMR spectroscopy. The mixture was heated to 50 °C for 48 hrs without showing any visible change or indication of

change by ^{1}H NMR spectroscopy. This contrasts with $[(Et_8N_4Me_2)Sm(THF)_2]$ and $[(C_5Me_5)_2Sm(THF)_2]$ which both cleave nitriles at 50 °C (in under 48 hrs). Increasing the temperature to 75 °C for a further 72 hrs resulted in a change of colour from a faint purple solution to brown, alongside the formation of dark coloured crystals. The crystalline product was shown to be a samarium(II) complex free of coordinated solvent; this is discussed in Section 2.2.7

2.2.7 Preparation of a Samarium(II) Complex Free of Ancillary Ligands

A samarium $(Et_8N_4Me_2)^{2-}$ complex free of ancillary coordinated ligands was synthesised by James and was found to react with dinitrogen, binding the small molecule between two macrocyclic units in the first reported end-on dinitrogen organosamarium complex.[268] The complex is more open to reaction with small molecules such as dinitrogen or carbon monoxide as there are no ancillary ligands to compete for coordination to the metal centre. The relatively simple synthesis of $[(Me_8N_2Ph_2)Sm(THF)_2]$ allowed for the investigation of the reaction of this more flexible ligand system with small molecules.

A solution of **8** in C_6D_6 was refluxed in a sealed vessel for 5 days, forming crystalline product upon cooling (Scheme 12). Single crystal X-ray diffraction of the dark product showed this to be a samarium(II) macrocyclic product **10**. Characterisation of this complex by NMR spectroscopy was attempted, although due to a mixture of products

coupled with the small scale of reaction (< 10 mg product), the characterisation of **10** rests on the single crystal X-ray diffraction. Two crystalline products were observed, colourless blocks and small dark coloured crystals, with only the latter being able to be characterised by single crystal X-ray diffraction. The colourless crystal may be a product of hydrolysis as a result of the long reaction time at high temperature. Despite numerous attempts, these products have not been reproduced, which is discussed further below.

Scheme 12: Preparation of the polymeric samarium complex free of coordinated solvent, **10.**

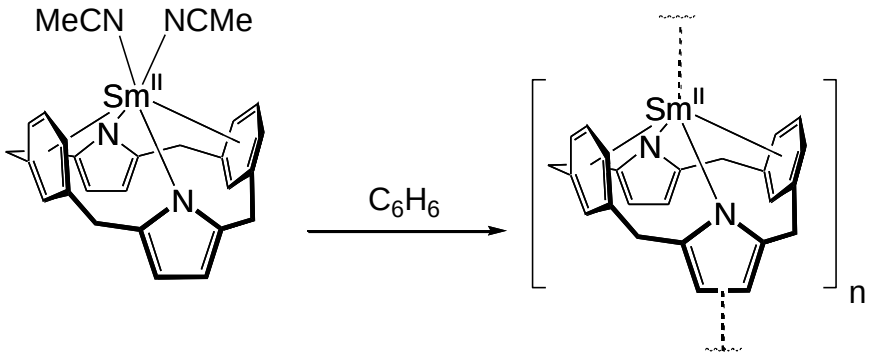

8 **10**

The crystal belongs to the tetragonal space group $I4_1/a$ (No. 88) with $a = b = 25.499(4)$, $c = 23.856(5)$ Å. The asymmetric unit contains one samarium complex and 2.5 benzene solvent molecules. The unit cell contains 16 macrocyclic molecules. The solid state structure can be seen in Figure 56.

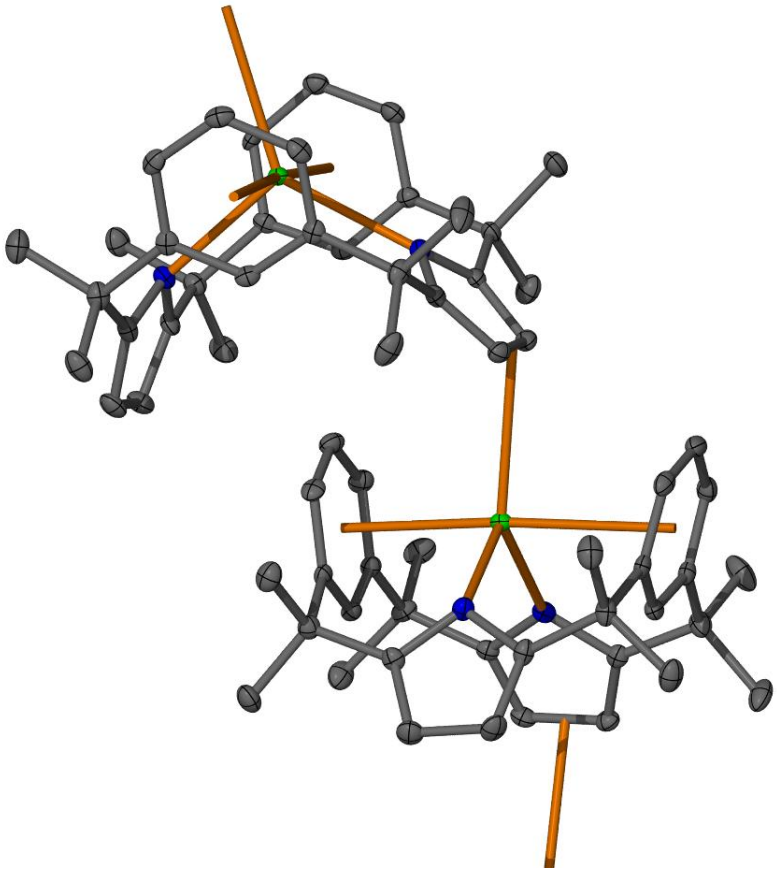

Figure 56: Molecular structure of [{($Me_8N_2Ph_2$)Sm}$_n$], (**10**) with thermal ellipsoids drawn at 50% probability (protons omitted for clarity).

The complex **10** has the macrocyclic ligand in a similar conformation and binding mode (η^6:η^1:η^6:η^1) to the bis(THF) complex. The high position of the metal in the macrocyclic cavity allows it to form a weak bond to an adjacent macrocycle, forming a polymeric chain. This weak bond formed between Sm^{II} and the η^2 C–C bond (centroid) on an adjacent macrocycle has a distance of 2.91 Å and results in significant desymmetrisation of the molecule due to this association. Selected measurements from the single crystal structure are compared with others in Table 6.

Table 6: Selected bond lengths and angles of the ancillary solvent free complex **10**, and bis- and mono-THF Sm complexes **3** and **4**. (L = $(Me_8N_2Ph_2)^{2-}$)

	$[LSm]_n$ (10)	**$[LSm(THF)_2]$ (3)**	**$[LSm(THF)]$ (4)**
M in cavity	High	High	Low
Sm–O or -(C-C) centroid	2.91	2.638(3)	2.523(4)
M–$\eta^x_{(Ph)}$ (Å)	2.68, 2.89 (η^6)	2.77 (η^6)	2.90, 2.91 (η^3)
$\theta_{(Ph)}$ (°)	174.9 (η^6)	167.6 (η^6)	NA
Φ (°)	19.8	27.6	33.5
M–$\eta^x_{(Py)}$ (Å)	2.548(2), 2.640(2)	2.614(3) (η^1)	2.53, 2.53 (η^5)
$\theta_{(Py)}$ (°)	NA	NA	131.6

If the conformation of the macrocycle in **10** were closer to that seen in the mono(THF) adduct, **4**, with the metal centre sitting deep in the ligand cavity, weak interactions between units may not be possible, thereby preventing the unsolvated complex from forming. The coordination number influenced ionic radii of Sm^{II} is apparent in comparing complexes **10** and **3**, that bind similarly to the macrocycle.

Attempts to reproduce this complex by the alternative route of heating $[(Me_8N_2Ph_2)Sm(THF)_2]$ under reduced pressure were unsuccessful. Only the more labile NCMe Lewis base adduct showed some success in desolvation. Unfortunately the desolvation to this product has proven difficult to replicate, particularly on the small scales in which these experiments have been done. Further work to identify a reliable synthesis of the unsolvated samarium complex will allow investigation of **10** with

weaker binding reagents that may not otherwise outcompete coordinating solvent molecules in the THF complex **3** or the NCMe complex **8**.

This unsolvated complex is anticipated to be very reactive. The samarium(II) metal centre is only weakly bound to the adjacent molecule and thus is open to accept more strongly binding ligands. There is great potential for small molecule activation, for example, where a small N_2 or CO molecule could react with the complex without having to outcompete ancillary solvent molecules.

Chapter 3

Reactivity Studies of *N*-Heterocycles with Samarium and Europium Calix[2]phenylene[2]pyrrolide

3.1 Introduction

As discussed in Chapter 1, Sm^{II} is commonly utilised in reactions in the form of SmI_2, which is a useful one electron reductant. Organosamarium complexes provide access to reactive samarium(II) within an adaptable steric and electronic environment.

The preparation of some simple samarium(II) macrocyclic complexes of calix[2]phenylene[2]pyrrolide has been established in Chapter 2. In this Chapter these precursor complexes are reacted with *N*-heterocycles of varying steric bulk and electronic characteristics.

Pyridine is a 6-membered aromatic heterocycle containing one nitrogen atom, and is more basic than nitriles or furans.[334] While it is structurally analogous to benzene, the shorter bonds between carbon and nitrogen within the heterocycle mean the hexagonal geometry is imperfect.[335] Pyridine (pyr) is used as an aromatic solvent that can coordinate to Lewis acidic metals through the lone pair of the nitrogen atom and is commonly used in lanthanide chemistry, with numerous examples of pyridine solvent

coordinating to form lanthanide-pyridine adducts.[293, 329, 336-342] For example an early study of lanthanide(III) salicaldehyde complexes (Ln = La, Pr, Nd, Sm, Eu, Tb) reacted with pyridine, bipyridine, quinoline and phenanthroline yielded $[Ln(pyr)_2(sal)_3]$, $[Ln(bipy)(sal)_3]$, $[Ln(quin)_2(sal)_3]$ and $[Ln(phen)(sal)_3]$ respectively, demonstrating that these heterocycles can coordinate as neutral ligands.[343] The reaction of $Sm(SePh)_3$ with selenium in pyridine to give the lanthanide chalcogenido cluster $[(pyr)_8Sm_8Se_6(SePh)_{12}]$ has a yield four times higher than the THF analogue.[344] This result was attributed to the higher basicity of the pyridine relative to THF.

Pyridine is not always an innocent ancillary ligand; it can also be reduced. For example the reaction of thulium diiodide with excess pyridine results in the reductive coupling of two pyridine radical anions through the C4 carbons (Figure 57).[345] The magnetic moment of the reductively coupled product (6.05 μ_B) lies between the ranges of Tm^{II} (4.5 μ_B) and Tm^{III} (7.0–7.5 μ_B). This decreased magnetic moment was attributed to exchange interaction between two trivalent thulium atoms.

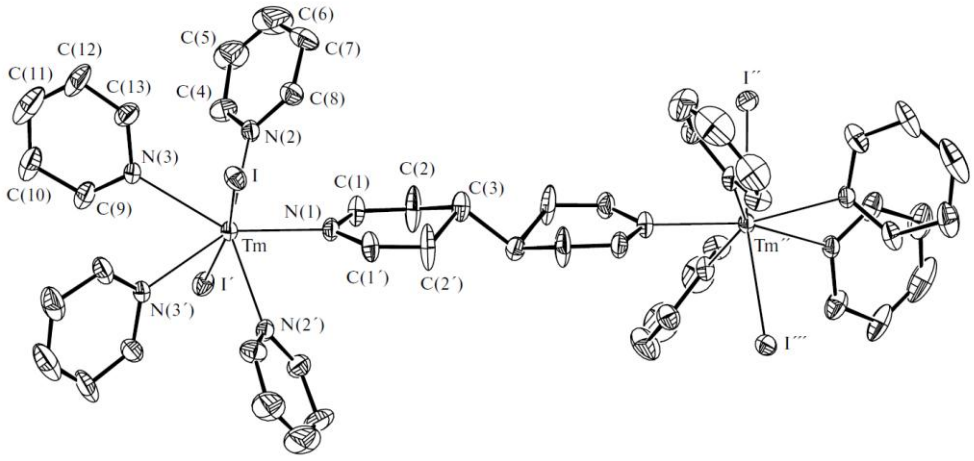

Figure 57: Reductively coupled $[\{TmI_2(C_5H_5N)_4\}_2(\mu_2\text{-}N_2C_{10}H_{10})]$, reproduced from literature.[345]

Evans noted a similar result in the reaction of $(C_5Me_5)_2Sm$ with pyridine, which formed $[\{(C_5Me_5)_2Sm(pyr)\}_2(\mu\text{-}N_2C_{10}H_{10})]$.[268] Thulium iodide is a stronger reducing agent than samarium diiodide, with a reduction potential of −2.0 V compared to −1.5 V for samarium diiodide. The redox potential of $[(C_5Me_5)_2Sm]$ is hard to measure due to insolubility, however an estimate of $E_{1/2}$ at −2.66 V vs ferrocene/ferrocenium has been based on the electrochemical reduction of $[(C_5Me_5)_3Sm]$ in THF at Sb, Au and Pt electrodes.[346]

Previous work has established that different ligand environments affect the reductive reactivity of a thulium(II) metal centre.[293] In comparing the reactivity of two similar thulium(II) complexes with pyridine, it was found that one reductively dimerises pyridine instantaneously (Figure 58), whilst the other reacts slowly via a coordinated adduct.[94, 293]

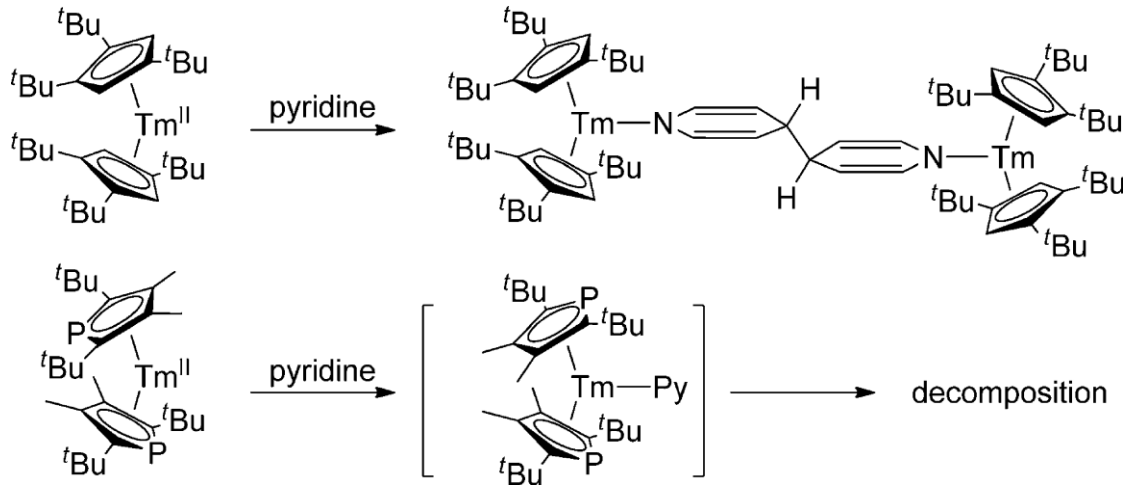

Figure 58: Reactivity of cyclopentadienyl- and phospholyl-based Tm(II) complexes with pyridine, reproduced from literature.[293, 336]

This is just one of a number of examples showing that a phospholyl thulium(II) complex is more stable and less reactive than an analogous cyclopentadienyl thulium(II) complex.[94, 195, 293, 336] Both ligands are of a similar size, indicating that the difference in reactivity lies within the electronic structure of the ligand. Maron and Nief concluded that the transfer of an electron from the thulium(II) to pyridine, the key step of this reaction, is more effective when the metal centre is bound to a cyclopentadienyl ligand instead of phospholyl.[94] Phospholyl ligands have been shown to be less electron-donating than cyclopentadienyl ligands of similar bulk when bound to uranium.[347] Cyclopentadienyl is a stronger electron donor than phospholyl, which in turn makes the Sm^{II}/Sm^{III} redox potential of coordinated samarium more negative.[336, 348, 349]

Bis(pentamethylcyclopentadienyl)samarium(II) reductively dimerises CO_2 to form an oxalate complex. Similar to the above pyridine reaction, this also involves the transfer of an electron from the metal to coordinated CO_2 as a first step.[350] Recent DFT computational work has successfully reproduced this experimentally observed behaviour in pentamethylcyclopentadienyl $(C_5Me_5)^-$ and phospholyl $(C_4Me_4P)^-$ complexes of thulium and samarium(II) (Figure 59) in reactions with pyridine and CO_2.[94] Calculated theoretical results were found to be consistent with observed experimental data. The phospholyl ligand was shown to have a stabilising effect in complexes with both samarium(II) and thulium(II).

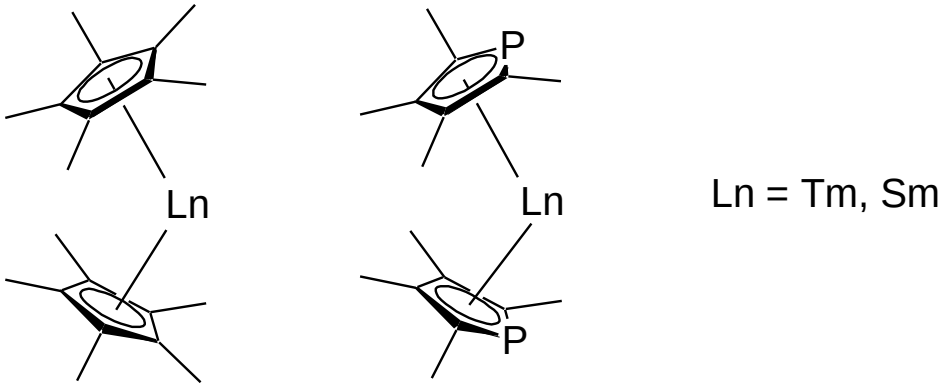

Figure 59: $[(C_5Me_5)_2Ln]$ and $[(C_4Me_4P)_2Ln]$ complexes investigated by DFT.[94]

Pentamethylcyclopentadienyl and tetramethylphospholyl are both π-binding ligands of similar size. The presence of phosphorus in the phospholyl ligand changes the electronic properties of the ligand. These two ligand types were the subject of a recent experimental and theoretical study of the reaction of pyridine and acridine with $[(C_5Me_5)_2Sm(THF)_2]$ and $[(C_4Me_4P)_2Sm]$.[336] With the more stabilising phospholyl ligand, a coordinated pyridine adduct, $[(C_4Me_4P)_2Sm(pyr)_2]$ was formed. Reaction of $[(C_5Me_5)_2Sm(THF)_2]$ with pyridine resulted in reductive coupling and oxidation of the samarium (Figure 60), similar to the $[(C_5Me_5)_2Tm^{II}]$ complex above. Interestingly, the phospholyl complex that did not reduce pyridine was able to reductively dimerise acridine, a better π-acceptor than pyridine.

The ligand environment of a lanthanide centre determines its reactivity, and therefore whether pyridine will form an adduct or be reductively coupled. The transfer of an electron from the metal centre to pyridine is the key step of the activation.

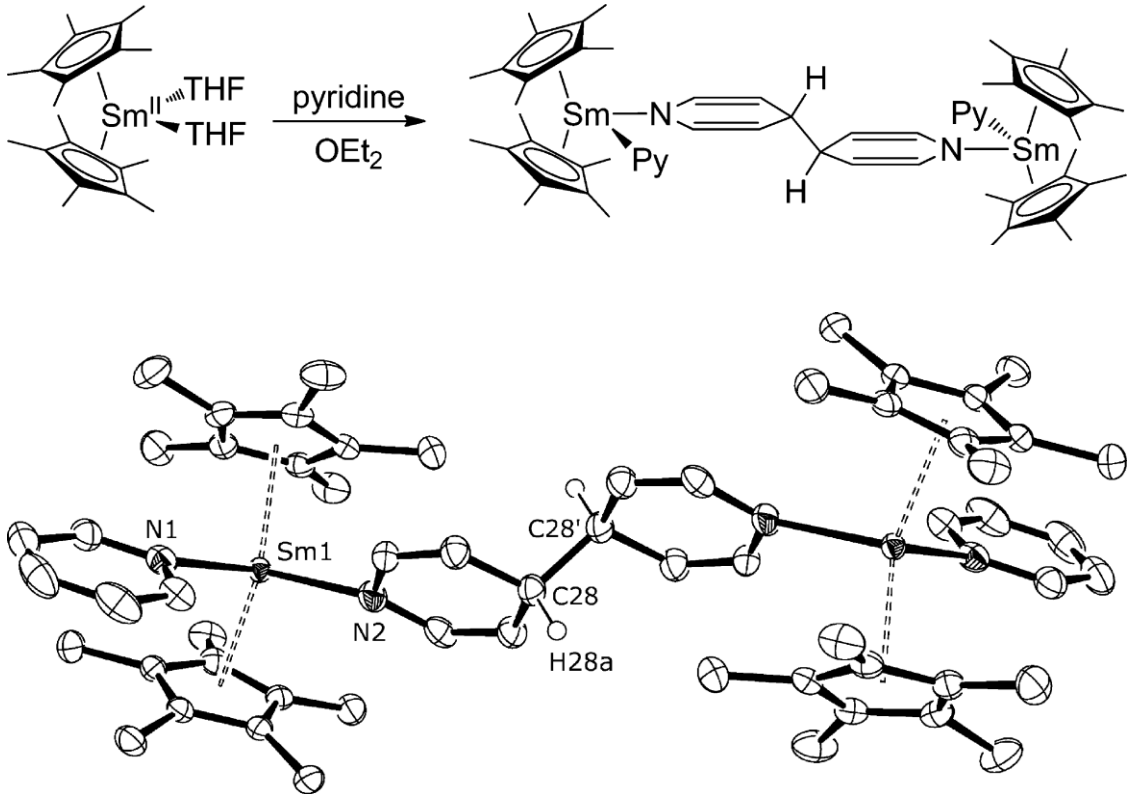

Figure 60: Reductive coupling of pyridine with $[(C_5Me_5)_2Sm(THF)_2]$ and X-ray structure of $[\{(C_5Me_5)_2Sm(pyr)\}_2\{\mu\text{-}(NC_5H_5\text{-}C_5H_5N)\}]$, reproduced from literature.[336]

When coordinated to samarium, for example, the metal-pyridine bond may be neutral (f^6-pyridine^0) or form a samarium(III) radical anion complex (f^5-L$^{\bullet-}$). Formation of a ytterbium(III) radical anion complex with 2,2'-bipyridine and phenanthroline was measured by Andersen using magnetic susceptibility,[351, 352] with supporting evidence provided by Morris using cyclic voltametry, UV-vis-near-IR electronic absorption and Raman spectroscopy.[353] The observed inconclusive oxidation state is supportive of the work by James, which indicates the metal centre is somewhere between Sm^{II} and Sm^{III}, indicating the partial transfer of an electron.[268]

Generally a longer Sm–N(pyr) bond is observed when pyridine is neutrally coordinated, and a shorter bond if the ligand has been reduced by the metal centre. Examples of samarium(II) complexes with neutral pyridine adducts have a lanthanide–nitrogen bond distance around 2.6-2.7 Å, for example SmI_2(3,5-dimethylpyr)$_4$ (Sm–N = 2.708(10) Å),[354] and [(tmp)$_2$Sm^{II}(pyr)$_2$] (Sm–N 2.644 Å) (tmp = 2,3,4,5-tetramethyl-1H-phosphol-1-yl).[336] Samarium(III) complexes generally have shorter Sm–N bond lengths, around 2.4-2.5 Å, as seen in [{$(C_5Me_5)_2Sm$}$_2${μ-(NC_5H_5-C_5H_5N)}] in Figure 60 above (Sm–N = 2.547 Å to neutral pyr ligand).[336] The limited number of literature compounds available does not allow for an in-depth analysis of coordination number-dependant bond lengths to be considered.

This is not a strict rule, and complexes with Sm–N bond lengths between the generally observed 2.4-2.5 Å for Sm^{III} and 2.6-2.7 Å for Sm^{II} are not uncommon. Therefore the M–N bond distance is not a definitive measure of whether a samarium metal centre is in the 2+ or 3+ oxidation state, and the sterics involved also influence bond lengths within a metal complex. There are examples of neutral pyridine adducts binding samarium(II) with significantly shorter bond lengths, such as [$(C_5Me_5)_2$(pyr)$_2$Sm] (Sm–N = 2.540 Å).[355] These complexes may be examples of a metal centre that is informally between samarium(II) and samarium(III). There are also examples of Sm^{III} complexes with longer bonds such as [$(C_5Me_5)_3$Sm^{III}(pyr)] (Sm–N = 2.656 Å)[338] and [$(C_5Me_5)_2$(pyr)SmOSm(pyr)$(C_5Me_5)_2$] (Sm–N 2.561-2.576 Å).[356]

In the present study, pyridine-based molecules of increasing size are used to investigate the binding capacity of Sm^{II} stabilised by the flexible $(Me_8N_2Ph_2)^{2-}$ ligand. Resulting products will be compared where appropriate to analogous complexes of the more rigid $(Et_8N_4Me_2)^{2-}$ ligand system introduced in Section 1.5. Figure 61 shows the two macrocyclic ligands side by side.

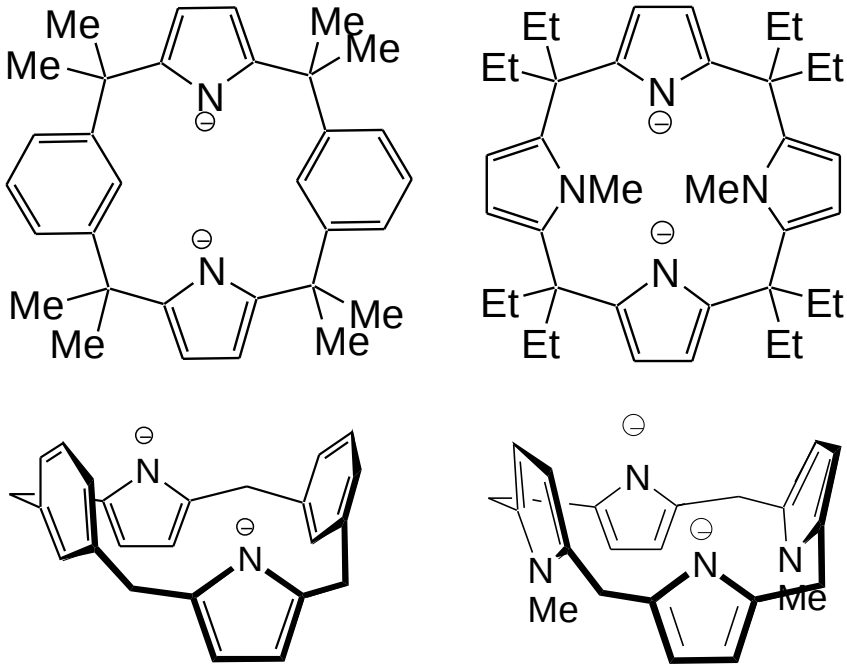

Figure 61: Flat and side-on diagrams of $(Me_8N_2Ph_2)^{2-}$ and $(Et_8N_4Me_2)^{2-}$ macrocyclic ligand systems (*meso*-alkyl groups omitted from side-on projections for clarity).

Whilst the more flexible system will adapt to accommodate ancillary ligands, as seen in Chapter 2, analogous complexes of the more rigid *N*-methylated ligand may instead see ancillary ligands forced to adopt less favoured binding modes. An example of this is seen in the binding of the large cyclooctatetraendiyl ligand to a $(Me_8N_2Ph_2)^{2-}$ samarium complex reported by Frey, and shown in Scheme 13.[307]

Scheme 13: Addition of COT to $[(Me_8N_2Ph_2)Sm^{II}(THF)]$ to form $[(Me_8N_2Ph_2)Sm^{III}(THF)]^+[(Me_8N_2Ph_2)Sm^{III}(COT)]^-$.[307]

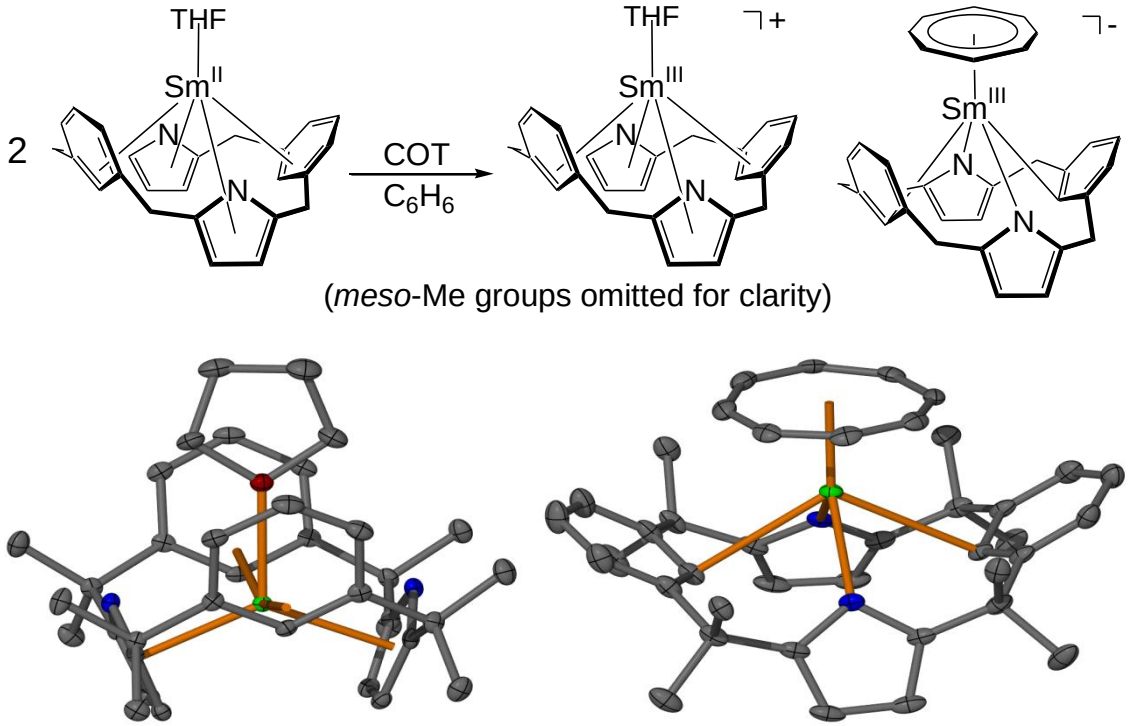

Here the samarium(II) complex reacts to form a separated cation/anion product. The cation is a Sm^{III} mono(THF) complex, the change in oxidation state demonstrated by changes to bond lengths between the ligand and metal, and in changes to the NMR spectrum of the complex in solution. The anion is a COT^{2-} complex, with the sterically bulky COT^{2-} binding η^8, forcing the macrocyclic ligand into an η^1:η^1:η^1:η^1 binding scheme. To achieve this the macrocyclic units splay outwards, resulting in a shallow macrocyclic cavity. The metal centre sits much higher in the macrocyclic cavity relative to the phenylene groups when compared to the cation. The anionic product is an example of the flexibility of the $(Me_8N_2Ph_2)^{2-}$ ligand and its adaptability in binding. By

contrast, the cyclooctatetraendiyl complex of $(Et_8N_4Me_2)^{2-}$ highlights the rigidity of this macrocycle, as shown in Scheme 14.

Scheme 14: Addition of COT to $[(Et_8N_4Me_2)Sm^{II}(THF)_2]$.

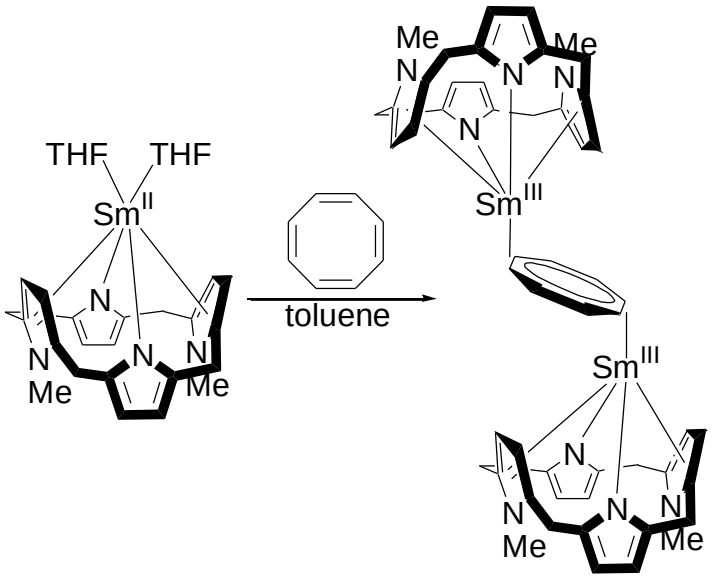

The $(Et_8N_4Me_2)^{2-}$ macrocycle is not flexible enough to accommodate the COT^{2-} ligand bound μ^8 to samarium 1:1, and instead the COT^{2-} is forced to bridge between two macrocyclic units, binding η^2 to each Sm^{III}. The COT complexes of these two related macrocyclic systems, shown side by side in Figure 62, emphasise their differences in conformational flexibility.

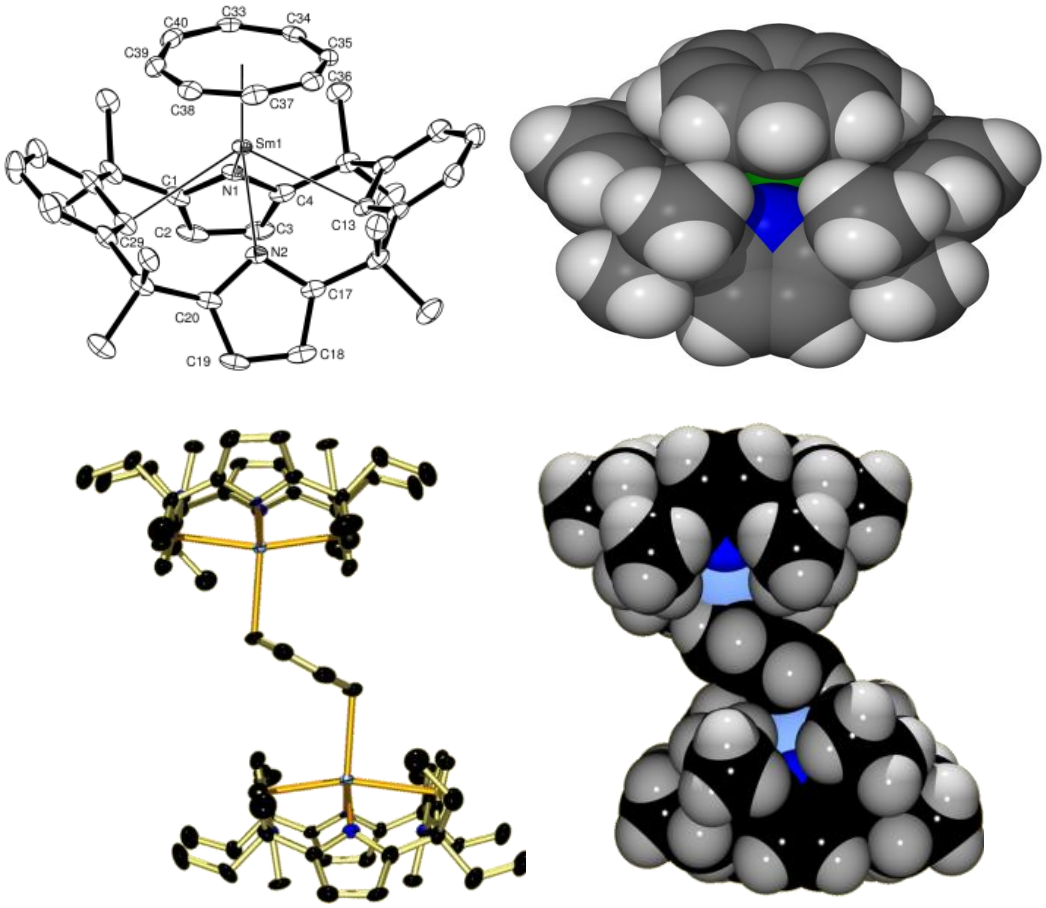

Figure 62: Side by side comparison of samarium COT complexes of the $(Et_8N_4Me_2)^{2-}$ and $(Me_8N_2Ph_2)^{2-}$ macrocyclic ligand systems.[266, 307]

Research Aim

The $(Me_8N_2Ph_2)^{2-}$ ligand with its flexibility in binding modes has the potential to form stable complexes with a range of lanthanide metal centres varying in size and oxidation state. We aim to utilise the adaptability of the ligand to prepare a series of lanthanide complexes to further investigate hapticity changes seen with a series of heterocyclic ligands of increasing bulk and varying electronic properties.

It is important to identify how reactive the flexible and adaptable $(Me_8N_2Ph_2)^{2-}$ ligand is in order to assess potential applications or possible further modifications. The precursor complex $[(Me_8N_2Ph_2)Sm(THF)_2]$ will be reacted with a series of pyridine-based heterocycles and close diazine analogues in order to investigate and assess its reductive strength. Identifying the reactivity of complexes of this ligand is an important step to determining its utility in synthesis.

Pyridine-based heterocycles of different reductive susceptibilities, sterics and electronic properties were selected. Previous work by James investigated the reductive ability of $(Et_8N_4Me_2)^{2-}$ lanthanide complexes and, where relevant, his results will be compared with related $(Me_8N_2Ph_2)^{2-}$ complexes in this Chapter.

3.2 Results and Discussion

Complexes in this Chapter include pyridine- and diazine-based ligands shown in Figure 63. Pyridine-based heterocycles are introduced in Section 3.2.1, and linked- and fused-ring heterocycles in Section 3.2.2. Diazines and related heterocycles are reported in Section 3.2.3 to establish the reductive capacity of samarium $(Me_8N_2Ph_2)^{2-}$ complexes in the presence of different electronic environments.

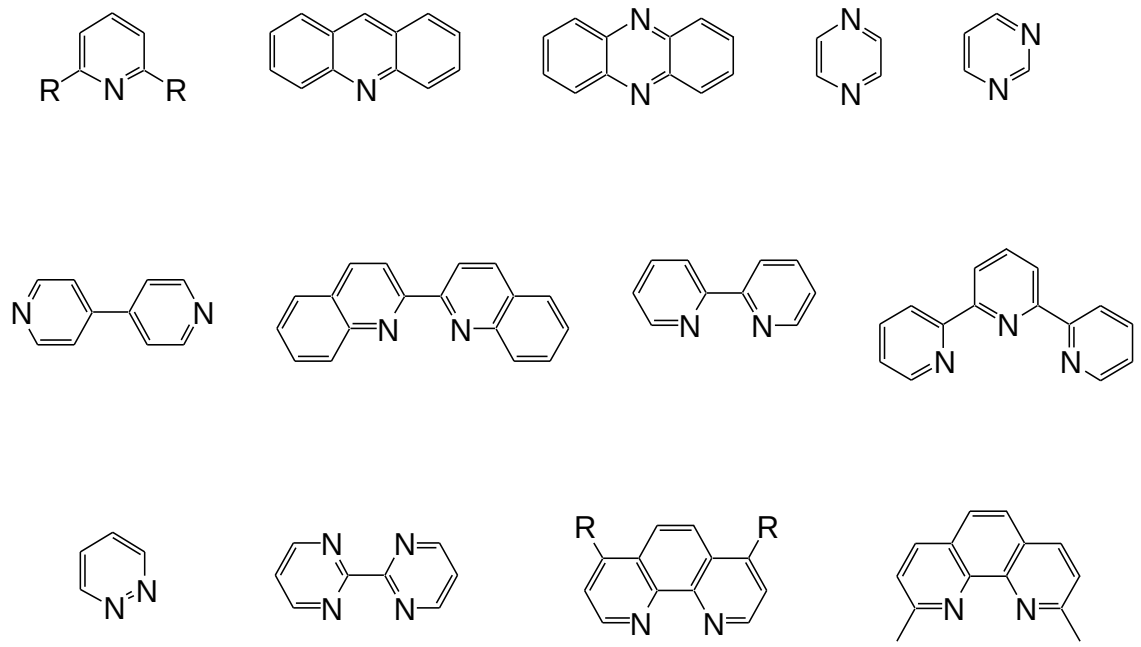

Figure 63: N-heterocyclic ligands investigated in this Chapter.

Reactions of $[(Me_8N_2Ph_2)Ln(THF)_x]$ (Ln = Sm, Eu; x = 1, 2) with the pyridine-based molecules were carried out in aromatic solvent. In most cases the reaction proceeded at room temperature, either immediately or over a 24 – 72 hr period. Products were typically isolated by crystallisation from solution, with some assisted by slow evaporation of solvent.

Many of these product complexes are sparingly soluble, preventing thorough characterisation in solution. Analysis by NMR spectroscopy was attempted for all soluble complexes obtained in sufficient yield, although the presence of a paramagnetic metal centre often resulted in only partial assignment of resonances. Therefore the characterisation of complexes and oxidation state in solution is limited in this work. Elemental analysis was attempted for all complexes, however the low solubility often

prevented successful recrystallisation, which resulted in satisfactory results for only a handful of products. Solid state crystal structures were obtained by single crystal X-ray diffraction.

3.2.1 The Reactivity of $(Me_8N_2Ph_2)Ln(II)$ Complexes with Pyridines

As established in Section 3.1, pyridine can coordinate metal centres through the lone pair localised on the nitrogen atom, and it is a well-known ligand in lanthanide chemistry. It was important to establish whether pyridine would displace THF in the samarium bis-THF precursor complex (**3**), and if there were differences between pyridine and THF complexes. As noted in the introduction to this Chapter, pyridine may coordinated to form an adduct or be reductively coupled depending on the stabilising ability of the ligand set. If the pyridine coordinates as a neutral adduct, this will be reflected in strong shifting of resonances in solution ^{1}H NMR spectra. It will also be apparent in the geometry of the single crystal molecular structure. As noted in Section 3.1, the bond length between the metal and coordinated pyridine (M–N) is approximately 2.7 Å for Sm^{2+}–pyr^0 and 2.5 Å for Sm^{3+}–$pyr^{\bullet-}$.

This Section looks at the pyridine-based heterocycles shown in Figure 64. Addition of 2,6-dimethyl substituents to pyridine is an example of a change in sterics compared to pyridine, whilst the triple fused-ring system of acridine has both

increased steric bulk and a more extended aromatic electronic structure better able to be reduced.

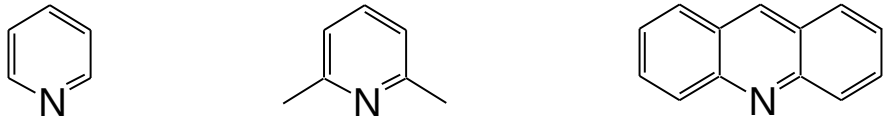

Figure 64: Pyridine, 2,6-dimethylpyridine and acridine are the focus of Section 3.2.1.

Pyridine

Addition of excess pyridine to a dark purple solution of $[(Me_8N_2Ph_2)Sm(THF)_2]$ in benzene formed (over 48 hours) dark purple coloured crystals of $[(Me_8N_2Ph_2)Sm(pyr)_2]$, **11**, as shown in Scheme 15.

Scheme 15: Reaction of $[(Me_8N_2Ph_2)Sm(THF)_2]$ with pyridine to produce $[(Me_8N_2Ph_2)Sm(pyr)_2]$, **11**.

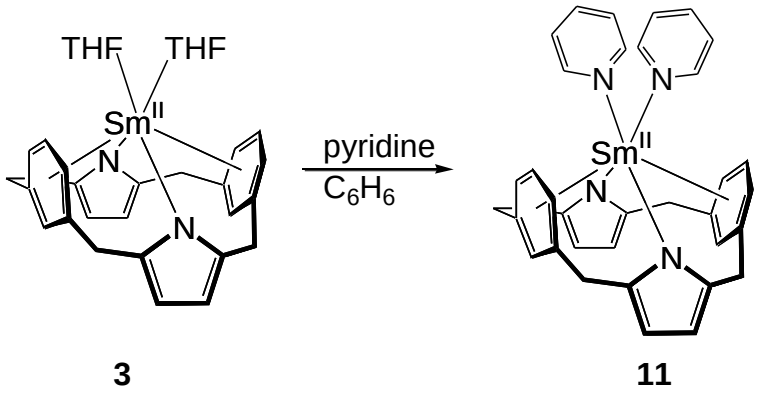

3 **11**

This complex is sparingly soluble in benzene, and was characterised by elemental analysis, NMR spectroscopy and single crystal X-ray diffraction. The observed and calculated elemental analysis were in good agreement. Although the complex was only

sparingly soluble in deuterated benzene, the pale blue solution was sufficient to obtain a ^{1}H NMR spectrum, although this could only be partially assigned.

Two resonances at −3.15 and 11.56 ppm are attributed to the 24 protons of the *meso*-methyl groups, which are oriented toward either face of the macrocycle. Two phenylene protons are observed as a very broad resonance at 132 ppm and are attributed to the protons located closest to the metal centre, on the phenylene C2 atom. The influence of the samarium(II) metal centre causes a dramatic shift of this resonance relative to the remainder of the spectrum, similar to the ^{1}H NMR spectrum of the bis(THF) complex **3**, and indicate the presence of a Sm^{II} centre.

A ^{13}C NMR spectrum was obtained, however the resonances observed were extremely weak in comparison to the C_6D_6 solvent resonance, even when data was collected over 14 hrs. During the 14 hr ^{13}C NMR data collection, the sample solution lost colour and formed yellow crystals. The colour change from blue to yellow is indicative of oxidation of the samarium metal to Sm^{III}.[140] This product was characterised by single crystal X-ray diffraction and its structure will be discussed below, following the targeted pyridine complexes.

Purple single crystals of the bis(pyr) product **11** suitable for X-ray diffraction crystallised from benzene solution over a 24 hr period. The crystal **11** belongs to the orthorhombic space group *P*ccn (No. 56) with a = 13.200(8), b = 14.090(2), c = 18.660(1) Å. The asymmetric unit cell consists of one half of the macrocyclic unit

with one bound pyridine, with a C_2 axis passing through the metal centre. The molecular structure is shown in Figure 65.

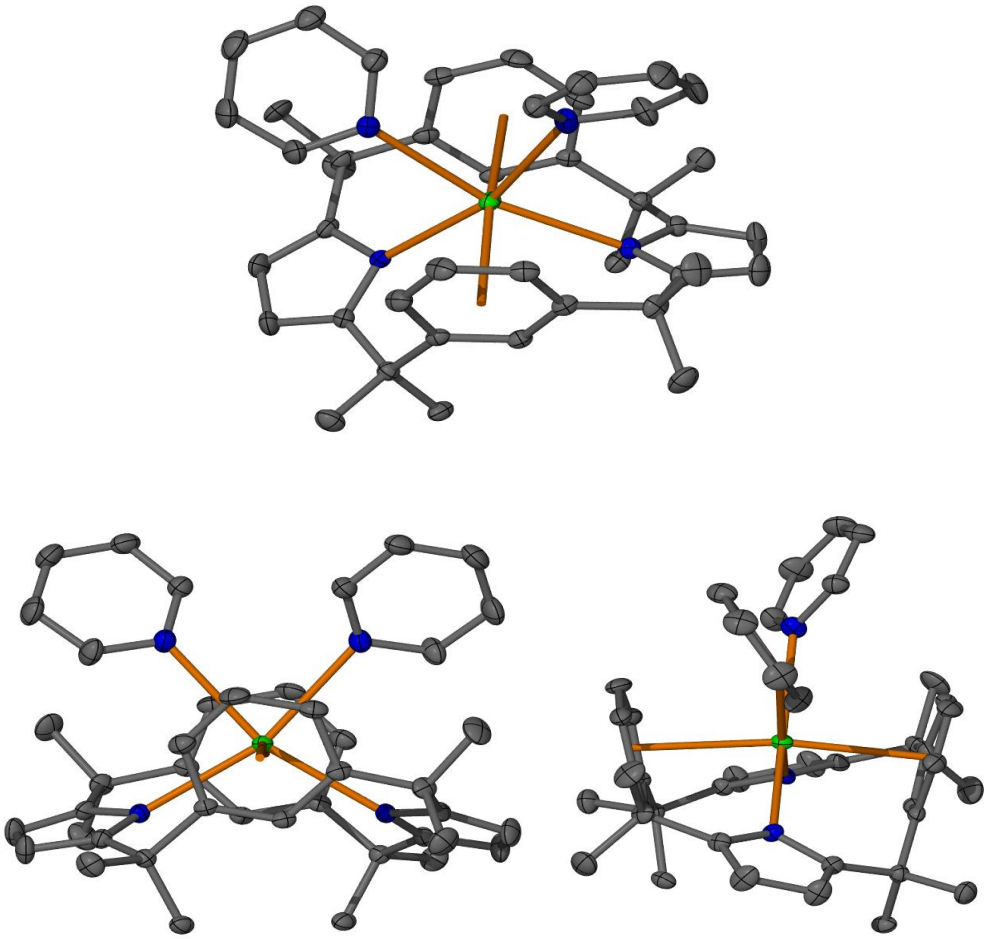

Figure 65: Molecular structure of $[(Me_8N_2Ph_2)Sm(pyr)_2]$, (**11**), with thermal ellipsoids drawn at 50% probability (protons omitted for clarity).

The metal centre sits high in the macrocyclic cavity, in an η^6:η^1:η^6:η^1 binding conformation similar to the analogous bis(THF) and bis(NCMe) complexes. Table 7 compares selected structural properties between these three single crystal structures.

The samarium–pyridine nitrogen bond length of 2.734(2) Å indicates that this is a samarium(II) complex, which is supported by the large chemical shift influences of the paramagnetic samarium(II) centre in the ^{1}H NMR spectrum.

Table 7: Selected bond lengths and angles of complexes **11**, **3** and **8** (L = $(Me_8N_2Ph_2)^{2-}$).

	[LSm(pyr)$_2$] **(11)**	**[LSm(THF)$_2$]** **(3)**	**[LSm(NCMe)$_2$]** **(8)**
M in cavity	High	High	High
M–L (Å)	2.734(2)	2.638(3)	2.648(9)
M– $\eta^x_{(Ph)}$ (Å)	2.77 (η^6)	2.77 (η^6)	2.72, 2.79 (η^6)
$\theta_{(Ph)}$ (°)	169.7 (η^6)	167.6 (η^6)	176.2 (η^6)
Φ (°)	25.5	27.6	18.7
M–$\eta^x_{(Py)}$ (Å)	2.592(3) (η^1)	2.614(3) (η^1)	2.589(6) (η^1)
$\theta_{(Py)}$ (°)	NA	NA	NA

A europium bis(pyr) complex was prepared in an analogous reaction combining pyridine with [$(Me_8N_2Ph_2)$Eu$(THF)_2$], **5**. The product, [$(Me_8N_2Ph_2)$Eu$(pyr)_2$], **12**, is analogous and crystallographically isomorphous to the samarium complex **11**. Single crystals of the europium bis(pyr) product **12** suitable for X-ray diffraction were crystallised from benzene solution (a = 13.200(8), b = 14.090(2), c = 18.660(3) Å). The europium—pyridine nitrogen bond distance is 2.747(2), similar to the samarium–pyridine bond seen in **11**, confirming that this is a samarium(II) complex.

The bis(pyr) complex **11** dissociated a pyridine ligand when heated to 110 °C in benzene for 72 hrs, yielding [$(Me_8N_2Ph_2)$Sm(pyr)], **13**, Scheme 16. This ligand

dissociation is analogous to the loss of a THF from the bis(THF) complex discussed in Chapter 2. This was a small scale reaction, thus the mono(pyr) complex **13** was characterised only by crystallographic analysis.

Scheme 16: Reaction of $[(Me_8N_2Ph_2)Sm(THF)_2]$ with pyridine to produce $[(Me_8N_2Ph_2)Sm(pyr)_2]$, **11** and solvent-driven formation of $[(Me_8N_2Ph_2)Sm(pyr)]$, **13**.

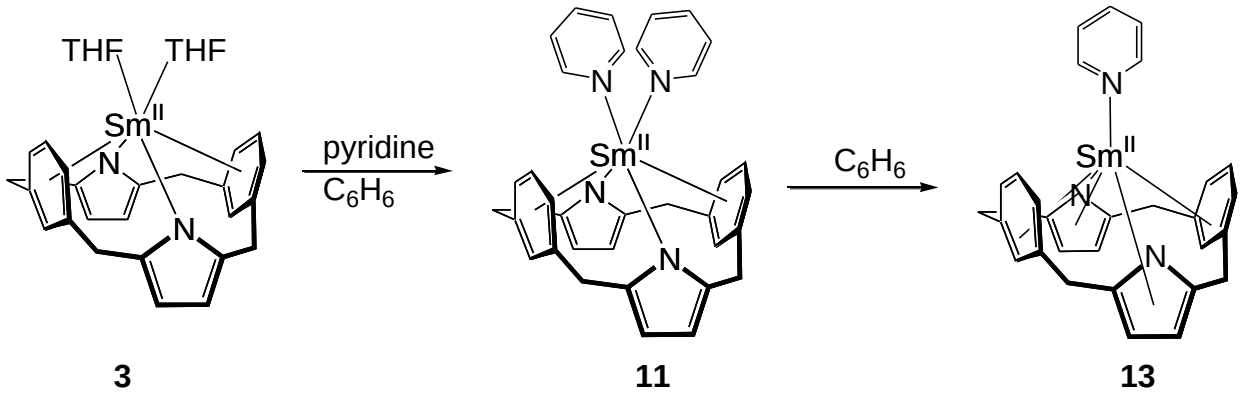

Single crystals of the purple mono(pyr) complex **13** suitable for X-ray diffraction were obtained from benzene. The crystal belongs to the triclinic space group *P*-1 (No. 2) with a = 9.3000(5), b = 10.0800(5), c = 16.2550(6) Å, α = 82.734(1), β = 87.629(2), γ = 75.065(2) °. This structure is shown in Figure 66.

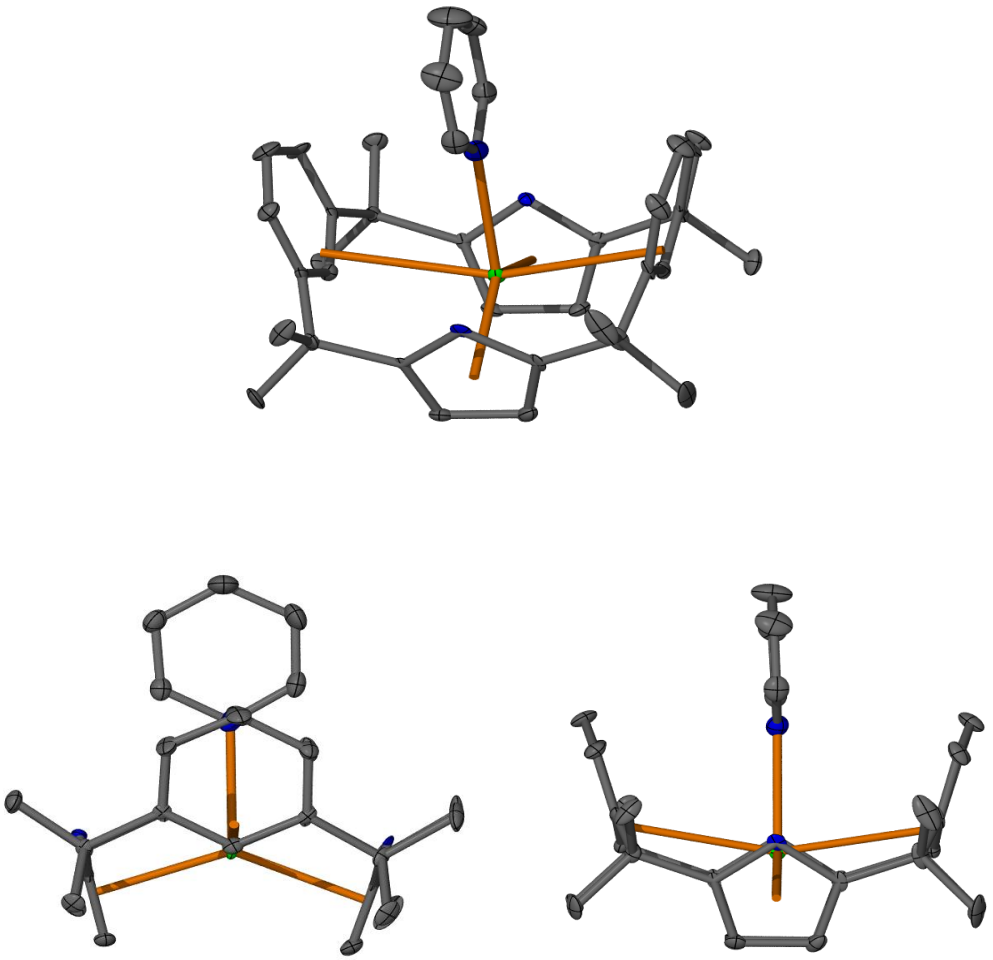

Figure 66: Molecular structure of [($Me_8N_2Ph_2$)Sm(pyridine)], (**13**) with thermal ellipsoids drawn at 50% probability (hydrogens omitted for clarity).

The macrocyclic ligand binds η^3:η^5:η^3:η^5 to the metal centre, with the pyrrolide units bound η^5 to the metal centre, which is seated deep in the macrocyclic cavity. The pyridine molecule is drawn into the macrocyclic cavity and coordinated at a M–N distance of 2.596(3) Å, indicative of Sm^{II}–(pyr).

Parallels can be seen between the coordination and structure of the pyridine and THF complexes. Metal centres in the bis(THF) complex **3** and bis(pyr) complexes **11** (Sm) and **12** (Eu) are each bound η^6:η^1:η^6:η^1 to the macrocycle, whilst the mono(THF) and mono(pyr) complexes (**4** and **13**, respectively) are bound η^3:η^5:η^3:η^5. The four samarium structures are compared in Table 8.

Table 8: Comparison of the mono- and bis-(pyr) and -(THF) complexes (L = $(Me_8N_2Ph_2)^{2-}$).

	[LSm(THF)$_2$] **(3)**	**[LSm(pyr)$_2$]** **(11)**	**[LSm(THF)]** **(4)**	**[LSm(pyr)]** **(13)**
M in cavity	High	High	Low	Low
M–L (Å)	2.638(3)	2.734(2)	2.523(4)	2.596(3)
M–$\eta^6_{(Ph)}$	2.77	2.77	NA (η^3)	NA (η^3)
$\theta_{(Ph)}$ (°)	167.6 (η^6)	169.7 (η^6)	NA (η^3)	NA (η^3)
Φ (°)	27.6	25.5	33.5	28.5
M–$\eta^x_{(Py)}$	2.614(3) (η^1)	2.592(3) (η^1)	2.53, 2.53 (η^5)	2.48, 2.49 (η^5)
$\theta_{(Py)}$ (°)	NA	NA	131.6	136.4

An Oxygen-bridged Pyridine Complex

As noted above, one sample of the samarium bis(pyr) complex (**11**) in C_6D_6 solution was observed to bleach to colourless, forming yellow crystals overnight. This colour change is characteristic of the oxidation of samarium(II) to samarium(III), and was attributed to a very slow leak of the Young's tube containing the solution. Single crystal X-ray diffraction identified the yellow crystals as an oxygen-containing product **14**, shown in Figure 67.

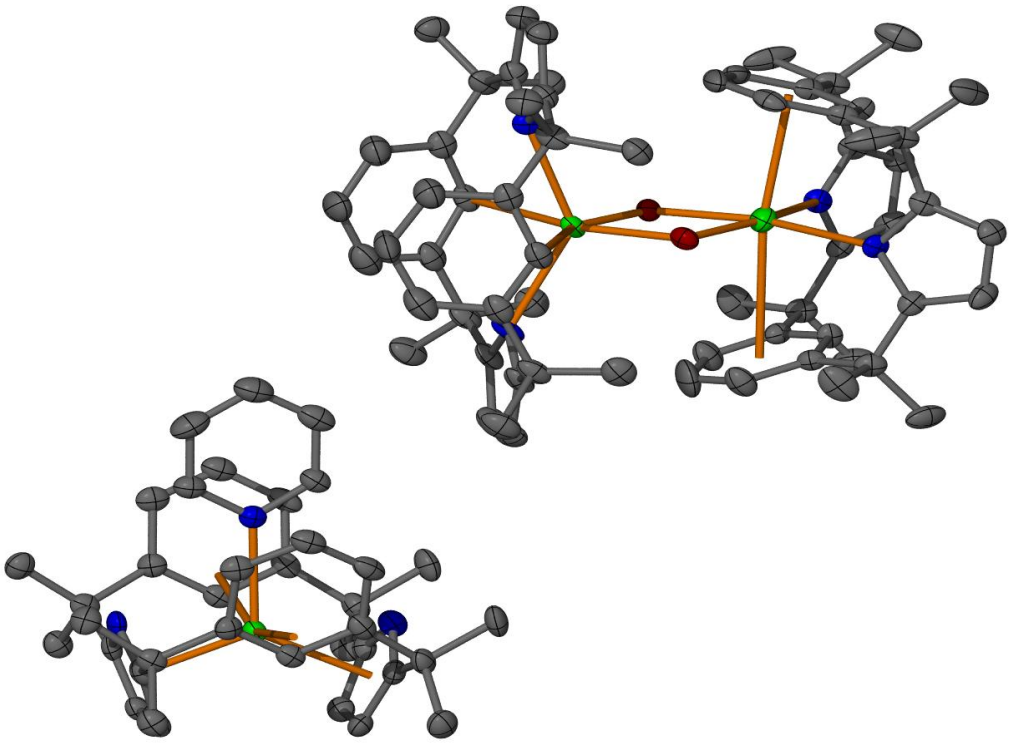

Figure 67: Structure of $[(Me_8N_2Ph_2)Sm^{III}(pyr)]^{+}{}_2[\{(Me_8N_2Ph_2)Sm^{III}(\mu\text{-}O)\}_2]^{2-}$ **14**.

Due to the proximity of the heavy samarium atoms and poor diffraction data, it is not possible to determine conclusively from this X-ray diffraction data whether these are bridging oxygens or hydroxides. However the Sm–N(pyridine) bond length in the pyridine component is 2.518(8) Å, shorter than that in the mono(pyr) complex (2.596(3) Å). This suggests that this may be a Sm(III) cation, contrasting with the Sm(II) mono-pyridine neutral adduct. This would establish the formula as $[(Me_8N_2Ph_2)Sm^{III}(pyr)]^{+}{}_2[\{(Me_8N_2Ph_2)Sm^{III}(\mu\text{-}O)\}_2]^{2-}$. The presence of the oxygen confirms that a slow leak of air into the vessel has formed this complex. Interestingly, two different binding modes of the macrocycle are seen in the dianion component, $\eta^6{:}\eta^1{:}\eta^6{:}\eta^1$ and a new $\eta^1{:}\eta^1{:}\eta^1{:}\eta^1$ mode where the samarium metal atom is 'pulled'

through to the other cavity face. This rogue decomposition product was not characterised further.

2,6-Dimethylpyridine

2,6-Dimethylpyridine (also known as 2,6-lutidine) is a sterically hindered weakly nucleophilic molecule.[357] A molar excess of 2,6-dimethylpyridine (432 μmol) was added to a benzene solution of [($Me_8N_2Ph_2$)Sm(THF)$_2$], **3**, (30 mg, 45 μmol) with no immediate change observed. Over a 72 hr period with slow evaporation, dark green crystals of [($Me_8N_2Ph_2$)Sm(2,6-dimethylpyr)], **15**, were obtained. The reaction is shown in Scheme 17. The crystalline product was very sparingly soluble in benzene and toluene. Due to the insolubility of this product characterisation rests on the X-ray crystal structure analysis.

Scheme 17: Reaction of 2,6-dimethylpyridine with [($Me_8N_2Ph_2$)Sm(THF)$_2$], **3**, to form [($Me_8N_2Ph_2$)Sm(2,6-dimethylpyr)], **15**.

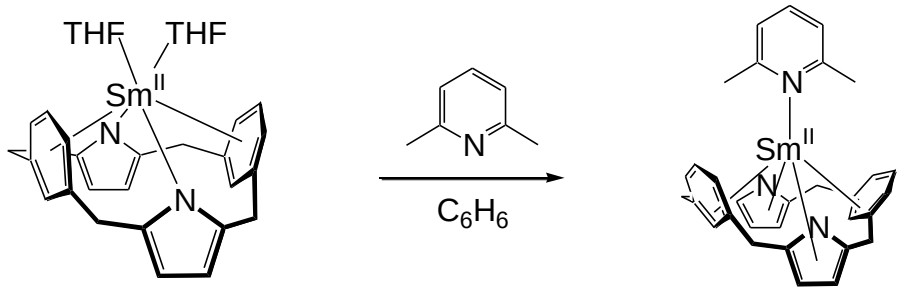

3 **15**

Dark green crystals of **15** suitable for X-ray diffraction were isolated from solution and washed with benzene. The crystal belongs to the orthorhombic space group *P*bca (No. 61) with a = 16.279(2), b = 17.542(2), c = 25.576(2) Å. The molecular structure is shown in Figure 68.

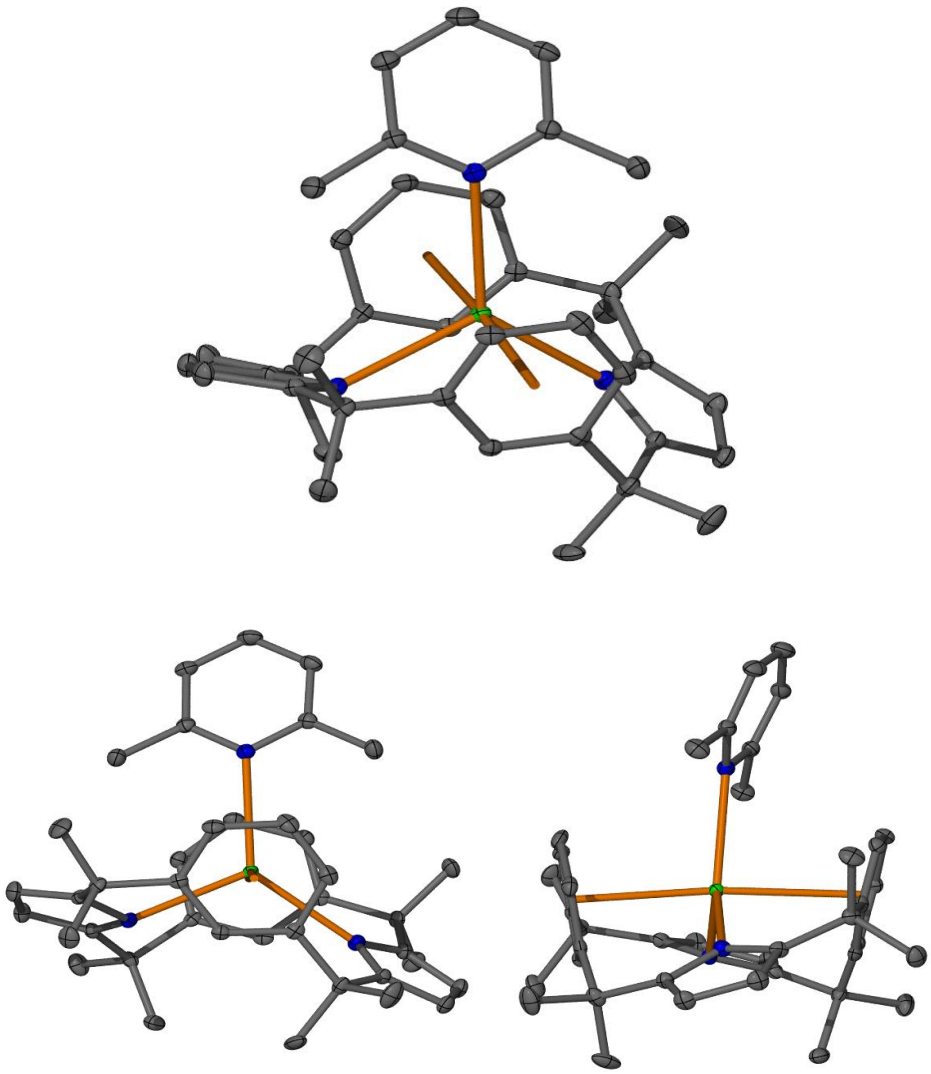

Figure 68: Molecular structure of [($Me_8N_2Ph_2$)Sm(2,6-dimethylpyr)], **15** with thermal ellipsoids drawn at 50% probability (protons omitted for clarity).

The metal centre sits high in the macrocyclic cavity, approximately between the centroids of the phenylenes. The metal centre is bound η^6:η^1:η^6:η^1 to the ligand, which differs from the mono(pyr) complex which binds low in η^3:η^5:η^3:η^5 fashion. The addition of the methyl groups to the pyridine causes this mono-ligated complex to adopt a binding mode more similar to the bis(pyr) **11** than the mono(pyr) **13**.

Table 9: Comparison of selected single crystal measurements between [($Me_8N_2Ph_2$)Sm(2,6-dimethylpyridine)] (**15**) and [($Me_8N_2Ph_2$)Sm(pyr)] (**13**) (L = $(Me_8N_2Ph_2)^{2-}$).

	[LSm(2,6-dimethylpyr)] (15)	**[LSm(pyr)] (13)**
M in cavity	High	Low
M–N (Å)	2.703(2)	2.596(3)
M–$\eta^6_{(Ph)}$ (Å)	2.68, 2.78	NA (η^3)
$\theta_{(Ph)}$ (°)	173.5 (η^6)	NA (η^3)
Φ (°)	20.1	28.5
M–$\eta^x_{(Py)}$ (Å)	2.534(2), 2.553(2) (η^1)	2.48, 2.49 (η^5)
$\theta_{(Py)}$ (°)	NA	136.4

As seen in the pyridine complexes **11** and **13**, the M–N bond distance of 2.703(2) Å indicates that the samarium metal centre is in a 2+ oxidation state. In comparison to the mono(pyr) complex **13**, which has approximately C_{2v} symmetry, the 2,6-dimethylpyridine complex has not only a different conformation and binding mode, but also distinctly inequivalent pyrrolide groups apparent from the distance of the Sm centre from the heterocyclic planes. The ancillary 2,6-dimethylpyrrolide sits within the macrocyclic cavity with a distinct lean towards one of the phenylene moieties. Crystal packing influences cannot be excluded as the cause of this structure.

Whilst the methyl groups on 2,6-dimethylpyridine are not a large steric addition, their proximity to the macrocyclic ligand are presumably affecting the macrocycle conformation, and therefore the binding mode to the metal centre (Figure 69). If the 2,6-dimethylpyridine complex were to have the same conformation and binding mode as the mono(pyr) analogue, lone pairs on the nitrogens of the η^5 pyrrolide units would be directed toward the methyl groups of the 2,6-dimethylpyridine, which is sterically unfavourable. The macrocycle instead changes conformation in order to accommodate the 2,6-dimethylpyridine ligand.

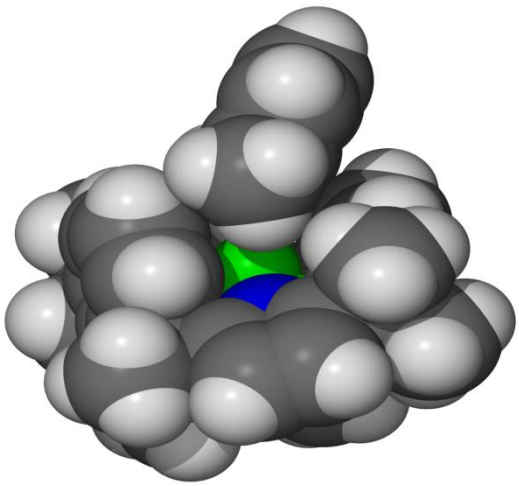

Figure 69: Spacefilling diagram of [($Me_8N_2Ph_2$)Sm(2,6-dimethylpyr)] **15** showing 2,6-dimethylpyridine coordination in the macrocyclic cavity.

Acridine

Acridine is a molecule with more steric bulk and a different electronic environment to pyridine and 2,6-dimethylpyridine. The fused tricyclic system of acridine is significantly larger and is a better π-acceptor than pyridine. With the extended aromatic

structure of acridine compared to pyridine, a reduced form of acridine would be expected to be more electronically stable than a pyridine analogue.

As noted in Section 3.1 acridine can be reductively coupled at the 7-position in the presence of reducing lanthanide(II) such as $[(C_5Me_5)_2Sm]$[135] or $[(C_4Me_4P)_2Sm]$.[336] The related macrocyclic ligand $[(Et_8N_4Me_2)Sm(THF)_2]$ also reductively dimerises acridine.[268]

As shown in Scheme 18, a solution of acridine in benzene was added to a solution of $[(Me_8N_2Ph_2)Sm(THF)_2]$, **3**, immediately resulting in a colour change from purple to green. A dark green crystalline product was collected after 72 hrs. This product is very sparingly soluble in benzene, preventing recrystallisation or analysis by NMR spectroscopy. Elemental analysis was unsuccessful despite multiple attempts, which may be explained by the presence of a second product. Under the microscope both green and purple crystals were observed in the crude product. Single crystal X-ray diffraction of the purple product was not successful despite multiple attempts, however green single crystals suitable for X-ray diffraction were found to be a reductively coupled product $[\{(Me_8N_2Ph_2)Sm\}_2(\mu$-7,7'-dihydro-biacridine$)]$, **16**, shown in Figure 70. The green crystal of complex **16** belongs to the monoclinic space group $P2_1/c$ (No. 14) with a = 24.641(5), b = 10.691(3), c = 31.206(5) Å, β = 101.476(6) °.

Scheme 18: Reaction of acridine with [($Me_8N_2Ph_2$)Sm($THF)_2$], **3**, to form [{($Me_8N_2Ph_2$)Sm}$_2$(μ-7,7'-dihydro-biacridine)], **16.**

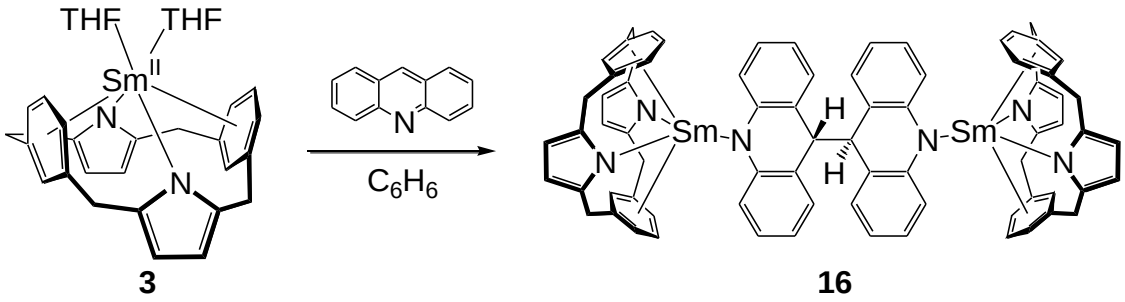

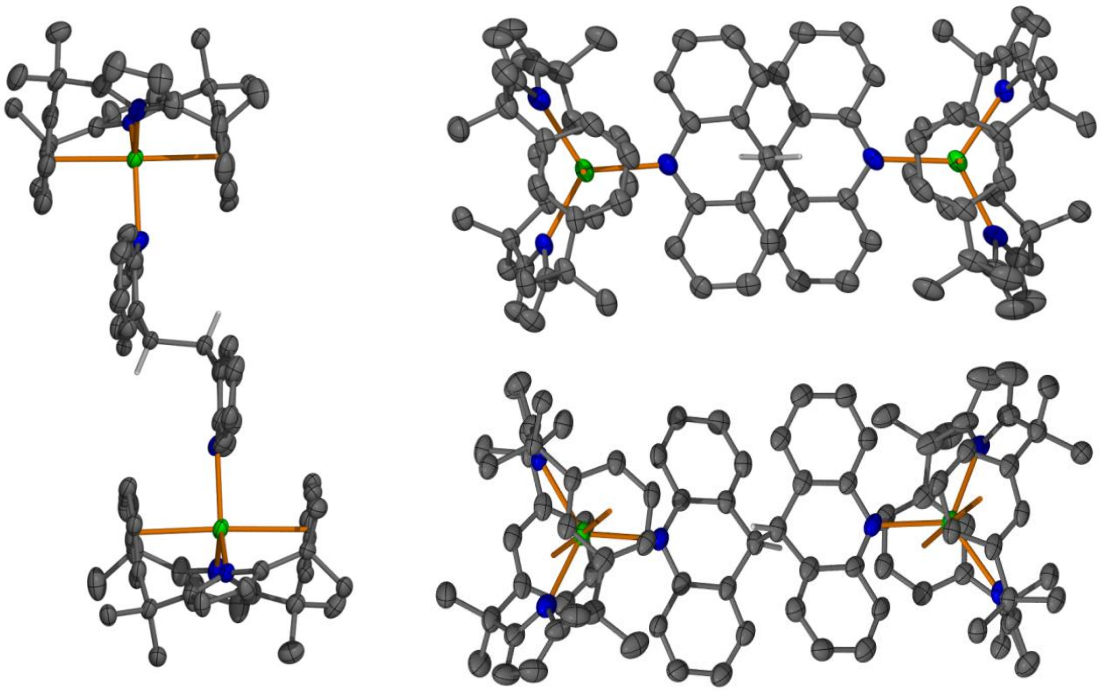

Figure 70: Molecular structure of [{($Me_8N_2Ph_2$)Sm}$_2$(μ-7,7'-dihydro-biacridine)], **16,** with thermal ellipsoids drawn at 50% probability.

The complex **16** contains reductively coupled acridine groups bound through C7 carbons. The Sm–N bond lengths to the acridine are 2.389(6) and 2.408(6) Å, indicating that the acridine has been reduced and the metal centre is samarium(III). This is consistent with Sm–N distances of 2.38 Å in the related reductively coupled phospholyl complex $[\{(\eta^5\text{-}C_4Me_4P)_2Sm\}_2(\mu\text{-}\eta_3\text{:}\eta_3\text{-}C_{13}H_9N)_2]$,[135] and 2.38 Å in $[\{(Et_8N_4Me_2)Sm\}_2(\mu\text{-}7,7'\text{-dihydro-biacridine})]$.[268] The macrocyclic geometry (η^6:η^1:η^6:η^1) is also consistent with the structures observed in the bis(THF), bis(pyridine) and 2,6-dimethylpyridine complexes. This geometry is also likely to be dictated in avoiding pyrrolide:acridine interactions which would expected to occur for a deeply-sitting Sm centre binding η^3:η^5:η^3:η^5.

3.2.2 The Reactivity of $(Me_8N_2Ph_2)Ln(L)$ Complexes with Linked or Fused Pyridine Ligands

This investigation into bulkier ligands was extended to related pyridine-based heterocycles, as shown in Figure 71. Linked pyridines in the form of 2,2'-bipyridine (bipy) and 2,2':6',2''-terpyridine (terpy) are also investigated and complexes of these larger bidentate and tridentate molecules are compared with analogous complexes of the related $(Et_8N_4Me_2)^{2-}$and $2(C_5Me_5)^-$ lanthanide complexes. The large fused-ring systems of 1,10-phenanthroline, structurally related to 2,2'-bipyridine, are included in this work. The investigation of these large delocalised systems are further expanded by including 4,7-disubstituted-1,10-phenanthrolines.

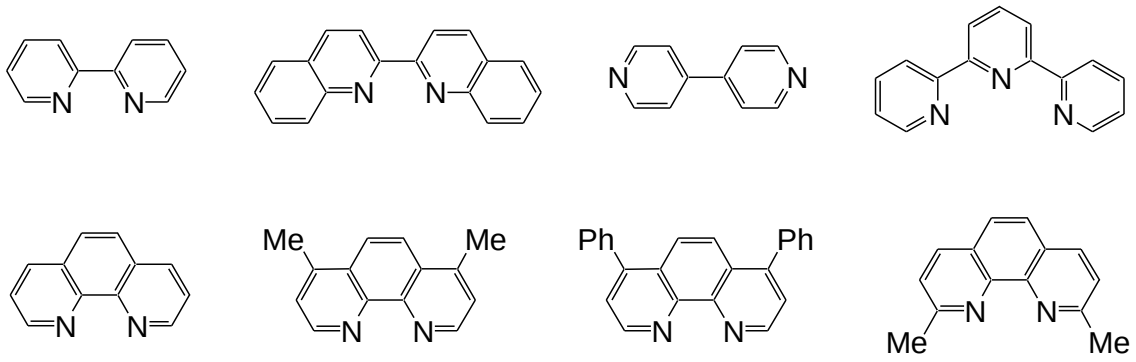

Figure 71: Linked pyridines 2,2'-bipyridine, 2,2'-biquinoline, 4,4'-bipyridine, 2,2';6',2"-terpyridine and fused pyridines 1,10-phenanthroline, 4,7-dimethyl- and 4,7-diphenyl-1,10-phenanthroline, 2,9-dimethyl-1,10-phenanthroline.

2,2'-Bipyridine

2,2'-Bipyridine is the molecule formed by two pyridines linked through the C2 carbons. Chelating bipyridines are well-established ligands in coordination chemistry of the lanthanides.[343, 351, 352, 358-361] Two nitrogen atoms are available to σ-bind a metal centre in addition to the π-accepting orbitals of the ring. 2,2'-Bipyridine is able to bind as a neutral ligand or be reduced by either one or two electrons. Even when bound as a neutral ligand the bipyridine can act as an 'electron reservoir'.[362] This flexibility in redox as well as relative ease of functionalisation make it a very useful ligand.

When reduced, the C–C bond linking the two pyridines shows the most significant change in bond distance, as shown in Table 10. When free or bound as a neutral ligand, this bond is approximately 1.50 Å in length. If the bipyridine is reduced the bond distance shortens.[363, 364] Neutrally chelated bipyridine retains the same non-coplanar

structure of the free bipyridine, but when reduced the bipy becomes more planar in structure.

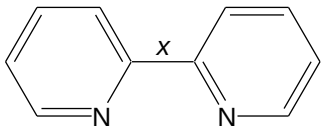

Bond distance *x* (Å)		Reference:
2,2'-Bipyridine (free)	1.49	365, 366
$[(C_5Me_5)_2Yb(bipy)]^+[(C_5Me_5)_2YbCl_2]^-$	1.49	352
$[(C_5Me_5)_2Ce^{III}(bipy)I]$	1.50	367
$[Sm^{III}(bipy)_2Cl_3(MeOH)]$	1.48	368
$(C_5Me_5)_2Sm^{III}(bipy)$	1.43	360
$(C_5Me_5)_2Yb^{III}(bipy)$	1.43	351, 352, 369
$[(Yb(bipy^{2-})(THF)_2)_3]$	1.41	370

Table 10: 2,2'-Bipyridine, with bond distances for selected complexes.

The first reported dianionic bipyridine lanthanide complex, $[\{Yb(bipy)(THF)_2\}_3]$, is shown in Figure 72. This is a trimeric ytterbium complex with each bipyridine forming a chelating bridge between two metal centres.[370] As noted in the above list, the C–C bond linking the two pyridines in this complex has an average bond distance of 1.41 Å, which is shorter again than the monoanionic examples.

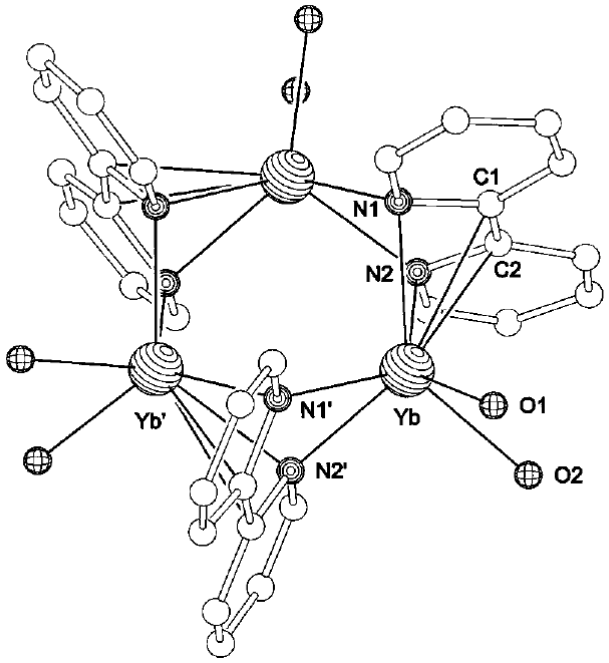

Figure 72: $[(Yb(bipy)(THF)_2)_3]$, reproduced from literature.[370]

Another measurement which can provide useful information is the bond length between the metal centre and the coordinated nitrogen atom of bipyridine. Presuming no steric influence, a shorter bond length generally indicates a reduced bipyridine ligand, whilst a complex will have longer M–N bond distances if the bipyridine ligand is neutral. A sample of these measurements are shown in Table 11.

Table 11: Metal–nitrogen bond distances in selected lanthanide bipyridine complexes (dca = $N(CN)^-$)

M–N distance (Å)		**Reference**
$[(C_5Me_5)_2Sm^{III}(bipy)]$	2.43	360
$[(C_5Me_5)_2Ce^{III}(bipy)I]$	2.633, 2.782	367
$[\{(dca)_3Sm^{III}(bipy)_2(H_2O)\}_n]$	2.633, 2.691	371
$[Sm^{III}(bipy)_2Cl_3(MeOH)]$	2.63 (averaged)	368
$[(Yb(bipy)(THF)_2)_3]$	2.51 (averaged)	370

The reaction of $[(C_5Me_5)_2Sm(THF)_2]$ with 2,2'-bipyridine yields $[(C_5Me_5)_2Sm(bipy)]$, shown in Figure 73.[360] Evans measured the magnetic susceptibility of this complex, finding it to be between the ranges usually observed for trivalent and divalent samarium complexes. Resonance shifts in the ^{13}C NMR spectrum were characteristic of samarium(III) rather than samarium(II), whilst IR spectroscopy also indicated the presence of a bipyridyl anion rather than a neutral bipyridine ligand. A UV spectrum of the product was more similar to a monoanionic bipyridyl than a free bipyridine. Bond lengths in the crystal structure were consistent with one electron reduction of bipyridine (bond *x* is 1.43 Å, Sm–N is 2.43 Å). Overall Evans concluded that structural and magnetic data indicated charge separation between the metal and bipyridyl ligand, forming what he described as a Sm^{III}(bipyridyl^{-}) compound.[360] The delocalised bipyridine system distributes additional electron density more effectively than in the case of pyridine (Section 3.1). The bipyridine is reduced to an anion without reductive coupling occurring.

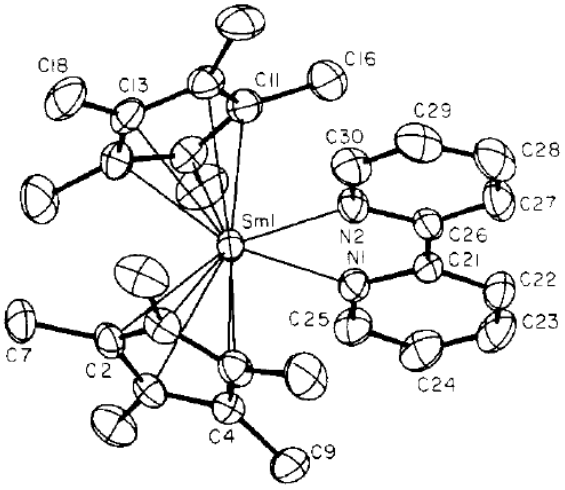

Figure 73: X-Ray crystallographic representation of $[(C_5Me_5)_2Sm(bipy)]$, reproduced from literature.[360]

When reacted with 2,2'-bipyridine, $[(C_5Me_5)_2Yb]$ forms $[(C_5Me_5)_2Yb(bipy)]$.[67, 352, 372] Recent work by Andersen on this ytterbium bipy complex yielded inconclusive characterisation data regarding the oxidation state of the metal centre, similar to the samarium analogue.[352] Proton NMR spectroscopy indicated a paramagnetic product containing a bipyridyl radical anion, which was supported by the IR spectrum and single crystal X-ray crystallography, with further evidence provided in a subsequent paper by Da Re.[353] The magnetic moment was found to be higher than expected for $[(C_5Me_5)_2Yb^{II}(bipy^0)]$, and lower than expected for $[(C_5Me_5)_2Yb^{III}(bipy^{-})]$. This is attributed to spin coupling between an electron from the bipyridyl radical anion and the ytterbium(III) metal centre. Lukens used $[(C_5Me_5)_2Yb(bipy)]$ to quantify exchange coupling in lanthanide single molecule magnets, concluding that there is strong exchange coupling between the lanthanide centre and strongly reducing radical ligands.[373]

A 2,2'-bipyridine complex of the $(Me_8N_2Ph_2)^{2-}$ ligand was targeted as a product for structural comparison with the related bis(pyr) complex **11**. A solution of $[(Me_8N_2Ph_2)Sm(THF)_2]$, **3**, and 2,2'-bipyridine in toluene yielded $[(Me_8N_2Ph_2)Sm(bipy)]$, (**17**), as fine dark crystals (Scheme 19). Elemental analysis of the product was in good agreement with calculated results. The ^{1}H NMR spectrum of **17** was obtained and showed resonances shifted both upfield and downfield in the range 136.50 – 144.50 ppm. Low solubility impeded further NMR spectroscopy techniques required to completely assign this spectrum.

Scheme 19: Reaction of 2,2'-bipyridine with of [($Me_8N_2Ph_2$)Sm($THF)_2$], **3**, to form [($Me_8N_2Ph_2$)Sm(bipy)], (**17**).

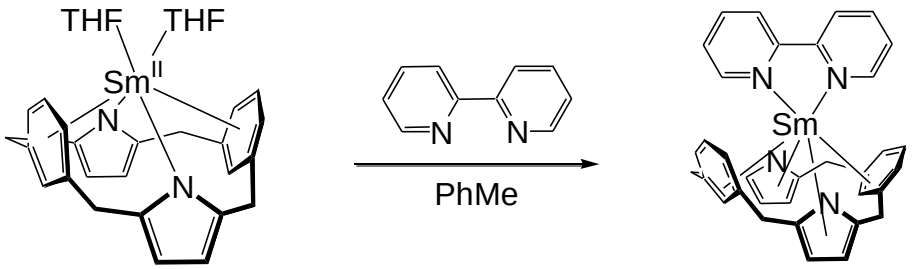

3 **17**

Dark green/purple single crystals of [($Me_8N_2Ph_2$)Sm(bipy)], **17**, were obtained by recrystallisation from toluene and analysed by single crystal X-ray diffraction. The crystal belongs to the monoclinic space group $P2_1/c$ (No. 14) with a = 10.6790(9), b = 17.4410(7), c = 18.5706(5) Å, β = 103.555(3) °. The asymmetric unit contains one macrocyclic unit.

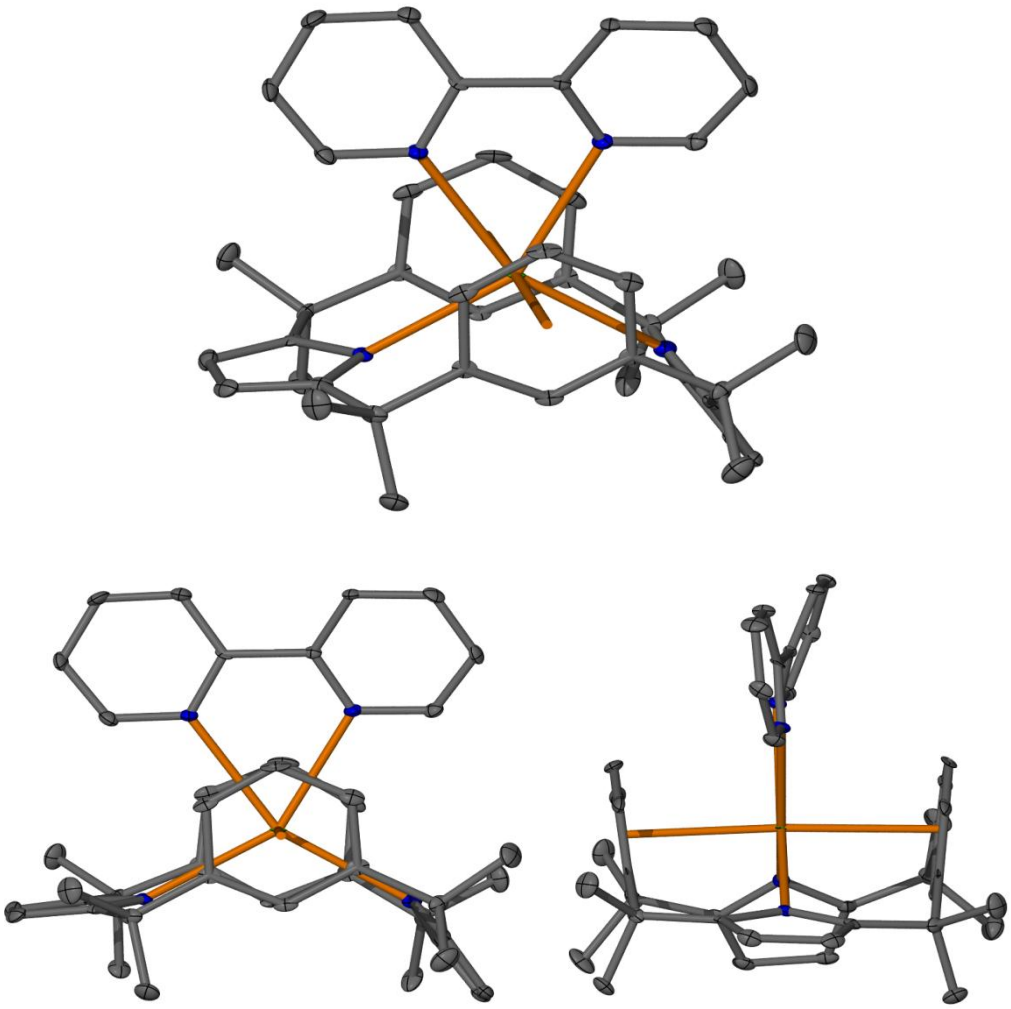

Figure 74: Molecular structure of [$Me_8N_2Ph_2Sm(bipy)$], (**17**), with thermal ellipsoids drawn at 50% probability (protons omitted for clarity).

Overall the macrocycle binds η^1:η^6:η^1:η^6 to the metal, with the bipyridine lying in the cavity formed between the two phenylene groups. The ^{1}H NMR spectrum and M–N distances of 2.668(2) and 2.705(2) Å indicate the metal centre is samarium(II).

The torsion angle of the two heterocyclic rings of bipyridine is 18.11 °, also indicative of a non-reduced state. The C–C bond bridging the two pyridines (bond *x* as per Table 10 above) is 1.484(3) Å, which alongside the torsion between the rings indicate that this is a neutral adduct and has not been reduced. Interestingly, a spacefilling structure (Figure 75) suggests that the bipy ligand would be able to fit closer in to the metal centre without distorting the macrocycle, as would be the case if it had been reduced. Asymmetry in the steepness of the pyrrolide rings and the subtleties of the bipy ligand position may stem from crystal packing influences.

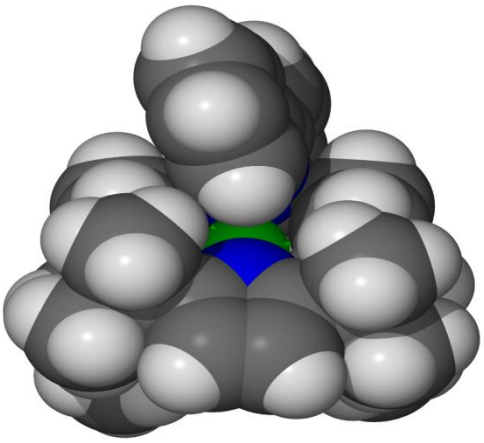

Figure 75: Spacefilling structure of [$Me_8N_2Ph_2Sm(bipy)$], (**17**).

In an analogous reaction of the related $(Et_8N_4Me_2)^{2-}$ macrocycle, the reaction forms a samarium(III) complex with the bipy reduced by a single electron to form a radical anion, $[(Et_8N_4Me_2)Sm^{III}(bipy^{\bullet-})]$.[268] This product is consistent with results for decamethylsamarocene, $[(C_5Me_5)_2Sm^{III}(bipy^{\bullet-})]$.[360] We can conclude that it is the influence of the macrocyclic ligand and not sterics alone that result in the poor reducing

ability of the $[(Me_8N_2Ph_2)Sm(THF)_2]$ complex relative to other ligand sets such as $2(C_5Me_5)^-$ or $(Et_8N_4Me_2)^{2-}$, which is consistent with previously described analogous complexes of NCMe.

Attempts to prepare further related products were also attempted by reacting $[(Me_8N_2Ph_2)Sm(THF)_2]$ with 4,4-bipyridine and 2,2'-biquinoline, Figure 76.

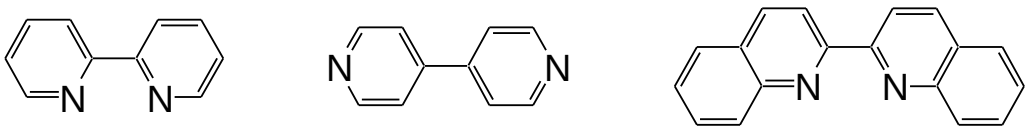

Figure 76: 2,2'-Bipyridine, 4,4'-bipyridine and 2,2-biquinoline (cuprione).

The 4,4'-bipyridine reaction was attempted in anticipation of a different reduction outcome to the 2,2'-bipy isomer. Whilst 4,4'-bipyridine can form 1:1 organolanthanide adducts such as $[(C_5Me_5)_2Yb(4,4'\text{-bipy})]$,[351] 4,4'-bipyridine would be better suited to bridge between two samarium centres than the 2,2'-bipy isomer, and therefore may be more likely to be doubly reduced. A samarium complex was prepared by reacting $[(Me_8N_2Ph_2)Sm(THF)_2]$ with 4,4'-bipyridine. Single crystal X-ray structure showed that the resulting complex, **18**, contained O/OH bridges, indicating that some water may have been present in the 4,4'-bipyridine reactant (Figure 77). Complex **18** is mostly likely to be $[\{(Me_8N_2Ph_2)Sm^{III}(\mu\text{-OH})\}_2]\cdot 4,4'\text{-bipy}\cdot 4C_6H_6\cdot 2H_2O$. Complexes of 4,4'-bipyridine were not pursued further in this work.

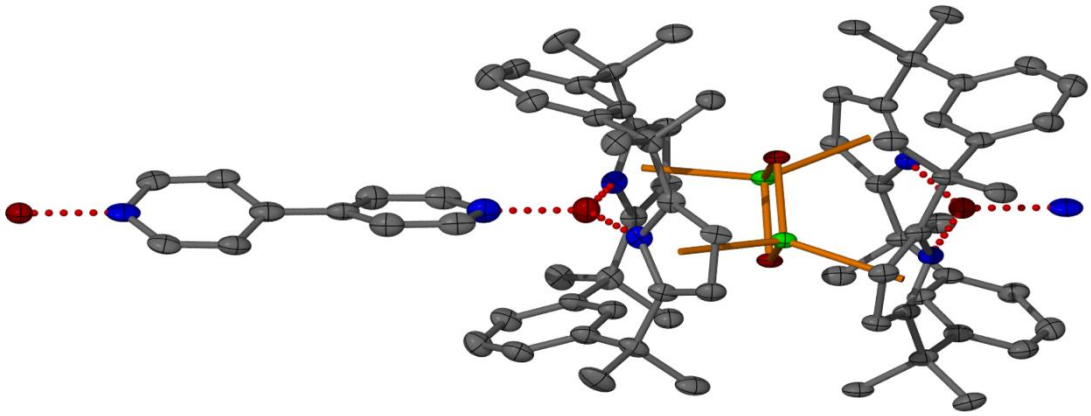

Figure 77: Crystal structure of complex **18**, $[\{(Me_8N_2Ph_2)Sm^{III}(\mu\text{-}OH)\}_2]\cdot 4,4'\text{-bipy}\cdot 4C_6H_6\cdot 2H_2O$.

Cuproine, or 2,2'-biquinoline was also reacted with $[(Me_8N_2Ph_2)Sm(THF)_2]$ in an attempt to determine how increasing steric bulk within the macrocyclic groove would affect the resulting complex. Small orange and purple crystals formed from a milky suspension of fine powder over 24 hrs, but despite repeated attempts no single crystals suitable for X-ray diffraction were isolated.

2,2'-bipyridine and the structurally related 1,10-phenanthroline ligand both bind through nitrogen to metals and share some electronic characteristics. 1,10-Phenanthrolines will be discussed later in this Chapter.

2,2':6',2''-Terpyridine

2,2';6',2''-Terpyridine (terpy) has three linked pyridine units, making it an appropriate neutral ligand to test the flexibility of this macrocyclic ligand. Tridentate coordinating

terpyridine is well established, with examples in *d*, *p* and *f* block chemistry. Few bidentate terpyridine complexes have been reported,[368, 374-380] and fewer monodentate examples are known.[381, 382] These unusual binding modes for terpyridine are formed through steric influence, where terpy is prevented from binding in tridentate fashion.

Previous work by James on a samarium complex of the related macrocyclic $(Et_8N_4Me_2)^{2-}$ ligand with terpy, Figure 78, was found to bind through only one of the three nitrogen atoms available on the terpyridine molecule. This is the first example of a monodendate 2,2':6,2"-terpyridine ligand bound to a lanthanide.[268] The rigid structure of the $(Et_8N_4Me_2)^{2-}$ macrocyclic ligand prevents the terpy from binding tridentate. Bidentate binding is sterically unfavourable in this case as the remaining unbound pyridine unit would have to be located in close proximity to the macrocyclic ligand.

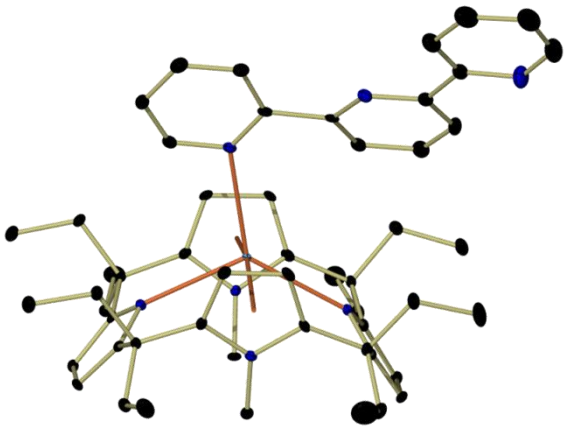

Figure 78: Crystal structure of $[(Et_8N_4Me_2)Sm(terpy)]$.[268]

As demonstrated earlier with the sterically bulky COT^{2-} ligand discussed in Section 3.1, the $(Me_8N_2Ph_2)^{2-}$ ligand can splay outwards to bind η^1:η^1:η^1:η^1 to the metal centre in order to accommodate a large ligand. Cyclooctatetraendiyl π-binds to the metal centre, occupying a large area of the coordination sphere of the metal. The COT^{2-} ligand is oblate, with steric bulk occupying a large cone angle. Terpyridine, on the other hand, is a more slender molecule, able to occupy a long 'arc' of the coordination sphere in a relatively narrow binding cleft. It is of interest to establish how the terpyridine molecule would bind to samarium in this large but flexible $(Me_8N_2Ph_2)^{2-}$ system.

A mixture of $[(Me_8N_2Ph_2)Sm(THF)_2]$, **3**, and terpyridine in benzene formed a very fine dark crystalline product over a 72 hr period (Scheme 20). Despite multiple attempts, elemental analysis of this product was not successful, which was likely due to the difficulty recrystallising this poorly soluble complex. Characterisation by NMR spectroscopy was not possible due to the sparing solubility of the complex.

Scheme 20: Reaction of $[(Me_8N_2Ph_2)Sm(THF)_2]$, **3**, with terpyridine to form $[(Me_8N_2Ph_2)Sm^{II}(terpy)]$, **19**.

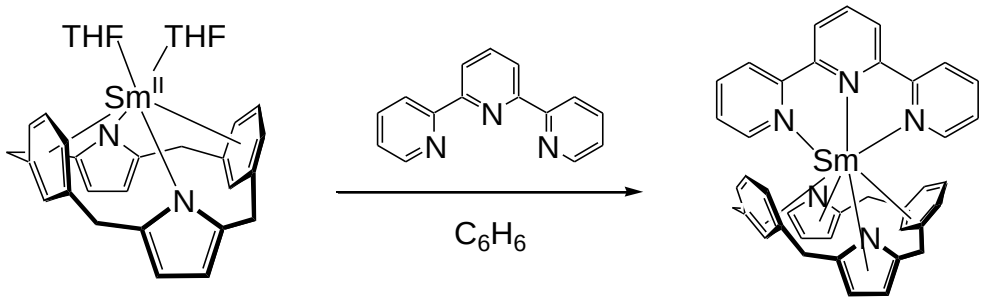

3 **19**

Dark orange-brown crystals suitable for X-ray diffraction were obtained by heating the complex in C_6D_6 in a sealed Young's tube at 70 °C for 72 hrs followed by slow cooling to room temperature. The product was identified as the 1:1 complex $[(Me_8N_2Ph_2)Sm^{II}(terpy)]$, **19**. The crystals belong to the monoclinic space group $P2_1/c$ (No. 14) with a = 13.962(1), b = 11.3406(9), c = 23.342(2) Å, β = 93.028(1) °. The molecular structure is shown in Figure 79.

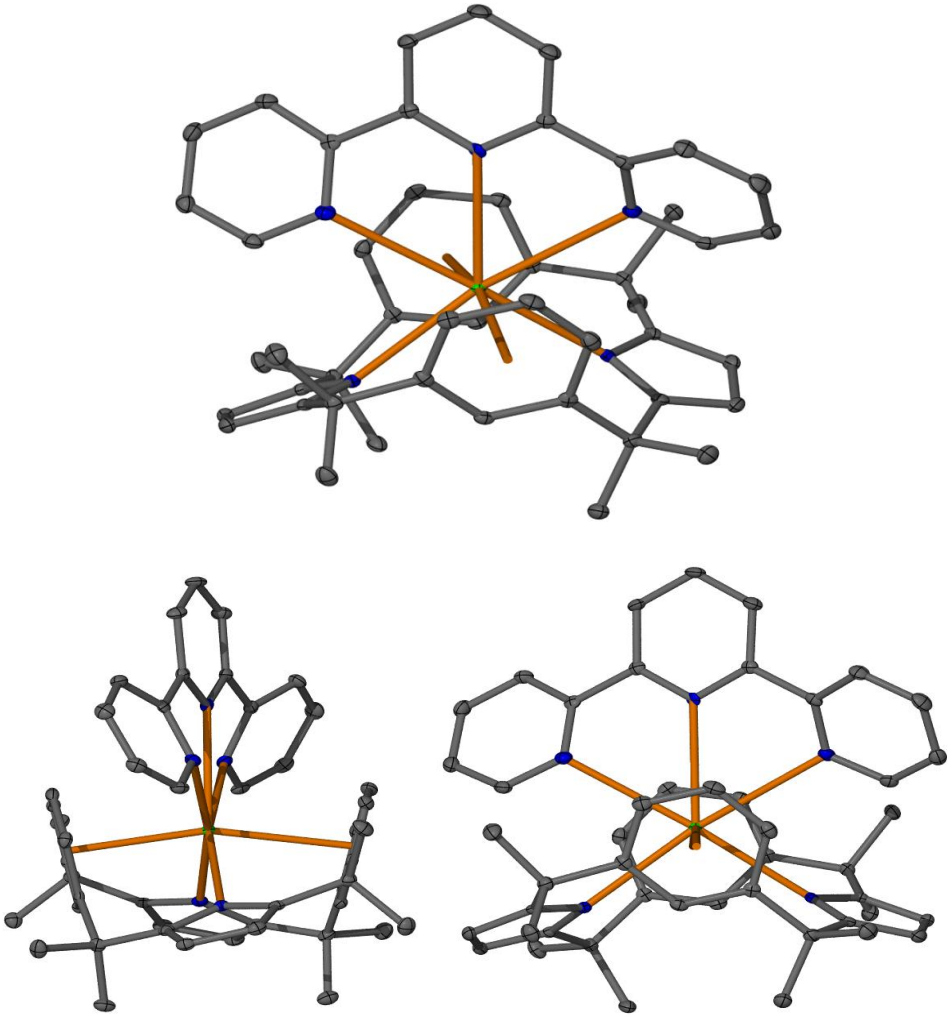

Figure 79: Molecular structure of $[(Me_8N_2Ph_2)Sm(terpy)]$, (**19**).

The tridentate terpyridine is σ-bound through the three nitrogen atoms to the metal centre. The relatively long Sm–N bond distances in comparison to complexes listed in Table 12 indicate that this is a Sm^{II} complex with a neutral terpyridine ligand. Torsion in the terpyridine ligand also indicates that it has not been reduced and is likely to be bound to the metal as a neutral adduct.

Table 12: M–N bond distances in organolanthanide terpyridine complexes.

Ln–N bond distance (Å)		**Terpy C–C bond**	**Ref.**
$[(Me_8N_2Ph_2)Sm^{II}(terpy)]$, (**19**)	2.965, 2.846, 2.927	1.488(3), 1.487(3)	Herein
$[(C_5Me_5)_2Sm^{III}(terpy)]$	2.498, 2.449, 2.498	1.446	348, 367
$[(C_5Me_5)_2Sm^{III}(terpy)]^+ PF_6^-$	2.515, 2.554, 2.518	1.477, 1.491	348
$[Sm^{III}(terpy)_3](ClO_4^-)_3$	2.591, 2.552, 2.603	1.480, 1.451	384

1,10-Phenanthroline

1,10-Phenanthroline is a tricyclic system containing two nitrogen atoms which is related to 2,2'-bipyridine in structure and coordination properties. Similar to bipyridine it is a commonly used ligand in coordinating *p*, *d* and *f* block metals, and substituted phenanthrolines are readily available. Unlike bipyridine the 1,10-phenanthroline (phen) molecule is conjugated throughout, allowing greater stabilisation through delocalisation. Phenanthroline ligands give metal complexes photophysical properties, such as luminescence.[368, 386] Phenanthroline systems investigated in this work are shown in Figure 80.

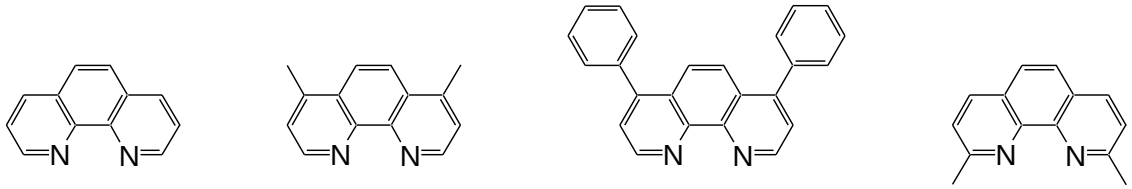

Figure 80: 1,10-Phenanthroline and 4,7-dimethyl-, 4,7-diphenyl- and 2,9-dimethyl-substituted molecules.

Each of these reactions was carried out on a small scale, with a solution of excess phenanthroline combined with the samarium(II) precursor [($Me_8N_2Ph_2$)Sm($THF)_2$] **3** in C_6H_6 or PhMe. The small scale of reaction in combination with low solubility of the resulting complexes in benzene and toluene prevented characterisation by NMR spectroscopy, and also precluded recrystallisation for elemental analysis.

Small dark single crystals of product were obtained from the reaction of 1,10-phenanthroline with [($Me_8N_2Ph_2$)Sm($THF)_2$] (**3**) in C_6H_6 after 72 hrs (Scheme 20), and these were analysed on the MX2 beamline at the Australian Synchrotron. The crystals suffered from bad decay in the beam, and whilst the structures clearly show the presence of a dianionic samarium complex coupled at the heterocycle, a detailed discussion of the structural metrics of [{($Me_8N_2Ph_2$)Sm}$_2$(μ-4,4'-dihydro-biphen)] (**20**) has not been pursued.

Scheme 21: Reaction of 1,10-phenantholine with $[(Me_8N_2Ph_2)Sm(THF)_2]$, **3**, to form $[\{(Me_8N_2Ph_2)Sm\}_2(\mu$-4,4'-dihydro-biphen)] (**20**).

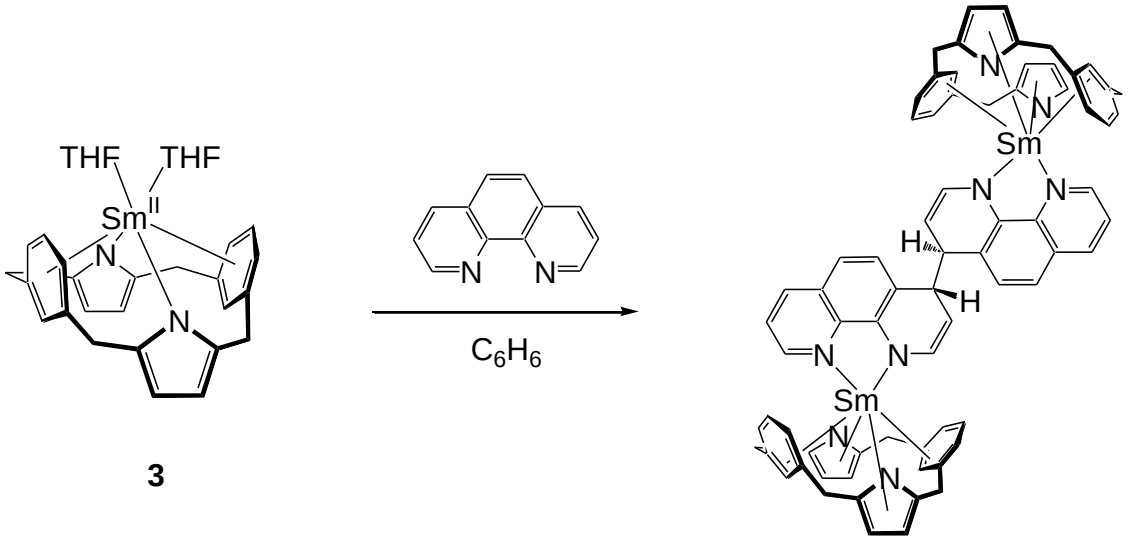

3 **20**

This reductive dimerisation of phenanthroline at the 4-position seen above has previously been reported for a ruthenium silylyne complex, observed in 90% yield after 9 days stirring over sodium amalgam.[387] The related macrocyclic complex, $[(Et_8N_4Me_2)Sm(THF)_2]$ also reductively dimerises 1,10-phenanthroline to form $[\{(Et_8N_4Me_2)Sm^{III}\}_2(\mu$-4,4'-dihydro-biphen)], similar to $[\{(Me_8N_2Ph_2)Sm^{III}\}_2(\mu$-4,4'-dihydro-biphen)], **20**.[268] In both of these complexes the Sm-N(phen) bond distances indicate that each metal is asymmetrically bound to the phenanthroline nitrogen atoms, (2.358(6) and 2.603(5) Å in $[\{(Et_8N_4Me_2)Sm^{III}\}_2(\mu$-4,4'-dihydro-biphen)], and 2.344(1) and 2.577(1) Å in $[\{(Me_8N_2Ph_2)Sm^{III}\}_2(\mu$-4,4'-dihydro-biphen)], **20**. In both cases the shorter bond distance is between samarium and the nitrogen on the phenylene that is located on the ring that is reductively coupled. This bonding is discussed in greater

length later in relation to the complex [{($Me_8N_2Ph_2$)Sm}$_2$(μ-4,4'-dihydro-bipyridazine)], (**31**).

In repeated attempts to obtain good quality structural data for the [{($Me_8N_2Ph_2$)Sm^{III}}$_2$(μ-4,4'-dihydro-biphen)] crystals, two lithium phenanthroline complexes of the $(Me_8N_2Ph_2)^{2-}$ ligand with different levels of phenanthroline solvation were identified by X-ray crystallography. Lithium is present from the previous metathetical exchange. The structures of [($Me_8N_2Ph_2$)Li_2(phen)] (**21**) and [($Me_8N_2Ph_2$)Li_2(phen)$_2$] (**22**) are shown in Figure 81. Characterisation of these rogue products was not pursued further.

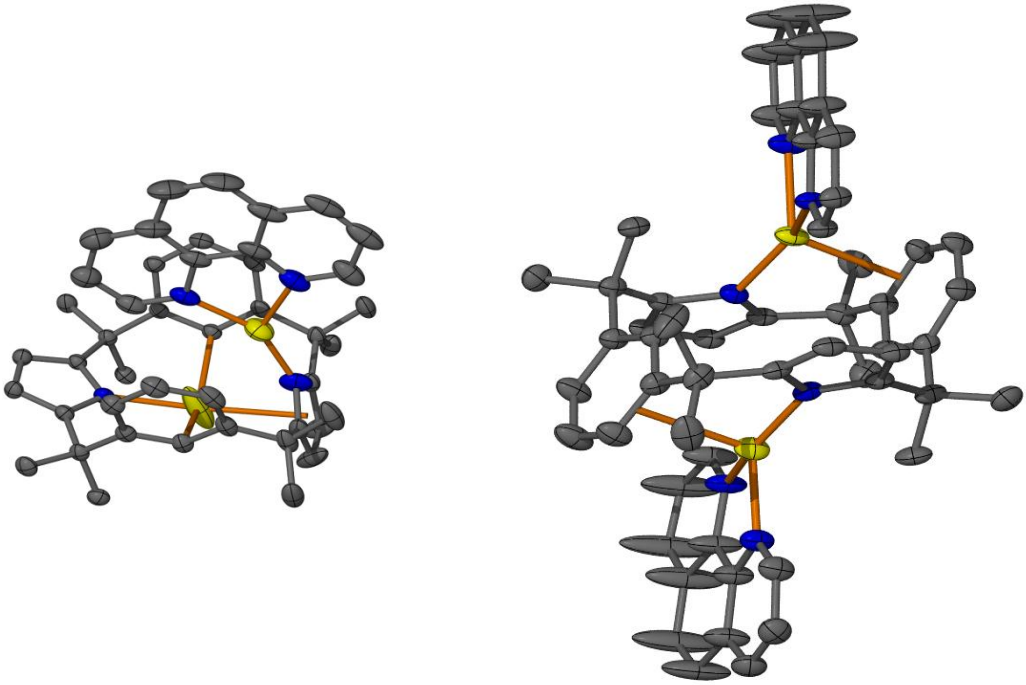

Figure 81: Lithium phenanthroline complexes **21** and **22** with the $(Me_8N_2Ph_2)^{2-}$ ligand system.

Whilst bipy and phen are similar in structure, the reductive dimerisation of 1,10-phen is in contrast to the bipy adducts formed in the reactions of these ligands with both $[(Me_8N_2Ph_2)Sm(THF)_2]$ and $[(Et_8N_4Me_2)Sm(THF)_2]$. In reactions with $[(C_5Me_5)_2Yb]$, both bipy and phen form radical anion ytterbium(III) complexes, $[(C_5Me_5)_2Yb^{III}(bipy^{\bullet-})]$ and $[(C_5Me_5)Yb^{III}(phen^{\bullet-})]$.[352, 353] Exchanging electron-donating methyl substituents on the cyclopentadienyl ring for two electron-withdrawing trimethylsilyl groups prevented the reduction of phenanthroline from occurring, instead forming a neutral adduct, $[\{1,3\text{-}(Me_3Si)_2C_5H_3\}_2Yb^{II}(phen)]$.[352]

4,7-Dimethyl-1,10-phenanthroline

To continue investigating the dimerisation of phenanthroline by the $(Me_8N_2Ph_2)^{2-}$ samarium complex, an analogous reaction with 4,7-dimethyl-1,10-phenanthroline was also performed. This heterocycle has methyl substituents in the coupling positions at 4 and 7.

This reaction was done under similar conditions as the previous 1,10-phenanthroline, and yielded pink crystals forming from the maroon-coloured solution over a period of 48 hrs (Scheme 22). Once again despite repeated attempts these small crystals suffered from decay during X-ray single crystal data collection. As in the case of complex **20**, whilst the structure of complex **23** is identifiable from X-ray crystallography, low quality data prevented a quantitative structural analysis.

Scheme 22: Reaction of 4,7-dimethyl-1,10-phenanthroline with [($Me_8N_2Ph_2$)Sm(THF)$_2$], **3**, to form [{($Me_8N_2Ph_2$)Sm}$_2${μ-4,4'-bis-(4,7-dimethylphen)}], **23**.

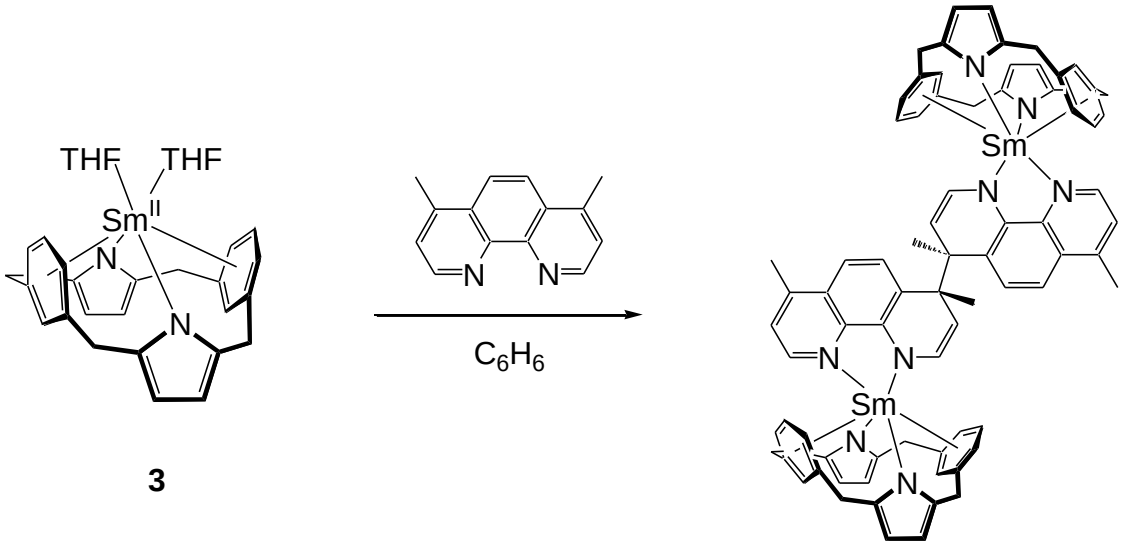

3 **23**

Interestingly, the steric and electronic influence of the methyl substituents do not prevent reductive coupling at the 4 and 7 positions of the phenanthroline, and the outcome is the same as the unsubstituted 1,10-phenanthroline, including the asymmetrical Sm–N(phen) bond lengths. The 4,7-dimethyl-1,10-phenanthroline samarium complex, [{($Me_8N_2Ph_2$)Sm}$_2${μ-4,4'-bis-(4,7-dimethylphen)}], **23**, is shown in Figure 82. Once again this is an analogous product to the related $(Et_8N_4Me_2)^{2-}$ macrocycle, which also saw reductive coupling at the 4 position under the same conditions to form [{($Et_8N_4Me_2$)Sm}$_2${μ-4,4'-bis-(4,7-dimethylphen)}].[268]

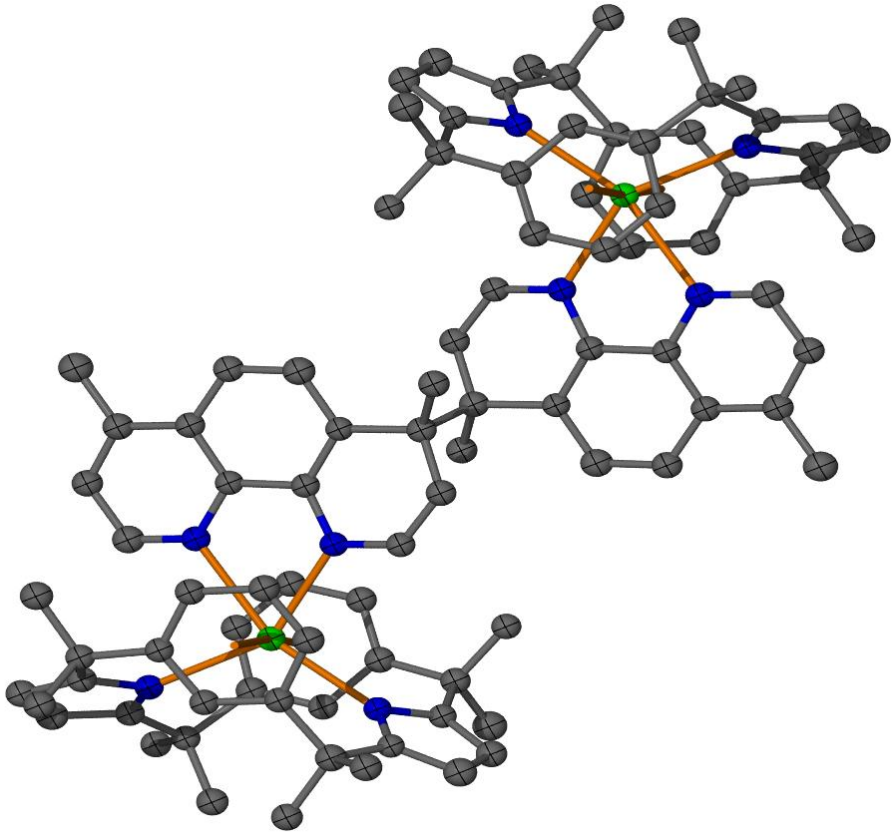

Figure 82: Reductively coupled [{($Me_8N_2Ph_2$)Sm}$_2${μ-4,4'-bis-(4,7-dimethylphen)}], **23**. Hydrogens omitted for clarity, isotropically refined atoms shown with arbitrary sized radii.

4,7-Diphenyl-1,10-phenanthroline (bathophenanthroline)

To further increase the steric bulk at the coupling position phenyl substitution at the 4 and 7 positions of phenanthroline was introduced. Under the same conditions as the previous two reactions, an immediate colour change from purple to teal was observed upon addition of the phenanthroline. Crystals of product formed from the solution over 48 hrs (Scheme 23).

Scheme 23: Reaction of 4,7-dimethyl-1,10-phenanthroline with [($Me_8N_2Ph_2$)Sm($THF)_2$], **3**, to form [($Me_8N_2Ph_2$)Sm(4,7-diphenyl-1,10-phenanthroline)], (**24**).

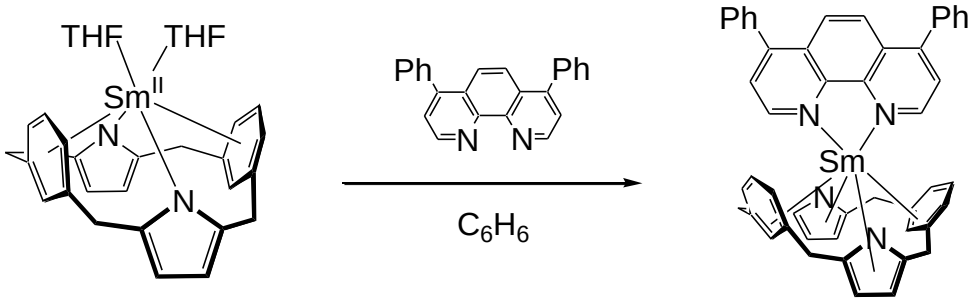

3 **24**

Dark green crystals of a 4,7-diphenyl-1,10-phenanthroline complex (**24**) were isolated from the teal green reaction mixture and washed with benzene. The crystal belongs to the triclinic space group *P*-1 (No. 2) with a = 12.966(2), b = 13.005(1), c = 16.313(2) Å, α = 83.437(3), β = 85.056(2), γ = 81.677(3) °. There are 2 molecules in the asymmetric unit. The structure is shown in Figure 83.

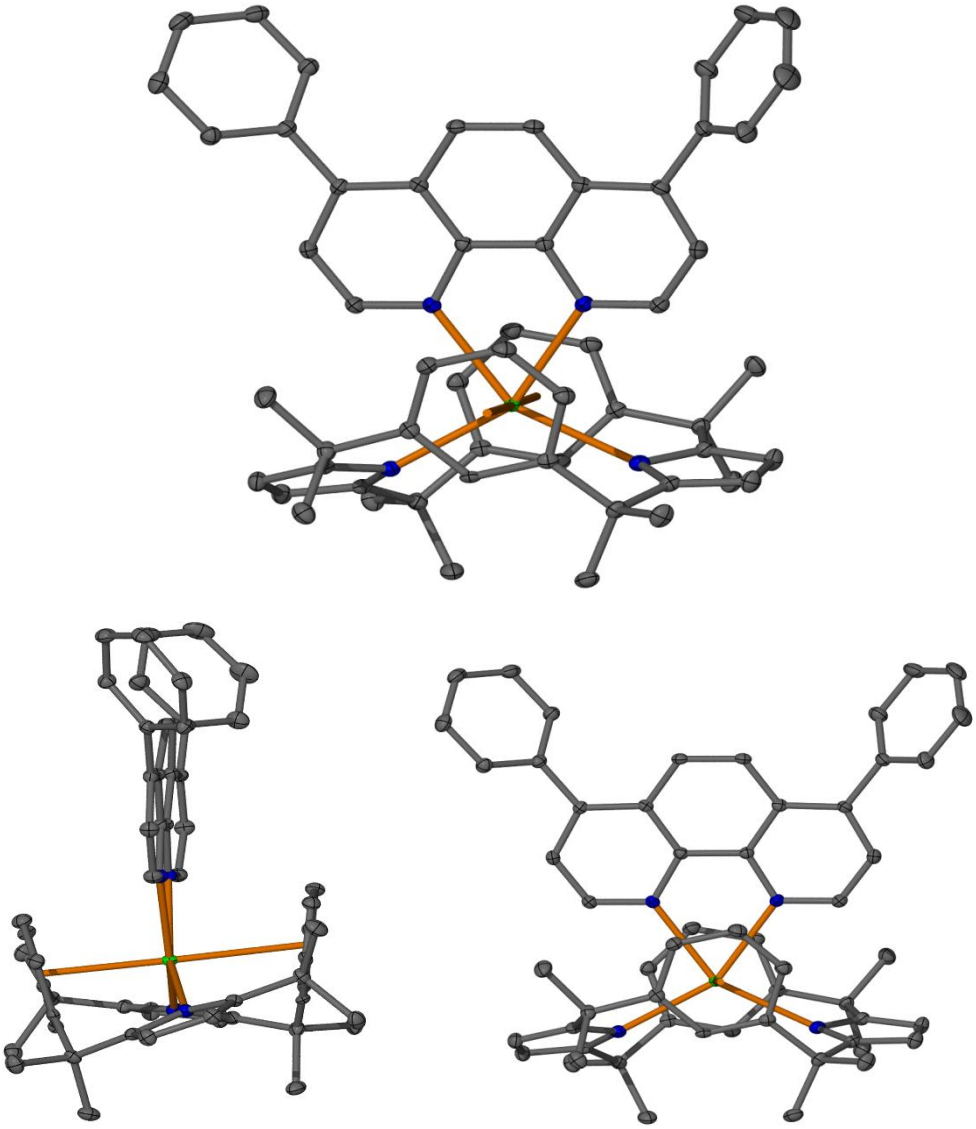

Figure 83: Molecular structure of [($Me_8N_2Ph_2$)Sm(4,7-diphenyl-1,10-phenanthroline)], (**24**) with thermal ellipsoids drawn at 50% probability (protons omitted for clarity).

The samarium metal centre sits high in the macrocyclic cavity, sandwiched between the two phenylene units. The phenylene groups bind η^6 to the metal, with the phenylene planes forming an angle of 20.0 °. The distances between the phenylene centroids and the metal are 2.66 and 2.84 Å. The ‘metallocene angle’ formed between the phenylene

centroids and the metal centre is 179.2 °. The two pyrrolide groups bind η^1 through the nitrogen at a distance of 2.452(2) and 2.474(2) Å from the metal centre. These pyrrolides are angled such that both pyrrolides are directed toward a point below the metal centre. The tilt of these pyrrolides and the staggering of the phenylene units indicate a slight twist of the macrocycle. The 4,7-diphenyl-1,10-phenanthroline is bound in the top of the macrocyclic cavity by σ-bonds to the two nitrogen atoms, with Sm–N distances of 2.439(2) and 2.452(2) Å. These bond lengths are indicative of a $[(Me_8N_2Ph_2)Sm^{III}(4,7\text{-diphenylphen}^{\bullet-})]$ complex as discussed in Section 3.1.

Once again the $(Et_8N_4Me_2)^{2-}$ product of reaction with 4,7-diphenyl-1-,10-phenanthroline is analogous in structure, forming as a 1:1 complex with samarium(III) and a phenanthroline radical anion ligand. These results show that by sufficiently increasing the steric bulk at the 4 position, reductive coupling can be prevented and instead a 1:1 complex becomes favourable.

A further reaction of the $[(Me_8N_2Ph_2)Sm(THF)_2]$ complex with 1,10-phenanthrolines introduced steric bulk directed towards the metal centre. The reaction of 2,9-dimethyl-1,10-phenanthroline with $[(Me_8N_2Ph_2)Sm(THF)_2]$ yielded very small crystals in a milky suspension of fine powder, however repeated attempts to identify the product proved unsuccessful, with single crystal X-ray diffraction identifying instead a poorly diffracting red crystal. Phenanthrolines complexes of the related $(Et_8N_4Me_2)^{2-}$ ligand yielded similar results, whilst reaction with the 2,9-dimethylphen formed a neutral Sm^{II} adduct.[268]

3.2.3 The Reactivity of $(Me_8N_2Ph_2)Ln(II)$ Complexes with Diazines

In this Section the reactions of diazines with the samarium precursor $[(Me_8N_2Ph_2)Sm(THF)_2]$, **3**, are described. The structures of the diazines pyrazine, phenazine, pyrimidine, 2,2'-bipyrimidine and pyridazine are shown in Figure 84. These diazines have two nitrogen atoms able to *σ*-bind a metal centre, and are more easily reduced than pyridine due to the additional electronegative nitrogen centre.[388] Carbon atoms of these heterocycles are even more electron deficient than those of pyridine, also due to the presence of an additional nitrogen atom.[335, 389]

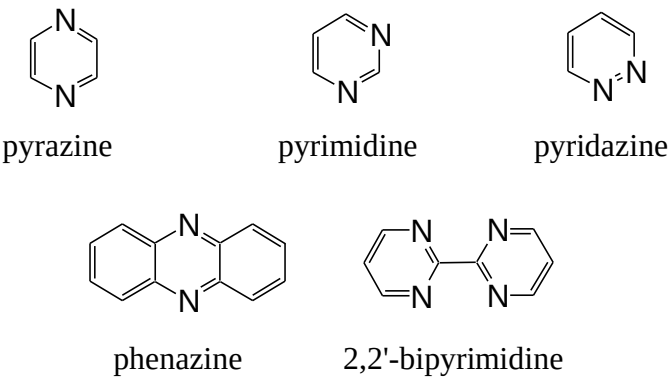

Figure 84: Diazines reacted with $[(Me_8N_2Ph_2)Sm(THF)_2]$, **3** in this work.

Pyrazine

Pyrazine (*p*-diazine) is a symmetrical planar diazine with two nitrogen atoms occupying *para* positions. The carbon–carbon bond lengths and internal bond angles in pyrazine

are similar to those of benzene (Figure 85).[390] Whilst similar in size to pyridine, the electronic characteristics of this molecule differ. The nitrogens are open to direct electrophilic attack, but the carbon atoms are deficient in electron density.[390] Pyrazine is known as an easily reducible molecule.

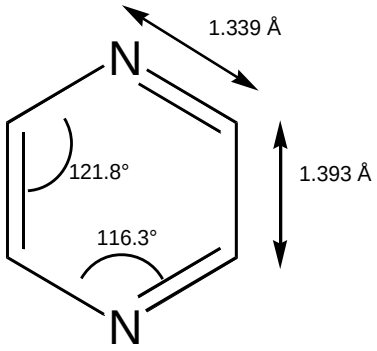

Figure 85: Bond lengths and angles in pyrazine.[390]

A pyrazine ligand can bind 1:1 to a metal centre as a neutral adduct, it may bind 1:2 to form a bridge between metal centres, or it may be reduced. Pyrazine adducts are observed in $[(C_5H_4Bu^t)_3Ce^{III}(pyrazine)]$ and $[(C_5Me_5)_2Yb^{II}(pyrazine)]$.[341, 351]

With nitrogen atoms at opposite ends of the heterocycle, pyrazine is also able to act as a bridging ligand between metal centres, and can be utilised to form chains, layers or 3D network structures.[391-394] Lanthanide complexes with pyrazine bridging ligands include $[\{Dy^{III}(H_2O)_2(hfac)_3\}_2(pyrazine)]$ (hfac = hexafluroroacetylacetonato) and the ytterbium complex, $[(C_5H_5)_3Yb(NC_4H_4N)Yb(C_5H_5)_3]$ (Figure 86).[395]

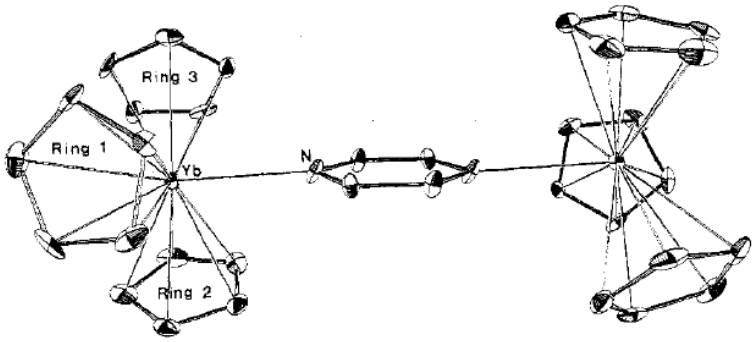

Figure 86: A Yb complex containing a bridging pyrazine ligand, $[(C_5H_5)_3Yb(NC_4H_4N)Yb(C_5H_5)_3]$, reproduced from literature.[395]

The addition of pyrazine to a solution of $[(Me_8N_2Ph_2)Sm(THF)_2]$ (**3**) yielded dark crystals over a 7 day period. This product was characterised by NMR spectroscopy and single crystal X-ray diffraction, and found to be the stable samarium(II) adduct, $[(Me_8N_2Ph_2)Sm(pyrazine)]$, **25**.

Scheme 24: Reaction of $[(Me_8N_2Ph_2)Sm(THF)_2]$ with pyrazine to form $[(Me_8N_2Ph_2)Sm(pyrazine)]$, **25**.

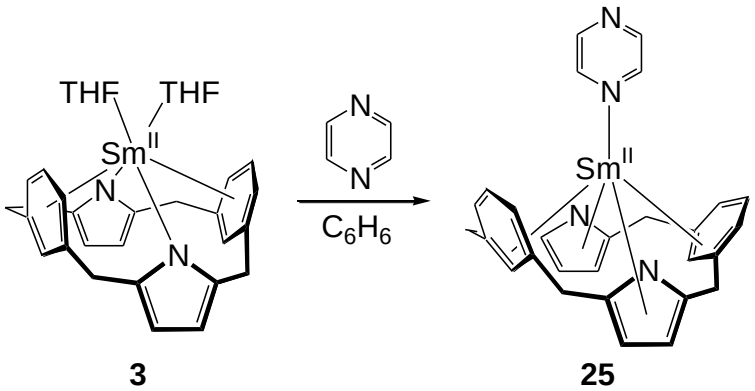

3 **25**

Dark purple crystals of **25** suitable for X-ray diffraction were obtained from the reaction mixture and washed with benzene. The crystals belong to the triclinic space group

P-1 (No. 2) with a = 9.419(1), b = 10.244(1), c = 16.297(2) Å, α = 82.796(2), β = 87.725(9), γ = 75.284(3) °. The asymmetric unit cell contains one molecule of [($Me_8N_2Ph_2$)Sm(pyrazine)].

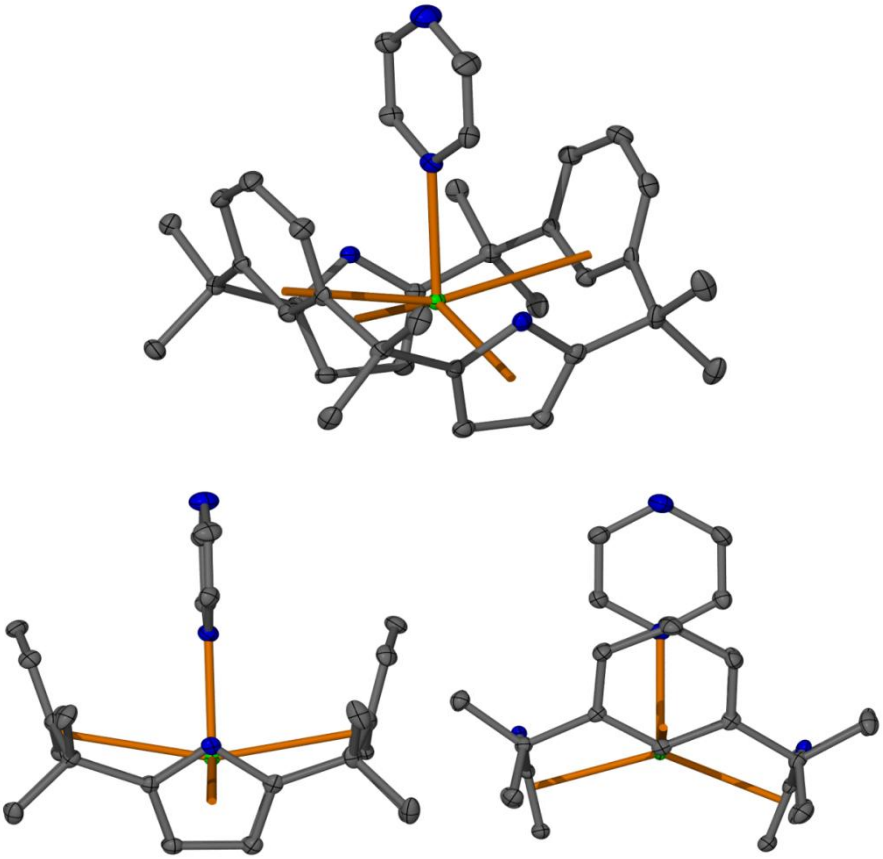

Figure 87: Molecular structure of [($Me_8N_2Ph_2$)Sm(pyrazine)], (**25**) with thermal ellipsoids drawn at 50% probability (protons omitted for clarity).

The samarium(II) complex **25** forms an adduct with pyrazine, with Sm–N bond length (metal to pyrazine) of 2.645(3) Å, indicating no ligand reduction or metal oxidation has occurred. This is somewhat surprising because samarium(II) is a stronger reducing agent than ytterbium, and as reported by Raymond above, is quite capable of reducing the pyrazine ligand.[395]

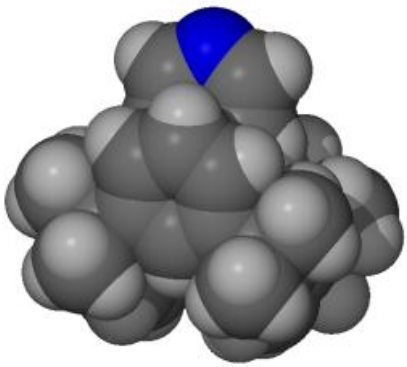

Figure 88: Spacefilling structure of [($Me_8N_2Ph_2$)Sm(pyrazine)] **25**.

A spacefilling structure of the pyrazine adduct, Figure 88, shows that a second samarium macrocycle unit is sterically prevented from binding to the uncoordinated nitrogen centre in the η^5:η^3:η^5:η^3 binding mode, as the phenylene group extends more than halfway over the face of the coordinated pyrazine. It is surprising however, that this flexible, adaptable ligand does not change coordination mode to bind η^1:η^6:η^1:η^6 as seen in [($Me_8N_2Ph_2$)SmCl], (**7**), and [($Me_8N_2Ph_2$)Sm(2,6-Me_2-pyridine)], (**15**), which would conceivably allow the coordination of a second unit (Figure 89).

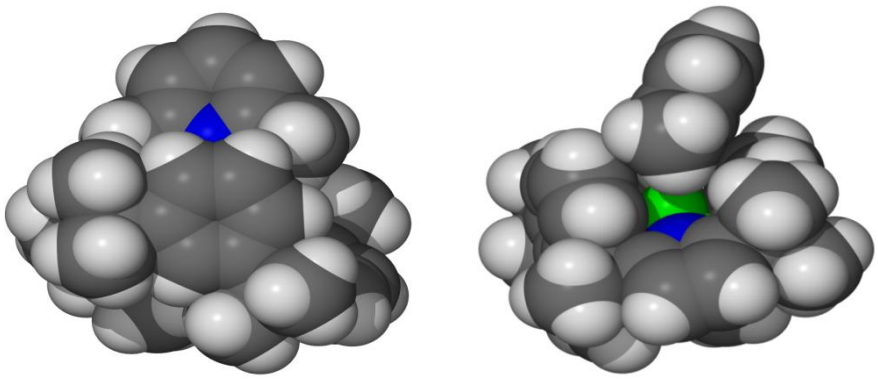

Figure 89: Spacefilling structures of [($Me_8N_2Ph_2$)Sm(2,6-dimethylpyr)], **15**.

Addition of pyrazine to a benzene solution of the europium mono-THF precursor **6**, yielded orange plate crystals of [($Me_8N_2Ph_2$)Eu^{II}(pyrazine)], **26**, analogous to **25**. Single crystals obtained from the reaction were analysed by X-ray diffraction and found to be isomorphous to the samarium analogue. The crystal belongs to the triclinic space group *P*-1 (No. 2) with a = 9.4220(4), b = 10.2560(4), c = 16.320(2) Å, α = 82.819(4), β = 87.760(9), γ = 75.265(4) °. As with the isomorphous samarium complex, there is one macrocyclic complex in the asymmetric unit.

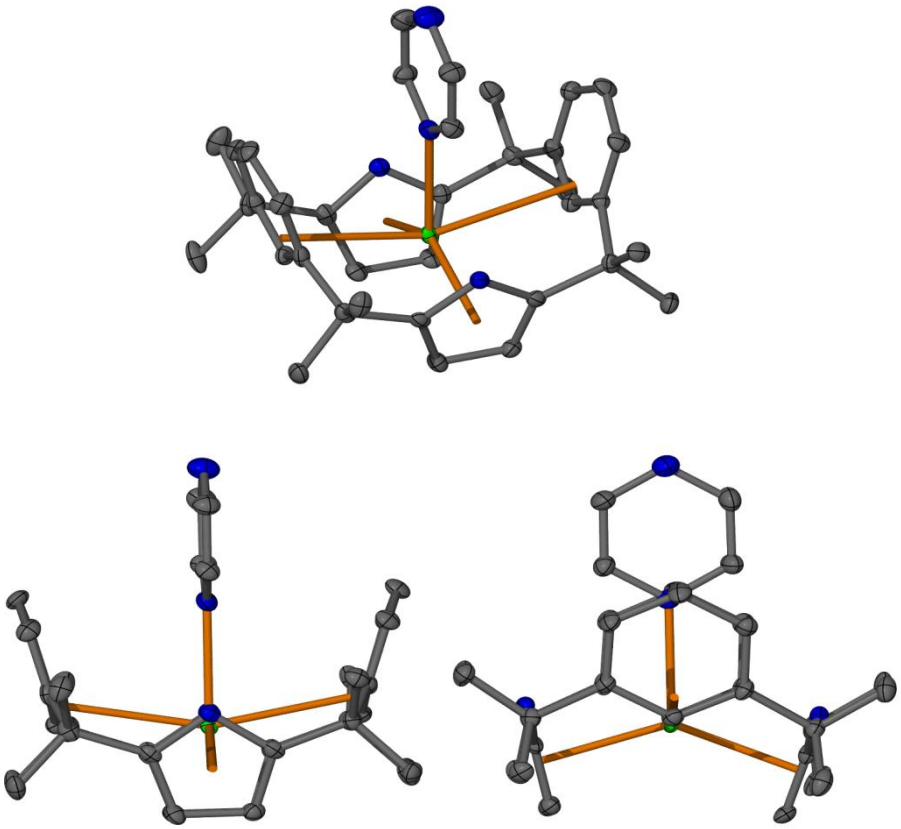

Figure 90: Molecular structure of [($Me_8N_2Ph_2$)Eu(pyrazine)], (**26**) with thermal ellipsoids drawn at 50% probability (protons omitted for clarity).

In both the samarium and europium complexes **25** and **26** the metal centre sits low in the macrocyclic cavity. The M–N bond distances are 2.653(3) (Sm) and 2.642(5) Å (Eu), indicating that both metal centres are lanthanide(II). The macrocycle has a symmetrical conformation with little or no twisting, similar to the mono(THF) Sm and Eu complexes **4** and **6**. The coordinated pyrazine is aligned along the binding groove of the macrocycle, between the phenylene moieties.

The metal centre binds η^5:η^3:η^5:η^3 to the ligand. The phenylene units are splayed outwards further than in previous examples in this work, at angles of 28.2 ° (Sm) and 28.6 ° (Eu) to each other. The two pyrrolide groups coordinate η^5 to the metal, with centroid–M distances of 2.51, 2.51 (Sm) and 2.51/2.52 (Eu) Å. The angle formed between pyrrolide centroid-metal-centroid is 137.3 (Sm) and 137.8° (Eu).

Phenazine

Phenazine has a structure similar to pyrazine, with three fused rings, Figure 91. These extra annulated rings will increase steric influence alter the electronic properties and may result in different redox behaviour of lanthanide complexes compared to the pyrazine complex above.

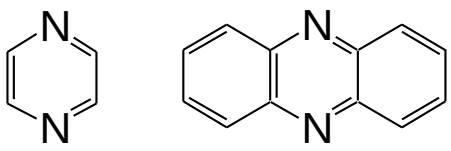

Figure 91: Pyrazine and phenazine.

Reaction of $[(Me_8N_2Ph_2)Sm(THF)_2]$, **3**, with phenazine results in a 2:1 complex (Scheme 25). In this complex the coordinated phenazine ligand bridges between two samarium metal centres. Both metal centres are oxidised to samarium(III), resulting in a two electron reduction of phenazine.

Scheme 25: Reaction of $[LSm(THF)_2]$, **3**, with phenazine to form $[(LSm)_2(phenazine^{2-})]$, **27**, $(L = Me_8N_2Ph_2)^{2-}$.

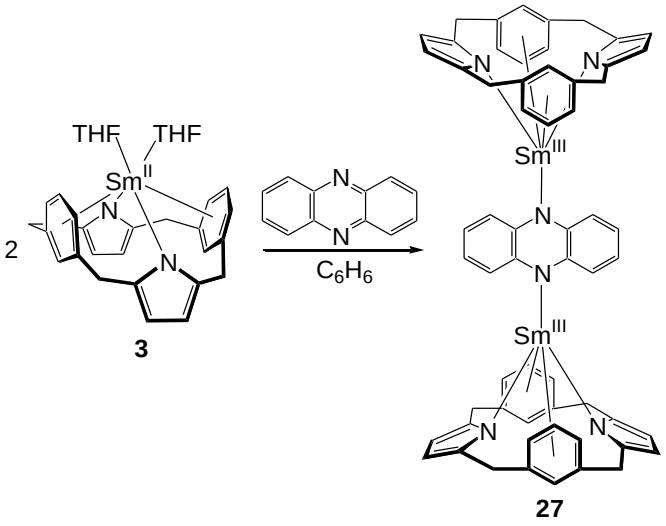

Dark crystals of complex (**27**) were obtained by slow evaporation from benzene. The crystal belongs to the monoclinic space group $P2_1/n$ (No. 14) with a = 11.9550(8), b = 16.065(1), c = 18.500(1) Å, β = 104.176(1) °. There is one macrocycle in the asymmetric unit, shown in Figure 92.

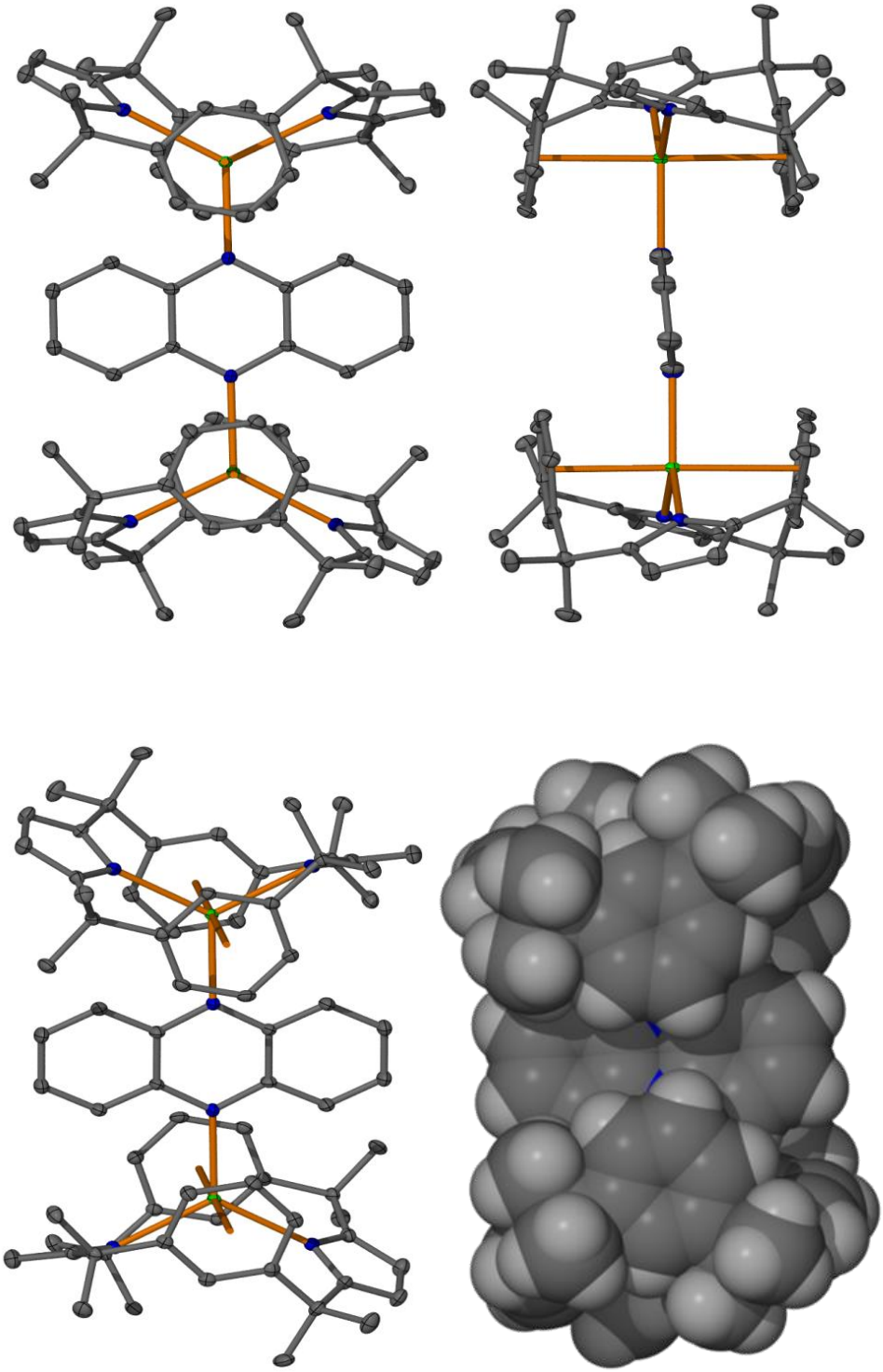

Figure 92: Molecular structure of [($Me_8N_2Ph_2$)Sm(phenazine)], (**27**) with spacefilling structure.

The phenazine binds 1:2 to the samarium macrocycle, which adopts a η^6:η^1:η^6:η^1 binding mode, similar to the [$(Me_8N_2Ph_2)Sm^{III}Cl$] **7** complex introduced in Section 2.2.5. The Sm–N bond distance (2.355(2) Å) also suggests that both metal centres are samarium(III).

There are numerous examples of phenazine being reduced by lanthanides to form similar bimetallic complexes. Reaction of [$(C_5Me_5)_2Sm$] with phenazine produces [{$(C_5Me_5)_2Sm$}$_2$(μ-phenazine)], which has a 2.36 Å Sm–N bond, also indicating a samarium(III) metal centre.[135] [$(C_5Me_5)Ln(BPh_4)$] (Ln = Sm, Yb) also reduces phenazine to give [{$(C_5Me_5)_2Ln$}$_2$(μ-$C_{12}H_8N_2$)].[396] Similarly phenazine is doubly reduced by a uranium COT complex to form bimetallic [{$(C_5Me_5)(COT)U$}$_2$(μ-phenazine)], another structurally similar product.[397] Trivalent [$(C_5Me_5)_3Ln$] (Ln = Sm, La) can act as a one-electron reductant in a sterically induced reduction (even for the relatively uncrowded La complex), and also reduces phenazine to give [{$(C_5Me_5)_2Ln$}$_2$(μ-$C_{12}N_2H_8$)].[160, 398]

It is interesting that the $(Me_8N_2Ph_2)^{2-}$ ligand system will form a stable 1:1 adduct with pyrazine ([$(Me_8N_2Ph_2)Sm$(pyrazine)], **25**) but reduces phenazine to form a bimetallic complex as seen in [{$(Me_8N_2Ph_2)Sm$}$_2$(phenazine^{2-})], **27**. Phenazine has different electronic properties to pyrazine, most notably the presence of the annulated benzene rings, making it more able to be reduced by [$(Me_8N_2Ph_2)Sm(THF)_2$], **3**. The samarium(III) sits higher within the macrocyclic cavity, binding η^6:η^1:η^6:η^1 and

allowing the phenazine to bind to two samarium(III) centres (see space filling diagram in Figure 92 above).

Pyrimidine

Pyrimidine has high electron density at the two nitrogens in positions 1 and 3, which leaves the 2, 4 and 6 positions relatively low on π electron density (Figure 93).[389] The electron deficiency at these positions enhances the reactivity at these positions.[399] The two nitrogens are positioned *meta* within the ring which amplifies their individual electronic effects on the structure in comparison to pyrazine or pyridazine.[389, 399] While the carbon in the 5-position is less electron deficient, it is slightly activated by the inductive effect of the nitrogens, and electrophilic attack or diazo-coupling can readily take place at the C5 position.[399] An unsubstituted diazine is more open to nucleophilic attack than the less electron-deficient pyridine.[335] Addition of a nucleophilic radical to pyrimidine can reportedly occur at C2 or C4.[388]

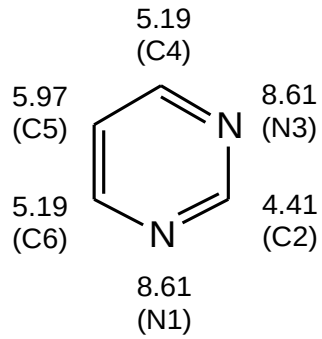

Figure 93: Electron density on pyrimidine atoms (sum of σ and π components).[389]

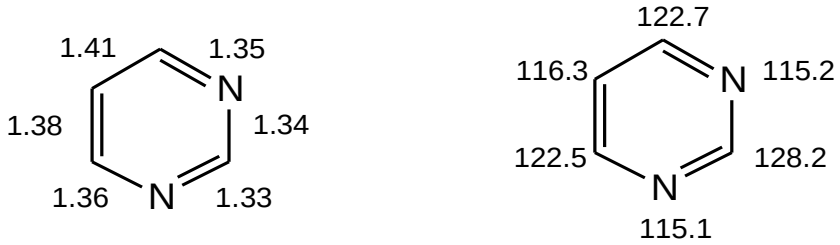

Figure 94: Bond lengths (Å) and internal angles of pyrimidine (°).[400]

Reaction of [$(Me_8N_2Ph_2)Sm(THF)_2$], **3**, with pyrimidine (*m*-diazine) yielded two products as shown in Scheme 26. The major product was identified as purple crystalline [$(Me_8N_2Ph_2)Sm$(pyrimidine)] (**28**), with an orange crystalline minor product found to be [{$(Me_8N_2Ph_2)Sm$}$_2$(μ-dihydro-bipyrimidine)] (**29**). The two products were not able to be separated, therefore characterisation relies on single crystal X-ray diffraction as NMR spectroscopy and elemental analysis of the mixture did not provide useful results.

Scheme 26: Reaction of (**3**), to form [LSm(pyrimidine)] (**28**), and [$(LSm)_2$(μ-dihydro-bipyrimidine)] (**29**).(L = $(Me_8N_2Ph_2)^{2-}$)

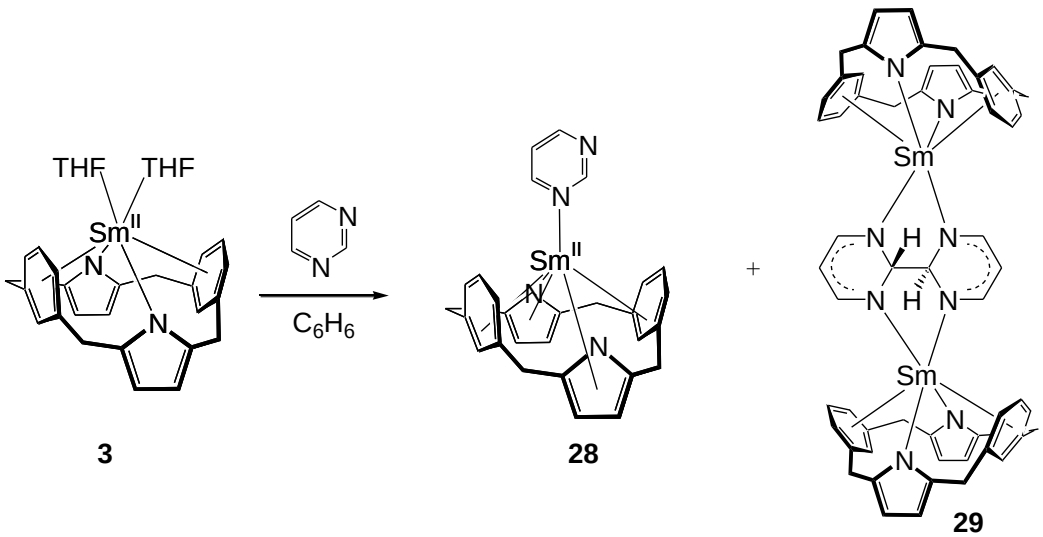

Purple crystals of the 1:1 adduct, [($Me_8N_2Ph_2$)Sm(pyrimidine)], **28**, were grown from benzene. The crystal belongs to the orthorhombic space group $P2_12_12_1$ (No. 19) with a = 10.263(3), b = 15.4140(5), c = 18.907(1) Å. The unit cell contains 4 macrocyclic units. The molecular structure is shown in Figure 95.

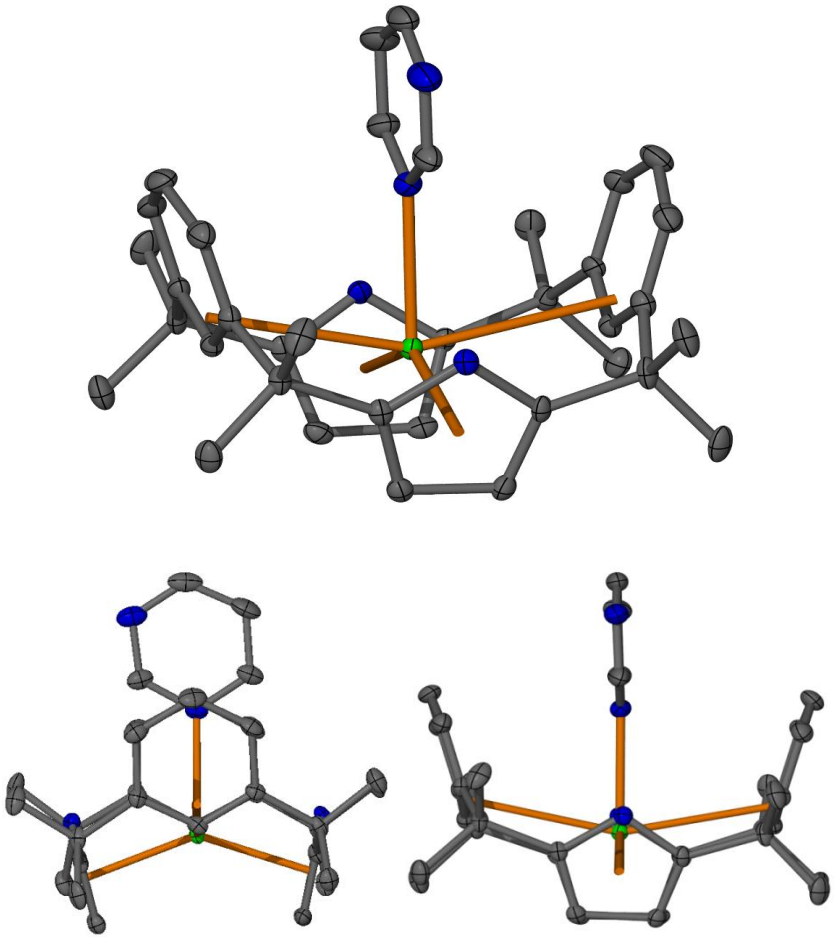

Figure 95: Molecular structure of [($Me_8N_2Ph_2$)Sm(pyrimidine)], (**28**) with thermal ellipsoids drawn at 50% probability (protons omitted for clarity).

The molecular structure of **28** shares conformational characteristics with the pyrazine complex **25** and mono-pyridine complex **13** (Table 13). The samarium metal centre is

located low in the macrocyclic cavity and the coordinated pyrimidine binds within the groove formed by the two phenylene moieties. The phenylene units of the macrocycle were observed to be splayed outwards, with each phenylene binding η^3 to the metal centre. Overall the macrocycle binds η^3:η^5:η^3:η^5 to the metal.

Table 13: Selected properties of similar single crystal structures **28**, **25** and **13**, (L = $(Me_8N_2Ph_2)^{2-}$).

	[LSm(pyrimidine)] (28)	**[LSm(pyrazine)] (25)**	**[LSm(pyridine)] (13)**
M in cavity	Low	Low	Low
M–N (Å)	2.621(3)	2.645(3)	2.596(3)
M–$\eta^6_{(Ph)}$ (Å)	NA (η^3)	NA (η^3)	NA (η^3)
$\theta_{(Ph)}$ (°)	NA (η^3)	NA (η^3)	NA (η^3)
Φ (°)	28.2	28.2	28.5
M–$\eta^x_{(Py)}$ (Å)	2.51, 2.52 (η^5)	2.50, 2.51 (η^5)	2.48, 2.49 (η^5)
$\theta_{(Py)}$ (°)	141.3	137.3	136.4

The Sm–N bond distance of 2.621(3) Å indicates an oxidation state of Sm(II), with the pyrimidine coordinated as a neutral Lewis base adduct, similar to the pyrazine and mono-pyridine complexes **25** and **13**.

Lanthanide complexes with neutral pyrimidine adduct ligands, for example, $[(C_5H_4R)_3Ce^{III}(pyrimidine)]$ (R = *t*Bu, $SiMe_3$) have been previously reported.[341] There are numerous examples of neutral pyrimidine adducts with transition metals, such as $[(pyrimidine)_4M(NCS)_2]$ (M = Co, Ni),[401] or $[(C_6H_6)RuCl_2(pyrimidine)]$,[402] amongst others.[403-405]

An orange crystalline minor product was also observed under the microscope when preparing crystals of the above purple major product for single crystal X-ray diffraction. These crystals were isolated by hand and analysed by single crystal X-ray diffraction. Crystals of the orange crystalline minor product were identified as a 2:1 complex containing reductively coupled pyrimidine, [{($Me_8N_2Ph_2$)Sm}$_2$(μ-2,2'-dihydro-bipyrimidine)], **29**. The crystals belong to the monoclinic space group *C*2/c (No. 15) with a = 32.527(3), b = 10.8540(15), c = 20.001(3) Å, β = 122.988(3)°. The unit cell contains 4 molecules, with half of a molecule in the asymmetric unit. The pyrimidines are coupled through the C2 atom, with the two samarium metal centres each bridging between nitrogen atoms from each of the coupled pyrimidine groups.

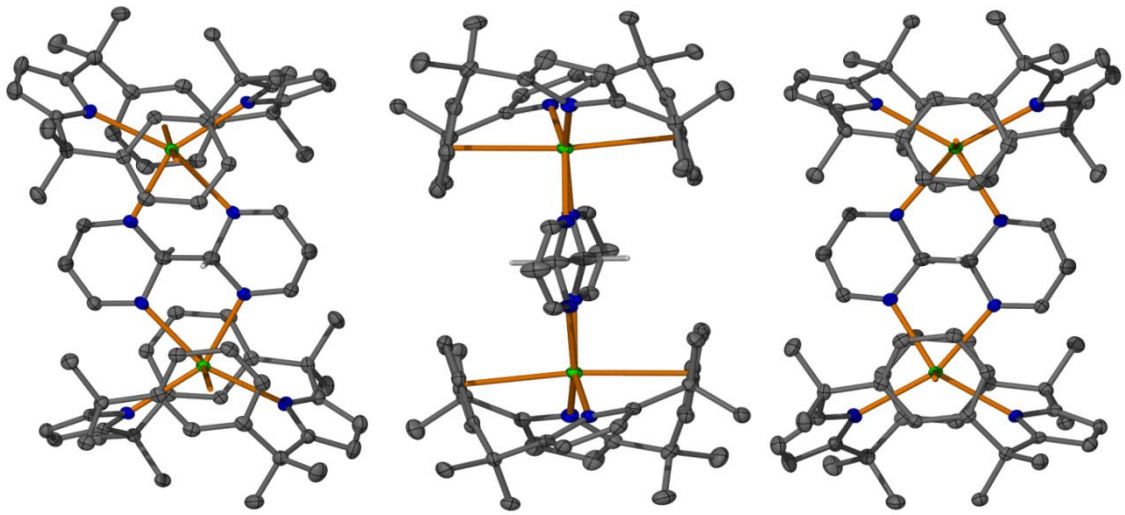

Figure 96: Molecular structure of the coupled minor product [{($Me_8N_2Ph_2$)Sm}$_2$(μ-2,2'-dihydro-bipyrimidine)], (**29**) with thermal ellipsoids drawn at 50% probability (except for C2, protons have been omitted for clarity).

A search of the literature has not uncovered any previous reports of pyrimidine reductively coupling. The Sm–N bond lengths of 2.44(3) and 2.489(3) Å are consistent with a reduced *N*-heterocyclic species. The pyrimidines have coupled through their C2 carbons, the atom with the least electron density in the heterocycle. The 2,2'-bipyrimidine formed has protons on the coupled C2 carbons, which means the ligand is not planar.

2,2'-Bipyrimidine

The coupled pyrimidine moeity in **29** is structurally related to 2,2'-bipyrimidine (Figure 97), which is known as a chelating ligand able to form 2:1 complexes similar to (**29**). A 2,2'-bipyrimidine complex was prepared in order to compare and contrast it's single crystal molecular structure with the coupled pyrimidine product.

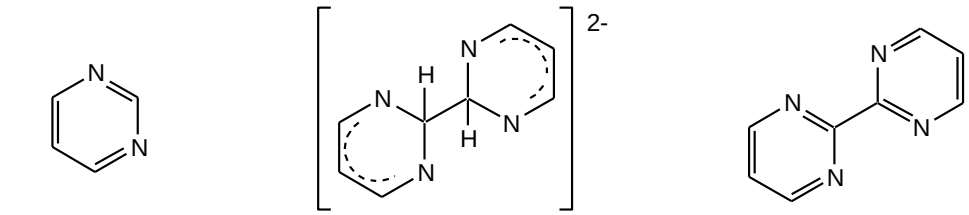

pyrimidine

reductively coupled
$(2,2'\text{-bipyrimidine}H_2)^{2-}$

2,2'-bipyrimidine

Figure 97: Pyrimidine, coupled pyrimidine (as seen in complex **29**), and 2,2'-bipyrimidine.

A stoichiometric amount of 2,2'-bipyrimidine in benzene was added to a purple solution of $[(Me_8N_2Ph_2)Sm(THF)_2]$, **3**, immediately forming a dark green solution (Scheme 27).

A crystalline product was observed after 18 hrs, and continued to form over the following 72 hrs. Blue crystals suitable for single crystal X-ray diffraction were isolated and washed with benzene. The product is insoluble in benzene, preventing analysis by NMR spectroscopy or sufficient purification for elemental analysis.

Scheme 27: Reaction of [($Me_8N_2Ph_2$)Sm($THF)_2$], **3**, with 2,2'-bipyrimidine to form [{($Me_8N_2Ph_2$)Sm}$_2$(2,2'-bipyrimidine)], (**30**).

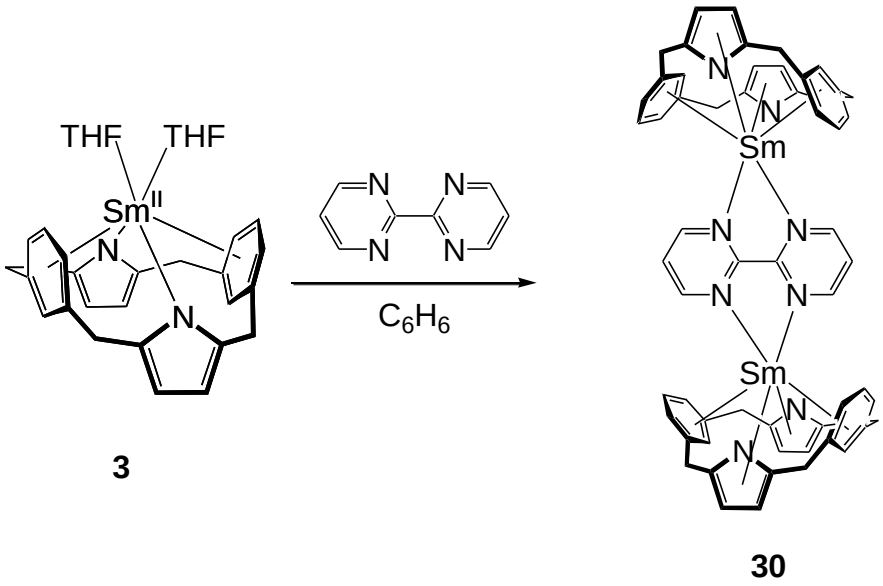

3 **30**

Crystals of [{($Me_8N_2Ph_2$)Sm}$_2$(2,2'-bipyrimidine)], (**30**), belong to the monoclinic space group *C*2/c (No. 15) with a = 32.380(1), b = 10.818(3), c = 20.061(1) Å, β = 122.976(4)°. As shown in Figure 98, this complex shares a very similar structure to the coupled pyrimidine complex **29**, and their crystal structures are isomorphous. Selected distances and angles of these two similar Sm complexes are shown in Table 14, and indicate that this is also a Sm(II) complex.

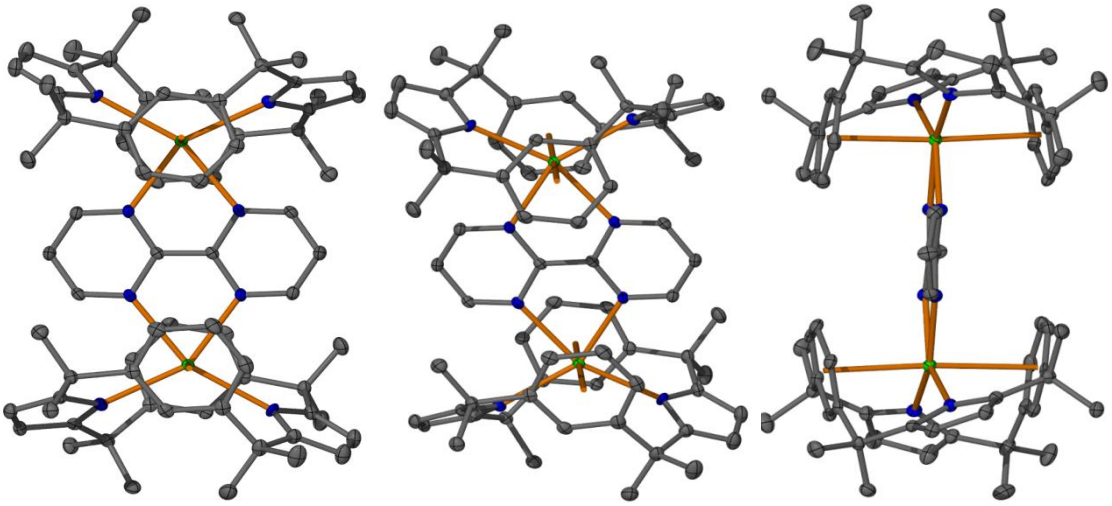

Figure 98: Molecular structure of [{($Me_8N_2Ph_2$)Sm}$_2$(2,2'-bipyrimidine)], (**30**) with thermal ellipsoids drawn at 50% probability (protons omitted for clarity).

Table 14: Selected bond and angle measurements of [{($Me_8N_2Ph_2$)Sm}$_2$(bipyrimidine)] (**30**) and [{($Me_8N_2Ph_2$)Sm}$_2$(μ-2,2'-drihydro-bipyrimidine)] (**29**) (L = $(Me_8N_2Ph_2)^{2-}$).

	[(LSm)$_2$(bipyrimidine)] (30)	**[(LSm)$_2$(μ-2,2'-dihydro-2,2'-bipyrimidine)] (29)**
M in cavity	High	High
M–N (Å)	2.436(3), 2.486(3)	2.444(3), 2.489(3)
M–$\eta^x_{(Ph)}$ (Å)	2.66, 2.71 (η^6)	2.70, 2.76 (η^6)
$\theta_{(Ph)}$ (°)	175.6	172.4
Φ (°)	19.1	24.0
M–$\eta^x_{(Py)}$ (Å)	2.442(2), 2.459(3) (η^1)	2.451(3), 2.467(3) (η^1)

Similar bridging 2,2'-bipyrimidine complexes such as [{$(C_5Me_5)_2Ln$}$_2$(μ_2-2,2'-bipyrimidine)] for Ln = Gd, Dy, Tb, Yb are known.[351, 406] The Yb complex is an adduct, whilst the Gd, Tb and Dy complexes have a bipyrimidyl dianion bridging between two lanthanide(III) metal atoms. Related bimetallic lanthanide(III) complexes with 2,2'-bipyrimidine and acetylacetonate ligands have been prepared with the aim of doping organic light-emitting diodes (OLEDs).[407]

Pyridazine

Pyridazine (*o*-diazine) is a 1,2-diazine, containing two adjacent nitrogen atoms, Figure 99. The nitrogen atoms attract more electron density, which as a result gives the other atoms in the ring a partially positive charge. This has the effect of making the pyridazine an unappealing target for electrophilic attack.[408]

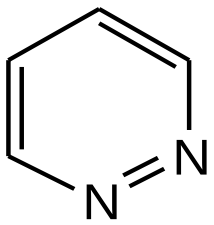

Figure 99: Pyridazine.

Reaction of [$(Me_8N_2Ph_2)Sm(THF)_2$], **3**, with pyridazine yields the samarium complex [{$(Me_8N_2Ph_2)Sm$}$_2$(μ-4,4'-dihydro-bipyridazine)], **31**, (Scheme 28). Orange crystals of complex **31** were isolated, washed and recrystallised from benzene. Single crystals suitable for X-ray diffraction were obtained and found to belong to the monoclinic

space group $P2_1/n$ (No. 14) with a = 11.741(3), b = 19.847(4), c = 16.898(4) Å, β = 110.218(8) °. The pyridazine coordinates through both nitrogen atoms to a samarium metal centre. Two complexes are coupled through the C4 carbons of the pyridazines, as seen in Figure 100.

Scheme 28: Reaction of [($Me_8N_2Ph_2$)Sm($THF)_2$], (**3**), with pyridazine to form [{($Me_8N_2Ph_2$)Sm}$_2$(μ-4,4'-dihydro-bipyridazine)] (**31**).

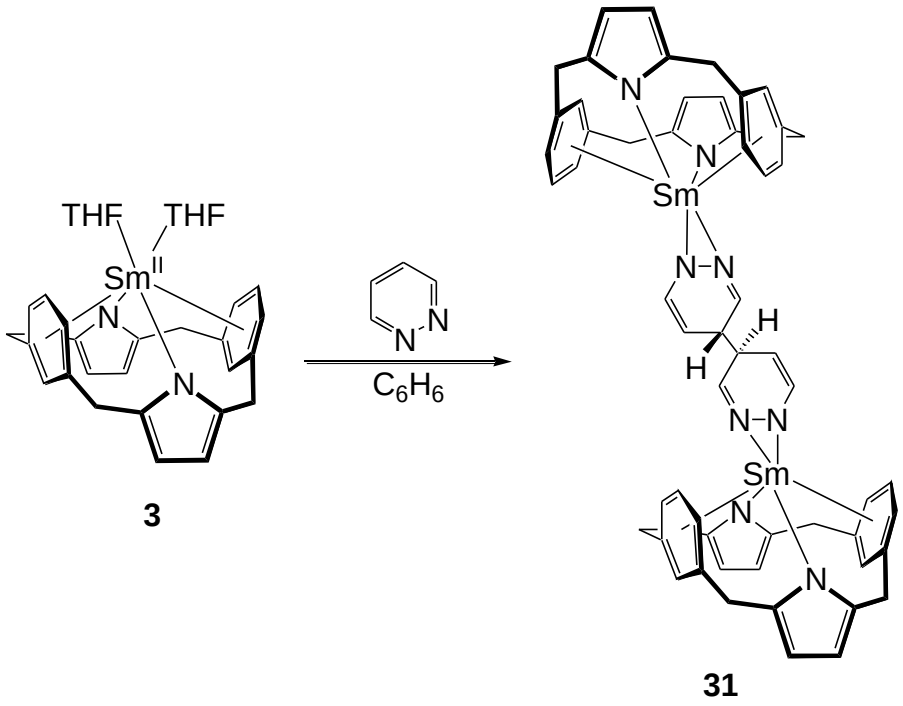

3 **31**

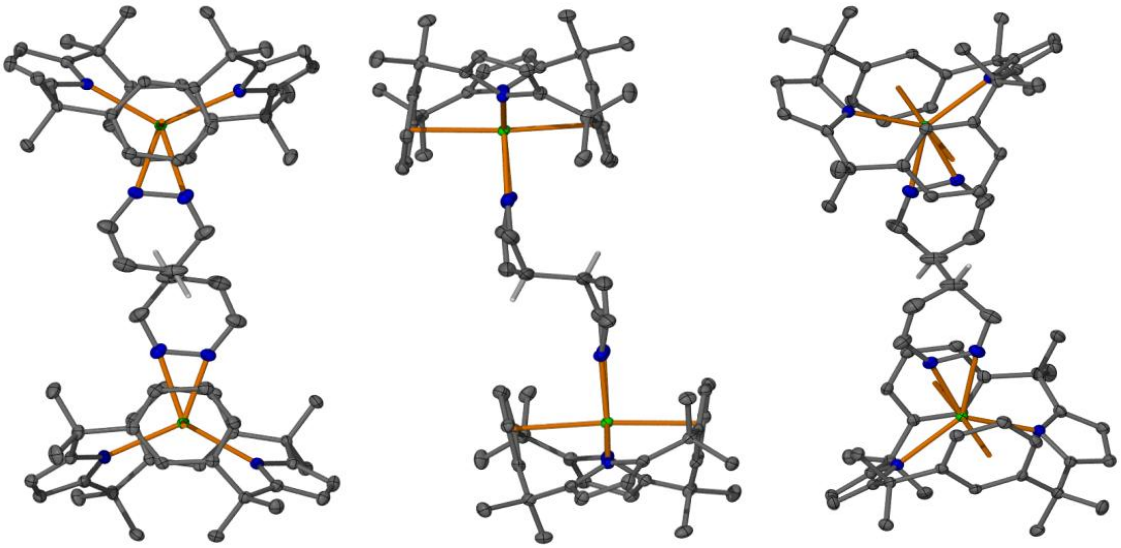

Figure 100: Molecular structure of [{($Me_8N_2Ph_2$)Sm}$_2$(μ-4,4'-dihydro-bipyridazine)] (**31**) with thermal ellipsoids drawn at 50% probability (except for C4, protons omitted for clarity).

The metal centre sits high in the macrocyclic cavity, approximately between the centroids of the phenylenes, allowing the metal to bind both nitrogens of one pyrimidine moeity. The metal centre is bound η^1:η^6:η^1:η^6 to the macrocyclic ligand. The pyridazine molecule sits in the top of the macrocyclic cavity, located between the two phenylene groups. The pyridazine is coupled to a second pyridazine samarium macrocycle molecule through their C4 carbons. The pyridazine is distorted in shape, with the C4 carbons pulled toward each other and away from the plane of the diazine. Table 15 lists selected measurements of the single crystal molecular structure.

Table 15: Selected bond and angle measurements of [{($Me_8N_2Ph_2$)Sm}$_2$(μ-4,4'-dihydro-bipyridazine)] (**31**) and [{($Me_8N_2Ph_2$)Sm}$_2$(μ-2,2'-dihydro-2,2'-bipyrimidine)])] (**29**) (L = $(Me_8N_2Ph_2)^{2-}$).

	[(LSm)$_2$(μ-4,4'-dihydro-bipyridazine)] (31)	**[(LSm)$_2$(μ-2,2'-dihydro-2,2'-bipyrimidine)] (29)**
M in cavity	High	High
M–N (Å)	2.319(3), 2.440(3)	2.444, 2.489
M–$\eta^x_{(Ph)}$ (Å)	2.63, 2.69 (η^6)	2.700, 2.764 (η^6)
$\theta_{(Ph)}$ (°)	175.1 (η^6)	172.4
Φ (°)	18.0	24.0
M–$\eta^x_{(Py)}$ (Å)	2.442(2), 2.451(2) (η^1)	2.451, 2.467 (η^1)

The reaction of [(C_5Me_5)$_2$Sm(THF)$_2$] with pyridazine in toluene forms [{(C_5Me_5)$_2$Sm(THF)}$_2$(μ-bipyridazine)] as a yellow-orange powder, Figure 101.[360] Similar to **31**, two pyridazine molecules couple through the C4 carbons, forming a bipyridazine moiety, despite the [{(C_5Me_5)$_2$Sm(THF)}$_2$(μ-bipyridazine)] having less steric bulk than the macrocyclic complex. Each pyridazine ring binds through both nitrogens to a Sm^{III} atom, and consistent with the structure of **31**, these two bonds differ by approximately 0.12 Å in length. Evans writes that this difference in bond distance suggests two different bond types, a single bond (Sm–NR_2) and coordination of a lone pair (Sm←:NR_3).[360] The pyridazine does not initially form a dianion bound to two Sm^{III} ions, but rather an intermediate one electron reduction product that then couples through the C4 position to form the final product, consistent with the most electron density being located at the 1 and 4 positions.

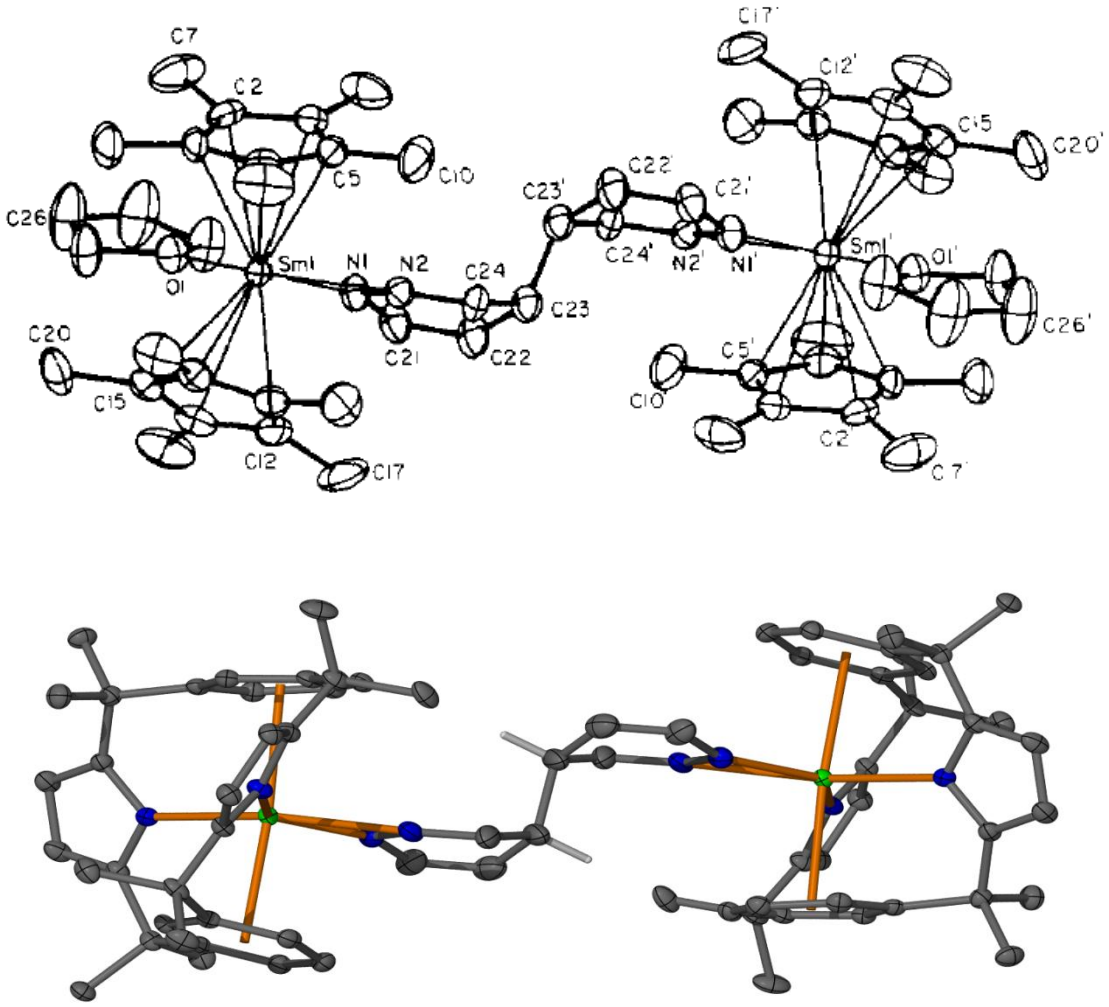

Figure 101: [{$(C_5Me_5)_2Sm(THF)\}_2$(μ-dihydro-bipyridazine)], reproduced from literature (above)[360] and [{$(Me_8N_2Ph_2)Sm\}_2$(μ-4,4'-dihydro-bipyridazine)], **31**, (below).

An analogous reaction of decamethylytterbocene does not reduce the pyridazine, and instead forms the neutral bis-pyridazine adduct [$(C_5Me_5)_2Yb$(*o*-pyridazine)$_2$].[351] When reacted with pyridazine trivalent [$Ce(C_5H_4tBu)_3$] also forms a Lewis base adduct, [$Ce(C_5H_4tBu)_3$(pyridazine)], the first reported η^2-coordinated pyridazine in a mononuclear complex.[341]

3.3 Conclusions

The series of complexes reported in this Chapter showcase the flexibility of the $(Me_8N_2Ph_2)^{2-}$ ligand. This macrocyclic ligand responds to the environment of its metal centre by adopting different binding modes which result in a change in size of the macrocyclic cavity. Hapticity changes push or pull the metal centre in or out of the cavity, and the macrocycle can twist to accommodate large ligands.

This work indicates that the $(Me_8N_2Ph_2)^{2-}$ ligand is very capable of stabilising low valent *f* elements. The macrocycle may be able to stabilise some of the more reactive lanthanide(II) ions, leading to some interesting and important chemistry.

The reactivity of lanthanide complexes of $(Me_8N_2Ph_2)^{2-}$ has also been extensively investigated for a range of heterocycles, with some interesting results. Where lanthanide(II) complexes such as $[(C_5Me_5)_2Sm]$ have reduced heterocycles, and in turn formed samarium(III) products, the adaptable $(Me_8N_2Ph_2)^{2-}$ ligand has instead tended to bind the less reducible heterocycles to form samarium(II) neutral adducts. Reductive reactivity was observed in some cases, with the $(Me_8N_2Ph_2)^{2-}$ samarium(II) complexes reductively coupling some heterocycles to form 2:1 samarium(III) products.

In the case of pyrazine and phenazine, the former produced an samarium(II) adduct whilst the latter was reduced and formed a 2:1 product. Reaction of $[(Me_8N_2Ph_2)Sm(THF)_2]$ with pyrimidine formed a samarium(II) adduct as a major

product, along with a 2:2 dihydro-2,2'-bipyrimidine complex. This minor product was found to be isomorphous to the 2,2'-bipyrimidine complex, despite the chemical differences in the bridging ligands.

Chapter 4

Conclusions

This work has described the synthesis and characterisation of lanthanide complexes of the macrocyclic calix[2]phenylene[2]pyrrolide ligand. Samarium(II), samarium(III) and europium(II) complexes have been prepared, characterised and discussed.

Chapter 1 provided a background of lanthanide and organolanthanide chemistry, introducing the ubiquitous cyclopentadienyl and pentamethylcyclopentadienyl ligands. A variety of alternative ligand sets were described, with a focus on pyrrolide chemistry and in particular the tetrapyrrolic macrocycle calix[4]pyrrole. A broad introduction to modifications to the calix[4]pyrrole macrocycle was given, outlining additions to the macrocycle at the *meso*-carbons or to the pyrrole moiety on the nitrogen atom or the carbon backbone. Background information on further modifications through changing the heteroatom, the heterocycle, or the number of heterocyclic units were described. A *trans*-*N*,*N'*-dimethylated calix[4]pyrrolide ligand utilised in past work within our research group was introduced, alongside the calix[2]phenylene[2]pyrrole macrocycle that forms the focus of this thesis. Recent advances in lanthanide(II) chemistry were described.

Chapter 2 described the synthesis of *meso*-octamethylcalix[2]phenylene[2]pyrrolide complexes with potassium, lithium, samarium and europium. The convenience of the lithium complex over potassium as a precursor to lanthanide complexes is highlighted. The efficiency of subsequent preparation of samarium(II) complexes which are (largely)

free of *N*-confused macrocyclic product is noted. Simple samarium(II) adducts with THF demonstrate the range of flexibility of the macrocyclic ligand, whilst the preparation of an NCMe adduct provided an unexpected property; unlike other lanthanide nitriles, reductive cleavage does not occur on the nitrile, instead a samarium(II) complex free of coordinated solvent was observed. A samarium(III) chloride complex was prepared and characterised. Europium(II) complexes with THF and NCMe were characterised for comparison with the analogous samarium complexes.

Chapter 3 described complexes prepared by reacting THF adducts of the lanthanide(II) precursor with a series of pyridines and diazines, largely with investigation based on structural characteristics as determined by single crystal X-ray diffraction. Examples of neutral mono- and bis- adducts, possible single electron ligand reduction and reductively dimerised products were reported.

This thesis has revealed a number of avenues for future work. The ancillary-ligand-free samarium macrocycle is a desirable target for reactivity studies with the activation of small molecules, as was observed for the related $(Et_8N_4Me_2)^{2-}$ ligand. The bis(NCMe) complex not undergoing the usual reductive cleavage is an interesting property that warrants further explanation. In comparison to other ligand systems, samarium(II) complexes of this $(Me_8N_2Ph_2)^{2-}$ macrocyclic ligand tend to have weaker reductive properties. The flexibility and adaptability of the $(Me_8N_2Ph_2)^{2-}$ macrocyclic ligand are convenient for preparing stable organolanthanide complexes, and it would be of interest to prepare complexes with lanthanide and actinide metal centres with their different

sizes, reactivities and electronic properties. Already thorium and uranium complexes with the $(Me_8N_2Ph_2)^{2-}$ ligand have been prepared and reported.[409]

Chapter 5

Experimental

General Experimental Information

With the exception of the air-stable preparation of calix[2]phenylene[2]pyrrole, all manipulations on a scale over 100 mg were performed under an atmosphere of high purity argon using standard Schlenk techniques. Smaller scale manipulations and storage of samples were performed in an atmosphere of dry nitrogen in a glove box. Solvents (THF, PhMe, hexanes) were dried using an Innovative Technologies Solvent Purification system and stored over a sodium or potassium mirror as appropriate. Deuterated benzene was dried over sodium, fractionally distilled and freeze-degassed before use. Acetonitrile used in the preparation of the air-stable calix[2]phenylene[2]pyrrolide was used as received. NMR solvents were dried over sodium using benzophenone indicator and trap-to-trap distilled before use. Volatile liquid reagents were purchased from commercial sources and dried over 4 Å sieves and then distilled trap-to-trap prior to use. Volatile solid reagents were purchased from commercial sources and sublimed prior to use. Non-volatile solid reagents were purchased from commercial sources and heated under vacuum before use.

NMR spectra were recorded in $CDCl_3$ or C_6D_6 using a Varian Mercury Plus 300 NMR operating at 299.91 MHz (^1H) and 75.42 MHz (^{13}C). Proton spectra were referenced to residual solvent resonances for $CDCl_3$ (7.26 ppm) or C_6D_6 (7.16 ppm).

Elemental Analyses were undertaken at the Central Science Laboratory, University of Tasmania by Dr. Thomas Rodemann using a ThermoFinnigan Flash EA 1112 Elemental Analyser.

Data for single crystal structures obtained by X-ray diffraction were collected using the macromolecular crystallography MX1 and MX2 beamlines at the Australian Synchrotron, Victoria, with crystals mounted on Hampton Scientific cryoloops. Data was collected at −173 °C on a single axis goniometer with 360 ° rotation at maximum resolution using a fixed detector. Blu-Ice software[410] was used to operate the diffractometer and data was reduced using XDS.[411, 412] Structures were solved and refined by Assoc. Prof. Michael Gardiner using direct methods with SHELXS-97[413] and refined using full-matrix least-squares routines against F^2 with SHELXL-97[413] and visualised using X-SEED.[414] Unless otherwise specified, all non-hydrogen atoms were refined anisotropically and all hydrogens placed in calculated positions. Calculated hydrogens were refined using a riding model with fixed C–H distances of 0.95 (sp^2-CH), 0.99 (sp^3-CH, CH_2), 0.98 Å (CH_3). The thermal parameters of all calculated hydrogen atoms were estimated as $U_{iso}(H) = 1.2\ U_{eq}(C)$, except for CH_3 where $U_{iso}(H) = 1.5\ U_{eq}(C)$. Details are provided electronically as .CIF files in the Appendix and are named according to the complex number referred to within this thesis.

Synthesis of $Me_8N_2Ph_2H_2$, 1

This is a modification of Sessler's preparation[272] by Frey.[229]

1,3-bis(1,1'-dimethylhydroxymethyl)benzene (13.51 g, 69.5 mmol) was stirred with pyrrole (4.5 mL, 69.5 mmol) in 800 mL acetonitrile for 15 minutes until dissolved, forming a pale straw-coloured solution. Scandium triflate (120 mg, 244 μmol) in acetonitrile (5 mL) was added and the mixture left without stirring for 7 days. Over this time the yellow solution darkened to a deep green and product formed as colourless rosette crystals. The product was collected by filtration and washed with acetonitrile. The supernatant was reduced *in vacuo* and formed a second crop of product over three days. The combined solids were washed with acetonitrile and purified by sublimation at 220 °C / 1 x 10^{-3} mmHg to yield $Me_8N_2Ph_2H_2$ as colourless crystals (1.41 g, 9%).

^{1}H NMR (299.91 MHz, $CDCl_3$, 25 °C; partially assigned): δ =1.52 (s, 24H, *meso*-CH_3), 5.97 (d, 4H, pyrrolide CH), 6.62 (s, br, 2H, NH), 6.75 (s, 2H, phenylene CH), 7.21 (m, 6H, phenylene CH).

^{13}C NMR (75.42 MHz, $CDCl_3$, 25 °C): δ = 30.4, 39.4, 103.4, 122.7, 126.9, 127.9, 139.8, 149.4.

Synthesis of $[(Me_8N_2Ph_2)Li_2(THF)_4]$, 2

Colourless crystals of **1** $Me_8N_2Ph_2H_2$ (2.3804 g, 5.3 mmol) were suspended in hexane/THF (50 mL) in a flamed-out Schlenk flask under argon. *N*-Butyl lithium (6.6 mL of 1.6 M solution in hexane, 10.56 mmol) was injected, immediately forming a milky suspension which was stirred at room temperature for one hour. Filtration yielded the desired product as a white powder (3.576 g, 90%) which was dried under vacuum and stored under nitrogen. **2** is soluble in THF and insoluble in hexane. The ^{1}H NMR spectrum was consistent with that obtained by Fisk in earlier work on this complex.[415] Crystals suitable for X-ray diffraction analysis were grown from a THF solution layered with hexane.

^{1}H NMR (299.91 MHz, THF-D_8, 25 °C; partially assigned): δ = 1.57 (s, 24H, *meso*-CH_3), 5.72 (s, 4H, pyrrolide CH), 6.90 (m, 6H, phenylene CH), 8.25 (s br, 2H, phenylene CH).

Synthesis of $[(Me_8N_2Ph_2)Sm(THF)_2]$, 3

The colourless powder $[(Me_8N_2Ph_2)Li_2(THF)_4]$ (960 mg, 130 μmol) was dissolved in THF (5 mL) prior to the addition of SmI_2 (12.8 mL of 0.1M solution in THF, 130 μmol). The clear solution darkened immediately upon addition of the samarium diiodide, and the resulting dark brown solution was stirred for two hours to ensure completion of reaction. Purple crystals formed in the solution over two hours at room temperature

without stirring. The mixture was cooled in the freezer a further 6 hours to yield more crystalline product. The dark orange mother liquor was removed by cannula and the purple crystals dried under vacuum, losing solvent to yield **3** as a fine purple powder (921 mg, 98%) which was stored under nitrogen. This bis(THF) product **3** is sparingly soluble in benzene. A ^{1}H NMR spectrum was obtained and found to be consistent with results reported by Frey,[315] with an additional very broad resonance identified at 120 ppm. Low solubility prevented the collection of useful ^{13}C and 2D NMR spectra.

^{1}H NMR (299.91 MHz, C_6D_6, 25 °C; partially assigned): δ = −4.48 (br, 8H, THF), −3.12 (s, 12H, *meso*-CH_3), −1.42 (br, 8H, THF), 5.91 (br, 4H), 6.43 (br, 4H), 7.66 (s, 2H), 10.46 (s, 12H, *meso*-CH_3), 120 (br, 2H, phenylene CH).

Synthesis of [(Me$_8$N$_2$Ph$_2$)Sm(THF)], 4

Recrystallisation of **3** from benzene or toluene yields purple crystals of the mono(THF) complex **4** in near-quantitative yield. As with complex **3**, the ^{1}H NMR spectrum of **4** was found to be consistent with results reported by Frey,[315] with an additional very broad resonance identified at 120 ppm. Low solubility prevented the collection of useful ^{13}C and 2D NMR spectra.

^{1}H NMR (299.91 MHz, C_6D_6, 25 °C; partially assigned): δ = -12.33 (br, 4H, THF), -4.10 (s, 4H, THF), -3.83 (s, 12H, *meso*-CH_3), 5.47 (br, 4H, aromatic CH) 6.97 (s, 4H,

aromatic CH), 7.16 (s, 2H, aromatic CH), 10.29 (s, 12H, *meso*-CH_3), 120 (br, 2H, phenylene CH).

Synthesis of [$(Me_8N_2Ph_2)Eu(THF)_2$], 5

A colourless solution of **2** [$(Me_8N_2Ph_2)Li_2(THF)_4$] (300 mg, 399 μmol) in 2 mL THF was prepared under nitrogen. Bright green europium diodide was added ($EuI_2.THF_2$, 227 mg, 413 μmol), with the mixture immediately changing to an orange colour. Large orange crystals formed over the following 12 hours (231 mg, 96%). Solid state crystal structure and elemental analysis confirm this product to be [$(Me_8N_2Ph_2)Eu(THF)_2$], **5**, isomorphous to the samarium analogue **3**.

Elemental analysis: ($C_{40}H_{52}N_2O_2Eu$, MW = 744.83)

Calc.: C, 64.50; H, 7.04; N, 3.76

Found: C, 64.53; H, 6.91; N, 3.56.

Synthesis of [$(Me_8N_2Ph_2)Eu(THF)$], 6

Recrystallisation of **5**, [$(Me_8N_2Ph_2)Eu(THF)_2$], from benzene yields fine orange crystals of [$(Me_8N_2Ph_2)Eu(THF)$], **6**, in quantitative yield. A solid state crystal structure isomorphous to the samarium analogue **4** was obtained for this product, but no further characterisation was pursued.

Synthesis of [(Me$_8$N$_2$Ph$_2$)SmCl], 7

Two drops of *t*BuCl were added to a solution of [(Me$_8$N$_2$Ph$_2$)Sm(THF)$_2$], **3**, (50 mg, 67 μmol) in 3 mL benzene. An immediate colour change from dark purple to bright orange was observed. Slow evaporation of the solution yielded red-orange crystals suitable for X-ray diffraction, which were removed from the liquor and washed with benzene. A second crop of product was collected yielding a total of 25 mg (62%). This complex has very low solubility in C_6D_6.

^{1}H NMR (299.91 MHz, C_6D_6, 25 °C, partially assigned): δ = 1.45 (s, 12H, *meso*-CH_3), 1.92 (s, 12H, *meso*-CH_3), 3.59 (s, 2H), 4.56 (s, 2H), 5.31 (s, 4H, aromatic CH), 7.32 (s, 4H, aromatic CH).

Elemental analysis: ($C_{32}H_{36}N_2SmCl$, MW = 634.46)

Calculated:	C, 60.58;	H, 5.72;	N, 4.42
Found:	C, 60.59;	H, 5.68;	N, 4.19.

Synthesis of [(Me$_8$N$_2$Ph$_2$)Sm(NCMe)$_2$], 8

A dark purple solution of [(Me$_8$N$_2$Ph$_2$)Sm(THF)$_2$] (17 mg, 23 μmol) in benzene (2 mL) was prepared under an atmosphere of nitrogen at room temperature. Acetonitrile (1 drop, 26 mmol) was added to the solution with no immediate change observed. Over a

72 hour period the solution paled in colour, resulting in a colourless solution containing large dark red/purple crystals suitable for X-ray diffraction analysis (14 mg, 90%).

^{1}H NMR (299.91 MHz, C_6D_6, 25 °C; partially assigned): δ = -3.13 (s, 12H, CH_3), 10.64 (s, 12H, CH_3).

Elemental analysis: ($C_{42}H_{46}N_4Sm$, MW = 757.21)

Calculated:	C, 63.48;	H, 6.22;	N, 8.23
Found:	C, 63.53;	H, 6.38;	N, 7.83.

Synthesis of $[(Me_8N_2Ph_2)Eu(NCMe)_2]$, 9

Two drops of acetonitrile were added to a benzene solution of $[(Me_8N_2Ph_2)Eu(THF)_2]$, (**5**), (20 mg, 27 μmol) Orange needle crystals formed over 72 hrs of slow evaporation (17 mg, 93%). A solid state crystal structure was obtained for this product but no further characterisation was pursued.

Synthesis of $[\{(Me_8N_2Ph_2)Sm\}_n]$, 10

A clear purple solution of $[(Me_8N_2Ph_2)Sm(NCMe)_2]$, (**8**), (10 mg, 14 μmol) in C_6D_6 was heated to 50 °C for 48 hrs, then raised to 75 °C for a further 72 hours before being cooled slowly to room temperature. The resulting clear brown solution contained dark and colourless crystals (mass not recorded). X-ray diffraction of the dark crystals

showed 1:1 samarium macrocyclic units forming a polymeric chain with no ancillary ligands. Further characterisation was not obtained due to the small yield of product. Attempts to reproduce the unsolvated complex have proven unsuccessful.

Synthesis of [(Me$_8$N$_2$Ph$_2$)Sm(pyridine)$_2$], 11

A dark purple solution of [(Me$_8$N$_2$Ph$_2$)Sm(THF)$_2$] (**3**) (28 mg, 36 μmol) in benzene was prepared under an atmosphere of nitrogen. A molar excess of pyridine (3 drops) was added to the purple solution. Small dark blue crystals formed over 48 hrs, with the solution losing colour slowly as the crystals grow in size over 7 days. The resulting clear blue-grey liquor was removed by pipette, yielding dark purple crystals suitable for X-ray diffraction (28 mg, 98%). Low solubility impeded characterisation by NMR spectroscopy, which is partially assigned below.

^{1}H NMR (299.91 MHz, C_6D_6, 25 °C; partially assigned): δ = -3.15 (s, 12H, CH_3), 11.56 (s, 12H, CH_3), 132 (very broad, 2H, aromatic CH).

Elemental analysis: ($C_{42}H_{46}N_4Sm$, MW = 757.21)

Calculated:	C, 66.62;	H, 6.12;	N, 7.40
Found:	C, 66.55;	H, 6.41;	N, 7.19.

Synthesis of [(Me$_8$N$_2$Ph$_2$)Eu(pyridine)$_2$], 12

A molar excess of pyridine was added to an orange solution of [(Me$_8$N$_2$Ph$_2$)Eu(THF)$_2$], **5**, (25mg, 34 μmol) in benzene. Crystals formed over 72 hrs (20 mg, 79%) and were characterised by single crystal X-ray diffraction.

Synthesis of [(Me$_8$N$_2$Ph$_2$)Sm(pyridine)], 13

A pale blue benzene solution of [(Me$_8$N$_2$Ph$_2$)Sm(pyr)$_2$], **11**, (17 mg, 22 μmol) in a sealed Youngs tube was heated to 80 °C for 5 days, then raised to 110 °C for a further 3 days before being slowly cooled to room temperature. Purple plate crystals of mono(pyr) complex **13** were isolated from the solution (yield not recorded) and washed with a small amount of benzene and were characterised single crystal X-ray diffraction.

Synthesis of an oxygen-containing (Me$_8$N$_2$Ph$_2$)$^{2-}$ samarium complex, 14

This complex is described from yellow crystals obtained from a C_6D_6 solution of [(Me$_8$N$_2$Ph$_2$)Sm(pyr)], **13**, which had lost colour during an overnight ^{13}C NMR spectral analysis. Yellow crystals of [(Me$_8$N$_2$Ph$_2$)Sm^{III}(pyr)]$^{+}{}_2$[{(Me$_8$N$_2$Ph$_2$)Sm^{III}(μ-O)}$_2$]$^{2-}$ were obtained and characterised by single crystal X-ray diffraction. As this was a rogue decomposition product, further characterisation was not pursued.

Synthesis of [($Me_8N_2Ph_2$)Sm(2,6-dimethylpyridine)], 15

[($Me_8N_2Ph_2$)Sm(THF)], **4**, (30 mg, 45 μmol) was dissolved in 1 mL benzene, and one drop (a molar excess) of 2,6-dimethylpyridine added. No immediate colour change was observed. After 72 hrs slow evaporation dark green crystals (24 mg, 97 %) suitable for single crystal X-ray diffraction were isolated from the dark liquor and washed with benzene. Characterisation by NMR spectral analysis was prevented by insolubility.

Synthesis of [{($Me_8N_2Ph_2$)Sm}$_2$(μ-7,7'-dihydro-biacridine)], 16

A clear solution of acridine (5 mg, 28 μmol) in benzene (0.5 mL) was added to a dark purple solution of [($Me_8N_2Ph_2$)Sm($THF)_2$], **3**, (22 mg, 28 μmol) in benzene (1 mL) immediately forming a green solution which yielded two crops of dark green crystals over 72 hours (15 mg, 35%). These crystals are only sparingly soluble in benzene, preventing characterisation by either elemental analysis or NMR spectroscopy. Two crystal types were observed under the microscope; green crystals were characterised by single crystal X-ray diffraction and found to be [{($Me_8N_2Ph_2$)Sm}$_2$(μ-7,7'-dihydro-biacridine)], **16**, whilst the purple crystal product was not able to be identified despite repeated attempts at single crystal X-ray diffraction.

Synthesis of [($Me_8N_2Ph_2$)Sm(2,2'-bipyridine)], 17

A clear solution of 2,2'-bipyridine (5 mg, 32 μmol) in toluene (0.5 mL) was added to a dark purple solution of [($Me_8N_2Ph_2$)Sm($THF)_2$], **3**, (20 mg, 27 μmol) in toluene (1 mL),

with an immediate colour change to a dark green. Fine needle crystals formed alongside block crystals over 12 hours. The crude crystalline product was washed with toluene and recrystallised to yield purple blocks suitable for X-ray diffraction (20 mg, 98%). The dark crystals form a green solution in C_6D_6. A ^1H NMR spectrum was obtained in C_6D_6, however due to dramatic shifting of resonances it was unable to be reliably assigned. Attempts to obtain a useful ^{13}C NMR spectrum were unsuccessful, with only very weak resonances observed.

Elemental analysis: ($C_{42}H_{44}N_4Sm$, MW = 755.20)

Calculated:	C, 66.80;	H, 5.87;	N, 7.42
Found:	C, 66.93;	H, 5.73,	N, 7.19.

Synthesis of [($Me_8N_2Ph_2$)Sm(4,4'-bipyridine)], 18

Addition of crystalline 4,4'-bipyridine to a saturated solution of dark purple [($Me_8N_2Ph_2$)Sm(THF)$_2$], **3**, resulted in the formation of a milky purple suspension. Reducing the volume by slow evaporation over 24 hrs yielded crystals suitable for single crystal X-ray diffraction.

Reaction of [($Me_8N_2Ph_2$)Sm(THF)] with cuprione (2,2-biquinoline)

Cuprione (8 mg, 31 μmol) in benzene was added to a solution of [($Me_8N_2Ph_2$)Sm(THF)], **4**, (25 mg, 37 μmol) in benzene (3 mL), with an immediate

colour change from dark purple to a bright red solution. Over 6 hours a fine red-grey powder settled out from solution. The mother liquor was decanted and filtered through a glass wool plug. Upon very slow evaporation over 24 hrs small orange crystals formed, however attempts to characterise the product by X-ray single crystal diffraction were unsuccessful.

Synthesis of [(Me$_8$N$_2$Ph$_2$)Sm(2,2':6',2''-terpyridine)], 19

A clear solution of 2,2';6',2''-terpyridine (5 mg, 21 μmol) in benzene (0.5 mL) was added to a dark purple solution of [(Me$_8$N$_2$Ph$_2$)Sm(THF)$_2$], **3**, (16 mg, 22 μmol) in benzene (1 mL). Over 72 hours a very fine dark orange solid formed from the dark blue solution. The solution was pipette away and the product isolated and washed with benzene. A second crop of product was isolated from the mother liquor with slow evaporation, giving a total yield of 11 mg (62%). These dark orange crystals proved too insoluble for NMR spectroscopy, but were able to be characterised by single crystal X-ray diffraction.

Synthesis of [{(Me$_8$N$_2$Ph$_2$)Sm}$_2$(μ-4,4'-dihydro-biphen)], 20

1,10-Phenanthroline (5 mg, 28 μmol) was added to a solution of [(Me$_8$N$_2$Ph$_2$)Sm(THF)$_2$], **3**, (20 mg, 27 μmol) in benzene. Small dark crystals formed over 72 hrs, and were analysed by single crystal X-ray diffraction on the MX2 beamline

at the Australian Synchrotron. The crystals suffered decay in the beam, but the structure was able to be characterised using the data collected.

Synthesis of [(Me$_8$N$_2$Ph$_2$)Li$_2$(phen)], 21 and [(Me$_8$N$_2$Ph$_2$)Li$_2$(phen)$_2$], 22

These two complexes were identified by single crystal X-ray diffraction during repeated attempts to characterise the samarium complex [{(Me$_8$N$_2$Ph$_2$)Sm}$_2$(μ-4,4'-biphen)], **20**. These rogue products were not characterised beyond single crystal X-ray diffraction .

Synthesis of [{(Me$_8$N$_2$Ph$_2$)Sm}$_2${μ-4,4'-bis-(4,7-dimethylphen)}], 23

[(Me$_8$N$_2$Ph$_2$)Sm(THF)$_2$], **3**, (30 mg, 45 μmol) was dissolved in 3 mL benzene and combined with 4,7-dimethyl-1,10-phenanthroline (8 mg, 40 μmol) in 1 mL benzene to form a maroon-brown solution. Pink crystals were collected from the solution after 72 hrs and washed with benzene. A second crop of product was collected, with a total yield of 18 mg, 71%. The crystals were characterised by single crystal X-ray diffraction.

Synthesis of [(Me$_8$N$_2$Ph$_2$)Sm(4,7-diphenylphen)], 24

[(Me$_8$N$_2$Ph$_2$)Sm(THF)$_2$], **3**, (30 mg, 45 μmol) was dissolved in 3 mL benzene and combined with 4,7-diphenyl-1,10-phenanthroline (15 mg, 45 μmol) in 1 mL benzene to form a teal coloured solution. Green crystals were collected from the solution after 72

hrs and washed with benzene. A second crop of product was collected, with a total yield of 34 mg, 97%. The crystals were characterised by single crystal X-ray diffraction.

Reaction of [(Me$_8$N$_2$Ph$_2$)Sm(THF)$_2$] with neocuprione

Neocuprione (10 mg, 48 μmol) in benzene was added to a solution of [(Me$_8$N$_2$Ph$_2$)Sm(THF)], **4**, (25 mg, 34 μmol) in benzene (3 mL), immediately forming a milky suspension of fine purple-brown powder which settled out of the green-brown solution. The powder was removed by filtration, and slow evaporation of the mother liquor yielded red and orange crystals however attempts to discern their structure by X-ray diffraction were unsuccessful. The small scale of reaction prevented characterisation by NMR spectroscopy and these products were not pursued further.

Synthesis of [(Me$_8$N$_2$Ph$_2$)Sm(pyrazine)], 25

[(Me$_8$N$_2$Ph$_2$)Sm(THF)$_2$], **3**, (43 mg , 58 μmol) was dissolved in 2 mL benzene, making a dark solution. A solution of pyrazine (5 mg, 62 μmol) in 1 mL benzene was added dropwise. Over 7 days dark purple prism crystals formed, which were collected and washed with benzene. A second crop of crystals were grown from the liquor, total yield of 37 mg, 94%.

^{1}H NMR (299.91 MHz, C_6D_6, 25°C; partially assigned): δ = -3.75 (s, 12H, CH_3), 10.98 (s, 12H, CH_3).

Synthesis of [(Me$_8$N$_2$Ph$_2$)Eu(pyrazine)], 26

A solution of [(Me$_8$N$_2$Ph$_2$)Eu(THF)$_2$], **5**, (25 mg, 34 μmol) in benzene was prepared, and solution of pyrazine (6 mg, 75 μmol) in benzene was added dropwise. Orange plate crystals of **26** formed over 72 hours and were characterised by single crystal X-ray crystallography.

Synthesis of [{(Me$_8$N$_2$Ph$_2$)Sm}$_2$(phenazine)], 27

Bright yellow crystals of phenazine (5 mg, 28 μmol) were dissolved in 1 mL benzene and added to a solution of [(Me$_8$N$_2$Ph$_2$)Sm(THF)$_2$], **3**, (38 mg, 55 μmol). An immediate colour change was observed from dark purple to orange. Over 12 hrs dark crystals formed from the orange solution, which were washed with benzene. Yield of 35 mg, 100%.

Elemental analysis: ($C_{76}H_{80}N_6Sm_2$, MW = 1378.24)

Calculated:	C, 66.23;	H, 5.85;	N, 6.10
Found:	C, 67.31;	H, 6.19;	N, 5.44

Synthesis of [(Me$_8$N$_2$Ph$_2$)Sm(pyrimidine)], 28 and [{(Me$_8$N$_2$Ph$_2$)Sm}$_2$(μ-dihydro-bipyrimidine)], 29

A dark purple solution of [(Me$_8$N$_2$Ph$_2$)Sm(THF)$_2$], **3**, (50 mg, 68 μmol) in PhMe was prepared and pyrimidine (5 mg, 68 μmol) added. No colour change was observed. Over 7 days dark crystals formed in the solution. The liquor was pipetted away from the crystals and kept to grow a second crop or product. The crystals were washed with a small amount of benzene, yielding below 10 mg. The product was washed with benzene, in which it is only slightly soluble. Note that attempts to recrystallise the product were unsuccessful.

On inspection under the microscope it was observed that the product contains two crystal types. The major product is the dark purple adduct, (**28**), whilst the orange minor product, (**29**), is coupled with a bond formed ortho to each of the nitrogens of two pyrimidine ligands. The two products were not able to be separated, therefore characterisation relies on single crystal X-ray diffraction.

Synthesis of [{(Me$_8$N$_2$Ph$_2$)Sm}$_2$(2,2'-bipyrimidine)], 30

2,2'-Bipyrimidine (10 mg, 0.6 μmol) in 1 mL benzene was added to a solution of [(Me$_8$N$_2$Ph$_2$)Sm(THF)$_2$], **3**, in 3 mL benzene. The mixture immediately changed from purple to a dark green colour, with crystals forming over 4 days. Dark blue crystals were collected and washed with benzene, with a second crop of crystals growing over

the following 48 hrs. Total yield of 34 mg, 45%. Whilst the crystal was characterised by single crystal X-ray diffraction, insolubility prevented characterisation by NMR spectroscopy.

Synthesis of [{($Me_8N_2Ph_2$)Sm}$_2$(μ-4,4'-bipyridazine)], 31

A molar excess of pyridazine (1 drop) was added to a solution of [($Me_8N_2Ph_2$)Sm(THF)$_2$], **3**, (43 mg, 58 μmol) in benzene (3 mL). The mixture formed a clear bright orange solution, which formed orange crystals overnight (9 mg, 23%). Whilst the crystal was characterised by single crystal X-ray diffraction, insolubility prevented characterisation by NMR spectroscopy.

Chapter 6

References

1. P. Thyssen and K. Binnemans, in *Handbook on the Physics and Chemistry of Rare Earths*, eds. J.-C. G. B. Karl A. Gschneidner and K. P. Vitalij, Elsevier, 2011, vol. 41, pp. 1-93.

2. H. C. Aspinall, *Chemistry of the f-Block Elements*, CRC Press, 2001.

3. F. Nief, *Eur. J. Inorg. Chem.*, 2001, 891-904.

4. H. B. Kagan, M. Sasaki and J. Collin, *Pure Appl. Chem.*, 1988, **60**, 1725-1730.

5. N. Kaltsoyannis and P. Scott, *The f elements*, Oxford University Press, 1999.

6. S. Cotton, *Lanthanide and Actinide Chemistry*, Wiley, 2007.

7. L. R. Morss, *Chem. Rev.*, 1976, **76**, 827-841.

8. W. J. Evans, N. T. Allen and J. W. Ziller, *Angew. Chem. Int. Ed.*, 2002, **41**, 359.

9. J. J. Katz, G. T. Seaborg and L. R. Morss, *The Chemistry of the Actinide Elements*, 2nd edn., Chapman and Hall, London, 1986.

10. L. R. Morss, *Handbook on the Physics and Chemistry of Rare Earths*, Elsevier Science, Amsterdam, 1994.

11. D. F. Shriver and P. W. Atkins, *Inorganic Chemistry*, 3rd Edition edn., Oxford University Press, 1999.

12. G. Molander and J. A. C. Romero, *Chem. Rev.*, 2002, **102**, 2161.

13. S. Hong and T. J. Marks, *Acc. Chem. Res.*, 2004, **37**.

14. Z. M. Hou and Y. Wakatsuki, *Coord. Chem. Rev.*, 2002, **231**, 1-22.

15. U. Schuchardt, F. Fabri, R. B. Muterle and W. de Oliveira, *Polymer*, 2006, **47**, 4544-4548.

16. D. M. Cui, Z. C. Zhang and X. L. Liu, *J. Polym. Sci. Pol. Chem.*, 2008, **46**, 6810-6818.

17. F. T. Edelmann, in *Struct Bond*, 2010, vol. 137, pp. 109-163.

18. G. Q. Yu, Y. L. Li, Y. H. Qu and X. L. Li, *Macromolecules*, 1993, **26**, 6702-6705.

19. C. Iftner, F. Bonnet, F. Nief, M. Visseaux and L. Maron, *Organometallics*, 2011, **30**, 4482-4485.

20. H. Yasuda, Y. Nakayama, Y. Satoh, Z. Q. Shen, X. F. Ni, M. Inoue and S. Namba, *Polym. Int.*, 2004, **53**, 1682-1685.

21. D. Baudry-Barbier, N. Andre, A. Dormond, C. Pardes, P. Richard, M. Visseaux and C. J. Zhu, *Eur. J. Inorg. Chem.* 1998, 1721-1727.

22. H. Schumann, M. Glanz, J. Gottfriedsen and S. Dechert, *Advances on Organometallic Catalysts and Olefin Polymerization in China and Germany*, 2001, 226-232.

23. E. N. Kirillov, E. A. Fedorova, A. A. Trifonov and M. N. Bochkarev, *Appl. Organomet. Chem.*, 2001, **15**, 151-156.

24. M. N. Bochkarev, I. L. DFedushkin, A. A. Fagin, T. V. Petrovskava, J. Ziller, W,, R. N. R. Broomhall-Dillard and W. J. Evans, *Agnew. Chem., Int. Ed. Engl.*, 1997, **36**, 133.

25. F. T. Edelmann, *Coord. Chem. Rev.*, 2011, **255**, 1834-1920.

26. D. J. Wilson and D. K. Jenkins, *Polym. Bull.*, 1992, **27**, 407-411.

27. V. S. Sastri, J. R. Perumareddi, V. R. Rao, G. V. S. Rayudu and J.-C. G. Bunzli, *Modern Aspects of Rare Earths and Their Complexes*, Elsevier, 2003.

28. Y. Shimizu, F. C. Lin, Y. Takao and M. Egashira, *J. Am. Ceram. Soc.*, 1998, **81**, 1633-1643.

29. E. L. Brosha, R. Mukundan, D. R. Brown and F. H. Garzon, *Sensor Actuat. B: Chem.*, 2002, **87**, 47-57.

30. N. F. Szabo, H. Du, S. A. Akbar, A. Soliman and P. K. Dutta, *Sensor Actuat. B: Chem.*, 2002, **82**, 142-149.

31. R. Ramamoorthy, P. K. Dutta and S. A. Akbar, *J. Mater. Sci.*, 2003, **38**, 4271-4282.

32. G. A. Molander, *Chem. Rev.*, 1992, **92**, 29-68.

33. R. J. Mears, L. Reekie, I. M. Jauncey and D. N. Payne, *Electron Lett.*, 1987, **23**, 1026-1028.

34. S. V. Eliseeva and J. C. G. Bunzli, *New J. Chem.*, 2011, **35**, 1165-1176.

35. M. A. Katkova and M. N. Bochkarev, *Dalton Trans.*, 2010, **39**, 6599-6612.

36. R. Taube and M. R. Kunze, *Z. Anorg. Allg. Chem*, 2010, **636**, 2454-2461.

37. B. S. Richards, *Sol. Energ. Mat. Sol. Cells*, 2006, **90**, 1189-1207.

38. Q. Y. Zhang and X. Y. Huang, *Prog. Mater. Sci.*, 2010, **55**, 353-427.

39. M. Nyman, M. A. Rodriguez, L. E. S. Rohwer, J. E. Martin, M. Waller and F. E. Osterloh, *Chem. Mater.*, 2009, **21**, 4731-4737.

40. Y. He, Y. Wu, T. Sheng and X. Wu, *J. Hazard. Mater.*, 2010, **180**, 675-682.

41. L. D. Carlos, R. A. S. Ferreira, V. D. Bermudez, B. Julian-Lopez and P. Escribano, *Chem. Soc. Rev.*, 2011, **40**, 536-549.

42. S. V. Eliseeva, D. N. Pleshkov, K. A. Lyssenko, L. S. Lepnev, J.-C. G. Bünzli and N. P. Kuzmina, *Inorg. Chem.*, 2010, **49**, 9300-9311.

43. J. L. Major and T. J. Meade, *Acc. Chem. Res*, 2009, **42**, 893-903.

44. K. N. Allen and B. Imperiali, *Curr. Opin.Chem. Biol.*, 2010, **14**, 247-254.

45. L. Cheng, K. Yang, S. Zhang, M. Shao, S. Lee and Z. Liu, *Nano. Res.*, 2010, **3**, 722-732.

46. B. Song, C. D. B. Vandevyver, A.-S. Chauvin and J.-C. G. Bunzli, *Org. Biomol. Chem.*, 2008, **6**, 4125-4133.

47. J. J. Croat, *J. Appl. Phys.*, 1997, **81**, 4804-4809.

48. R. Sessoli and A. K. Powell, *Coord. Chem. Rev.*, 2009, **253**, 2328-2341.

49. K. Bernot, F. Pointillart, P. Rosa, M. Etienne, R. Sessoli and D. Gatteschi, *Chem. Commun.*, 2010, **46**, 6458-6460.

50. M. Andruh, J.-P. Costes, C. Diaz and S. Gao, *Inorg. Chem.*, 2009, **48**, 3342-3359.

51. T. M. Jahns, G. B. Kliman and T. W. Neumann, *IEEE Trans. Ind. Appl.*, 1986, **IA-22**, 738-747.

52. M. Ooshima, A. Chiba, T. Fukao and M. A. Rahman, *IEEE Trans. Ind. Electron*, 1996, **43**, 292-299.

53. J. A. Barclay, *J. Alloys. Compd.*, 1994, **207–208**, 355-361.

54. K. A. Gschneidner and V. K. Pecharsky, Patent US 5537826 A, Jul 23, 1996.

55. V. K. Pecharsky and J. K. A. Gschneidner, *Phys. Rev. Lett.*, 1997, **78**, 4494-4497.

56. V. K. Pecharsky and K. A. Gschneidner Jr, *J. Magn. Magn. Mater.*, 1999, **200**, 44-56.

57. K. A. Gschneidner and V. K. Pecharsky, *Annu. Rev. Mater. Sci.*, 2000, **30**, 387-429.

58. K. A. GschneidnerJr, V. K. Pecharsky and A. O. Tsokol, *Rep. Prog. Phys.*, 2005, **68**, 1479.

59. G. J. Miller, *Chem. Soc. Rev.*, 2006, **35**, 799-813.

60. D. Z. Huang, X. Y. Wang, G. M. Li, Z. Liu, Z. H. Peng, S. Q. Huang and S. W. Dong, in *Future Material Research and Industry Application, Pts 1 and 2*, ed. K. S. Thaung, 2012, vol. 455-456, pp. 1552-1560.

61. C. F. Li, X. H. Li, Q. L. Li, J. H. Guo and X. H. Li, *J. Anal. At. Spectrom.*, 2011, **26**, 2012-2022.

62. I. T. Uysal, J. X. Zhao, S. D. Golding, M. G. Lawrence, M. Glikson and K. D. Collerson, *Chem. Geol.*, 2007, **238**, 63-71.

63. G. Caro, B. Bourdon, J. L. Birck and S. Moorbath, *Geochim. Cosmochim. Acta*, 2006, **70**, 164-191.

64. G. T. Seaborg, *Radiochim. Acta*, 1993, **61**, 115-122.

65. P. Caravan, J. J. Ellison, T. J. McMurry and R. B. Lauffer, *Chem. Rev.*, 1999, **99**, 2293-2352.

66. C. J. Burns and B. E. Bursten, *Comments on Inorganic Chemistry*, 1989, **9**, 61-93.

67. C. H. Booth, M. D. Walter, D. Kazhdan, Y. J. Hu, W. W. Lukens, E. D. Bauer, L. Maron, O. Eisenstein and R. A. Andersen, *J. Am. Chem. Soc.*, 2009, **131**, 6480-6491.

68. W. J. Evans, *New. J. Chem.*, 1995, **19**, 525-533.

69. Shannon, *Acta. Cryst. A*, 1976 **32** 751-767.

70. W. J. Evans, J. L. Shreeve, J. W. Ziller and R. J. Doedens, *Inorg. Chem.*, 1995, **34**, 576-585.

71. W. J. Evans, *Inorg. Chem.*, 2007, **46**, 3435-3449.

72. W. J. Evans, R. Dominguez and T. P. Hanusa, *Organometallics*, 1986, **5**, 263-270.

73. M. N. Bochkarev, I. L. Fedushkin, A. A. Fagin, T. V. Petrovskaya, J. W. Ziller, R. N. R. BroomhallDillard and W. J. Evans, *Angew. Chem. Int. Ed.*, 1997, **36**, 133-135.

74. M. N. Bochkarev, A. A. Fagin, I. L. Fedushkin, A. A. Trifonov, E. N. Kirillov, I. L. Eremenko and S. E. Nefedov, *Mater. Sci. Forum*, 1999, **315-3**, 144-153.

75. W. J. Evans, *J. Organomet. Chem.*, 2002, **652**, 61-68.

76. N. B. Mikheev, S. A. Kulyukhin, A. N. Kamenskaya, I. A. Rumer and N. A. Konovalova, *Radiochemistry*, 2004, **46**, 521-535.

77. L. R. Morss and M. C. McCue, *Inorg. Chem.*, 1975, **14**, 1624-1627.

78. P. Anderson, *Expert Opin. Pharmacother.*, 2006, **7**, 1475-1486.

79. O. Sartor, *Rev. Urol.*, 2004, **6**, S3-S12.

80. B. Ira, Patents US2843539 A, July 15 1958.

81. J. Collin, J. L. Namy and H. B. Kagan, *Nouv. J. Chim.*, 1986, **10**, 229-232.

82. S. Zhiquan and J. Ouyang, in *Handbook on the Physics and Chemistry of Rare Earths*, eds. Karl A. Gschneidner, Jr. and E. LeRoy, Elsevier, 1987, vol. Volume 9, pp. 395-428.

83. J. Zhang, A. G. MacPhee, J. Lin, E. Wolfrum, R. Smith, C. Danson, M. H. Key, C. L. S. Lewis, D. Neely, J. Nilsen, G. J. Pert, G. J. Tallents and J. S. Wark, *Science*, 1997, **276**, 1097-1100.

84. M. T. McCulloch and G. J. Wasserburg, *Science*, 1978, **200**, 1003-1011.

85. S. Claesson, J. Pallister and M. Tatsumoto, *Contr. Mineral. and Petrol.*, 1984, **85**, 244-252.

86. J. T. Chesley, A. N. Halliday and R. C. Scrivener, *Science*, 1991, **252**, 949-951.

87. A. Prinzhofer, D. A. Papanastassiou and G. J. Wasserburg, *Geochim. Cosmochim. Acta*, 1992, **56**, 797-815.

88. J. L. Namy, P. Girard and H. B. Kagan, *Nouv. J. Chim.*, 1977, **1**, 5-7.

89. P. Girard, J. L. Namy and H. B. Kagan, *J. Am. Chem. Soc.*, 1980, **102**, 2693-2698.

90. G. A. Molander and J. A. Mckie, *J. Org. Chem.*, 1992, **57**, 3132-3139.

91. A. Krief and A. M. Laval, *Chem. Rev.*, 1999, **99**, 745-777.

92. J. A. Soderquist, *Aldrichim. Acta*, 1991, **24**, 15.

93. H. B. Kagan and J. L. Namy, *Tetrahedron*, 1986, **42**, 6573-6614.

94. S. Labouille, F. Nief and L. Maron, *J. Phys. Chem. A*, 2011, **115**, 8295-8301.

95. R. A. Flowers Ii and E. Prasad, in *Handbook on the Physics and Chemistry of Rare Earths*, eds. J.-C. G. B. Karl A. Gschneidner and K. P. Vitalij, Elsevier, 2006, vol. Volume 36, pp. 393-473.

96. F. Machrouhi, B. Hamann, J. L. Namy and H. B. Kagan, *Synlett*, 1996, 633-&.

97. W. J. Evans, N. T. Allen and J. W. Ziller, *J. Am. Chem. Soc.*, 2000, **122**, 11749-11750.

98. L. J. Nugent, Lauberea.Pg, G. K. Werner and Vandersl.Kl, *J. Organomet. Chem.*, 1971, **27**, 365-&.

99. K. O. Hodgson, K. Mares, D. F. Starjs and A. Streitwieser, Jr, *J. Am. Chem. Soc.*, 1973, **95**, 8650-8658.

100. R. D. Fischer, in *Fundamental and Technological Aspects of Organo-f-Element Chemistry*, eds. T. Marks and I. Fragalà, Springer Netherlands, 1985, vol. 155, pp. 277-326.

101. R. D. Fischer, in *Organometallics of the f-Elements*, eds. T. J. Marks and R. D. Fischer, Springer Netherlands, 1979, vol. 44, pp. 337-377.

102. W. Jahn, K. Yünlü, W. Oroschin, H.-D. Amberger and R. D. Fischer, *Inorg. Chim. Acta*, 1984, **95**, 85-104.

103. J. J. Uebel and R. M. Wing, *J. Am. Chem. Soc.*, 1972, **94**, 8910-&.

104. Cockeril.Af, G. L. O. Davies, R. C. Harden and D. M. Rackham, *Chem. Rev.*, 1973, **73**, 553-588.

105. T. A. Gerken and W. M. Ritchey, *J. Magn. Reson.*, 1976, **24**, 155-164.

106. A. D. Sherry, C. R. Malloy, F. M. H. Jeffrey, W. P. Cacheris and C. F. G. C. Geraldes, *J. Magn. Reson.*, 1988, **76**, 528-533.

107. B. McGarvey, in *Organometallics of the f-Elements*, eds. T. Marks and R. D. Fischer, Springer Netherlands, 1979, vol. 44, pp. 309-336.

108. Evans, *J. Organomet. Chem.*, 1987, **326**, 299-306.

109. J. Jensen and A. R. Mackintosh, *Rare Earth Magnetism: Structures and Excitations*, Clarendon Press, Oxford, 1991.

110. R. Fischer, *NMR of Paramagnetic Molecules*, 1973, 521-553.

111. T. J. Kealy and P. L. Pauson, *Nature*, 1951, **168**, 1039.

112. G. Wilkinson, M. Rosenblum, M. C. Whiting and R. B. Woodward, *J. Am. Chem. Soc.*, 1952, **74**, 2125-2126.

113. P. F. Eiland and R. Pepinsky, *J. Am. Chem. Soc.*, 1952, **74**.

114. W. J. Evans and B. L. Davis, *Chem. Rev.*, 2002, **102**.

115. G. Wilkinson and J. M. Birmingham, *J. Am. Chem. Soc.*, 1954, **76**, 6210.

116. J. M. Birmingham and G. Wilkinson, *J. Am. Chem. Soc.*, 1956, **78**, 42-44.

117. Calderaz.F, Pappalar.R and S. Losi, *J. Inorg. Nucl. Chem.*, 1966, **28**, 987-&.

118. S. Manastyrskyj, M. Dubeck and R. E. Maginn, *Inorg. Chem.*, 1963, **2**, 904-&.

119. R. E. Maginn, Manastry.S and M. Dubeck, *J. Am. Chem. Soc.*, 1963, **85**, 672-&.

120. S. Manastyrskyj and M. Dubeck, *Inorg. Chem.*, 1964, **3**, 1647-&.

121. E. O. Fischer and H. Fischer, *Angew. Chem. Int. Edit.*, 1964, **3**, 132-&.

122. G. W. Watt and F. O. Drummond, *J. Am. Chem. Soc.*, 1966, **88**, 5926-&.

123. J. L. Namy, J. Collin, J. Zhang and H. B. Kagan, *J. Organomet. Chem.*, 1987, **328**, 81-86.

124. S. Agarwal, N. E. Brandukova-Szmikowski and A. Greiner, *Macromol. Rapid Comm.*, 1999, **20**, 274-278.

125. A. Streitwieser and U. Mueller-Westerhoff, *J. Am. Chem. Soc.*, 1968, **90**, 7364-7364.

126. F. Mares, K. Hodgson and Streitwi.A, *J. Organomet. Chem.*, 1970, **24**, C68-&.

127. F. Mares, K. O. Hodgson and Streitwi.A, *J. Organomet. Chem.*, 1971, **28**, C24-&.

128. W. J. Evans, I. Bloom, H. W. E. and J. L. Atwood, *J. Am. Chem. Soc.*, 1981, **103**, 6507.

129. W. J. Evans, L. R. Chamberlain, T. A. Ulibarri and J. W. Ziller, *J. Am. Chem. Soc.*, 1988, **110**, 6423-6432.

130. W. J. Evans, L. A. Hughes and T. P. Hanusa, *J. Am. Chem. Soc.*, 1984, **106**, 4270-4272.

131. W. J. Evans, L. A. Hughes and T. P. Hanusa, *Organometallics*, 1986, **5**, 1285-1291.

132. R. A. Andersen, J. M. Boncella, C. J. Burns, J. C. Green, D. Hohl and N. Rosch, *J. Chem. Soc. Chem. Comm.*, 1986, 405-407.

133. T. A. Ulibarri, J. W. Ziller and W. J. Evans, *Abstr. Pap. Am. Chem. S.*, 1988, **196**, 377-INOR.

134. W. J. Evans, T. A. Ulibarri and J. W. Ziller, *J. Am. Chem. Soc.*, 1990, **112**, 2314-2324.

135. W. J. Evans, S. L. Gonzales and J. W. Ziller, *J. Am. Chem. Soc.*, 1994, **116**, 2600-2608.

136. W. J. Evans, D. G. Giarikos, C. B. Robledo, V. S. Leong and J. W. Ziller, *Organometallics*, 2001, **20**, 5648-5652.

137. W. J. Evans, T. A. Ulibarri and J. W. Ziller, *J. Am. Chem. Soc.*, 1990, **112**, 219-223.

138. W. J. Evans, D. B. Rego, J. W. Ziller, A. G. DiPasquale and A. L. Rheingold, *Organometallics*, 2007, **26**, 4737-4745.

139. W. J. Evans, G. W. Rabe and J. W. Ziller, *J. Organomet. Chem.*, 1994, **483**, 21-25.

140. W. J. Evans, *Polyhedron*, 1987, **6**, 803-835.

141. W. J. Evans, D. K. Drummond, L. R. Chamberlain, R. J. Doedens, S. G. Bott, H. M. Zhang and J. L. Atwood, *J. Am. Chem. Soc.*, 1988, **110**, 4983-4994.

142. W. J. Evans, T. A. Ulibarri and J. W. Ziller, *J. Am. Chem. Soc.*, 1988, **110**, 6877-6879.

143. B. M. Schmiege, J. W. Ziller and W. J. Evans, *Inorg. Chem.*, 2010, **49**, 10506-10511.

144. P. L. Watson and G. W. Parshall, *Acc. Chem. Res*, 1985, **18**, 51-56.

145. W. J. Evans and D. K. Drummond, *J. Am. Chem. Soc.*, 1988, **110**, 2772-2774.

146. W. J. Evans, R. A. Keyer, H. Zhang and J. L. Atwood, *J. Chem. Soc. Chem. Comm.*, 1987, 837-838.

147. C. J. Burns and R. A. Andersen, *J. Am. Chem. Soc.*, 1987, **109**, 941-942.

148. W. J. Evans, L. A. Hughes, D. K. Drummond, H. M. Zhang and J. L. Atwood, *J. Am. Chem. Soc.*, 1986, **108**, 1722-1723.

149. C. J. Burns and R. A. Andersen, *J. Am. Chem. Soc.*, 1987, **109**, 5853-5855.

150. W. J. Evans and D. K. Drummond, *J. Am. Chem. Soc.*, 1986, **108**, 7440-7441.

151. W. J. Evans, D. K. Drummond, S. G. Bott and J. L. Atwood, *Organometallics*, 1986, **5**, 2389-2391.

152. W. J. Evans, S. L. Gonzales and J. W. Ziller, *J. Am. Chem. Soc.*, 1991, **113**, 9880-9882.

153. W. J. Evans, S. L. Gonzales and J. W. Ziller, *J. Chem. Soc. Chem. Comm.*, 1992, 1138-1138.

154. W. J. Evans, A. L. Wayda, W. E. Hunter and J. L. Atwood, *J. Chem. Soc. Chem. Comm.*, 1981, 706-708.

155. W. J. Evans, S. C. Engerer, P. A. Piliero and A. L. Wayda, *J. Chem. Soc. Chem. Comm.*, 1979, 1007-1008.

156. G. Jeske, H. Lauke, H. Mauermann, H. Schumann and T. J. Marks, *J. Am. Chem. Soc.*, 1985, **107**, 8111-8118.

157. W. J. Evans, J. W. Grate, L. A. Hughes, H. Zhang and J. L. Atwood, *J. Am. Chem. Soc.*, 1985, **107**, 3728-3730.

158. W. J. Evans, S. L. Gonzales and J. W. Ziller, *J. Am. Chem. Soc.*, 1991, **113**, 7423-7424.

159. T. D. Tilley and R. A. Andersen, *Inorg. Chem.*, 1981, **20**, 3267-3270.

160. W. J. Evans, J. M. Perotti, S. A. Kozimor, T. M. Champagne, B. L. Davis, G. W. Nyce, C. H. Fujimoto, R. D. Clark, M. A. Johnstone and J. Ziller, W, *Organometallics*, 2005, **24**, 3916-3931.

161. W. J. Evans and S. E. Foster, *J. Organomet. Chem.*, 1992, **433**, 79-94.

162. W. J. Evans, K. J. Forrestal and J. W. Ziller, *Angew. Chem. Int. Ed.*, 1997, **36**, 774-776.

163. W. J. Evans, K. J. Forrestal and J. W. Ziller, *J. Am. Chem. Soc.*, 1998, **120**, 9273-9282.

164. G. W. Nyce, J. W. Ziller and W. J. Evans, *Abstr. Pap. Am. Chem. S.*, 2001, **221**, U740-U741.

165. W. J. Evans, B. L. Davis, T. M. Champagne and J. W. Ziller, *P. Natl. Acad. Sci. USA*, 2006, **103**, 12678-12683.

166. K. J. Forrestal, W. J. Evans and J. W. Ziller, *Abstr. Pap. Am. Chem S.*, 1996, **211**, 298-INOR.

167. G. W. Nyce, R. A. Clark, J. W. Ziller and W. J. Evans, *Abstr. Pap. Am. Chem S.*, 1999, **217**, U1006-U1006.

168. W. J. Evans, G. W. Nyce and J. W. Ziller, *Abstr. Pap. Am. Chem S.*, 1999, **217**, U37-U37.

169. W. J. Evans, G. W. Nyce, K. J. Forrestal and J. W. Ziller, *Organometallics*, 2002, **21**, 1050-1055.

170. W. J. Evans, G. W. Nyce and J. W. Ziller, *Angew. Chem. Int. Ed.*, 2000, **39**, 240.

171. W. J. Evans, G. W. Nyce, M. A. Johnston and J. W. Ziller, *J. Am. Chem. Soc.*, 2000, **122**, 12019-12020.

172. F. T. Edelmann, *Angew. Chem. Int. Ed.*, 1995, **34**, 2466-2488.

173. M. P. Hogerheide, J. Boersma and G. vanKoten, *Coord. Chem. Rev.*, 1996, **155**, 87-126.

174. F. T. Edelmann, D. M. M. Freckmann and H. Schumann, *Chem. Rev.*, 2002, **102**, 1851-1896.

175. S. T. Liddle, *P. Roy. Soc. a-Math Phy.*, 2009, **465**, 1673-1700.

176. S. A. Cotton, *Coord. Chem. Rev.*, 1997, **160**, 93-127.

177. C. Eaborn, P. B. Hitchcock, K. Izod and J. D. Smith, *J. Am. Chem. Soc.*, 1994, **116**, 12071-12072.

178. H. Schumann, J. Muller, N. Bruncks, H. Lauke, J. Pickardt, H. Schwarz and K. Eckart, *Organometallics*, 1984, **3**, 69-74.

179. H. Schumann, H. Lauke, E. Hahn and J. Pickardt, *J. Organomet. Chem.*, 1984, **263**, 29-35.

180. W. Q. Weng, K. Kunze, A. M. Arif and R. D. Ernst, *Organometallics*, 1991, **10**, 3643-3647.

181. K. Kunze, A. M. Arif and R. D. Ernst, *B. Soc. Chim. Fr.*, 1993, **130**, 708-711.

182. D. Baudry, F. Nief and L. Ricard, *J. Organomet. Chem.*, 1994, **482**, 125-130.

183. J. H. Jin, S. C. Jin, Z. S. Jin and W. Q. Chen, *J. Chem. Soc. Chem. Comm.*, 1991, 1328-1329.

184. R. D. Ernst and T. H. Cymbaluk, *Organometallics*, 1982, **1**, 708-713.

185. J. Sieler, A. Simon, K. Peters, R. Taube and M. Geitner, *J. Organomet. Chem.*, 1989, **362**, 297-303.

186. H. Schumann and A. Dietrich, *J. Organomet. Chem.*, 1991, **401**, C33-C36.

187. L. N. Bochkarev, T. A. Stepantseva, L. N. Zakharov, G. K. Fukin, A. I. Yanovsky and Y. T. Struchkov, *Organometallics*, 1995, **14**, 2127-2129.

188. A. L. Wayda, J. L. Atwood and W. E. Hunter, *Organometallics*, 1984, **3**, 939-941.

189. W. A. Herrmann, F. C. Munck, G. R. J. Artus, O. Runte and R. Anwander, *Organometallics*, 1997, **16**, 682-688.

190. A. C. Hillier, W. J. Sommer, B. S. Yong, J. L. Petersen, L. Cavallo and S. P. Nolan, *Organometallics*, 2003, **22**, 4322-4326.

191. P. L. Arnold, Z. R. Turner, A. I. Germeroth, I. J. Casely, R. Bellabarba and R. P. Tooze, *Dalton Trans.*, 2010, **39**, 6808-6814.

192. P. L. Arnold, J. McMaster and S. T. Liddle, *Chem. Commun.*, 2009, 818-820.

193. S. T. Liddle and D. P. Mills, *Dalton Trans.*, 2009, 5592-5605.

194. D. Barbier-Baudry, A. Dormond and M. Visseaux, *J. Organomet. Chem.*, 2000, **609**, 21-28.

195. F. Nief, B. T. de Borms, L. Ricard and D. Carmichael, *Eur. J. Inorg. Chem.*, 2005, 637-643.

196. F. Nief and L. Ricard, *J. Organomet. Chem.*, 1994, **464**, 149-154.

197. P. L. Arnold, F. G. N. Cloke and P. B. Hitchcock, *Chem. Commun.*, 1997, 481-482.

198. W. J. Evans, R. Anwander, M. A. Ansari and J. W. Ziller, *Inorg. Chem.*, 1995, **34**, 5-6.

199. B. J. Deelman, M. Booij, A. Meetsma, J. H. Teuben, H. Kooijman and A. L. Spek, *Organometallics*, 1995, **14**, 2306-2317.

200. P. Poremba, M. Noltemeyer, H. G. Schmidt and F. T. Edelmann, *J. Organomet. Chem.*, 1995, **501**, 315-319.

201. W. J. Evans, R. N. R. Broomhall-Dillard and J. W. Ziller, *J. Organomet. Chem.*, 1998, **569**, 89-97.

202. R. Anwander, F. C. Munck, T. Priermeier, W. Scherer, O. Runte and W. A. Herrmann, *Inorg. Chem.*, 1997, **36**, 3545-3552.

203. M. D. Walter, D. J. Berg and R. A. Andersen, *Organometallics*, 2007, **26**, 2296-2307.

204. A. Recknagel, M. Noltemeyer and F. T. Edelmann, *J. Organomet. Chem.*, 1991, **410**, 53-61.

205. J. A. Moore, A. H. Cowley and J. C. Gordon, *Organometallics*, 2006, **25**, 5207-5209.

206. A. A. Trifonov, E. N. Kirillov, M. N. Bochkarev, H. Schumann and S. Muehle, *Russ. Chem. Bull.* , 1999, **48**, 382-384.

207. A. A. Trifonov, Y. A. Kurskii, M. N. Bochkarev, S. Muehle, S. Dechert and H. Schumann, *Russ. Chem. Bull.* , 2003, **52**, 601-606.

208. A. A. Trifonov, E. A. Fedorova, V. N. Ikorskii, S. Dechert, H. Schumann and M. N. Bochkarev, *Eur. J. Inorg. Chem.*, 2005, 2812-2818.

209. C. L. Pan, W. Chen and J. F. Song, *Organometallics*, 2011, **30**, 2252-2260.

210. A. R. Petrov, O. Thomas, K. Harms, K. A. Rufanov and J. Sundermeyer, *J. Organomet. Chem.*, 2010, **695**, 2738-2746.

211. F. Y. Zhou, J. Wu, M. S. Lin, Y. Zhao, J. A. Wu, Y. Zhang, W. Li and Y. H. Li, *Z. Anorg. Allg. Chem.*, 2011, **637**, 117-121.

212. S. Gambarotta, G. Aharonian and G. P. A. Yap, *Organometallics*, 2002, **21**, 4257-4263.

213. K. C. Jantunen, B. L. Scott, J. C. Gordon and J. L. Kiplinger, *Organometallics*, 2007, **26**, 2777-2781.

214. D. Jacoby, C. Floriani, A. Chiesivilla and C. Rizzoli, *J. Am. Chem. Soc.*, 1993, **115**, 7025-7026.

215. M. Dennstedt and J. Zimmerman, *J. Am. Chem. Soc.*, 1887, **20**, 2449.

216. M. Dennstedt and J. Zimmerman, *J. Am. Chem. Soc.*, 1888, **21**, 1478.

217. M. Dennstedt, *J. Am. Chem. Soc.*, 1890, **23**, 1370.

218. V. V. Chelintzev and B. V. Tronov, *J. Russ. Phys. Chem. Soc.*, 1916, **48**, 127.

219. H. Fischer and H. Orth, *Die Chemie des Pyrrols*, Akademische Verlagsgesellschaft m.b.H, , Leipzig, 1934.

220. P. Rothemund and C. L. Gage, *J. Am. Chem. Soc.*, 1955, **77**, 3340-3342.

221. D. Jacoby, C. Floriani, A. Chiesivilla and C. Rizzoli, *J. Chem. Soc. Chem. Comm.*, 1991, 790-792.

222. P. A. Gale, J. L. Sessler, V. Kral and V. Lynch, *J. Am. Chem. Soc.*, 1996, **118**, 5140-5141.

223. V. Blangy, C. Heiss, V. Khlebnikov, C. Letondor, H. Stoeckli-Evans and R. Neier, *Angew. Chem. Int. Ed.*, 2009, **48**, 1688-1691.

224. L. Cuesta and J. Sessler, L., *Chem. Soc. Rev.*, 2009, **38**, 2497-2812.

225. J. L. Sessler, A. Andrievsky, V. Kral, P. Sansom, K. Shreder, P. A. Gale and B. L. Iverson, *Abstr. Pap. Am. Chem S.*, 1996, **212**, 185-INOR.

226. W. E. Allen, P. A. Gale, C. T. Brown, V. M. Lynch and J. L. Sessler, *J. Am. Chem. Soc.*, 1996, **118**, 12471-12472.

227. J. L. Sessler, Abstracts of Papers, 243rd ACS National Meeting & Exposition, United States, March, 2012.

228. P. A. Gale, J. L. Sessler and V. Kral, *Chem. Commun.*, 1998, 1-8.

229. D. Jacoby, C. Floriani, A. Chiesivilla and C. Rizzoli, *J. Chem. Soc. Chem. Comm.*, 1991, 220-222.

230. C. Floriani, *Chem. Commun.*, 1996, 1257-1263.

231. C. Floriani, *Pure Appl. Chem.*, 1996, **68**, 1-8.

232. L. Bonomo, E. Solari, G. Martin, R. Scopelliti and C. Floriani, *Chem. Commun.*, 1999, 2319-2320.

233. J. Jubb and S. Gambarotta, *Inorg. Chem.*, 1994, **33**, 2503-2504.

234. D. Bhattacharya, S. Maji, K. Pal and S. Sarkar, *Inorg. Chem.*, 2009, **48**, 6362-6370.

235. D. Bhattacharya, S. Dey, S. Maji, K. Pal and S. Sarkar, *Inorg. Chem.*, 2005, **44**, 7699-7701.

236. F. Franceschi, E. Solari, R. Scopelliti and C. Floriani, *Angew. Chem. Int. Ed.*, 2000, **39**, 1685-+.

237. L. Bonomo, C. Stern, E. Solari, R. Scopelliti and C. Floriani, *Angew. Chem. Int. Ed.*, 2001, **40**, 1449-+.

238. C. Floriani, E. Solari, G. Solari, A. Chiesi-Villa and C. Rizzoli, *Angew. Chem. Int. Ed.*, 1998, **37**, 2245-2248.

239. J. Jubb, S. Gambarotta, R. Duchateau and J. H. Teuben, *J. Chem. Soc. Chem. Comm.*, 1994, 2641-2642.

240. D. Jacoby, C. Floriani, A. Chiesivilla and C. Rizzoli, *J. Am. Chem. Soc.*, 1993, **115**, 3595-3602.

241. J. Jubb, D. Jacoby, C. Floriani, A. Chiesivilla and C. Rizzoli, *Inorg. Chem.*, 1992, **31**, 1306-1308.

242. S. Deangelis, E. Solari, C. Floriani, A. Chiesivilla and C. Rizzoli, *Organometallics*, 1995, **14**, 4505-4512.

243. J. Jubb and S. Gambarotta, *J. Am. Chem. Soc.*, 1994, **116**, 4477-4478.

244. J. Jubb and S. Gambarotta, *J. Am. Chem. Soc.*, 1993, **115**, 10410-10411.

245. J. I. Song and S. Gambarotta, *Angew. Chem. Int. Ed.*, 1995, **34**, 2141-2143.

246. E. Campazzi, E. Solari, C. Floriani and R. Scopelliti, *Chem. Commun.*, 1998, 2603-2604.

247. S. Gambarotta, T. Dube and G. P. A. Yap, *Angew. Chem. Int. Ed.*, 1999, **38**, 1432-1435.

248. E. Campazzi, E. Solari, R. Scopelliti and C. Floriani, *Inorg. Chem.*, 1999, **38**, 6240-6245.

249. E. Campazzi, E. Solari, R. Scopelliti and C. Floriani, *Inorg. Chem.*, 1999, **38**, 6240-6245.

250. E. Campazzi, E. Solari, R. Scopelliti and C. Floriani, *Chem. Commun.*, 1999, 1617-1618.

251. P. A. Gale, J. W. Genge, V. Kral, M. A. McKervey, J. L. Sessler and A. Walker, *Tetrahedron Lett.*, 1997, **38**, 8443-8444.

252. J. L. Sessler, P. Anzenbacher, K. Jursikova, H. Miyaji, J. W. Genge, N. A. Tvermoes, W. E. Allen, J. A. Shriver, P. A. Gale and V. Kral, *Pure Appl. Chem.*, 1998, **70**, 2401-2408.

253. W. H. Brown, Hutchins.Bj and Mackinno.Mh, *Can. J. Chem.*, 1971, **49**, 4017-&.

254. D.-W. Yoon, D. E. Gross, V. M. Lynch, J. L. Sessler, B. P. Hay and C.-H. Lee, *Angew. Chem. Int. Ed.*, 2008, **47**, 5038-5042.

255. D.-W. Yoon, D. E. Gross, V. M. Lynch, J. L. Sessler, B. P. Hay and C.-H. Lee, *Angew. Chem. Int. Ed.*, 2008, **47**, 5038-5042.

256. C.-H. Lee, H. Miyaji, D.-W. Yoon and J. L. Sessler, *Chem. Commun. (Cambridge, U. K.)*, 2008, 24-34.

257. P. A. Gale, J. L. Sessler, W. E. Allen, N. A. Tvermoes and V. Lynch, *Chem. Commun.*, 1997, 665-666.

258. H. Miyaji, W. Sato, J. L. Sessler and V. M. Lynch, *Tetrahedron Lett.*, 2000, **41**, 1369-1373.

259. R. Timmermann, R. Mattes and B. Franck, *Angew. Chem. Int. Ed.*, 1987, **26**, 64-65.

260. B. Franck and C. Wegner, *Angew. Chem. Int. Ed.*, 1975, **14**, 424-424.

261. Y. Furusho, H. Kawasaki, S. Nakanishi, T. Aida and T. Takata, *Tetrahedron Lett.*, 1998, **39**, 3537-3540.

262. J. Wang, A. K. J. Dick, M. G. Gardiner, B. F. Yates, E. J. Peacock, B. W. Skelton and A. H. White, *Eur. J. Inorg. Chem.*, 2004, 1992-1995.

263. J. Wang, M. G. Gardiner, E. J. Peacock, B. W. Skelton and A. H. White, *Dalton Trans.*, 2003, 161-162.

264. J. Wang, R. I. J. Amos, A. S. P. Frey, M. G. Gardiner, M. L. Cole and P. C. Junk, *Organometallics*, 2005, **24**, 2259-2261.

265. J. Wang, M. G. Gardiner, B. W. Skelton and A. H. White, *Organometallics*, 2005, **24**, 815-818.

266. A. S. P. Frey, M. G. Gardiner, D. N. Stringer and B. F. Yates, *Organometallics*, 2007, **26**, 1299-1302.

267. N. W. Davies, A. S. P. Frey, M. G. Gardiner and J. Wang, *Chem. Commun.*, 2006, 4853-4855.

268. A. N. James, *Steric and Electronic Investigations into Samarium(II) Dinitrogen, Heteroalkyne and Heterocycle Reductions*, PhD thesis, University of Tasmania, 2011.

269. T. Nakabuchi, Y. Matano and H. Imahori, *Organometallics*, 2008, **27**, 3142-3152.

270. M.-X. Wang, *Chem. Commun.*, 2008, 4541-4551.

271. M. Stępień and L. Latos-Grażyński, *Acc. Chem. Res*, 2004, **38**, 88-98.

272. J. L. Sessler, W. S. Cho, V. Lynch and V. Kral, *Chem. Eur. J.*, 2002, **8**, 1134-1143.

273. M. Staffilani, K. S. B. Hancock, J. W. Steed, K. T. Holman, J. L. Atwood, R. K. Juneja and R. S. Burkhalter, *J. Am. Chem. Soc.*, 1997, **119**, 6324-6335.

274. M. G. Gardiner, S. M. Lawrence, C. L. Raston, B. W. Skelton and A. H. White, *Chem. Commun. (Cambridge)*, 1996, 2491-2492.

275. B. Castellano, A. ZanottiGerosa, E. Solari, C. Floriani, A. ChiesiVilla and C. Rizzoli, *Organometallics*, 1996, **15**, 4894-4896.

276. J. L. Atwood, M. G. Gardiner, C. Jones, C. L. Raston, B. W. Skelton and A. H. White, *Chem. Commun. (Cambridge)*, 1996, 2487-2488.

277. A. Rosa, G. Ricciardi, M. Rosi, A. Sgamellotti and C. Floriani, *J. Chem. Soc. Dalton Trans.*, 1993, 3759-3766.

278. L. Cuesta and J. L. Sessler, *Chem. Soc. Rev.*, 2009, **38**, 2716-2729.

279. V. Kral, P. A. Gale, P. Anzenbacher, K. Jursikova, V. Lynch and J. L. Sessler, *Chem. Commun.*, 1998, 9-10.

280. M. J. Chmielewski and J. Jurczak, *Tetrahedron Lett.*, 2005, **46**, 3085-3088.

281. K.-B. Jung, S. K. Kim, V. M. Lynch, D.-G. Cho and J. L. Sessler, *Chem. Commun. (Cambridge, U. K.)*, 2012, **48**, 2495-2497.

282. H. Schumann and W. Genthe, in *Handbook on the Physics and Chemistry of Rare Earths*, eds. Karl A. Gschneidner, Jr. and E. LeRoy, Elsevier, 1984, vol. Volume 7, pp. 445-571.

283. H. Schumann, J. A. Meese-Marktscheffel and L. Esser, *Chem. Rev.*, 1995, **95**, 865.

284. K. Izod, *Angew. Chem. Int. Ed.*, 2002, **41**, 743-+.

285. S. Salot and J. C. Warf, *J. Am. Chem. Soc.*, 1968, **90**, 1932-&.

286. R. Navaneethakrishnan and J. C. Warf, *Inorg. Chem.*, 1976, **15**, 2849-2852.

287. J. Doyle and A. G. Sykes, *J. Chem. Soc. A*, 1968, 2836-&.

288. W. J. Evans, *Adv. Organomet. Chem.*, 1985, **24**, 131-177.

289. W. J. Evans, J. W. Grate, H. W. Choi, I. Bloom, W. E. Hunter and J. L. Atwood, *J. Am. Chem. Soc.*, 1985, **107**, 941-946.

290. M. C. Cassani, M. F. Lappert and F. Laschi, *Chem. Commun.*, 1997, 1563-1564.

291. P. B. Hitchcock, M. F. Lappert, L. Maron and A. V. Protchenko, *Angew. Chem. Int. Ed.*, 2008, **47**, 1488-1491.

292. W. J. Evans, N. T. Allen and J. W. Ziller, *J. Am. Chem. Soc.*, 2001, **123**, 7927-7928.

293. F. Nief, F. Jaroschik, X. F. Le Goff and L. Ricard, *Organometallics*, 2007, **26**, 3552-3558.

294. J. Cheng, J. Takats, M. J. Ferguson and R. McDonald, *J. Am. Chem. Soc.*, 2008, **130**, 1544-1545.

295. F. Jaroschik, F. Nief, X. F. Le Goff and L. Ricard, *Organometallics*, 2007, **26**, 1123-1125.

296. M. N. Bochkarev, I. L. Fedushkin, S. Dechert, A. A. Fagin and H. Schumann, *Angew. Chem. Int. Ed.*, 2001, **40**, 3176-+.

297. F. Jaroschik, A. Momin, F. Nief, X. F. Le Goff, G. B. Deacon and P. C. Junk, *Angew. Chem. Int. Ed.*, 2009, **48**, 1117-1121.

298. W. J. Evans and D. S. Lee, *Can. J. Chem.*, 2005, **83**, 375-384.

299. F. Nief, *Dalton Trans.*, 2010, **39**, 6589-6598.

300. W. J. Evans, *Coord. Chem. Rev.*, 2000, **206-207**, 263-283.

301. I. L. Fedushkin, M. N. Bochkarev, S. Dechert and H. Schumann, *Chem. Eur. J.*, 2001, **7**, 3558-3563.

302. M. N. Bochkarev, A. A. Fagin and G. V. Khoroshenkov, *Russ. Chem. Bull.* , 2002, **51**, 1909-1914.

303. M. N. Bochkarev, I. L. Fedushkin, S. Dechert, A. A. Fagin and H. Schumann, *Angew. Chem. Int. Ed.*, 2001, **40**, 3176.

304. W. J. Evans, N. T. Allen and J. Ziller, W,, *J. Am. Chem. Soc.*, 2000, **122**, 11749.

305. F. Nief, D. Turcitu and L. Ricard, *Chem. Commun.*, 2002, 1646.

306. S. Ilango, B. Vidjayacoumar and S. Gambarotta, *Dalton Trans.*, 2010, **39**, 6853-6857.

307. A. S. P. Frey, *Structural and Reductive Chemistry of Low-valent Lanthanide Complexes Featuring Modified Porphyrinogens,* PhD thesis, University of Tasmania, 2009.

308. S. Kobayashi, I. Hachiya, M. Araki and H. Ishitani, *Tetrahedron Lett.*, 1993, **34**, 3755-3758.

309. S. Kobayashi, I. Hachiya, H. Ishitani and M. Araki, *Synlett*, 1993, 472-474.

310. K. Ishihara, Y. Karumi, M. Kubota and H. Yamamoto, *Synlett*, 1996, 839-+.

311. K. Ishihara, M. Kubota, H. Kurihara and H. Yamamoto, *J. Org. Chem.*, 1996, **61**, 4560-4567.

312. K. Ishihara, M. Kubota and H. Yamamoto, *Synlett*, 1996, 265.

313. B. Karimi and L. Ma'mani, *Synthesis-Stuttgart*, 2003, 2503-2506.

314. B. Karimi and L. Ma'mani, *Tetrahedron Lett.*, 2003, **44**, 6051-6053.

315. A. S. P. Frey, unpublished work, University of Tasmania, 2008.

316. N. Kuhn, M. Kockerling, S. Stubenrauch, D. Blaser and R. Boese, *J. Chem. Soc. Chem. Comm.*, 1991, 1368-1370.

317. N. Kuhn, G. Henkel and S. Stubenrauch, *Angew. Chem. Int. Ed.*, 1992, **31**, 778-779.

318. N. Kuhn, G. Henkel, J. Kreutzberg, S. Stubenrauch and C. Janiak, *J. Organomet. Chem.*, 1993, **456**, 97-106.

319. M. Westerhausen, M. Wieneke, H. Noth, T. Seifert, A. Pfitzner, W. Schwarz, O. Schwarz and J. Weidlein, *Eur. J. Inorg. Chem.*, 1998, 1175-1182.

320. H. D. Hausen, J. Todtmann and J. Weidlein, *J. Organomet. Chem.*, 1994, **466**, C1-C4.

321. J. Jubb, P. Berno, S. Hao and S. Gambarotta, *Inorg. Chem.*, 1995, **34**, 3563-3566.

322. S. Deangelis, E. Solari, C. Floriani, A. Chiesivilla and C. Rizzoli, *J. Chem. Soc. Dalton Trans.*, 1994, 2467-2469.

323. T. Dubé, J. Guan, S. Gambarotta and G. P. A. Yap, *Chem. Eur. J.*, 2001, **7**, 374-381.

324. K. K. Fonda and L. M. Vallarino, *Inorg. Chim. Acta*, 2002, **334**, 403-410.

325. W. H. Zachariasen, *The Actinide Elements*, McGraw-Hill, New York, 1954.

326. W. J. Evans, T. A. Ulibarri and J. W. Ziller, *Organometallics*, 1991, **10**, 134-142.

327. W. J. Evans, E. Montalvo, D. J. Dixon, J. W. Ziller, A. G. DiPasquale and A. L. Rheingold, *Inorg. Chem.*, 2008, **47**, 11376-11381.

328. X. F. Li, S. Eggers, J. Kopf, W. Jahn, R. D. Fischer, C. Apostolidis, B. Kanellakopulos, F. Benetollo, A. Polo and G. Bombieri, *Inorg. Chim. a-Art Let.*, 1985, **100**, 183-199.

329. G. B. Deacon, C. M. Forsyth, R. H. Newnham and T. D. Tuong, *Aust. J. Chem.*, 1987, **40**, 895-906.

330. W. J. Evans, T. J. Mueller and J. W. Ziller, *Chem. Eur. J.*, 2010, **16**, 964-975.

331. W. J. Evans, E. Montalvo, S. E. Foster, K. A. Harada and J. W. Ziller, *Organometallics*, 2007, **26**, 2904-2910.

332. W. J. Evans and D. K. Drummond, *Organometallics*, 1988, **7**, 797-802.

333. M. G. Gardiner, A. N. James, C. Jones and C. Schulten, *Dalton Trans.*, 2010, **39**, 6864-6870.

334. V. Gutmann, *Coord. Chem. Rev.*, 1976, **18**, 225-255.

335. J. A. Joule and K. Mills, *Heterocyclic Chemistry*, Wiley, 2013.

336. S. Labouille, F. Nief, X.-F. Le Goff, L. Maron, D. R. Kindra, H. L. Houghton, J. W. Ziller and W. J. Evans, *Organometallics*, 2012, **31**, 5196-5203.

337. K. Mashima, Y. Nakayama, T. Shibahara, H. Fukumoto and A. Nakamura, *Inorg. Chem.*, 1996, **35**, 93-99.

338. G. Deacon, B. Gatehouse, S. Platts and D. Wilkinson, *Aust. J. Chem.*, 1987, **40**, 907-914.

339. Pascal C. Leverd, D. Rinaldo and M. Nierlich, *Eur. J. Inorg. Chem.*, 2001, **2001**, 2021-2025.

340. Y. Cui, H. L. Ngo, P. S. White and W. Lin, *Chem. Commun.*, 2002, 1666-1667.

341. T. Mehdoui, J. C. Berthet, P. Thuery and M. Ephritikhine, *Dalton Trans.*, 2004, 579-590.

342. R. K. Agarwal and V. Kumar, *Phosphorus, Sulfur Silicon Relat. Elem.*, 2010, **185**, 1469-1483.

343. K. K. Rohatgi and S. K. Sen Gupta, *J. Inorg. Nucl. Chem.*, 1972, **34**, 3061-3071.

344. D. Freedman, T. J. Emge and J. G. Brennan, *Inorg. Chem.*, 1999, **38**, 4400-4404.

345. I. L. Fedushkin, V. I. Nevodchikov, M. N. Bochkarev, S. Dechert and H. Schumann, *Russ. Chem. Bull.* , 2003, **52**, 154-159.

346. A. M. Bond, G. B. Deacon and R. H. Newnham, *Organometallics*, 1986, **5**, 2312-2316.

347. P. Gradoz, D. Baudry, M. Ephritikhine, M. Lance, M. Nierlich and J. Vigner, *J. Organomet. Chem.*, 1994, **466**, 107-118.

348. K. D. John, J. M. Veauthier, E. J. Schelter, C. N. Carlson, B. L. Scott, R. E. Da Re, J. D. Thompson, J. L. Kiplinger and D. E. Morris, *Inorg. Chem.*, 2008, **47**, 5841-5849.

349. P. L. Watson, T. H. Tulip and I. Williams, *Organometallics*, 1990, **9**, 1999-2009.

350. W. J. Evans, C. A. Seibel and J. W. Ziller, *Inorg. Chem.*, 1998, **37**, 770-776.

351. D. J. Berg, J. M. Boncella and R. A. Andersen, *Organometallics*, 2002, **21**, 4622-4631.

352. M. Schultz, J. M. Boncella, D. J. Berg, T. D. Tilley and R. A. Andersen, *Organometallics*, 2001, **21**, 460-472.

353. R. E. Da Re, C. J. Kuehl, M. G. Brown, R. C. Rocha, E. D. Bauer, K. D. John, D. E. Morris, A. P. Shreve and J. L. Sarrao, *Inorg. Chem.*, 2003, **42**, 5551-5559.

354. G. H. Maunder and A. Sella, *Polyhedron*, 1998, **17**, 63-68.

355. M. R. MacDonald, J. W. Ziller and W. J. Evans, *Inorg. Chem.*, 2011, **50**, 4092-4106.

356. W. J. Evans, B. L. Davis, G. W. Nyce, J. M. Perotti and J. W. Ziller, *J. Organomet. Chem.*, 2003, **677**, 89-95.

357. H. C. Brown and X. R. Mihm, *J. Am. Chem. Soc.*, 1955, **77**, 1723-1726.

358. C. Kaes, A. Katz and M. W. Hosseini, *Chem. Rev.*, 2000, **100**, 3553-3590.

359. S. Herzog and K. Gustav, *Z. Anorg. Allg. Chem*, 1966, **346**, 162-&.

360. W. J. Evans and D. K. Drummond, *J. Am. Chem. Soc.*, 1989, **111**, 3329-3335.

361. M. N. Bochkarev, I. L. Fedushkin, V. I. Nevodchikov, V. K. Cherkasov, H. Schumann, H. Hemling and R. Weimann, *J. Organomet. Chem.*, 1996, **524**, 125-131.

362. W. Kaim, R. Reinhardt, E. Waldhor and J. Fiedler, *J. Organomet. Chem.*, 1996, **524**, 195-202.

363. S. J. Kraft, P. E. Fanwick and S. C. Bart, *Inorg. Chem.*, 2010, **49**, 1103-1110.

364. I. L. Fedushkin, T. V. Petrovskaya, F. Girgsdies, V. I. Nevodchikov, R. Weimann, H. Schumann and M. N. Bochkarev, *Russ. Chem. Bull.* , 2000, **49**, 1869-1876.

365. L. L. Merritt and E. D. Schroeder, *Acta. Crystallogr.*, 1956, **9**, 801-804.

366. F. E. Kuhn, M. Groarke, E. Bencze, E. Herdtweck, A. Prazeres, A. M. Santos, M. J. Calhorda, C. C. Romao, I. S. Goncalves, A. D. Lopes and M. Pillinger, *Chem. Eur. J.*, 2002, **8**, 2370-2383.

367. T. Mehdoui, J. C. Berthet, P. Thuery, L. Salmon, E. Riviere and M. Ephritikhine, *Chem. Eur. J.*, 2005, **11**, 6994-7006.

368. R. Kumar and U. P. Singh, *J. Mol. Struct.*, 2008, **875**, 427-434.

369. M. Schultz, J. M. Boncella, D. J. Berg, T. D. Tilley and R. A. Andersen, *Organometallics*, 2002, **21**, 460-472.

370. I. L. Fedushkin, T. V. Petrovskaya, F. Girgsdies, R. D. Kohn, M. N. Bochkarev and H. Schumann, *Angew. Chem. Int. Ed.*, 1999, **38**, 2262-2264.

371. A. Q. Wu, F.-K. Zheng, W.-T. Chen, L.-Z. Cai, Guo, J.-S. Huang, Z.-C. Dong and Y. Takano, *Inorg. Chem.*, 2004, **43**, 4839-4845.

372. M. D. Walter, D. J. Berg and R. A. Andersen, *Organometallics*, 2006, **25**, 3228-3237.

373. W. W. Lukens, N. Magnani and C. H. Booth, *Inorg. Chem.*, 2012, **51**, 10105-10110.

374. A. J. Canty, N. Chaichit, B. M. Gatehouse, E. E. George and G. Hayhurst, *Inorg. Chem.*, 1981, **20**, 2414-2422.

375. G. B. Deacon, J. M. Patrick, B. W. Skelton, N. C. Thomas and A. H. White, *Aust. J. Chem.*, 1984, **37**, 929-945.

376. S. D. Cummings, *Coord. Chem. Rev.*, 2009, **253**, 449-478.

377. E. W. Abel, N. J. Long, K. G. Orrell, A. G. Osborne, H. M. Pain and V. Sik, *J. Chem. Soc. Chem. Comm.*, 1992, 303-304.

378. E. W. Abel, V. S. Dimitrov, N. J. Long, K. G. Orrell, A. G. Osborne, V. Sik, M. B. Hursthouse and M. A. Mazid, *J. Chem. Soc. Dalton Trans.*, 1993, 291-298.

379. E. W. Abel, K. G. Orrell, A. G. Osborne, H. M. Pain, V. Sik, M. B. Hursthouse and K. M. A. Malik, *J. Chem. Soc. Dalton Trans.*, 1994, 3441-3449.

380. E. W. Abel, K. G. Orrell, A. G. Osborne, H. M. Pain and V. Sik, *J. Chem. Soc. Dalton Trans.*, 1994, 111-116.

381. F. P. Pruchnik, F. Robert, Y. Jeannin and S. Jeannin, *Inorg. Chem.*, 1996, **35**, 4261-&.

382. A. A. Sidorov, G. G. Aleksandrov, E. V. Pakhmutova, A. Y. Chernyad'ev, I. L. Eremenko and I. I. Moiseev, *Russ. Chem. Bull.* , 2005, **54**, 588-599.

383. A. Figuerola, J. Ribas, X. Solans, M. Font-Bardia, M. Maestro and C. Diaz, *Eur. J. Inorg. Chem.*, 2006, 1846-1852.

384. L. I. Semenova, A. N. Sobolev, B. W. Skelton and A. H. White, *Aust. J. Chem.*, 1999, **52**, 519-529.

385. Y. Fukuda, A. Nakao and K. Hayashi, *J. Chem. Soc. Dalton Trans.*, 2002, 527-533.

386. J. M. Stanley, C. K. Chan, X. P. Yang, R. A. Jones and B. J. Holliday, *Polyhedron*, 2010, **29**, 2511-2515.

387. S. D. Grumbine, R. K. Chadha and T. D. Tilley, *J. Am. Chem. Soc.*, 1992, **114**, 1518-1520.

388. J. A. Joule and K. Mills, *Heterocyclic Chemistry*, Wiley, 2010.

389. N. A. Ogorodnikova, *J. Mol. Struct.:THEOCHEM*, 1993, **279**, 71-78.

390. T. Eicher, S. Hauptmann and A. Speicher, *The Chemistry of Heterocycles: Structures, Reactions, Synthesis, and Applications 3rd, Completely Revised and Enlarged Edition*, Wiley, 2013.

391. H. Zhou, G.-W. Diao, S.-Y. Qian, X.-Z. Yang, A.-H. Yuan, Y. Song and Y.-Z. Li, *Dalton Trans.*, 2012, **41**, 10690-10697.

392. H. Zhou, A.-H. Yuan, S.-Y. Qian, Y. Song and G.-W. Diao, *Inorg. Chem.*, 2010, **49**, 5971-5976.

393. Y. Ma, G.-F. Xu, X. Yang, L.-C. Li, J. Tang, S.-P. Yan, P. Cheng and D.-Z. Liao, *Chem. Commun.*, 2010, **46**, 8264-8266.

394. F. Pointillart and K. Bernot, *Eur. J. Inorg. Chem.*, 2010, 952-964.

395. E. C. Baker and K. N. Raymond, *Inorg. Chem.*, 1977, **16**, 2710-2714.

396. W. J. Evans, J. R. Walensky, T. M. Champagne, J. W. Ziller, A. G. DiPasquale and A. L. Rheingold, *J. Organomet. Chem.*, 2009, **694**, 1238-1243.

397. W. J. Evans, M. K. Takase, J. W. Ziller, A. G. DiPasquale and A. L. Rheingold, *Organometallics*, 2009, **28**, 236-243.

398. W. J. Evans, K. A. Miller, D. S. Lee and J. W. Ziller, *Inorg. Chem.*, 2005, **44**, 4326-4332.

399. D. J. Brown, *The Chemistry of Heterocyclic Compounds, The Pyrimidines*, Wiley, 2009.

400. P. Wheatley, *Acta Crystallogr.*, 1960, **13**, 80-85.

401. M. Wriedt, S. Sellmer and C. Nather, *Inorg. Chem.*, 2009, **48**, 6896-6903.

402. J. G. Malecki, *Transit. Metal. Chem.*, 2010, **35**, 801-808.

403. F. D. Rochon, G. Masserweh and N. Nedelec, *Inorg. Chim. Acta*, 2003, **346**, 197-206.

404. F. D. Rochon and M. Fakhfakh, *Inorg. Chim. Acta*, 2009, **362**, 1455-1466.

405. L. Arizaga, R. Gonzalez, R. Chiozzone, C. Kremer, M. F. Cerda, D. Armentano, G. De Munno, F. Lloret and J. Faus, *Polyhedron*, 2008, **27**, 552-558.

406. S. Demir, J. M. Zadrozny, M. Nippe and J. R. Long, *J. Am. Chem. Soc.*, 2012, **134**, 18546-18549.

407. G. Zucchi, T. Jeon, D. Tondelier, D. Aldakov, P. Thuery, M. Ephritikhine and B. Geffroy, *J. Mater. Chem.*, 2010, **20**, 2114-2120.

408. R. N. Castle, *The Chemistry of Heterocyclic Compounds, Pyridazines*, Wiley, 2009.

409. P. L. Arnold, J. H. Farnaby, R. C. White, N. Kaltsoyannis, M. G. Gardiner and J. B. Love, *Chem. Sci.*, 2014, **5**, 756-765.

410. T. M. McPhillips, S. E. McPhillips, H. J. Chiu, A. E. Cohen, A. M. Deacon, P. J. Ellis, E. Garman, A. Gonzalez, N. K. Sauter, R. P. Phizackerley, S. M. Soltis and P. Kuhn, *J. Synchrotron Radiat.*, 2002, **9**, 401-406.

411. W. Kabsch, *J. Appl. Crystallogr.*, 1988, **21**, 916-924.

412. W. Kabsch, *Acta Crystallogr. D*, 2010, **66**, 125-132.

413. G. M. Sheldrick, *Acta Crystallogr. A*, 2008, **64**, 112-122.

414. L. J. Barbour, *Supramol. Chem.*, 2001, **1**, 189-191.

415. G. Fisk, *Macrocyclic Samarium Complexes of High Conformational Freedom*, BSc(Hons) thesis, University of Tasmania, 2007.